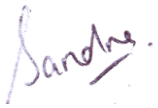
## Declaration

All of work presented in this thesis was performed entirely by me and no part of my thesis has been accepted or is currently being submitted for any other degree or diploma in this university or elsewhere. My research was carried out under the supervision of Professor Nicholas B. La Thangue and Dr. Amanda S. Coutts, Department of Oncology, Medical Science Division, University of Oxford.



Sandra Maniam

September 2013

## Abstract

Strap is a DNA damage responsive p53 cofactor, reflecting its control by the DNA damage signalling pathway. This study identified Strap at the mitochondria where it is damage regulated and can augment p53-dependent cytochrome c release leading to apoptosis. Moreover, p53 and Strap facilitate each other's localisation from the mitochondria to the nucleus during the DNA damage response. Two ATM/ATR phosphorylation consensus sites in Strap were identified by mass spectrometry and phosphorylation of all the ATM/ATR consensus sites resulted in mitochondrial localisation of Strap during DNA damage. Targeting Strap to the mitochondria depletes cellular ATP when cells favour energy production through oxidative phosphorylation and sensitises cells to p53-dependent damage-induced apoptosis. These results thus imply that Strap co-ordinates different arms of the p53 response, and might be responsible for integrating its mitochondrial and nuclear functions.

(134 words)

## Acknowledgements

First and foremost I would like to thank my supervisor Prof Nick La Thangue who gave me the opportunity to work in his lab which allowed me to explore my scientific interest. My DPhil will not be possible without the financial support from the Malaysian Ministry of Higher Education and University Putra Malaysia. To my collaborators, Benedikt Kessler's group, Ester Hammond's group and also to Mike Stratford, I am indeed grateful for their support and willingness to share their knowledge and expertise which accelerated the progress of this study.

To Amanda, words can't express my gratitude to you. You have been like a mentor, sister and a friend. Thank you for always believing in me and most importantly never giving up in me, it means a great deal. To Panos and Shonagh, thank you for lifting my spirits whenever I'm down. I would be lost without your guidance and friendship these past years. Lab experiments are not always rewarding and DPhil has been an enormous challenge. There are those people, however, who made the challenge much easier. I would like to take this opportunity to thank my lab mates where I would not have survived my most testing days without them.

To my dearest family whose been supporting me closely from far distance, I thank you for being patience and putting up with all my stress-acquired behaviour. I am indeed truly blessed to have you by my side. There are many more I would like to thank, but time, space, and modesty compel me to stop here.

# Table of Contents

Declaration ..... **i**
Abstract ..... **ii**
Acknowledgements ..... **iii**
Table of Contents ..... **iv**
List of Figures ..... **vii**
List of Tables ..... **ix**
List of Abbreviations ..... **x**
**Chapter 1**
Introduction ..... **1**
1.1 DNA damage response ..... 2
1.2 Cancer ..... 5
1.3 Mitochondrial Biology ..... 7
1.4 Metabolic reprogramming ..... 10
1.5 Apoptosis ..... 15
1.6 The OXPHOS system in mitochondria ..... 25
1.7 p53 ..... 29
1.8 p53 cofactors ..... 39
1.9 Project overview ..... 45
**Chapter 2**
Materials and Methods ..... **47**
2.1 Cell lines ..... 48
2.2 Plasmid Expression Vectors ..... 49
2.3 Transfection ..... 50
2.4 Small interfering RNA transfection ..... 50
2.5 Drug treatments ..... 51
2.6 Western Blotting ..... 51
2.7 Immunoprecipitation ..... 53
2.8 Immunofluoresence ..... 55
2.9 Mass spectrometry gel and tryptic digestion ..... 56
2.10 Mitochondrial Extraction ..... 58
2.11 Oligomerisation Assay ..... 58
2.12 Proteinase K digestion ..... 59
2.13 Reporter Assay ..... 59
2.14 xCELLigence ..... 60
2.15 Reverse Transcriptase Polymerase Chain Reaction ..... 60

2.16 TMRE staining ..... 62
2.17 Nuclear extraction ..... 62
2.18 ATP synthase specific activity ..... 63
2.19 Total ATP levels ..... 63
2.20 Flow cytometry ..... 63
**Chapter 3**
Results: Cell line development and proteomic analysis ..... **64**
3.1 Strap derivatives stable cell lines ..... 65
3.2 Inducible cell lines ..... 70
3.3 Introduction to proteomic analysis ..... 74
3.4 Proteomic analysis of the OB fold ..... 75
3.5 Proteomic analysis of the OB fold under damage ..... 79
3.6 Discussion ..... 81
**Chapter 4**
Results: Strap at the mitochondria ..... **84**
4.1 Strap is localised at the mitochondria ..... 85
4.2 Influence of p53 on mitochondrial Strap ..... 90
4.3 Regulation of nuclear and mitochondrial Strap and p53 ..... 92
4.4 Strap and p53 interact at mitochondria ..... 93
4.5 Strap reduces mitochondrial p53 levels ..... 98
4.6 Strap augments BAK oligomerisation and cytochrome c release ..... 101
4.7 Strap augments apoptosis in the presence of p53 ..... 111
4.8 Summary ..... 115
**Chapter 5**
Results: Proteomic analysis of L-Strap ..... **119**
5.1 Generation of mitochondrial targeted Strap ..... 120
5.2 Proteomic analysis of L-Strap ..... 121
5.3 Proteomic analysis of L-Strap under damage ..... 127
5.4 Post-translational modifications ..... 130
5.5 Discussion ..... 132
**Chapter 6**
Results: Strap and cellular metabolism ..... **135**
6.1 Strap interacts with ATP synthase subunit-β ..... 136
6.2 Regulation of Strap during OXPHOS ..... 139
6.3 Strap influences ATP/ADP levels during OXPHOS ..... 145
6.4 L-Strap augments apoptosis during OXPHOS in the presence of p53 ..... 152
6.5 Regulation of Strap during hypoxia ..... 159

6.6 Summary ..... 163
**Chapter 7**
Results: Strap derivatives ..... **166**
7.1 Proteomic analysis of the OB fold ..... 167
7.2 Characterization of Strap ATM/ATR consensus sites ..... 171
7.3 Impact of ATM/ATR phosphorylation on Strap at the mitochondria ..... 176
7.4 Strap derivatives and p53 ..... 180
7.5 Strap and 3D mutant augment apoptosis in the presence of p53 ..... 182
7.6 Summary ..... 185
**Chapter 8**
Discussion ..... **187**
8.1 Strap at the mitochondria ..... 188
8.2 Shuttling of mitochondrial Strap and p53 ..... 191
8.3 Strap at the mitochondria induces p53-dependent apoptosis ..... 194
8.4 Strap and cellular metabolism ..... 197
8.5 Regulation of Strap during hypoxia ..... 203
8.6 ATM/ATR phosphorylation of Strap ..... 205
8.7 Conclusions and future directions ..... 209
**Chapter 9**
References ..... **213**

# List of Figures

Figure 1.1 The DNA damage response cascade. ..... 4
Figure 1.2 Mitochondrial evolution and mtDNA overview. ..... 9
Figure 1.3 Regulation of metabolism in cancer cells. ..... 14
Figure 1.4 The intrinsic apoptotic pathway. ..... 16
Figure 1.5 Classification of the BCL-2 family proteins. ..... 18
Figure 1.6 Mitochondrial OXPHOS complexes. ..... 27
Figure 1.7 The functional domains and PTM sites of p53. ..... 31
Figure 1.8 p53 and cell metabolism. ..... 38
Figure 1.9 Regulation of Strap during cellular stress response. ..... 44
Figure 3.1 Strap TPR motif and OB fold. ..... 67
Figure 3.2 Functional analyses of Strap stable cell lines. ..... 69
Figure 3.3 Development of OB fold inducible cell line. ..... 72
Figure 3.4 Wild type Strap augments apoptosis in response to damage. ..... 73
Figure 3.5 Immunoprecipitation and mass spectrometry of the OB fold. ..... 76
Figure 3.6 Analysis of OB fold interacting proteins. ..... 78
Figure 3.7 Immunoprecipitation of OB fold under damage. ..... 80
Figure 4.1 Strap is localised at the mitochondria. ..... 86
Figure 4.2 Validation of Strap at mitochondria. ..... 88
Figure 4.3 Strap is localised at the outer mitochondrial membrane. ..... 89
Figure 4.4 Mitochondrial Strap is damage regulated. ..... 91
Figure 4.5 Strap levels are influenced by the presence of p53. ..... 94
Figure 4.6 Strap mRNA levels are not affected by damage. ..... 95
Figure 4.7 Strap interacts with p53 at the mitochondria. ..... 96
Figure 4.8 Evaluation of mitochondrially targeted p53. ..... 97
Figure 4.9 Depletion of Strap enhances mitochondrial p53 levels. ..... 99
Figure 4.10 Strap and p53 in the mitochondrial and nuclear fractions. ..... 100
Figure 4.11 Strap enhances cytochrome c release in the presence of p53. ..... 102
Figure 4.12 Strap enhances BAK oligomerisation in p53 dependent manner. ..... 104
Figure 4.13 Evaluation of mitochondrially targeted Strap. ..... 105
Figure 4.14 Strap augments cytochrome c release in the presence of L-p53. ..... 106
Figure 4.15 Stably expressing cell lines and control for mitochondrial membrane potential staining. ..... 108
Figure 4.16 Strap enhances mitochondrial membrane depolarization in the presence of p53. ..... 110
Figure 4.17 Strap augments cleaved PARP-1 levels in the presence of p53. ..... 112
Figure 4.18 Strap enhances cell death in the presence of p53 upon damage treatment. ..... 114
Figure 5.1 Generation of L-Strap. ..... 122
Figure 5.2 Immunoprecipitation of L-Strap. ..... 124
Figure 5.3 Analysis of L-Strap interacting proteins. ..... 126
Figure 5.4 Immunoprecipitation of L-Strap under damage. ..... 128
Figure 5.5 Analysis of L-Strap interacting proteins under damage. ..... 129
Figure 5.6 PTMs identified from L-Strap mass spectrometry analysis. ..... 131
Figure 6.1 Identification of an interacting partner of L-Strap. ..... 137
Figure 6.2 Strap interacts with ATP synthase subunit-β. ..... 138
Figure 6.3 Strap levels in glucose and galactose supplemented media. ..... 140
Figure 6.4 Interaction between Strap and ATP synthase subunit-β. ..... 142

Figure 6.5 Strap and p53 interaction in glucose or galactose supplemented media. ..... 144
Figure 6.6 Depletion of Strap increases cellular ATP/ADP ratio. ..... 146
Figure 6.7 Strap depletes cellular ATP/ADP ratio. ..... 147
Figure 6.8 Strap influences the mitochondrial membrane potential and ATP synthase activity. ..... 149
Figure 6.9 ATP synthase activity and ATP/ADP ratio in the presence and absence of p53 ..... 151
Figure 6.10 Strap induces apoptosis in a p53-dependent manner. ..... 154
Figure 6.11 L-Strap induces apoptosis during OXPHOS in a p53-dependent manner in the presence of damage. ..... 156
Figure 6.12 ATP depletion mediates L-Strap induced apoptosis. ..... 158
Figure 6.13 Strap levels during hypoxia. ..... 160
Figure 6.14 Transcriptional regulation of Strap during hypoxia. ..... 162
Figure 7.1 Phosphorylation sites identified via mass spectrometry. ..... 169
Figure 7.2 Strap is phosphorylated. ..... 170
Figure 7.3 Localisation of Strap derivatives. ..... 172
Figure 7.4 Strap derivative is localised to mitochondria. ..... 173
Figure 7.5 HA-3D is predominantly in the mitochondrial fraction. ..... 175
Figure 7.6 Strap levels in the presence and absence of ATM. ..... 177
Figure 7.7 Levels of Strap at mitochondria in the presence of ATM and/or ATR inhibitor. ..... 179
Figure 7.8 Strap and 3D mutant in the presence of p53. ..... 181
Figure 7.9 Strap and 3D mutant augment apoptosis in the presence of p53. ..... 184
Figure 8.1 Evolutionarily conserved nuclear export sequences in Strap. ..... 193
Figure 8.2 Model. ..... 210

# List of Tables

**Table 1.1** The components of the intrinsic apoptotic pathway……23

**Table 2.1** Media used for maintaining cell lines……..47

**Table 2.2** Primer sequences for Strap derivatives……...49

**Table 2.3** siRNA sequences for depleting Strap…… …….50

**Table 2.4** List of antibodies…….53

**Table 2.5** RTPCR primer sequences……60

# List of Abbreviations

| | |
|---|---|
| 911 | Rad9-Rad1-Hus1 |
| AIF | Apoptosis inducing factor |
| AMPK | Adenosine monophosphate-activated protein kinase |
| APAF-1 | Apoptotic protease activating factor-1 |
| ARF | Alternate reading frame of the cyclin-dependent kinase inhibitor 2A locus |
| ARF-BP1 | ARF-binding protein-1 |
| ATRIP | ATR interacting protein |
| ATM | Ataxia-telangiectasia mutated |
| ATP | Adenosine triphosphate |
| ATR | Ataxia-telangiectasia mutated and Rad-3 related protein |
| BAD | BCL-2 associated death promoter |
| BAK | BCL-2 antagonist killer |
| BAX | BCL-2 associated X protein |
| BCL-2 | B-cell lymphoma 2 |
| BCL-XL | B-cell lymphoma-extra large |
| BH | BCL-2 homology |
| BID | BH3 interacting domain death agonist |
| BIR | Baculovirus inhibitor of apoptosis repeats |
| CBP | Cyclic AMP response element-binding protein |
| cDNA | Complementary deoxyribonucleic acid |
| CHK1 | Checkpoint kinase 1 |
| CHK2 | Checkpoint kinase 2 |
| COXIV | Cytochrome c oxidase IV |

| | |
|---|---|
| DAVID | Database for annotation, visualization and integrated discovery |
| DKO | Double knock out |
| DNA | Deoxyribonucleic acid |
| DSB | Double-strand break |
| eIF | Eukaryotic initiation factor |
| ErbB2 | Neuro/glioblastoma derived oncogene homolog (avian) |
| FACS | Fluorescence activated cell sorting |
| FADH | Flavin adenine dinucleotide |
| GADD45 | Growth arrest and DNA-damage-inducible-45 |
| GAPDH | Glyceraldehyde-3-phosphate dehydrogenase |
| GFP | Green fluorescent protein |
| GLS2 | Glutaminase-2 |
| GLUT | Glucose transporter |
| GPX1 | Glutathione peroxidase 1 |
| GSH | Glutathione |
| GTP | Guanosine triphosphate |
| HA | Haemagglutinin |
| HAUSP | Herpesvirus-associated ubiquitin specific protease |
| HRE | Hypoxia response elements |
| IAP | Inhibitor of apoptotosis protein |
| IF1 | ATPase inhibitory factor 1 |
| IgG | Immunoglobulin G |
| IMS | Intermembrane space |
| IP | Immunoprecipitation |
| JMY | Junction-mediating and regulatory protein |
| KEAP1 | Kelch-like ECH-associated protein |

| | |
|---|---|
| LC/MS-MS | Liquid-chromatography-coupled tandem mass spectrometry |
| Luc | Luciferase |
| MCL-1 | Myeloid cell leukaemia sequence 1 |
| MDM2 | Mouse double minute 2 |
| MEFs | Mouse embryonic fibroblasts |
| MEP50 | Methylosome protein 50 |
| MITO | Mitochondria |
| MOMP | Mitochondrial outer membrane permeabilisation |
| MRN | MRE11, Rad50, NSB1 |
| mRNA | messenger ribonucleic acid |
| mtDNA | Mitochondrial deoxyribonucleic acid |
| NAC | N-Acetylcysteine |
| NADH | Nicotinamide adenosine dinucleotide |
| NADPH | Nicotinamide adenosine dinucleotide phosphate hydrogenase |
| NES | Nuclear export signal |
| NOXA | Phorbol-12-myristate-13-acetate-induced protein 1 |
| NT | Non targeting |
| OB | Oligonucleotide/Oligosaccharide binding domain |
| OMM | Outer mitochondrial membrane |
| OSCP | Oligomycin sensitivity-conferring protein |
| OXPHOS | Oxidative phosphorylation |
| PANTHER | Protein analysis through evolutionary relationships |
| PARP | Poly-(ADP ribose)-polymerase |
| PCNA | Proliferating cell nuclear antigen |
| PCR | Polymerase chain reaction |
| PGAM5 | Phosphoglycerate mutase family 5 |
| PHGDH | Phosphoglycerate dehydrogenase |

| | |
|---|---|
| PI(3,4,5)P3 | Phosphoinositide-3,4,5 triphosphate |
| PI(4,5)P2 | Phosphoinositide-4,5 biphosphate |
| PI3K | Phosphoinositide-3-kinase |
| PKM2 | Pyruvate Kinase M2 |
| PPP | Pentose phosphate pathway |
| PRMT5 | Protein arginine methyltransferase 5 |
| PTEN | Phosphatase and tensin homologue deleted on chromosome 10 |
| PTM | Post-translational modification |
| PTP | Permeability transition pores |
| PUMA | p53 upregulated modulator of apoptosis |
| RING | Really interesting new gene |
| RNA | Ribonucleic acid |
| ROS | Reactive oxygen species |
| RPA | Replication protein A |
| RTPCR | Reverse transcription polymerase chain reaction |
| SCO2 | Synthesis of cytochrome c oxidase 2 |
| SDS-PAGE | Sodium dodecyl sulphate-polyacrylamide gel electrophoresis |
| siRNA | Small interfering ribonucleic acid |
| SMAC | Second mitochondria-derived activator of caspases |
| snRNP | Small nuclear ribonucleoprotein |
| ss | Single-strand |
| SSB | Single-strand break |
| Strap | Stress responsive activator of p300 |
| TCA | Tricarboxylic acid |
| TIGAR | Tp53-induced glycolysis and apoptosis regulator |
| TIM | Translocase of inner membrane |

| | |
|---|---|
| TL | Total cell lysate |
| TOM | Translocase of outer membrane |
| TPR | Tetratricopeptide repeats |
| TRAP1 | TNF-receptor associated protein 1 |
| tRNA | Transfer ribonucleic acid |
| UV | Ultraviolet |
| VDAC | Voltage-dependent anion channel |
| XIAP | X-linked inhibitor of apoptosis |

**Amino Acids**

| | |
|---|---|
| A | Alanine |
| C | Cysteine |
| D | Aspartic acid |
| E | Glutamic acid |
| F | Phenylalanine |
| G | Glycine |
| H | Histidine |
| I | Isoleucine |
| K | Lysine |
| L | Leucine |
| M | Methionine |
| N | Asparagine |
| P | Proline |
| Q | Glutamine |
| R | Arginine |
| S | Serine |
| T | Threonine |

| | |
|---|---|
| V | Valine |
| W | Tryptophan |
| Y | Tyrosine |

**Nucleotide**s

| | |
|---|---|
| A | Adenine |
| C | Cytosine |
| G | Guanine |
| T | Thiamine |
| U | Uracil |

**Chemicals**

| | |
|---|---|
| AEBSF | 4-(2-Aminoethyl) benzenesulfonyl fluoride hydrochloride |
| BMH | Bismaleimidohexane |
| BSA | Bovine serum albumin |
| CCCP | Carbonyl cyanide 3-chlorophenylhydrazone |
| DAPI | 4',6-diamidino-2-phenylindole |
| DMEM | Dulbecco's modified Eagle's medium |
| DMSO | Dimethyl sulfoxide |
| dNTP | Deoxynucleotide triphosphate |
| DTT | Dithiothreitol |
| ECL | Enhanced chemiluminescence |
| EDTA | Ethylenediaminetetraacetic acid |
| EGTA | Ethylene glycol tetraacetic acid |
| FCS | Foetal calf serum |
| HCl | Hydrochloric acid |
| HEPES | Hydroxyethyl piperazineethanesulfonic acid |
| HRP | Horseradish peroxidase |

| | |
|---|---|
| LB | Luria Broth |
| NP-40 | Nonidet P40 substitute |
| ONPG | Ortho-nitrophenyl-β-D-galactopyranoside |
| PBS | Phosphate-buffered saline |
| PI | Propidium iodide |
| TBS | Tris-buffered saline |
| TMRE | Tetramethylrhodamine ethyl ester |
| Tween-20 | Polysorbate-20 |
| DFO | Desferrioxamine |
| CCCP | Carbonyl cyanide m-chloro phenyl hydrazone |

**Unit**

| | |
|---|---|
| bp | Basepair |
| g, mg, μg | Gram, milligram, microgram |
| hr, min, sec | Hour, minute, second |
| kDA | Kilodalton |
| kJ | KiloJoule |
| l, ml, μl | Litre, millilitre, microlitre |
| M, mM, μM, nM | Molar, millimolar, micromolar, nanomolar |
| nm | Nanometre |
| $^{o}$C | Degree celcius |
| V | Volts |
| v/v | Volume/volume |
| w/v | Weight/volume |

# Chapter 1:

# Introduction

## 1.1 DNA damage response

Cells are continually exposed to damaging agents such as ultraviolet (UV) light, and in order for tissues to remain healthy, cells must detect any damage to their DNA and prevent it from being passed on to their progeny. DNA damage is detected during checkpoints, when a signalling cascade may be initiated in response to DNA damage that triggers the DNA repair process, thus maintaining genomic integrity (**Figure 1.1**). The DNA damage response is mediated by two key players, ataxia telangiectasia mutated (ATM) and ataxia-telangiectasia mutated and Rad-3 related protein (ATR) protein kinases (Harper and Elledge, 2007). ATM primarily responds to double-strand breaks (DSBs) whilst ATR responds to single-strand breaks (SSBs) (Harper and Elledge, 2007).

DSBs are the most deleterious type of DNA damage as, when they are present, a cell does not have an intact complimentary strand as a template for the DNA repair process (Shiloh and Ziv, 2013). DSBs can occur following exposure to ionising radiation (IR), or to topoisomerase II inhibitors (proteins that prevent the separation of DNA strands during DNA replication). DSBs are also found at chromosome ends where they are associated with aging (Shiloh and Ziv, 2013). Following the generation of DSBs, the MRN (MRE11, Rad50, NSB1) complex is one of the first to be recruited to the DSB sites. Here, it acts as a DSB sensor for ATM and aids its recruitment to DSB sites (Harper and Elledge, 2007). Under normal conditions ATM exists as an inactive dimer but when it is recruited to the DSB sites, the dimer dissociates and autophosphorylates at multiple residues, which is important in maintaining its activation (Shiloh and Ziv, 2013).

The ATR-mediated checkpoint pathway also has a crucial role in regulating the cellular response to DNA replication stress. ATR is activated by SSBs and is thought to be present at stalled replication forks during nucleotide excision repair and at telomeres (Brown and Baltimore, 2000). SSBs can lead to loss of a single nucleotide during DNA replication and, where the SSBs are at telomeres, can also result in damaged 5' and/or 3' termini (Brown and Baltimore, 2000). Single-stranded DNA (ssDNA) at the site of the lesion is bound by replication protein A (RPA), which concurrently binds to ssDNA and ATR-interacting protein (ATRIP) and, in turn, recruits ATR (Fokas et al., 2013). The Rad9-Rad1-Hus1 (911) complex also binds to ssDNA where it recruits TopBP1, which binds to phosphorylated Rad9 and activates ATR (Fokas et al., 2013). ATR phosphorylates check point kinase1 (CHK1) which leads to suppression of DNA replication and cell cycle progression (Fokas et al., 2013).

A direct target of both ATM and ATR is the histone H2A variant H2AX (Ciccia and Elledge, 2010). Upon DNA damage, H2AX molecules are phosphorylated at residue S139, located at the carboxy (C)-terminus of H2AX. Once phosphorylated, H2AX is known as γH2AX. Many DNA repair and/or checkpoint proteins accumulate on γH2AX which serves to open up the chromatin structure and form a platform for the accumulation of DNA damage response and repair (Ciccia and Elledge, 2010). γH2AX was shown to directly recruit MDC1, which acts to amplify H2AX phosphorylation. The assembly of several damage response mediator proteins forms the IR-induced foci (IRIF). 53BP1, checkpoint kinase 2 (CHK2) and p53 are examples of proteins that are activated and recruited to IRIFs to mediate the DNA damage response (Ciccia and Elledge, 2010).

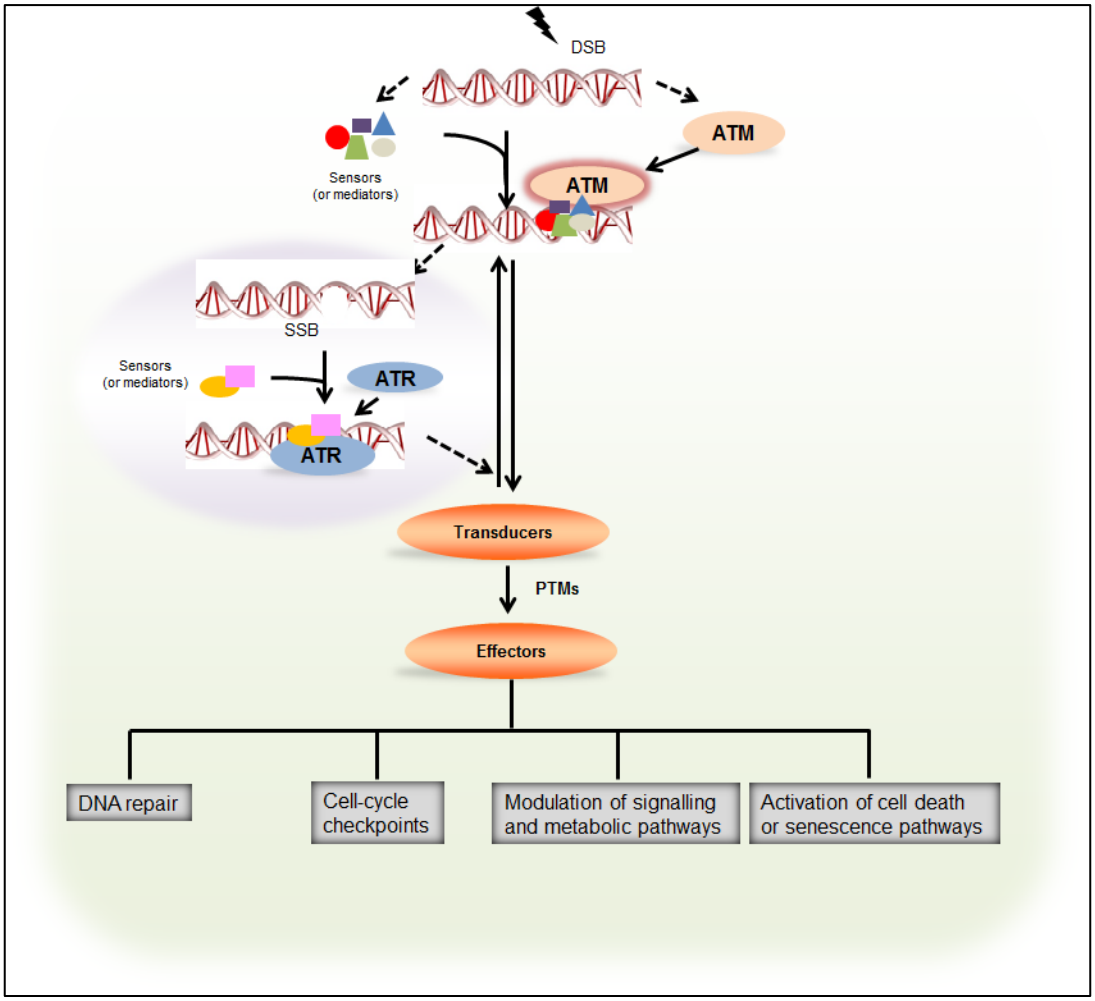



**Figure 1.1 The DNA damage response cascade.**

DNA damage response is initiated by the large protein complexes which include sensors or mediators at the double-strand breaks (DSB). Activity within these foci accompanied by post-translational modifications (PTMs) leads to the activation of ATM kinase which in turn activates both DNA repair and cell death response pathways. Single-strand break (SSB) produced from the processing of an initial DSB acts as an assembly point for the generation of a large complex that will activate the ATR kinase. This is accompanied by the activation of transducers mainly by PTMs that lead to the modulation of pathways that trigger both cell survival and cell death. Adapted from (Shiloh and Ziv, 2013).

The DNA damage response regulates the decision as to whether a cell should undergo apoptosis, senescence, cell cycle arrest, or DNA repair (Ciccia and Elledge, 2010). Defective regulation of the signalling pathways that drive a cell into any of these activities can result in incorrect DNA replication and genomic instability after DNA damage.

### 1.2 Cancer

Cancer results in 7.6 million deaths (approximately 13% of all deaths) in 2008 (Ferlay et al., 2010). The inability of cells to respond to stress and to repair damage underlies many forms of cancer. Cells are constantly challenged by stress originating from either extrinsic sources, such as chemical carcinogens that can induce modifications to DNA, or from the cellular environment, such as the production of free radicals which stimulate oxidative stress.

Despite possessing repair mechanisms that respond to different types of insults, cells may undergo incomplete DNA repair leading to the insertion of an incorrect base during DNA replication. This ultimately leads to the synthesis of an altered protein. Mutation of an oncogene, or the gene coding for a tumour suppressor or another protein that governs cell proliferation may lead to the development of cells that are resistant to death. Somatic mutations evolve when a cell containing unrepaired DNA damage divides, passing mutations onto its progeny. If left undetected, for example, when the mutation leads to the inactivation of a checkpoint protein, the genome can become unstable, leading to an enhanced mutation rate and the generation of multiple mutations over time (Poirier, 2004). The accumulation of

somatic mutations can be increased by extrinsic and intrinsic stress and the number of mutations vary with different types of cancer (Stratton, 2011; Vogelstein et al., 2013).

Past research has identified many oncogenes and tumour suppressors that are frequently altered in human tumours. These altered genes affect key signalling pathways that govern the cell cycle and thus have the potential to be therapeutic targets. Multiple classes of chemotherapy drugs are used, mainly in combination, to target cancer cells more effectively. In recent years, it has become apparent that differences in the genetic background of cancer patients results in varying responses to chemotherapy. This has led to an increased research focus on pharmacogenomics. Cancer pharmacogenomics relates to the study of germline genetic variants that contribute to a chemotherapy-induced phenotype (Wheeler et al., 2013).

A fundamental characteristic of cancer cells is their ability to sustain indefinite cycles of proliferation. Growth-promoting signals govern entry and progression of cells through the cell cycle thereby ensuring the homeostasis of cell number and maintenance of normal tissue architecture and function. In 2000, Hanahan and Weinberg outlined the acquired capabilities of cancer cells as "hallmarks of cancer" which include the ability to sustain growth signals, avoid growth suppressors, invade and metastasise to other tissues, induce angiogenesis, resist cell death and proliferate indefinitely (Hanahan and Weinberg, 2000). In 2011, these hallmarks were updated to include the ability of cancer cells to maintain the tumour microenvironment (Hanahan and Weinberg, 2011). Among the ways cancer cells

achieve this is by metabolic reprogramming which involves altering energy metabolism in order to fuel their growth and division (Hanahan and Weinberg, 2011). Mitochondria have long been recognised as the powerhouses of the cell and have recently received recognition as a potential target for therapeutic intervention of cancer.

### 1.3 Mitochondrial Biology

Most cells contain hundreds of mitochondria. Mitochondria are thought to have arisen 1.5 billion years ago from an endosymbiotic relationship between a bacterium and an ancestor of today's eukaryotic cells, in which the bacterium existed within the eukaryotic cell. Mitochondria have retained many vestiges of their bacterial ancestry, including a double membrane and a circular genome (Vafai and Mootha, 2012; Wallace, 1999). They resemble microbes in that they are typically about 1 mm in diameter and constantly divide and fuse to form a dynamic network (Vafai and Mootha, 2012). To increase its replication rate, the mammalian mitochondrial genome has reduced in size by transferring many essential genes to the nucleus (**Figure 1.2**). Once the mitochondrial proteins encoded by these genes are translated, they are imported back into the mitochondria (Wallace, 1999).

The mitochondrial genome is a dense circular molecule which accounts for only 0.0005% of the human genome, and constitutes no more than 1% of cellular DNA mass. Mitochondrial genes lack introns, and intergenic regions are absent or reduced to a few nucleotides (Kazak et al., 2012). The mammalian mitochondrial genome has retained only 13 genes coding for polypeptides, all of which are

required for oxidative phosphorylation (OXPHOS). The mitochondrial genome also encodes 12S and 16S ribosomal ribonucleic acid (rRNA) and 22 transfer ribonucleic acid (tRNA) genes that are required for mitochondrial protein synthesis (**Figure 1.2**). Studies in yeast demonstrated that the mitochondrial genome is arranged in nucleoprotein complexes within the nucleoid of a mitochondrion (Chen and Butow, 2005). The average number of copies of the mitochondrial genome per nucleoid is around six in cultured human cells (Holt et al., 2007). Mitochondrial DNA (mtDNA) mutations have been found in various cancers and seem to alter mitochondrial metabolism, enhance tumourigenesis and/or permit cancer cell adaptation to the changing environment of a tumour (Wallace, 2012).

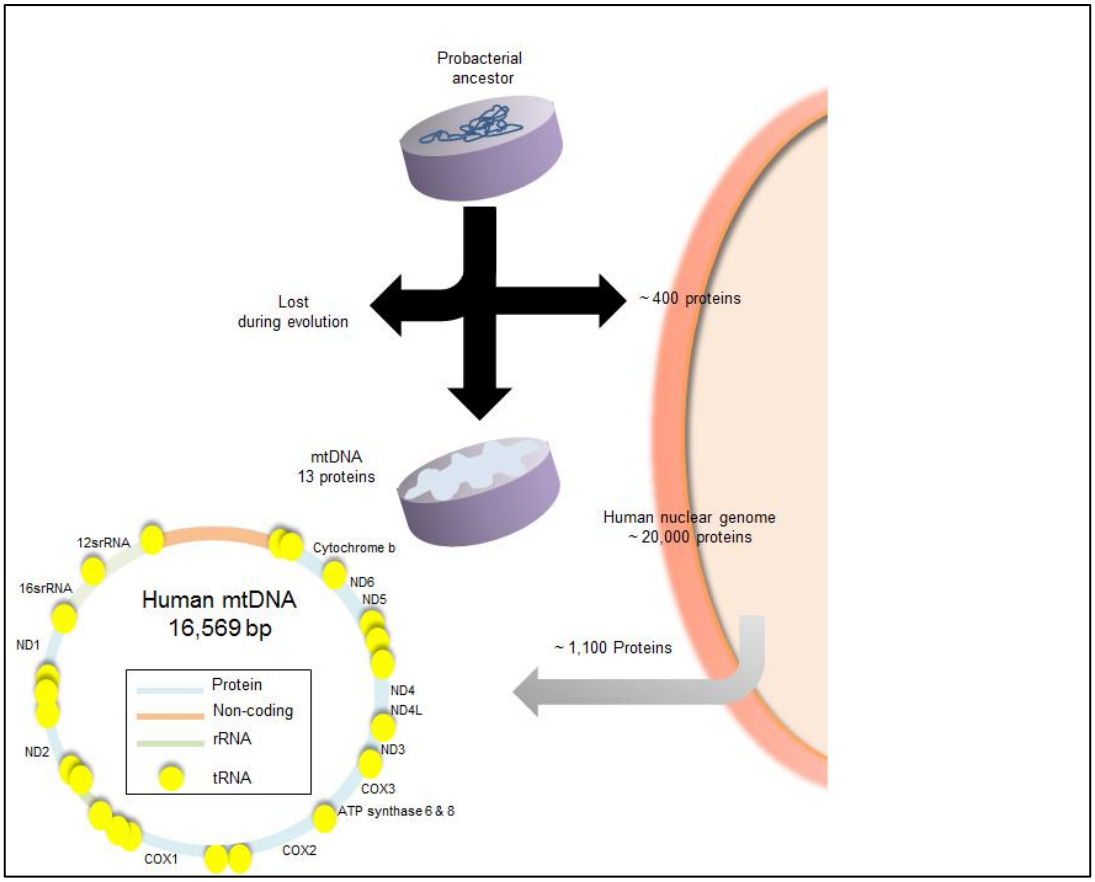



**Figure 1.2 Mitochondrial evolution and mtDNA overview.**

The mitochondrial genome codes for 13 proteins and at least 1,100 additional nuclear encoded mitochondrial proteins. Of these proteins, about 400 have proteobacterial origin. The mitochondrial genome contains 37 genes, 13 of which code for proteins required for OXPHOS, and the rest code for the RNA elements needed for their translation, including 22 tRNAs. In addition, there are two non-coding regions. ND- Nicotinamide adenosine dinucleotide dehydrogenase. Adapted from (Kazak et al., 2012; Vafai and Mootha, 2012).

### 1.4 Metabolic reprogramming

Contrary to normal undifferentiated cells which mainly rely on OXPHOS to produce energy for cellular processes, most cancer cells instead rely on glycolysis as their primary energy source. The phenomenon where cancer cells preferentially use glycolysis to metabolise glucose in the presence of oxygen was identified by Otto Warburg and was later known as aerobic glycolysis or the 'Warburg effect'(Schulze and Harris, 2012). At that time, Warburg hypothesised that the switch to energy production by glycolysis in cancer cells was due to irreversible mitochondrial damage leading to permanent impairment of aerobic respiration (Warburg, 1956). However, this hypothesis was disputed as most cancer cells retain functional mitochondria (Schulze and Harris, 2012). Nonetheless, the 'Warburg effect' is one of the best studied metabolic phenotypes of cancer cells.

Both normal and cancer cells utilise glucose and glutamine as sources of energy and also use them for biosynthesis of macromolecules. The high rate of glucose metabolism in cancer cells is facilitated by an increase in glucose transport by one or more isoenzymes of the glucose transporters (GLUT 1-4) (Thorens and Mueckler, 2010). Glucose molecules are phosphorylated by hexokinases to form glucose-6-phosphate (**Figure 1.3**). Glucose-6-phosphate can either be used to generate pyruvate through glycolysis or will be fed into the pentose phosphate pathway (PPP) to generate ribose-5-phosphate and nicotinamide adenosine dinucleotide phosphate-oxidase (NADPH) (**Figure 1.3**). Glutamine, on the other hand, is converted to glutamate in the cytosol by the enzyme glutaminase-1. Glutamate is then transported to the mitochondria where it is converted to α-ketoglutarate which enters the tricarboxylic acid (TCA) cycle resulting in the

generation of malate and citrate (**Figure 1.3**). Malate is converted to pyruvate and NADPH, whilst citrate is used for lipid synthesis.

The high proliferation rate in cancer cells requires increased energy, and the cells must achieve a balance between adenosine triphosphate (ATP) synthesis and biomass production. The enhanced glycolytic rate in cancer cells is required not only to meet the need for energy, but also to maintain the levels of glycolytic intermediates needed for the biosynthesis of macromolecules. The biosynthetic activities required for proliferating cancer cells involve high rates of nucleotide synthesis, amino acid synthesis and lipogenesis. Glycolysis provides essential molecules for both nucleotide and amino acid synthesis. The pentose phosphate pathway (PPP) results in the oxidative generation of NADPH and reductive nucleotide biosynthesis (**Figure 1.3**). The oxidation of glucose-6-phosphate generates NADPH and non-oxidative interconversion of phosphorylated sugars are required for nucleotide biosynthesis (**Figure 1.3**).

The tumour suppressor p53, whose gene is one of the most commonly mutated in human cancers, is a transcription factor that regulates the expression of genes involved in diverse biological functions including cellular energy metabolism. p53 dampens the glycolysis pathway by inhibiting the expression of GLUT1, GLUT4 and Tp53-induced glycolysis and apoptosis regulator (TIGAR) which leads to a reduced glycolysis rate (Bensaad et al., 2006; Schwartzenberg-Bar-Yoseph et al., 2004). Interestingly, TIGAR was also shown to reduce reactive oxygen species (ROS) and protect against ROS sensitive apoptosis via its biphosphatase activity

(Bensaad et al., 2006) and its association with hexokinase-2 during hypoxia (Cheung et al., 2012). Inhibition of glycolysis severely impairs the ATP generation and renders cancer cells highly dependent on this metabolic pathway for survival.

Regulation of cancer cell metabolism is also commonly influenced by activation of the phosphatidylinositol-3-kinase (PI3K)-Akt signalling pathway and stabilisation of HIF. PI3K-Akt is highly mutated in human tumours (Jones and Thompson, 2009) and its deregulation promotes cancer cell metabolism via multiple pathways. Binding of growth factors such as receptor tyrosine kinases or G protein-coupled receptors to PI3K stimulates its phosphorylation. Phosphorylated PI3K interacts with Akt which causes conformational changes in Akt and promotes its phosphorylation (Osaki et al., 2004). Phosphorylated Akt triggers glycolysis in a dose-dependent fashion by prompting cells to increase their glucose utilisation without increasing oxygen consumption (Elstrom et al., 2004). Constitutively active Akt mediates the translocation of GLUT4 to the plasma membrane and enhances glucose uptake (Kohn et al., 1996).

HIF stabilisation occurs under conditions of low oxygen. HIF is a heterodimeric transcription factor consisting of HIFα and HIFβ subunits (Cairns et al., 2011). HIFβ is a nuclear protein that binds to hypoxic response element (HRE) and activates the transcription of target genes. HIFα has two isoforms, HIF1α and HIF2α both of which are activated under low oxygen conditions (Cairns et al., 2011). Under normoxic conditions, HIFα levels are suppressed through oxygen-dependent hydroxylation by prolyl hydroxylase (Jones and Thompson, 2009). The E3 ubiquitin

ligase, Von-Hippel-Lindau (VHL), recognises the hydroxylated HIF and targets it for ubiquitin-mediated proteosomal degradation (Cairns et al., 2011; Jones and Thompson, 2009). HIF1α activates the transcription of genes involved in aerobic glycolysis, including glucose transporters, glycolytic enzymes and lactate dehydrogenase A (LDHA). HIF2α is associated with the chronic hypoxic response (Holmquist-Mengelbier et al., 2006).

The generation of pyruvate is an important metabolic control point in cellular metabolism as it can either be converted to lactate and $NAD^+$ by LDHA, which is important for continuation of glycolysis, or it can be converted to acetyl co-enzyme-A by pyruvate dehydrogenase (PDH) for entry to TCA cycle and mitochondrial respiration. HIF1α activates pyruvate dehydrogenase kinase 1 which phosphorylates and inhibits PDH, thus actively shunting pyruvate away from the mitochondrial respiration pathway and the TCA cycle (Kim et al., 2006; Papandreou et al., 2006). Reprogramming of core metabolism in tumours confers a selective growth advantage such as the ability to evade apoptosis and/or enhance cell proliferation, promotes tumour growth and progression.

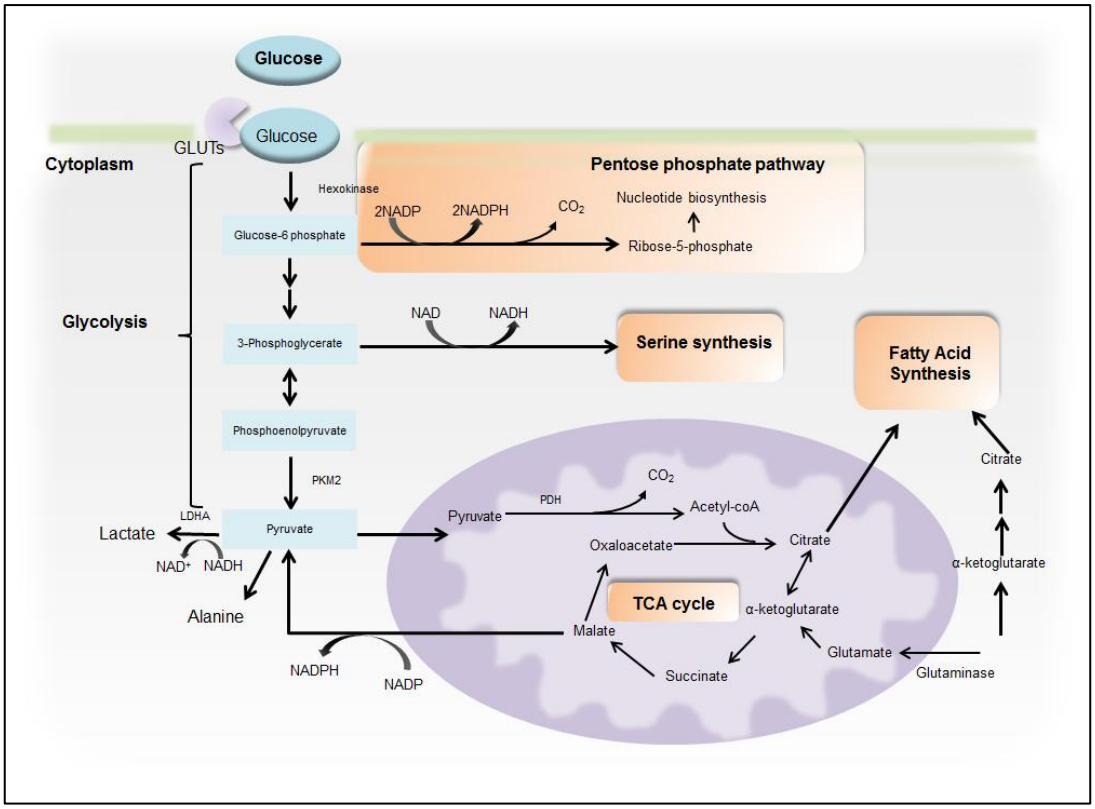



**Figure 1.3 Regulation of metabolism in cancer cells.**

Metabolism in cancer cells includes glycolysis, lactate production, the pentose phosphate pathway (PPP), glutaminolysis, the TCA cycle, and fatty acid and nucleotide biosynthesis. Glucose can be processed by glycolysis which leads to the generation of lactate and pyruvate. The latter is a substrate for the TCA cycle. Glutamine is deaminated to form glutamate which is also fed into the TCA cycle for energy production. Adapted from (Levine and Puzio-Kuter, 2010).

## 1.5 Apoptosis

Evasion of cell death has been recognised as one of the main alterations that dictates malignant growth (Hanahan and Weinberg, 2000). Apoptosis was intensively investigated for the past 40 years and was identified as a major defence strategy that prevents cells from acquiring tumourigenic potential (Olsson and Zhivotovsky, 2011). Apoptosis can be triggered by either intrinsic (mitochondrial) or extrinsic pathway.

The intrinsic apoptotic pathway is tightly regulated by the BCL-2 (B-cell lymphoma 2) family of proteins, and is mainly activated by internal stimuli emanating from cellular damage sensors (such as p53) or physicochemical alterations produced by stressed cells (*e.g.*, ROS or DNA damage). Mitochondria play a fundamental role in the intrinsic apoptotic pathway by releasing key effector proteins such as cytochrome c and SMAC (second mitochondria derived activator of caspase). These effector proteins are released by mitochondria in response to compromised integrity of the outer mitochondrial membrane (OMM) in a process known as mitochondrial outer membrane permeabilisation (MOMP) (**Figure 1.4**). This release initiates caspase activation in the cytosol, leading to caspase-mediated proteolysis of target proteins (Taylor et al., 2008).

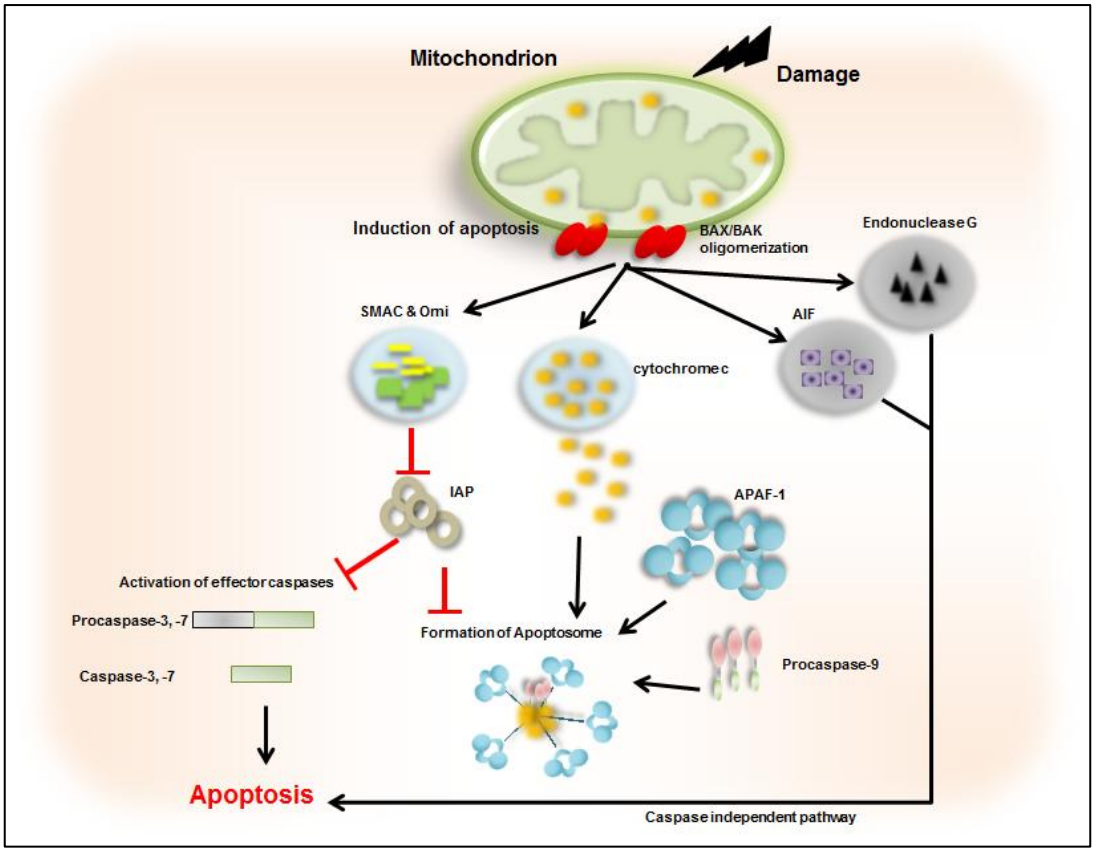



**Figure 1.4 The intrinsic apoptotic pathway.**

Stimuli initiating the intrinsic apoptotic pathway activate BCL-2 proapoptotic proteins such as BAX and BAK which promote MOMP. Following MOMP, soluble (SMAC/Omi/cytochrome c) and insoluble (AIF/endonuclease G) proteins are released from the intermembrane space into the cytosol. Cytochrome c binds to APAF-1, inducing oligomerisation and the formation of the apoptosome which, in turn, recruits procaspase-9. Activated caspase-9 cleaves and activates executioner caspases, leading to apoptosis. SMAC and Omi neutralise the inhibitory effect of IAP. The insoluble proteins, AIF and endonuclease G activate the caspase independent pathway following their translocation to the nucleus, where they promote DNA fragmentation.

BCL-2 family proteins

In mammals, there are at least 12 BCL-2 family proteins some of which inhibit apoptosis and some induce apoptosis. All BCL-2 family members have conserved homology within their core BCL-2 homology (BH)-domain and have similar secondary structure. The BCL-2 family of apoptotic regulators can be divided into three classes (**Figure 1.5**). The antiapoptotic proteins (BCL-2, BCL-XL, MCL-1) have up to four BH domains and promote cell survival by inhibiting proapoptotic proteins. The second class is the multidomain members (BAX, BAK, Bok) which, like their antiapoptotic counterparts, also contain multiple BH domains but instead promote apoptosis. Thirdly, the BH3-only proteins (NOXA, p53 upregulated modulator of apoptosis [PUMA], BID) have a conserved BH3 domain that is required for their proapoptotic role (Youle and Strasser, 2008).

In healthy cells, basal levels of antiapoptotic proteins prevent the activation of proapoptotic proteins. This is interaction is mediated via the BH3 groove or also known as the hydrophobic groove (**Figure 1.5**). The BH3 groove interaction is involved when the antiapoptotic proteins block the upstream of the intrinsic apoptosis by sequestering the BH3-only proteins or when they block downstream apoptosis by sequestering activated BAX and BAK (Westphal et al., 2011).

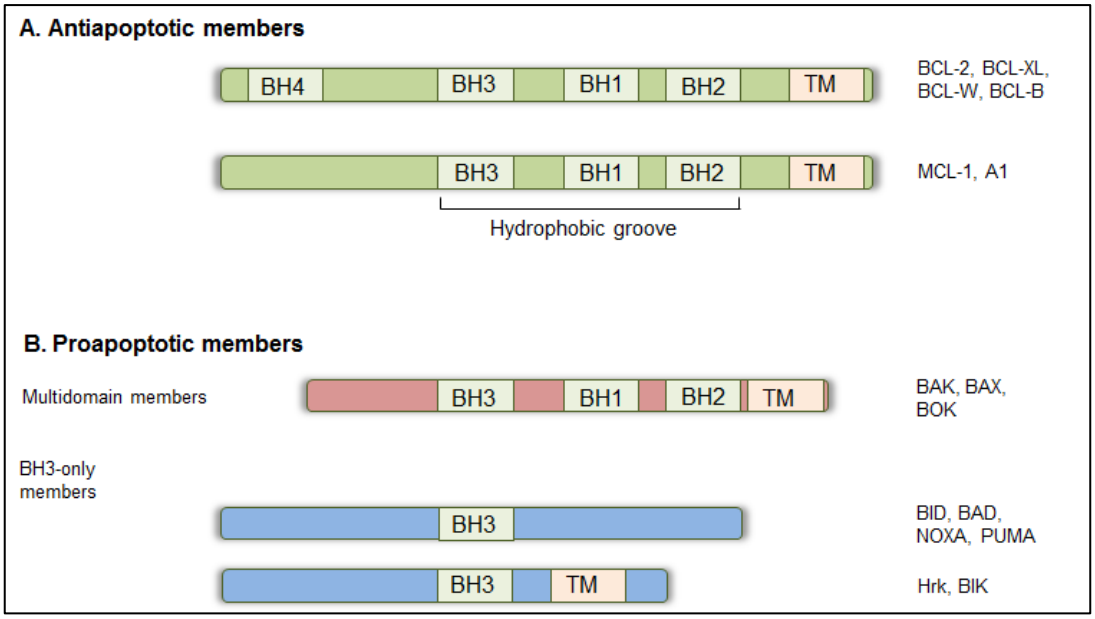



**Figure 1.5 Classification of the BCL-2 family proteins.**

The antiapoptotic family members have multiple BH domains. The BH1, BH2 and BH3 domains fold to form a hydrophobic groove (BH3 groove) that interacts with the BH3-only proteins to inhibit apoptosis. The proapoptotic members of the BCL-2 family can be subdivided into at least two groups; the multidomain proteins, a direct activator of apoptosis and the BH3-only proteins which induces apoptosis either by directly activating the proapoptotic proteins or indirectly by relieving the inhibitory effect of the antiapoptotic proteins. BH- BCL-2 homology domain; TM- transmembrane domain. Adapted from (Youle and Strasser, 2008).

Upon apoptotic signals, the BH3-only proteins are activated and competitively bind to the BH3 groove of the antiapoptotic proteins through the BH3 domains (Westphal et al., 2011). This displaces and activates BAX and BAK. Interestingly, the BH3-only proteins can also directly bind and activate the proapoptotic proteins, BAX and BAK (Westphal et al., 2011). The activation of BAX and/or BAK commits cells to apoptosis.

Activation of BAX and/or BAK is essential in triggering intrinsic apoptosis, as this event irreversibly commits the majority of cells to die (**Figure 1.4**). An early step of BAX activation is its translocation from the cytosol to the OMM (Wolter et al., 1997). This translocation is not required for BAK as it is already inserted at the OMM in healthy cells (Wolter et al., 1997). The activation of BAX/BAK can be explained by two models; the direct and the indirect activation model. In the direct model, BH3-only direct activators (*e.g.,* BID) are sequestered by the BCL-2 antiapoptotic proteins (*e.g.,* BCL-XL). Upon stress stimuli, the de-repressor BH3-only protein *(e.g.,* BAD) is induced. The de-repressor will displace the direct activator and liberate it to activate BAX.

In the indirect model, similar to the direct model, BAX and BAK are kept inactive by the antiapoptotic BCL-2 proteins under normal conditions. However, in contrast to the direct pathway, apoptosis signalling by the indirect pathway is activated when the BH3-only proteins bind and neutralise the antiapoptotic proteins, rather than activating BAK/BAX itself, allowing BAX/BAK to oligomerise and permeabilise the OMM. Example of activation of proapoptotic protein using the indirect model is

when BAX is activated by cleaved BH3-only protein BID, (Walensky and Gavathiotis, 2011). BID is an example of a BH3-only protein that is activated by caspase cleavage. Caspase-8 cleaves BID by removing its amino (N)-terminus and exposing its BH3 domain. Truncated BID translocates to the mitochondria where it suppresses the inhibitory effect of BCL-XL and promotes apoptosis (Li et al., 1998). Examples of other BH3-only proteins using the indirect model are PUMA and NOXA. These proteins are also direct transcriptional target of p53. PUMA and NOXA localise to the mitochondria via their BH3 domain and interact with the antiapoptotic BCL-2 family members such as MCL-1 and suppress the inhibitory effect of the proapoptotic proteins, thus promoting apoptosis (Nakano and Vousden, 2001; Oda et al., 2000). In this model, no direct interaction between the BH3-only proteins and BAX/BAK is required. Once the OMM is permeabilised, soluble proteins such as cytochrome c and SMAC, diffuse from the intermitochondrial membrane space (IMS) into the cytosol where they promote caspase activation (Giam et al., 2008) (**Figure 1.4**).

The formation of pore by OMM permeabilisation involves major conformation changes in BAX and BAK, followed by homooligomerisation (Westphal et al., 2011). Upon activation of BAK, the N-terminal region opens up to expose its BH3 domain. In the absence of proteins that suppress BAK (such as BCL-XL and MCL-1), the exposed BH3 domain binds to the hydrophobic region of another BAK molecule to form a homodimer. These homodimers subsequently bind to one another, resulting in the formation of BAK multimers which disrupt the OMM (Dewson et al., 2008). BAX has a C-terminal hydrophobic α-helix that acts as a transmembrane anchor when and inserts into the OMM under conditions of cellular

stress. The BH3 domains of BAX asymmetrically interact with the BH1 domain of antiapoptotic BCL-2 proteins such as BCL-XL. This has an inhibitory effect on BAX which is reversed by competitive binding of BH3-only proteins. This insertion of BAX to the OMM unmasks the BH domains that are pertinent for BAX oligomerisation (Renault and Manon, 2011).

One of the key differences between BAK and BAX is their localisation; BAX resides predominantly at the cytosol whilst BAK is localised to the OMM (Wolter et al., 1997). The importance of multidomain proapoptotic members BAX and BAK in the regulation of apoptosis is demonstrated by the fact that BAX/BAK double knockout (DKO) mice are embryonic lethal, with only a small percentage of these mice surviving for nine hours after birth. The hepatocytes of these mice show only moderate levels of apoptosis. BAX/BAK DKO mouse embryonic fibroblasts (MEFs) are resistant to apoptosis induced by high doses of staurosporine, etoposide and UV light (Wei et al., 2001).

Tumour suppressor p53 was shown to interact with BAK and BAX to induce mitochondria-dependent apoptosis. p53 directly binds and activates BAK (Leu et al., 2004). The p53-BAK complex disrupts MCL-1-BAK interaction and this induces mitochondrial-dependent apoptosis (Leu et al., 2004). Interestingly, Myc-induced adenosine monophosphate-activated protein kinase (AMPK) triggers mitochondrial accumulation of p53 which was shown to enhance the conformational activation of BAK without disrupting the BH3-groove which is essential for the BAK-BCL-XL interaction (Nieminen et al., 2013). p53 promotes apoptosis by

transcriptional activating the human *BAX* gene. Interestingly the p53 transcription-independent function involves mitochondrial p53 directly activating BAX and neutralising the antiapoptotic members of the BCL-2 family, BCL-XL and BCL-2 (Chipuk et al., 2004). This interaction disrupts the MOMP inhibitory complex formed by BCL-XL and BCL-2 which leads to increased release of cytochrome c and activation of caspases and chromatin degradation (Mihara et al., 2003; Vaseva and Moll, 2009).

MOMP leads to release of proteins, such as cytochrome c, into the cytosol which triggers apoptosis (Kilbride and Prehn, 2012). MOMP also releases caspase-independent effectors, such as apoptosis inducing factor (AIF) and endonuclease G (**Figure 1.4**). During apoptosis, these proteins translocate to the nuclear compartment where they promote DNA fragmentation and chromatin condensation (Kilbride and Prehn, 2012). The individual components of the intrinsic apoptotic pathway are described below.

**Table 1.1 The components of the intrinsic apoptotic pathway**

| Apoptotic Component | Molecular Weight | Description |
|---|---|---|
| **Cytochrome C**<br>(Liu et al., 1996) | 16 kDa | • Resides at the inner mitochondrial membrane.<br>• Main apoptosis mediator released in response to damage. |
| **Inhibitor of apoptosis proteins**<br>**(IAPs)**<br>(Takahashi et al., 1998) | | • A family of proteins that inhibit the activation of caspase-3, -7 and -9.<br>• The most potent inhibitor is X-linked IAP. |
| **SMAC**<br>(Du et al., 2000; Shiozaki and Shi, 2004; Verhagen et al., 2000) | 27 kDa | • Possess typical mitochondrial targeting signal that is cleaved after mitochondria entry and resides at the IMS.<br>• Released to the cytosol and activates apoptosis by reversing the IAP mediated inhibition of caspases. |
| **Omi/HtrA2**<br>(Hegde et al., 2002; Suzuki et al., 2001) | 50 kDa | • Translocated to the mitochondria due to its mitochondrial targeting signal.<br>• The mature form binds to IAP and relieves its inhibitory effects. |
| **AIF**<br>(Modjtahedi et al., 2006) | 62 kDa | • Resides at the IMS.<br>• Complete absence of AIF is embryonically lethal.<br>• Contains two nuclear localisation signals.<br>• Released into the cytosol and translocates to nucleus and contributes to DNA fragmentation and nuclear condensation during damage. |
| **Endonuclease G** | 35 kDa | • Directly induces DNA fragmentation in caspase-independent manner. |

Caspases

Caspases are cysteine proteases that proteolytically cleave substrates after aspartic acid residues. Caspases serve as signalling mediators that orchestrate apoptotic execution pathways by cleaving subsets of cellular proteins and are thus intimately involved in apoptosis (MacKenzie and Clark, 2012). The cleavage of key proteins in the cell by caspases leads to the morphological and biochemical changes observed in apoptosis (Shiozaki and Shi, 2004). These proteins are synthesised as inactive zymogens that are rapidly converted to active proteases upon induction of apoptosis. Zymogens have a common organisation at the N-terminal region consisting of a large and a small subunit covalently linked by a sequence of amino acids referred to as the intersubunit linker (Shiozaki and Shi, 2004).

Caspases involved in apoptosis are generally divided into two groups, the initiators and the effectors. The initiator procaspases -8,-9 and -10 are found as monomers under physiological conditions and form dimers upon activation (MacKenzie and Clark, 2012). The cleavage of the intersubunit linker influences the stability of the dimer and is not necessary for its enzymatic activity. In contrast, the effector procaspases-3, -6 and -7 are generally stable dimers but are inactive in the absence of stress (MacKenzie and Clark, 2012). Activation of the dimers occurs after proteolytic cleavage of the intersubunit linker in response to apoptotic stimuli. Cleavage of the signalling components that induce the morphologic changes associated with apoptosis is predominantly carried out by caspase-3 (MacKenzie and Clark, 2012). Caspases were shown to cleave poly-(ADP ribose)-polymerase-1 (PARP-1) which separates its DNA binding domain from its catalytic domain.

PARP-1 is 116 kDa protein consisting of an N-terminal DNA binding domain, an automodification domain and a C-terminal catalytic domain (Jagtap and Szabo, 2005). The cleavage inactivates PARP-1 and serves as a marker of apoptosis (Jagtap and Szabo, 2005)

### 1.6 The OXPHOS system in mitochondria

Mitochondria are best known for their role in ATP production, which they do via OXPHOS. Carbon fuels are oxidised in the citric cycle to yield high energy electrons (Nunnari and Suomalainen, 2012). This electron motive force is converted into a proton motive force and this, in turn, is converted into a phosphoryl transfer potential. The flow of electrons from nicotinamide adenosine dinucleotide (NADH) or flavin adenine dinucleotide (FADH) to oxygen through protein complexes located in the mitochondrial inner membrane leads to the pumping of protons out of the matrix (**Figure 1.6**). The resulting uneven distribution of protons generates a pH gradient and a transmembrane electrical potential that creates the proton motive force. ATP is synthesised when protons flow back to the mitochondrial matrix through ATP synthase (Complex V) (Nunnari and Suomalainen, 2012). The membrane potential is essential for other mitochondrial functions, such as mitochondrial protein import, and is used to trigger molecular changes that alter mitochondrial behaviour in response to mitochondrial dysfunction (Nunnari and Suomalainen, 2012).

The mitochondrial electron transport chain is composed of five multimeric complexes (**Figure 1.6**). Complex 1 is the first and the largest enzyme of the OXPHOS cascade, and it catalyses the oxidation of NADH by ubiquinone (Papa et al., 2012). The electrons from NADH in Complex I are transferred to coenzyme Q which carries electrons from Complex I through the membrane to Complex III (**Figure 1.6**). Complex II consists of four enzymatic subunits that participate in both the electron transport chain (membrane associated) and the Krebs cycle (mitochondrial matrix associated) (Eng et al., 2003). Whilst associated with complex II, electrons are transferred to $FADH_2$ rather than to NADH, before they are transferred to coenzyme Q (**Figure 1.6**). Reduced coenzyme Q mediates electron transfer from Complex I and II to Complex III (**Figure 1.6**). Whilst associated with Complex III, electrons are transferred to cytochrome c which is the substrate for Complex IV. The reduced cytochrome c is reoxidised within Complex IV and this process is coupled to the reduction of one molecule of oxygen to form two molecules of water (Koopman et al., 2013). Complex V is the ATP synthase complex of the mitochondrial inner membrane and matrix, and utilises the transmembrane electrochemical proton gradient generated by the electron transport chain to drive the synthesis of ATP from ADP (Koopman et al., 2013) (**Figure 1.6**).

Induction of cell death is influenced by changes in the amount of ATP generated by the mitochondria, and this death may occur in various fashions depending on the level of ATP in the cell. In several cell types, it has been shown that intracellular ATP is required to initiate apoptosis (Eguchi et al., 1997; Leist et al., 1997). The intrinsic apoptotic pathway is initiated following activation of caspase-9, which requires APAF-1.

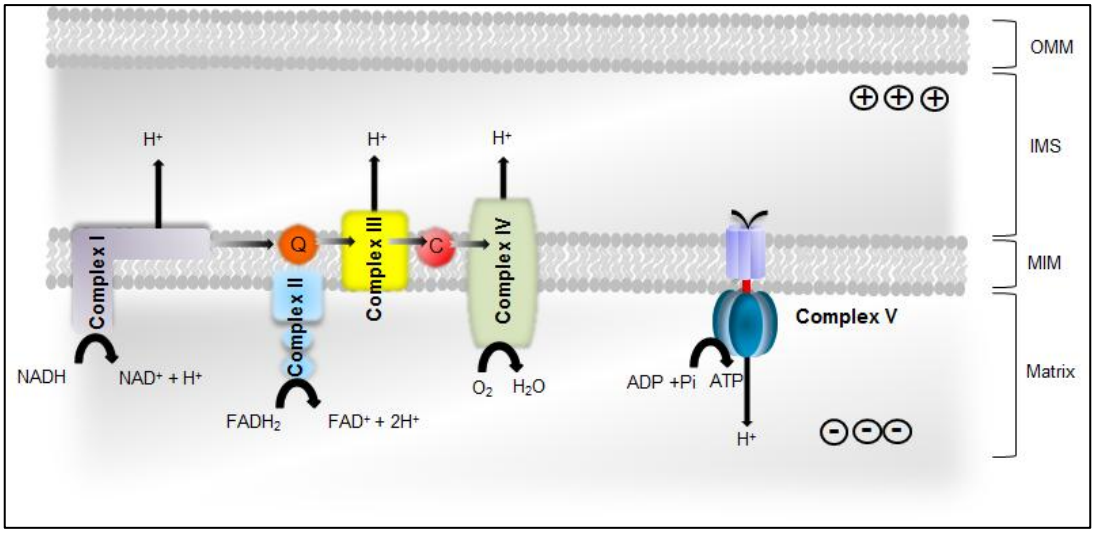



**Figure 1.6 Mitochondrial OXPHOS complexes.**

The mitochondrial electron transport chain consists of five multisubunit complexes that reside at the inner mitochondrial membrane (MIM). Complex I accepts electrons from the TCA cycle by-product, NADH. Complex II accepts electron from $FADH_2$. These electrons are passed to Complex III via coenzyme Q (Q). Electrons are subsequently transported to Complex IV via cytochrome c (C).The energy produced is used to transport protons ($H^+$) from the matrix to the IMS. At Complex V, a backflow of protons (from the IMS through to the mitochondrial matrix) is used to produce ATP from ADP. Adapted from (Koopman et al., 2013).

In the absence of apoptotic stimuli, APAF-1 exists in a monomeric form. In response to apoptotic stimuli, cytochrome c activates APAF-1 by binding to its C-terminus. Concurrently, ATP bound to the ATPase domain of APAF-1 is hydrolysed, and this promotes APAF-1 oligomerisation. The apoptosome consists of seven APAF-1 molecules which serve as a recruitment platform for proteins that trigger caspase-9 activation (Riedl and Salvesen, 2007). Interestingly, Izyumove *et al.* reported an induction of apoptosis in Hela cells in response to a 3-fold decrease in the level of intracellular ATP (Izyumov et al., 2004). This implies a complicated relationship between ATP levels and apoptosis whereby ATP is required for the apoptosis progression whilst the reduction in ATP was shown to trigger apoptosis.

Conversely, severe depletion of mitochondrial ATP (more than 70%) which is observed during anoxia or severe ischemia is linked to necrosis (Lemasters et al., 1999). Necrosis is the irreversible tissue destruction due to bioenergetic failure (Vaseva et al., 2012). Reduced ATP as little as 15 to 20% of normal levels due to mitochondrial injury can partially be replaced by glycolysis (Lemasters et al., 1999). During oxidative stress accompanied by ATP depletion, mitochondria undergo a permeability transition associated with the formation of permeability transition pore (PTP) (Javadov and Karmazyn, 2007). Opening of mitochondrial PTP which usually remain closed in the absence of cellular stress, results in uncoupling of OXPHOS and mitochondrial $F_1$-$F_O$ ATPase (ATP synthase complex operating in the reverse mode where ATP is being utilized) becomes activated (Javadov and Karmazyn, 2007). This ATPase consumes ATP generated by glycolysis, so that glycolysis will no longer be adequate to protect cell death (Lemasters et al., 1999). Severe depletion of ATP can also be caused by excess PARP-1 activation due to

ROS-induced DNA damage which consumes large amount of $NAD^+$ resulting in a massive ATP depletion (Leist et al., 1997). Severe ATP depletion accompanied by PTP opening results in mitochondrial swelling, OMM rupture and ultimately plasma membrane rupture (Javadov and Karmazyn, 2007). Perhaps modulating *in vivo* ATP availability might be an important strategy in inducing cell death and preventing tumour growth and progression.

**1.7 p53**

p53 mutations are the most common genetic alteration found in human cancer and perturbations of the p53 pathway are associated with oncogenesis and cancer progression (Vousden and Prives, 2009). p53 was initially identified as an oncogene that interacted with the T-antigen of the SV40 tumour virus (Lane and Crawford, 1979). The overexpression of mutant p53 in tumours and the ability of wild type p53 to supress transformation of cells led to the classification of wild type p53 as a tumour suppressor (Hainaut and Wiman, 2009).

p53 has a short half-life of 5-20 min at steady state, with the exact half-life dependent upon the specific cell type (Giaccia and Kastan, 1998). In response to cellular stress, the half-life of p53 is increased significantly to a few hours (Maltzman and Czyzyk, 1984). p53 levels are regulated through ubiquitination mainly by mouse double minute 2 (MDM2) and alternate reading frame of the cyclin-dependent kinase inhibitor 2A locus (ARF)-binding protein-1 (BP1) (ARF-BP1) (Leng et al., 2003). The ubiquitination process is highly dynamic and reversible. Polyubiquitination and monoubiquitination of p53 determine its

functionality. Polyubiquitination of p53 is associated with its destabilisation and proteasomal degradation whilst monoubiquitinated p53 is targeted for nuclear export. p53 ubiquitination is mainly mediated by the Really interesting new gene (RING) domain of MDM2. It has been shown that MDM2 and its homolog, MDMX can synergistically enhance p53 ubiquitination and proteasome-mediated degradation (Linares et al., 2003). MDM2 ubiquitinates p53 at six key lysine (K) residues located at the regulatory C-terminus of p53. These include K370, K372, K373, K381, K382 and K386 (**Figure 1.7**) (Dai and Gu, 2010). Besides MDM2, ARF-BP1 was shown to catalyse the ubiquitination of p53. ARF-BP1 ubiquitin ligase activity is strongly inhibited by the presence of ARF (Chen et al., 2005a). Ubiquitinated p53 can be rescued from proteosomal degradation by herpesvirus-associated ubiquitin specific protease (HAUSP)-mediated deubiquitination (Li et al., 2002).

p53 is a sequence-specific transcription factor that is activated during cellular stress. Once active, it promotes the transcription of various genes that regulate cell cycle progression, DNA repair, apoptosis, senescence, cellular metabolism and autophagy. High-affinity target gene promoters (those that promote cell cycle arrest) are activated by p53 under low levels of cellular stress and low-affinity target genes (those that promote apoptosis) require a higher degree of p53 activation (Carvajal and Manfredi, 2013). p53 acts as a transcription factor for various genes to mediate its apoptotic response. Among the target genes induced by p53 to exert its proapoptotic effects are *PUMA, NOXA* and *BAX* (Carvajal and Manfredi, 2013).

.

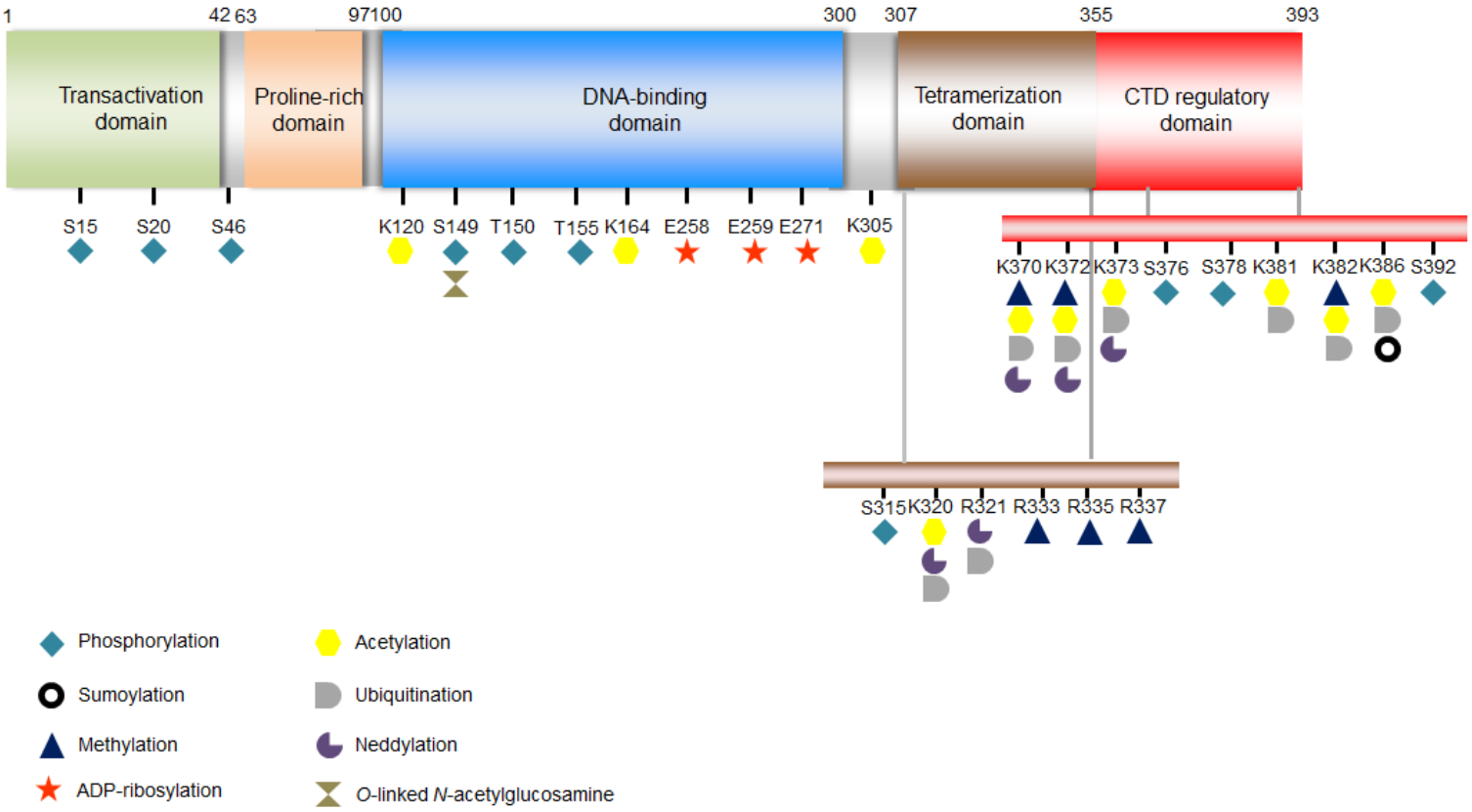



**Figure 1.7 The functional domains and PTM sites of p53.**

The p53 protein consists of 393 amino acids and is described as having five functional domains. The N-terminus consists of the transactivation and the proline-rich domain whilst the central core contains the DNA-binding domain. The C-terminus comprises the tetramerisation domain and the carboxy terminal (CTD) regulatory domain. Adapted from (Kruse and Gu, 2008).

p53 can effectively block cell cycle progression by activating the transcription of the cyclin-dependent kinase inhibitor p21, although several other p53 target genes such as *14-3-3 sigma* and *GADD45* also contribute to this response (Vousden and Prives, 2009). The induction of p21 expression upon DNA damage leads to temporary G1 block that allows cells to repair and survive safely until the damage has been removed (Vousden and Prives, 2009). A higher magnitude of damage activates irreversible cell cycle arrest or senescence which is an efficient tumour suppressor mechanism. The link between p53 and cellular senescence was initially proposed in PTEN-deficient prostate cancer (Chen et al., 2005b). A subsequent study showed that p53-induced cellular senescence is a major mechanism for tumour clearance when p53 is reactivated in p53-deficient hepatocarcinoma (Xue et al., 2007)

Besides apoptosis, cell cycle arrest and senescence, several studies have shown that p53 has a role in modulating both glycolysis and OXPHOS. The tumour suppressor p53 was found to enhance mitochondrial respiration and ATP generation by regulating the transcription of genes involved in aerobic respiration. *Synthesis of cytochrome oxidase 2 (SCO2)* was the first modulator of aerobic respiration to be identified as a direct transcriptional target of p53 (Matoba et al., 2006). Inactivation of p53 decreased SCO2-mediated oxygen consumption rate and cytochrome oxidase activity in cells (Matoba et al., 2006). Another p53 target gene that is involved in OXPHOS is *glutaminase-2* (*GLS-2*). GLS2 is a key enzyme in the conversion of glutamine to glutamate, a precursor in the biosynthesis of the ROS scavenger, glutathione (GSH). Induction of GLS2 by p53 increases cellular ATP production and aerobic respiration (Hu et al., 2010).

p53 modulates glycolysis through direct repression of genes encoding GLUT1 and GLUT4 and promotes activation of *TIGAR* which lowers the glycolytic rate (Bensaad et al., 2006; Thorens and Mueckler, 2010). Interestingly, p53 activation of genes that promote OXPHOS and limit glycolysis highlights another important function of p53 which is to limit oxidative stress. p53 protects the genome from oxidation by ROS, a major cause of DNA damage and genetic instability (Sablina et al., 2005). For example, TIGAR lowers intracellular ROS levels by increasing the activity of PPP which promotes the NADPH production, providing a survival function and protecting cells from oxidative stress-mediated damage (Bensaad et al., 2006). Similarly, inactivating p53 causes a reduction in GLS2 which results impaired reduced glutathione levels. This leads to enhanced levels of intracellular ROS and increased cellular sensitivity to ROS-dependent apoptosis (Hu et al., 2010; Suzuki et al., 2010). The antioxidant function of p53 in unstressed cells or during the initial stages of damage can also be mediated through proteins such as Sestrin 1, Sestrin 2, Glutathione peroxidase 1 (GPX1) and p53 induced nuclear protein 1 (p53INP) (Budanov et al., 2004; Budanov et al., 2002; Cano et al., 2009; Sablina et al., 2005; Velasco-Miguel et al., 1999) (**Figure 1.8**). It is interesting to note that the tumour development observed in $p53^{-/-}$ mice did not occur when these mice were supplemented with the antioxidant N-Acetylcysteine (NAC), suggesting that increased ROS in p53 deficient mice contributes to tumourigenesis. Interestingly, p53–mediated antioxidant function was recently reported during serine starvation where it induces p21-mediated G1 arrest and enhances glutathione levels, a known antioxidant (Maddocks et al., 2013). p53 however plays a dual role in regulating oxidative stress since increased ROS is observed when a p53-dependent apoptotic response is elicited (Liu et al., 2008).

p53 activation has been shown to induce autophagy and the basal levels of p53 have been shown to inhibit autophagy. Autophagy is a cellular stress adaptation which involves the activation of lysosomal pathway of cellular self-digestion (Tasdemir et al., 2008). p53 is a potent inducer of autophagy through transcriptional activation of damage-regulated autophagy modulator (DRAM) during starvation (Crighton et al., 2006). Conversely, changes in the cellular level of p53 can inhibit autophagy and promote cell survival (Tasdemir et al., 2008). This negative regulation seems to involve the transcription-independent effect of p53 as the cytoplasmic p53 derivative was shown to inhibit autophagy (Tasdemir et al., 2008).

The p53 protein is not active in cells unless it is first modified by other proteins. The transcriptional roles of p53 are regulated by an array of PTMs, the combination of which is dependent on the presence or absence of cellular stresses (**Figure 1.7**). Acetylation and phosphorylation of p53 have been shown to promote the expression of its targets whilst modifications such as NEDDylation, ubiquitination and sumoylation have been associated with suppression of p53-mediated transcription and nuclear export (Dai and Gu, 2010). Methylation has been associated with both enhancement and repression of p53 function, depending on the sites of modification (Dai and Gu, 2010). PTMs are thought to have significant role in cell fate determination by p53.

A transcription independent function of p53 was initially proposed when p53 lacking a DNA binding domain retained its ability to induce apoptosis when expressed in cells (Haupt et al., 1995). Subsequently, it was found that in response to stress, p53 localised to the mitochondria before its nuclear localisation (Erster et al., 2004; Marchenko et al., 2000; Mihara et al., 2003; Sansome et al., 2001; Zhao et al., 2005). Early after cell damage, monoubiquitination of cytoplasmic p53 by MDM2 targets it to the mitochondria (Marchenko et al., 2007). Mitochondrial p53 is either dimeric or has a higher-order oligomeric form, suggesting that the oligomerisation domain of p53 is pertinent for its localisation to the mitochondria (Pietsch et al., 2007). Interestingly, it was noted that the arginine variant at the codon 72 polymorphic variant of p53 is more strongly localised to the mitochondria (Dumont et al., 2003). Stress induced translocation of p53 to the mitochondria leads to the formation of a p53-BAK complex which is associated with the disruption of the antiapoptotic, MCL-1-BAK complex (Leu et al., 2004). p53 was shown to interact with the N-terminal of BAK through its DNA binding domain (Pietsch et al. 2007). p53 also interacts with BAX and this interaction facilitates MOMP and the activation of the intrinsic apoptotic pathway (Chipuk et al., 2004) (**Figure 1.8**).

p53 is well known for its apoptotic function and recently p53 was linked with necrosis, an irreversible form of tissue destruction activated by oxidative stress. In response to oxidative stress (hydrogen peroxide treatment), p53 accumulates at the mitochondria and directly interacts with cyclophilin D which triggers the opening of permeability transition pores (PTP) and mitochondrial permeability transition that lead to necrosis (Vaseva et al., 2012) (**Figure 1.8**). The deletion of proapoptotic proteins, BAX and BAK, had no effect on p53-mediated PTP opening and necrosis

which implies that the p53-induced necrosis is independent of its proapoptotic function at the mitochondria (Vaseva et al., 2012).

Vousden KH and Prives C once stated "If genius is the ability to reduce the complicated to the simple, then the study of p53 makes fools of us all" (Vousden and Prives, 2009). To date, p53 is known to be involved in apoptosis, necrosis, autophagy and senescence and p53 transcriptional activity regulates three out of the four known modes of cell death. The induction of senescence is transcriptionally regulated whilst necrosis involves direct interaction of p53 with PTP. Nuclear p53 induces apoptosis by enhancing transcription of proapoptotic genes and repressing antiapoptotic genes, whilst cytoplasmic p53 triggers mitochondria-induced apoptosis by interacting with the BCL-2 family proteins. p53 can either enhance or inhibit autophagy, depending on the stress stimuli. p53 is the best known transcription factor that operates both in the nucleus and cytoplasm and its localisation is an important determinant of its role. p53 shuttles between the cytoplasm and nucleus due to nuclear import and export signals in the C-terminus of the protein. Since p53 trafficking is important for p53 activation upon damage, perhaps there are other proteins that regulate p53 shuttling and this warrants further investigation.

Regulating cell cycle arrest, apoptosis and senescence are most well-understood functions of p53, which have been accepted as the main mechanisms for p53 to function as a tumour suppressor. Intriguingly, recent study on p53 demonstrated that the canonical functions of p53 in apoptosis, cell cycle arrest and senescence are not

absolutely required for its tumour suppression role (Li et al., 2012). The study used the acetylation-defective p53 mice which were deficient in cell cycle arrest, apoptosis and senescence. Interestingly, these mice did not develop early tumours and retained their ability to regulate energy metabolism and ROS production (Li et al., 2012). Importantly, this finding shed light on the importance of p53-mediated cellular metabolism regulation on tumour suppression although molecular mechanism of this regulation needs further elucidation. p53's ability to promote OXPHOS and inhibit glycolysis results in many unanswered questions such as how does p53 sense metabolic stress? Since apoptosis and cell cycle arrest may not be critical in p53-mediated tumour suppression, are additional downstream partners such as p53 cofactors are regulating this pathway? Are there any potential bridges between metabolism and the apoptotic machinery of p53? Understanding the metabolic function of p53 might help to identify the key therapeutic targets to combat cancer.

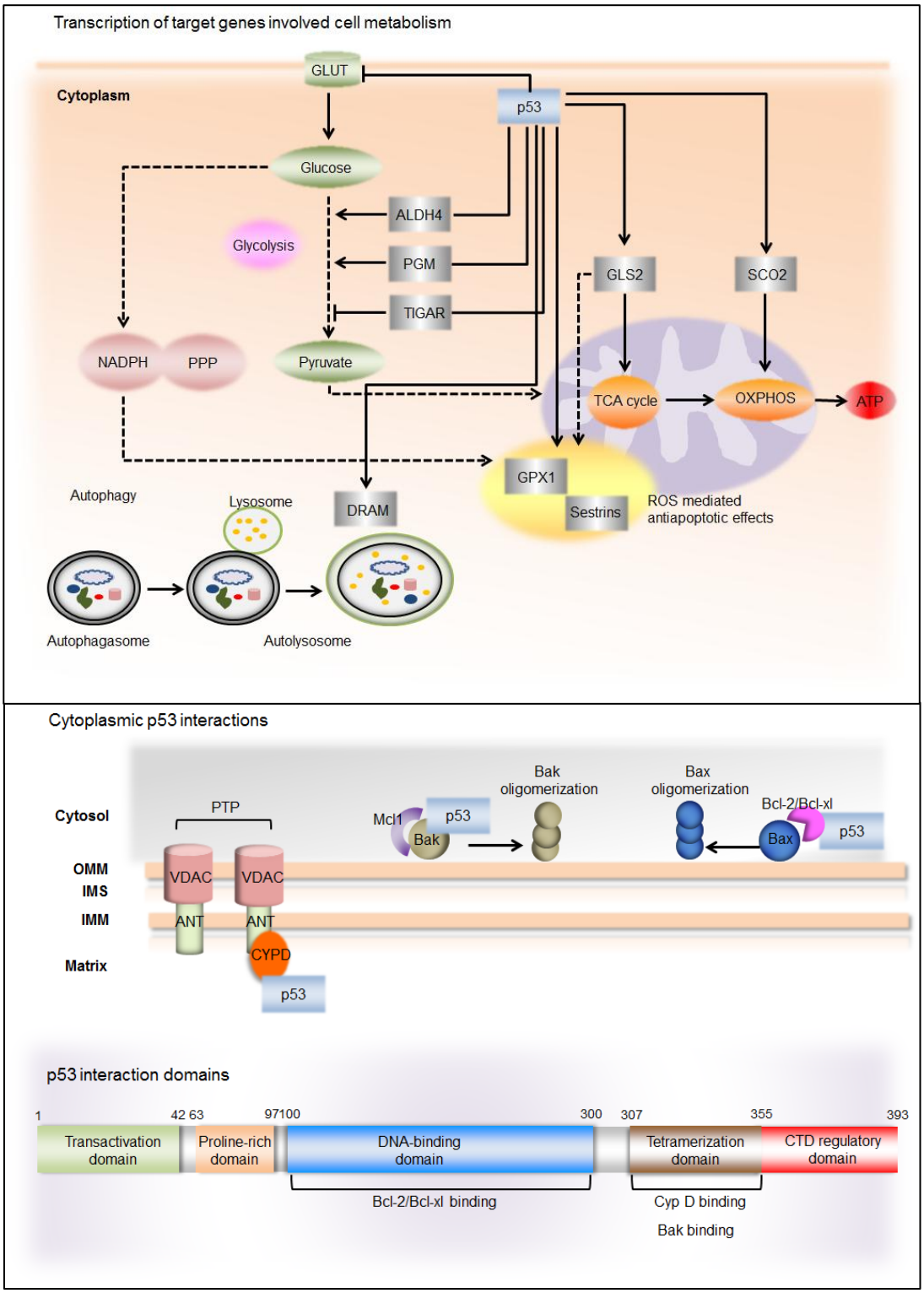



**Figure 1.8 p53 and cell metabolism.**

p53 transcriptionnally regulates glycolysis, OXPHOS and autophagy. The pro-survival mechanism of p53 is exerted by removal of mitochondrial ROS by transcriptional targets of p53. Direct interaction with the BCL-2 family and Permeability transition pores (PTP) allows p53 to mediate intrinsic apoptosis and necrosis, respectively. Adapted from (Shen et al., 2012).

### 1.8 p53 cofactors

p53 transcriptional activity at the nucleus is mainly regulated by its PTM which results in the recruitment of coactivators. p53 modification is necessary for the recruitment of transcription-associated factors which is associated with the induction of histone acetylation that contributes to the open statusof the chromatin. An increasing number of p53 cofactors have been shown to influence promoter-selective p53 transcriptional activity, thereby altering the balance between cell life and death. Several p53 cofactors are histone-modifying enzymes, such as histone acetyltransferase CREB-binding protein p300, PRMT1 and co-activator associated arginine methyltransferase (CARM1). p53 DNA-binding activity was shown to be enhanced by p300-mediated acetylation. p300 and cyclic AMP response element-binding protein (CBP) coactivators acetylate p53 and also act as a bridge linking p53 with the basal transcriptional machinery (Coutts and La Thangue, 2005). CBP/p300 promotes recruitment of p53 cofactors such as JMY and Strap that augment p53 response. Of interest, these two cofactors are described in more detail below.

#### JMY

Junction-mediating and regulatory protein (JMY) was initially identified from a yeast two-hybrid assay using truncated p300 protein as a bait (Shikama et al., 1999). JMY was shown to directly interact with p300 and augment p53 transcriptional activity by serving as a scaffold protein for the p300/CBP and p53 complex (Shikama et al., 1999). Interestingly, a variant of JMY (lacking the proline-rich domain at the C-terminus) was reported to possess enhanced ability to induce p53-

mediated cell cycle arrest compared to wild type JMY (Shikama et al., 1999). JMY is a stress responsive protein, both in the presence and absence of p53 (Coutts et al., 2007). Importantly, in a similar manner to p53, JMY is a target of MDM2-mediated ubiquitination, and it has been hypothesised that regulation of p53 is mediated through JMY's interaction with MDM2 (Coutts et al., 2007).

JMY's function relies heavily on its subcellular localisation. Cytoplasmic JMY was found to promote ARP2/3-independent actin nucleation (Zuchero et al., 2009). JMY becomes entirely cytoplasmic in differentiated cells and in non-damaged cells and appears to be enriched at the protruding periphery end of cells where it co-localises with actin (Coutts et al., 2009; Zuchero et al., 2009). In addition, JMY was found to promote cell migration during wound healing and invasiveness (Coutts et al., 2009; Zuchero et al., 2009). Besides cell motility, JMY influences cell adhesion by altering the expression and stability of E-cadherin protein (Coutts et al., 2009). Interestingly, stress-induced nuclear accumulation of JMY is not involved in cell motility instead it promotes p53 transcriptional activity (Coutts et al., 2009). This suggests a dual rule for JMY which involves both modification of transcription and cell motility. *JMY* was also found to be a HIF-1α responsive gene during hypoxia that enhances cell motility under hypoxic conditions (Coutts et al., 2011).

**Strap**

Using JMY as bait, Strap (Stress responsive activator of p300) was identified from a yeast two-hybrid assay (Demonacos et al., 2001). Strap was predicted to be composed of six tetratricopeptide (TPR) motifs based on multiple sequence alignment (Demonacos et al., 2001). Elucidation of Strap's crystal structure confirmed the presence of TPR motif but intriguingly, identified an OB (oligonucleotide/ oligosaccharide binding) fold at the C-terminus of Strap (Adams et al., 2012). Strap is upregulated in response to damage stimuli and was found to enhance the p300 and JMY interaction (Demonacos et al., 2001). The region that interacts with JMY was composed entirely of TPR motifs whilst the C-terminus of Strap interacted with p300 (Adams et al., 2012). Strap was also reported to enhance p53 transcriptional activity as well as p53-induced apoptosis (Demonacos et al., 2001) (**Figure 1.9**). Recent evidence suggests that Strap augments p53 transcriptional activity by its TPR motif whilst the converse was observed with the OB fold (Adams et al., 2012). Interestingly, the presence of Strap negates MDM2-mediated p53 degradation (Demonacos et al., 2001). This was supported by the finding that the half-life of p53 increases in the presence of Strap (Demonacos et al., 2001). Strap has been implicated in arginine methylation of p53 and promotes p53 methylation by aiding the recruitment of the protein arginine methyltransferase 5 (PRMT5) to the coactivator complex. This allows PRMT5 to methylate the arginine residues localised at the p53 tetramerisation domain and PRMT5 methylation enhances p53-dependent cell cycle arrest (Jansson et al., 2008).

Strap's subcellular localisation is influenced by ATM phosphorylation of serine (S)203 in response to DNA damage; an event which results in nuclear accumulation and enhanced p300 interaction of Strap (Demonacos et al., 2004). Phosphorylation by CHK2 was found to stabilise nuclear Strap in response to damage and cells expressing the CHK2 phosphomutant of Strap show impaired p53-mediated G2 arrest (Adams et al., 2008). This suggests a two-step sequential phosphorylation mechanism whereby Strap is first targeted by ATM kinase (Demonacos et al., 2004) followed by CHK2 (Adams et al., 2008) in the presence of DNA damage, which leads to nuclear accumulation and stabilisation of Strap (**Figure 1.9**).

Besides being a p53 cofactor, Strap has been reported to modulate nuclear hormone receptors such as the oestrogen receptor and the glucocorticoid receptor (GR) (Davies et al., 2011). Interaction between Strap and GR enhances GR protein stabilisation in a proteasome-dependent manner, and regulates GR transcriptional activity in a stress-dependent and gene-specific manner (Davies et al., 2011) (**Figure 1.9**). The role of Strap as a heat shock transcription factor 1(HSF-1) cofactor has been shown to regulate transcription of heat shock proteins. Strap enhances chromatin acetylation of *Hsp70* and *Hsp90* genes, possibly via its interaction with p300 during heat shock (Xu et al., 2008) (**Figure 1.9**). Depleting Strap during heat shock enhances cell death which suggests Strap promotes cell survival in response to heat shock (Xu et al., 2008).

More recently, Strap was reported to prevent apoptosis in acute myeloid leukaemia (AML) cells (Lynch et al., 2013). Surprisingly, reduced expression of the *BCL-2* gene and increased expression of proapoptotic genes were observed when Strap was depleted (Lynch et al., 2013). Similar results were observed in p300 depleted AML cells. Depletion of Strap or p300 influenced the stabilisation of Myc and its acetylation status, both of which are associated with induction of apoptosis (Lynch et al., 2013). Of note, AML cells harbour p53 mutant R174 which may suggest the antiapoptotic role of Strap is due to the absence of functional wild type p53.

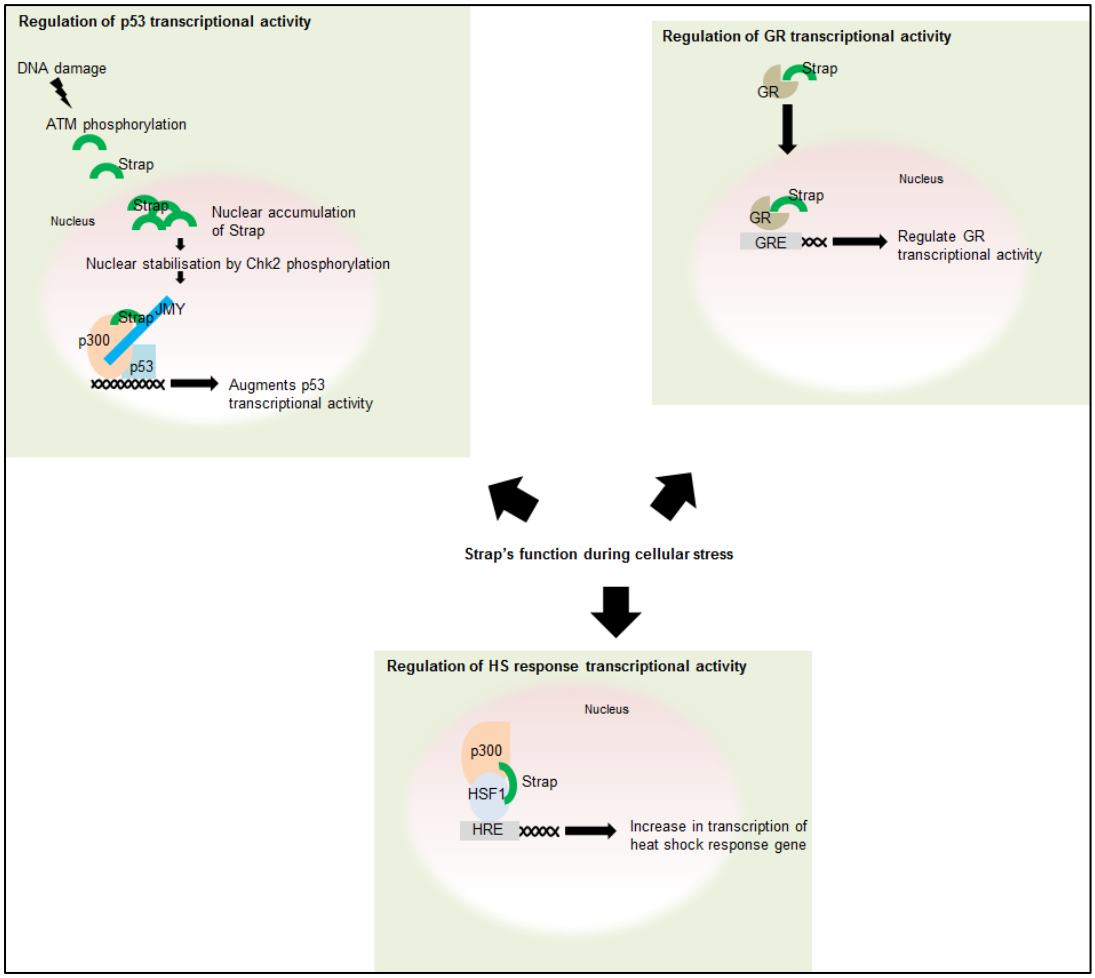



**Figure 1.9 Regulation of Strap during cellular stress response.**

Upon DNA damage, Strap is phosphorylated by ATM and CHK2 kinases leading to nuclear accumulation which facilitates the p53 response. During heat shock response, Strap is induced and recruited to HSE through interacting with HSF1/p300 complex. Transcription activation is facilitated through increase acetylation of chromatin mediated by the effect of Strap on p300 histone acetyltranseferase. Cellular stress regulates the interaction between GR and Strap which promotes GR stabilisation. Strap and GR complex translocates to the nucleus and binds to the GRE and regulates GR transcriptional activity. GR-glucocorticoid receptor, GRE-Glucocorticoid response element, HS- Heat shock, HRE-Heat shock response element, HSF1-Heat shock factor-1, GR-Glucocorticoid receptor, GRE-Glucocorticoid receptor element.

### 1.9 Project overview

Several reports have shown that pools of transcription factors with well characterised functions in the nucleus are also present at the mitochondria (Szczepanek et al., 2012; Wegrzyn et al., 2009). This study aims to elucidate the functional consequences of Strap at the mitochondria.

Strap is composed of two domains; the N-terminus comprises six tandem TPR motifs and the C-terminal region consists of a β-sheet OB fold (Adams et al., 2012). This structure provided new information on the complexity of Strap, which facilitated several lines of study documented here. The surprise discovery of Strap at mitochondria came about during proteomic analysis of the OB domain. Sequence and mass spectrometry analysis of Strap revealed three consensus sites for ATM/ATR kinase phosphorylation. The phosphorylation of all three sites in the presence of damage was found to mediate its mitochondrial localisation. Mitochondrial Strap promotes cytochrome c release via BAK oligomerisation in the presence of p53 during damage. Mitochondrial Strap shuttles p53 from the mitochondria to the nucleus. In a strategy to define the role of mitochondrial Strap, proteomic analysis of mitochondrially targeted Strap identified ATP synthase subunit-β as a potential interacting protein. Interestingly, mitochondrial Strap regulated OXPHOS by interacting with ATP synthase subunit-β to reduce ATP synthase activity. This results in p53-dependent cellular ATP depletion thereby promoting cell death.

Strap's crystal structure elucidation, together with new results on its role at the mitochondria emphasise the biological intricacy of cofactor activity during the p53 response. The discovery that Strap is recruited to mitochondria during DNA damage allows a better understanding of the transcription-independent role of Strap in the DNA damage response.

# Chapter 2

# Materials and Methods

## 2.1 Cell lines

All cell lines were grown at 37$^{o}$C in a humidified incubator with constant supply of 5% $CO_2$. The cells are generally maintained in Dulbecco's modified Eagle's medium (DMEM) or RPMI1640 (PAA Laboratories, Austria) with Foetal Calf serum (FCS) (Biosera, USA) in the presence of 10,000 units/ml penicillin/10,000 µg/ml streptomycin (Life Technologies Corp., USA). The maintenance media used for each cell line are summarized in Table 2.1.

**Table 2.1 Media used for maintaining cell lines.**

| Media | Cell line(s) |
|---|---|
| DMEM, 5% FCS (v/v), and 5% (v/v) penicillin/streptomycin. | U2OS, MCF-7, HCT116$^{+/+}$ and HCT116-/- (kindly provided by Dr. B. Vogelstein), HeLa, SAOS2. |
| RPMI, 5% FCS (v/v), and 5% (v/v) penicillin/streptomycin. | H1299. |
| DMEM, 5% FCS, 400 µg/ml G418 antibiotic (Promega, USA) and 5% (v/v) penicillin/streptomycin. | All stably transfected cell lines. |
| DMEM, 5% tetracycline negative FCS (v/v) (PAA Laboratories, Austria), 100 µg/ml G418 antibiotic, 150 µg/ml hygromycin B and 5% (v/v) penicillin/streptomycin. | U2OS Tet-On® gene expression System (Clontech Laboratories Inc., USA) mainly Flag-WT, Flag-OB, HA-WT, HA-3D, HA-L-Strap and empty vector control cell lines. |
| DMEM, 5% FCS (v/v), 100 µg/ml hygromycin B and 5% (v/v) penicillin/streptomycin. | GM1666 and GM1667 (kind gift from Dr. O'Neill E, University Oxford obtained from Shiloh Y). |

| Media | Cell line(s) |
|---|---|
| DMEM (25 mM glucose, 2 mM glutamine) supplemented with 5% (v/v) penicillin/streptomycin. | Glucose supplemented media. |
| Glucose free DMEM (Invitrogen, USA) supplemented with 10 mM Galactose (Sigma-Aldrich, USA), 5 mM HEPES (Invitrogen, USA), 2 mM Glutamine with 5% (v/v) penicillin/streptomycin. | Galactose supplemented media. |

## 2.2 Plasmid Expression Vectors

The following plasmids have previously been described: pcDNA3 HA-WT Strap, pcDNA3-HA-StrapS203A, pcDNA3-HA-StrapS203D (Demonacos et al., 2004), and pCMV-p53 (Demonacos et al., 2001). pcDNA3 (Invitrogen, USA), p3X Flag-CMV-7.1 expression vector (Sigma, St Louis), pCMV-β-galactosidase (Logan et al., 2005), pLuc-BAX (Miyashita and Reed, 1995), pLuc-GADD45(Kastan et al., 1992). Mitochondrial targeted p53 (L-p53) and the sucrose gradient mitochondrial sample were kindly provided by Dr. U. Moll (University of Stony Brook) and Dr. A. Storey (University of Oxford) respectively. The pcDNA3-HA-WT mutant derivatives S248A, S248D, S427A, S427D, S203A248A, S203D248D, S203A427A, S203D427D, S248A427A, S248D427D, S203A248A427A and S203D248D427D were cloned using oligonucleotides in accordance to Strategene's QuickChange® Multi Site-Directed Mutagenesis kit. The sequences of the primers are as listed in Table 2.2:

**Table 2.2 Primer sequences for Strap derivatives.**

| Plasmid | Primer Sequence |
|---|---|
| S248A | 5'-cccttgagggtttcgctcaggctgcagcg-3' |
| S248D | 5'-gcccttgagggtttcgatcaggctgcagcgct-3' |
| S427A | 5’-ccacagaactccagcgctcaagcctctgccacagtagcttcaagg-3’ |
| S427D | 5’-ccacagaactccagcgatcaagcctctgccacagtagcttcaagg-3’ |

## 2.3 Transfection

Required plasmid DNA was transfected using Gene Juice® transfection reagent (Merck, Germany) according to manufacturer’s protocol with slight modifications. A ratio of 1 µg of plasmid DNA to 1.5 µl of the transfection reagent was used. Briefly, the transfection reagent and serum free media (Life technologies Corp., USA) were incubated for 5 min. A complex of the required plasmid DNA and the mixture of transfection reagent and serum free media was incubated at room temperature for 10 min and added into each plate. Cells were harvested 24-72 hr after transfection.

## 2.4 Small interfering RNA transfection

Cells were plated and transfected for 72 hr using Oligofectamine (Life Technologies Corp., USA) following the manufacturer’s guidelines. A mixture of three siRNA was used at a final concentration of 90 nM (Adams et al., 2008; Davies et al., 2011). These and control siRNA were purchased from Dharmacon (Chicago, USA) and the sequences are as listed in Table 2.3.

**Table 2.3 siRNA sequences for depleting Strap**.

| Name | Sequence |
|---|---|
| Strap1 | 5'-ccagccuccuugagaguaa-3' |
| Strap2 | 5'ggaaaggacuauuccuuuu-3' |
| Strap3 | 5'-ccagctgggtgaggtgtac-3' |
| Non targeting | 5'-auguauuggccuguauuag-3' |

## 2.5 Drug treatments

Cells were treated with either UV light at 50 J/$m^2$, 2 µM of doxorubicin (Sigma-Aldrich, USA) or 40 µM of etoposide (Sigma Aldrich, USA) and harvested 6 hr later unless indicated otherwise. As for the inhibitors, cells were treated with either 10 mM caffeine (Sigma-Aldrich, USA), 10 µM ATM inhibitor (Calbiochem,Germany) or 10 µM ATM/ATR inhibitor (Calbiochem, Germany) and harvested after 6 hrs. Carbonyl cyanide 3-chlorophenylhydrazone (CCCP) and oligomycin were used as controls in TMRE (tetramethylrhodamine ethyl ester) staining for membrane depolarization and hyperpolarisation respectively. Cells were treated with 25 nM CCCP and 2 µM oligomycin and harvested an hour later.

## 2.6 Western Blotting

Media was removed from the plates and the cells were washed with PBS (Oxoid, USA). Cells were then manually lifted from the plates and harvested into pre-chilled microcentrifuge tubes (Eppendorf, Germany). Cells were pelleted at 800 x *g*, 2 min at 4$^{o}$C and the cell pellet was lysed according to the pellet size using TNN lysis buffer (150 mM NaCl, 50 mM Tris-HCl [pH 7.5], 5 mM EDTA, 0.5% NP-40, 50 mM NaF, 0.2 mM sodium orthovanadate and proteinase inhibitor cocktail [0.5

µg/ml leupeptin, 0.5 µg/ml pepstatin, 0.5 µg/ml aprotinin]) and incubated on ice for approximately 20 min. The lysed cells were centrifuged at 16,000 x *g* for 10 min at 4$^{o}$C to remove cell debris. The protein concentration was determined using Bradford reagent (Sigma-Aldrich, USA) and 20-80 µg of protein was loaded onto gels.

8-15% SDS-PAGE gels were prepared according to (Laemmli, 1970). The gels were run at 200 V until the loading dye reached the bottom of the gel in Tris/Glycine SDS running buffer. The gels were blotted onto nitrocellulose membrane (Whatman Inc., USA) in Towbin blotting buffer with 10% methanol (Towbin et al., 1979) and blotted for either 400 mA for 2 hr or 150 mA for approximately 16 hr at 8$^{o}$C. After blotting, the membrane was briefly rinsed with Ponceau S (Sigma-Aldrich, USA) to ensure complete transfer and absence of air bubbles during blotting. The membrane was blocked in 10% semi-skimmed milk/0.1% Tween-20/PBS for approximately 1 hr. The membrane was incubated with the primary antibody diluted in blocking solution for 16 hr at 8$^{o}$C. The membrane was briefly rinsed in 0.1% Tween-20/PBS (v/v) and incubated in its respective secondary antibody dissolved in the blocking solution for approximately 1 hr. After approximately 4-6 washes with 0.1% Tween-20/PBS, signal or protein expression was detected using either SuperSignal® West Dura Extended Duration Substrate or in-house made ECL (made from 2.5 mM Luminol, 396 µM Coumaric acid, 100 mM Tris-HCl (pH 8) and 0.02% hydrogen peroxide). For primary antibody to detect phosphorylation, TBS was used instead of PBS and BSA (Sigma-Aldrich, USA) was used instead of semi-skimmed milk in all washing and blocking solutions. All antibodies used are listed in Table 2.4.

## 2.7 Immunoprecipitation

Cells were harvested and lysed with TNN lysis buffer. After approximately 20 min incubation on ice, samples were spun at 16,000 x *g* for 10 min. 95-98% of the supernatant was subjected to overnight incubation with the designated antibody at 4$^{o}$C and the remaining 5-2% was kept for loading as an input. 30 µl protein A/G-agarose mix (Sigma-Aldrich, USA) was added to the overnight incubated lysates and incubated for one hour at 4$^{o}$C. Alternatively, for immunoprecipitation with either HA-agarose beads (Sigma-Aldrich, USA) or Flag-agarose beads (Sigma-Aldrich, USA); cell lysates were directly mixed with the beads and were subjected to overnight incubation. Following incubation, the beads were washed with lysis buffer approximately five times with centrifuging at 800 x *g* for 2 min at 4$^{o}$C. Eight-ten µl of 4x SDS loading buffer (62.5 mM Tris-HCl [pH 6.8], 25% glycerol, 2% SDS [Sigma-Aldrich, USA], 5% β-mercaptoethanol and 0.01% bromophenol blue) was added to the washed beads before boiling at 95-100$^{o}$C for 2 min to denature the protein and separate it from the beads. The elution was centrifuged at 16,000 x *g*, 1 min at room temperature prior to loading onto the gel.

**Table 2.4 List of antibodies.**

| Antibody | Species | Source |
|---|---|---|
| ATP synthase subunit-β | Mouse | BD Bioscience, USA |
| BAX | Rabbit | Cell Signaling Technology, Inc, USA |
| BCL-2 | Rabbit | Cell Signaling Technology, Inc, USA |
| BCL-XL | Rabbit | BD Bioscience, USA |
| Calnexin | Mouse | Millipore, USA |
| Cleaved Caspase 3 | Rabbit | Cell Signaling Technology, Inc, USA |
| Cytochrome C | Mouse | Santa Cruz Biotechnology, Inc, USA |
| Cytochrome Oxidase IV | Rabbit | Cell Signaling Technology, Inc, USA |
| E2F1(KH95) | Mouse | Santa Cruz Biotechnology, Inc,USA |
| Flag-M2 | Mouse | Sigma-Aldrich, USA |
| GFP | Goat | Santa Cruz Biotechnology, Inc, USA |
| HA-11 | Mouse | Covance, USA |
| p53(DO-1) | Mouse | Santa Cruz Biotechnology, Inc, USA |
| PARP-1 | Mouse | BD Bioscience, USA |
| PCNA (PC10) | Mouse | Santa Cruz Biotechnology, Inc, USA |
| Phospho ATM/ATR substrate | Rabbit | Cell Signaling Technology, Inc, USA |
| Strap | Mouse | OxFabs Antibody, UK |
| Strap (TTC5) | Rabbit | Sigma-Aldrich, USA |
| Syntaxin 6 | Mouse | Millipore, USA |
| β-actin | Mouse | Sigma-Aldrich, USA |
| α-Mouse IgG TrueBlot® ULTRA | HRP conjugated | eBioscience, Inc., USA |
| α-Rabbit IgG TrueBlot® ULTRA | HRP conjugated | eBioscience, Inc., USA |

| Antibody | Species | Source |
|---|---|---|
| α-Mouse IgG | HRP conjugated | Dako UK Ltd., UK |
| α-Rabbit IgG | HRP conjugated | Dako UK Ltd., UK |
| Alexa Fluor® 488 Donkey Anti-Mouse IgG | Fluorescein conjugated | Invitrogen,USA |
| Alexa Fluor® 488 Donkey Anti-Rabbit IgG | Fluorescein conjugated | Invitrogen,USA |
| Alexa Fluor® 594 Donkey Anti-Mouse IgG | Fluorescein conjugated | Invitrogen,USA |
| Alexa Fluor® 594 Donkey Anti-Rabbit IgG | Fluorescein conjugated | Invitrogen,USA |

**2.8 Immunofluoresence**

Cells were seeded onto 13 mm glass coverslips. Cells were fixed with 3.7% formaldehyde/PBS (v/v) except for ATP synthase subunit-β staining where cells were fixed with 100% methanol and incubated at room temperature for 10 min. For cells stained with MitoTracker®Red CMXRos (Invitrogen, USA), 100 nm of Mitotracker was added to each well 10 min prior to fixing the coverslips. Permeabilisation was performed for approximately 2-5 min with 0.5% TritonX-100/PBS (v/v), followed by incubation with primary antibody for an hour at room temperature in a humidified box. Coverslips were washed briefly with 0.025% Tween in PBS before adding secondary antibody for 30 min at room temperature.

Coverslips were mounted using Vectashield contained DAPI (4,6-diamino-2-phenylindole) after approximately 4-5 washes with 0.025% Tween in PBS.

**2.9 Mass spectrometry gel and tryptic digestion**

Cells were harvested and lysed with TNN lysis buffer. After approximately 20 min incubation on ice, samples were spun at 16,000 x *g* for 10 min. 98% of the supernatant was incubated with Flag agarose beads (Sigma, St Louis MO) for approximately 2 hrs at 4 ºC and the remaining 2% was kept for loading as an input. The beads were washed with lysis buffer for three times. The beads were eluted using 500 µg of FLAG peptide in 25 mM Tris-HCl pH 6.5 at 1,000 rpm for 1 hr at 4ºC. The samples were loaded in Nupage SDS loading buffer with Nupage sample reducing agent (Invitrogen, USA). The gel was silver stained using the SilverQuest$^{TM}$ Silver Staining Kit (Invitrogen, USA) according to manufacturer's instructions.

Following SDS–PAGE and staining, protein bands were excised and subjected to tryptic digestion as recommended by Kessler BM, University of Oxford and as described in (Jansson et al., 2008). The bands were cut into small pieces measuring approximately 1 $cm^2$ and were then incubated overnight in wash solution (50% methanol (Fisher Scientific,USA), 10% acetic acid, 40% ultrapure water) at room temperature. The wash solution was removed and the gel pieces rinsed in 200 µl wash solution for 2–3 hr at room temperature. The wash solution was then removed and the gel pieces dehydrated in 200 µl of acetonitrile (Fisher Scientific, USA) for 5 min at room temperature. After removing the acetonitrile, the samples were dried

for approximately 2 min in a vacuum centrifuge. 30 µl of 10 mM Dithiothreitol (DTT) (Sigma-Aldrich, USA) was added and the proteins were reduced for 30 min at room temperature. The DTT was removed and replaced with 30 µl of 100 mM iodoacetamide (Sigma-Aldrich, USA) and incubated for further 30 min. The solution was removed and replaced with another 200 µl of acetonitrile and incubated for 5 min before being dried for 2 min in a vacuum centrifuge. Following this, the gel pieces were rehydrated in 200 µl of 100 mM ammonium bicarbonate for 10 min at room temperature. After removing the ammonium bicarbonate, the gel pieces were then dehydrated again with 5 min incubation in 200 µl acetonitrile. The acetonitrile was removed and the gel pieces were dried for 2 min in a vacuum centrifuge. The gel pieces were further rehydrated for 10 min on ice in 30 µl of 20 ng/µl sequencing grade trypsin solution (Promega, USA) in 50 mM ammonium bicarbonate, with occasional vortex mixing. The samples were then centrifuged for 30 s and the excess trypsin solution was removed. 5 µl of 50 mM ammonium bicarbonate was added to each sample and the digestion was carried out overnight at 37°C. The next day, 30 µl of 50 mM ammonium bicarbonate was added to each digest and incubated at room temperature for 10 min with occasional gentle vortexing. The digests were centrifuged briefly and the supernatants were collected and transferred to new tubes. Next, 30 µl of extraction buffer (50% acetonitrile, 45% distilled water, 5% formic acid) was added to the tubes containing the gel pieces. These samples were incubated for 10 min at room temperature with occasional gentle vortex mixing. This step was repeated. The tubes containing the extracted peptides were transferred to a vacuum centrifuge and the volume of each samples were reduced to <20 µl by evaporation. The volume of each sample was

adjusted to 20 µl with 98% water, 2% acetonitrile, 0.1% formic acid prior to running on a mass spectrometer.

### 2.10 Mitochondrial Extraction

Mitochondrial fractions from cells seeded in 10 cm dishes were isolated using the Mitochondrial Isolation Kit for Cultured Cells (Pierce Biotechnology, USA and Sigma-Aldrich, USA) according to the manufacturer's instructions. Mitochondrial fraction prepared using conventional sucrose gradient method was a kind gift from Prof A.Storey, University of Oxford. Mitochondria isolation with higher yield and purity used in the immunoprecipitation and oligomerisation assays were obtained using the Mitochondrial Isolation Kit (Miltenyi Biotec, Germany) which uses magnetic microbeads to isolate functional human mitochondria from cells.

### 2.11 Oligomerisation Assay

Mitochondrial were isolated using the Mitochondrial Isolation Kit (Miltenyi Biotec, Germany) following the manufacturer's guidelines. The oligomerisation assay was performed as previously described (Meng et al., 2007) with slight modifications. Briefly, mitochondrial extracts were cross-linked with 1,6-Bismaleimidohexane (BMH) (Pierce Biotechnology, USA) at a final concentration of 100 µM. Crosslinking was allowed to proceed at 37$^{o}$C for 60 min. Samples were centrifuged at 14,000 x g for 20 min at 4$^{o}$C. The extracts were denatured with 4x SDS loading buffer and heated at 95-100$^{o}$C for 2 min before analysed using SDS-PAGE.

## 2.12 Proteinase K digestion

Mitochondrial fractions obtained from magnetic beads isolation protocol were used for proteinase K digestion as previously described (Mancini et al., 2009). Isolated mitochondria from U2OS cells were suspended in suspension buffer and treated with 0.2 mg/ml of proteinase K for 20 min on ice in the presence or absence of TritonX-100 (1% final concentration). 4-(2-Aminoethyl) benzenesulfonyl fluoride hydrochloride (AEBSF) was then added to a final concentration of 2 mM to stop the reaction.

## 2.13 Reporter Assay

Cells were seeded in 6 cm dishes and transfected with plasmid DNA along with 100 ng of β-galactosidase plasmid to measure transfection efficiency. Cells were harvested 48 hr after transfection, lysed with 125 µl of reporter lysis buffer (Promega, USA) and stored in -80$^{o}$C for approximately 20 min. The frozen lysate was thawed in 37$^{o}$C water bath. The thawed sample was centrifuged at 16,000 x *g* for 1 min at 4$^{o}$C. 50 µl of the sample was loaded into an opaque 96-well plate and the luciferase activity was measured using a luminometer which adds 100 µl of luciferase reagent (Promega, USA) per sample. All experiments were performed in triplicate.

Luciferase activity was normalized according to transfection efficiency by measuring β-galactosidase activity. An equal volume of the cell lysate and 2x β-galactosidase buffer (0.2 M $Na_2PO_4$ [pH 7.2], 2 mM $MgCl_2$, 0.7% β-Mercaptoethanol and 0.44 M Ortho-nitrophenyl-β-D-galactopyranoside [ONPG])

were loaded into a flat-bottomed 96-well plate. The enzyme activity was measured by the appearance of the yellow colour using a plate reader at 420 nm.

### 2.14 xCELLigence

Cells were seeded in 10 cm dishes. Cells were later trypsinized and counted using a haemocytometer. 5,000 cells in 100 µl media per well were plated on an E-plate 16. For the etoposide and doxorubicin treatment, 100 µl of drug at the desired concentration was added to the media in the E-plate 16. Alternatively, for the UV light treatment, cells were treated prior to trypsinization. Experiments were carried out using the RTCA DP instrument (Roche Diagnostic GmbH, Germany) which was placed in a humidified incubator maintained at 37ºC with 5% $CO_2$. The electronic sensors provide a continuous and quantitative measurement of cell index in each well. Cell index is a quantitative measure of cell number present in a well. The E-Plate 16 was monitored over the time frames indicated.

### 2.15 Reverse Transcriptase Polymerase Chain Reaction

Cells were seeded in 10 cm dishes. Cells were washed with PBS and pelleted by centrifugation at 800 x *g* for 2 min. The cell pellet was stored at -80$^{o}$C prior RNA extraction. RNA from the cells was extracted using TriZol® reagent according to the manufacturer's instructions. RNA was stored at -80$^{o}$C.

The amount of RNA was quantified using a NanoDrop (Thermo Fisher Scientific, USA). One µg of RNA was denatured at 65$^{o}$C for 5 min and reverse transcribed in a total volume of 15 µl (50 mM Tris-HCl pH7.5, 75 mM KCl, 3 mM MgCl2, 5 mM

Dithiothreitol, 10 mM dNTPs, 1U/µl ribonuclease inhibitor, 20 µM random hexamers and 5 U/µl moloney murine leukaemia virus reverse transcriptase (MMLV)) for 10 min at room temperature. This step was later continued at 37$^{o}$C for 1 hr and samples were stored at -20$^{o}$C.

10% of the synthesized cDNA served as a template for target cDNA amplification by polymerase chain reaction (PCR) in the presence of 0.5 µM of each specific primer (oligonucleotide sequences as listed in Table 2.5), 0.25 mM dNTPs (Promega, USA), 50 U of PAQ5000 DNA polymerase (Agilent Technologies, Inc. USA), 10% betaine (Sigma-Aldrich, USA) in 10X PAQ5000 PCR reaction buffer. Each cDNA template was amplified 25-30 cycles to reach an optimal quantitative result. PCR products were visualized on a 1% agarose gel containing 0.002% ethidium bromide (Sigma-Aldrich, USA).

**Table 2.5 RTPCR primer sequences.**

| Name | Sequence |
|---|---|
| Strap (Forward) | 5'-gaggaagtactcggttctgcc -3' |
| Strap (Reverse) | 5'-catatttatctaacgtcgccc-3' |
| 18s (Forward) | 5'-gataccgaacgagactctggc-3' |
| 18s (Reverse) | 5'-ccatccaatcggtagtagcg-3' |

### 2.16 TMRE staining

TMRE staining followed by flow cytometry analysis (Accuri C6, BD Bioscience, USA) was used to assess mitochondrial membrane potential. Cells were seeded in 10 cm dishes. 30-50% confluent dishes were stained with 55 nM TMRE for 40 min at 37$^{o}$C before harvesting for flow cytometry analysis. Culture media were removed and cells were washed with PBS before trypsinization. Trypsinized cells were pelleted at 1,000 rpm (Sorvall RT6000D, USA) for 5 min at 4$^{o}$C. Supernatant was removed and the pellets were washed again with 4 ml PBS. Cells were pelleted and resuspended in 500 µl of PBS. Samples were maintained at 37$^{o}$C throughout flow cytometry analysis. TMRE stained cells were detected in the FL2-A channel.

### 2.17 Nuclear extraction

Cells were seeded in 10 cm dishes. 50-75% confluent cells were harvested by removing the media and washed twice with PBS. Residual PBS was removed by tilting the plate and 1.2 ml of ice cold Buffer A (Protease inhibitor, 10 mM HEPES pH 7.9, 10 mM KCl, 0.1 mM EDTA and 0.1 mM EGTA pH 8.0) was added to the plate. Cells were lifted by manual scraping and suspended cells were left to sit on ice for 15 min. 75 µl of 10% NP-40 (Sigma Aldrich, USA) was added to dissolve the cellular membrane. The cells were mixed by vortexing for 10 s and pelleted at 16,000 x *g* for 1 min at 4$^{o}$C. The supernatant (cytoplasmic fraction) was removed to a fresh tube. The pellet (nuclear fraction) was lysed in 9 M Urea Lysis Buffer (9M Urea, 75 mM Tris-HCl pH 7.5 and 0.5M β-Mercaptoethanol).

### 2.18 ATP synthase specific activity

ATP synthase activity from total cell lysates was measured using the ATP synthase Specific Activity Microplate Assay kit (Abcam plc, UK) according to the manufacturer's instructions.

### 2.19 Total ATP levels

The total ATP levels were measured as described previously (Moss et al., 2010) with slight modifications. Cells were seeded in 10 cm dishes. 50-75% confluent cells were harvested by removing the media and washed once with PBS. Residual PBS was removed by tilting the plate and 200 µl of 5% Tricholoroacetic acid (w/v) were added per dish. The cells were pelleted at 16,000 x *g* for 5 min at 4$^{o}$C. The supernatant was removed to a fresh tube and subjected to HPLC analysis.

### 2.20 Flow cytometry

Cells were seeded on 10 cm dishes. Growth media were collected and adherent cells were lifted by adding 2 ml of trypsin (Lonza, Switzerland) per dish. The cells were pelleted at 1,000 rpm (Sorvall RT6000D, USA) for 5 min at 4$^{o}$C and washed once with PBS. The cells were pelleted again and fixed overnight in ice cold 70% ethanol/PBS (v/v). Fixed cells were washed once with PBS and stained in 4% (v/v) propidium idodide (Sigma-Aldrich, USA) in the presence of 125 U/ml RNAse A (Sigma-Aldrich, USA). Stained cells were analysed using flow cytometry (Accuri C6, BD Bioscience).

# Chapter 3

# Results: Cell line development and proteomic analysis

### 3.1 Strap derivatives stable cell lines

Strap was initially reported to comprise of six TPR motifs based on sequence analysis (Demonacos et al., 2001). Interestingly, recent elucidation of Strap's crystal structure revealed an atypical six TPR motifs that also contains an OB fold (Adams et al., 2012) (**Figure 3.1Ai**). The JMY and p300 interacting domains in Strap were previously determined by using *in vitro* translated truncations of Strap and its binding to various regions of p300 and JMY were assessed (Demonacos et al., 2001). The interacting domains in Strap are shown in **Figure 3.1Aii**. To further support the biochemical assay, the interaction between JMY and truncated Strap was investigated in U2OS cells stably expressing Flag-tagged JMY (Coutts et al., 2009). The stable cells were transiently transfected with either vector, wild type Strap, TPR motif or the OB fold. As expected, an increased association with JMY was observed with wild type Strap and TPR motif compared to the OB fold (**Figure 3.1Aiii**). The discovery of the OB fold prompted further investigation in the significance of both the TPR motif and OB fold in Strap's function, primarily in the DNA damage response. The OB fold construct generated consists of residues 220-440, which is inclusive of TPR6 and the linker (Adams et al., 2012).

U2OS (wild type p53) and SAOS2 (p53 null) cells stably expressing wild type Strap, TPR motif and OB fold were generated to investigate the functional requirements of the two different domains in the presence and absence of p53. The generation of stably-transfected cell lines served as an essential tool for a wide range of applications. In contrast to transient expression, constitutive expression allows long term as well as defined and reproducible expression of the protein of interest. Transfected cells were selected with the G418 antibiotic (400 µg/ml) and

positive clonal cells were pooled and expanded. Initial investigations of the stable cell lines by immunostaining showed that both the TPR motif and the OB fold had similar localisation as wild type Strap (**Figure 3.1B**).

To further asses the functional impact of the TPR motif and OB fold, impedance measurements were taken as an index of cell viability using the xCELLigence real time system. The xCELLigence system allows for label-free and dynamic monitoring of cellular changes in real time using impedance measurements. The system measures electrical impedance from cells plated in E-16 plates which contain numerous electrodes that are sensitive to cellular phenotype changes. The impedance measurement provides quantitative information about the biological status of the cells including number, viability and morphology (Stoddart, 2011). Impedance measured between electrodes in an individual well depends on electrode geometry, ionic concentration in the well and whether there are cells attached to the electrodes. In the absence of cells, the impedance measurement is determined by the ionic environment between the electrode and the solution (media) (Stoddart, 2011). Cells attached to the electrode surface will alter the ionic environment leading to an increase in the measurement of impedance (Atienza et al., 2005). The number of cells thus reflects the impedance value; for example a higher number of cells will give a higher impedance readout. The impedance measurement is displayed as cell index.

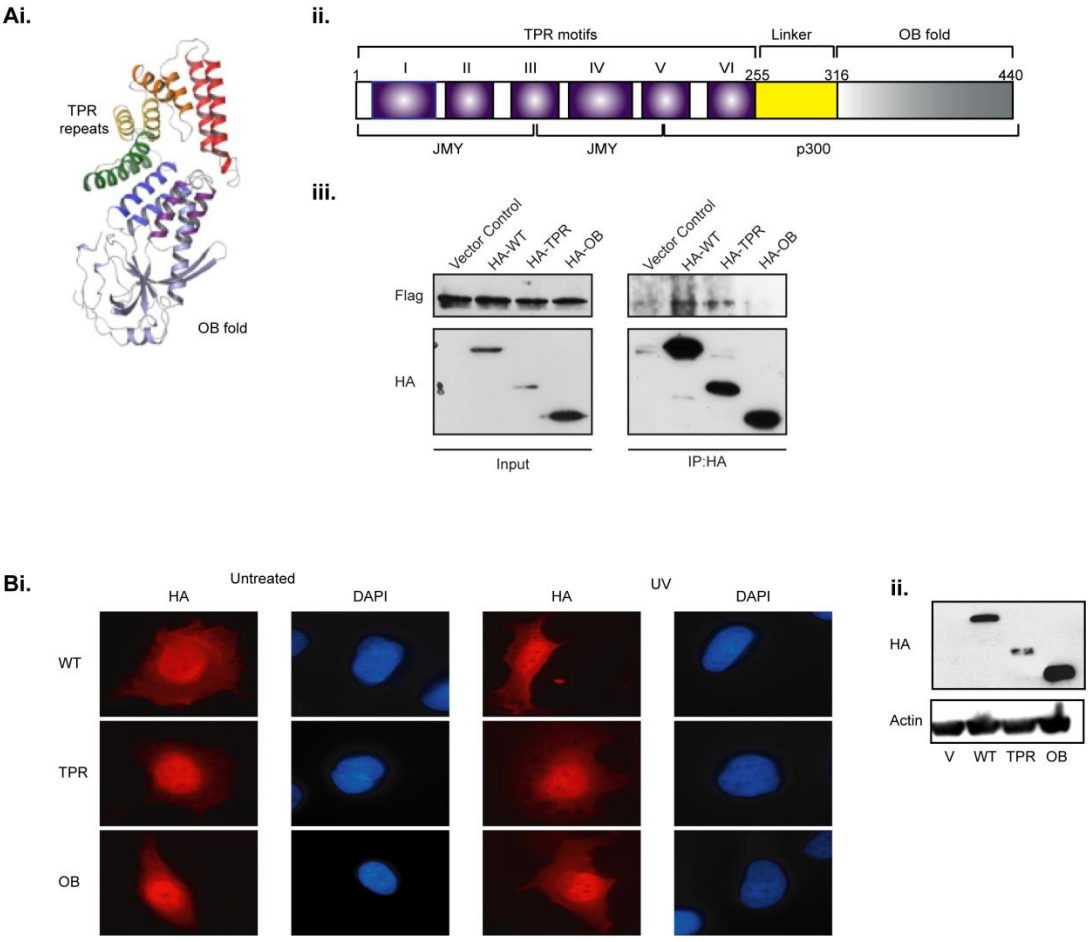



**Figure 3.1 Strap TPR motif and OB fold.**

**Ai.** Diagram of Strap's crystal structure which indicates the TPR motif and the OB fold (Adams et al., 2012).

**ii.** A cartoon of Strap showing the TPR motif in purple (1-271), with the OB fold (316-440) in grey.

**iii.** Ectopic Strap was immunoprecipitated from U2OS cells stably expressing Flag-tagged JMY, transfected with either 1 µg of wild type Strap (HA-WT), HA-TPR, HA-OB or vector control using anti-HA antibody. Anti-HA and anti-Flag antibody were used to detect ectopic Strap and JMY, respectively. 2% of the total sample volume was loaded as inputs.

**Bi.** U2OS cells stably expressing wild type Strap (HA-WT), HA-TPR, HA-OB and empty vector were either untreated or treated with UV light (50 J/m$^2$; 3 hr) as indicated. Samples were immunostained with anti-HA antibody to detect ectopic Strap. DAPI staining was used to visualise the nuclei. (Magnification X600.)

**ii.** Ectopic Strap was detected in U2OS cells stably expressing wild type Strap (HA-WT), HA-TPR, HA-OB and empty vector (V) using anti-HA antibody. Actin served as a loading control.

Stable cell lines created in both U2OS and SAOS2 cells were utilized in the xCELLigence system. Under normal conditions, the growth rates for wild type Strap, TPR motif and OB fold expressing cells were slightly reduced compared to the control U2OS cells (**Figure 3.2Ai**), and this was more apparent in SAOS2 cells (**Figure 3.2Aii**). Interestingly, in U2OS cells, a sharp decrease in cell index was apparent in wild type Strap overexpressing cells in response UV light treatment, which was less conspicuous in TPR motif and the OB fold overexpressing cells (**Figure 3.2Bi**). This was indicative of reduced cell viability in response to DNA damage for wild type Strap expressing cells compared to the TPR motif and OB fold expressing cells. In SAOS2 cells, both wild type Strap and TPR motif overexpressing cells demonstrated increased viability compared to the OB fold overexpressing cells under DNA damage condition (**Figure 3.2Bii**). In contrast, in the OB fold overexpressing cells, there was a decreased viability even in the absence of p53 suggesting that the OB fold alone may have p53-independent functions (**Figure 3.2Bii**).

Together, these data indicate the TPR motif and the OB fold have similar localisation as wild type Strap. U2OS stably expressing wild type Strap cells mediate p53-dependent reduced cell viability upon DNA damage treatment. Interestingly, this study suggests that the OB fold expressing cells have a p53-independent function in response to damage.

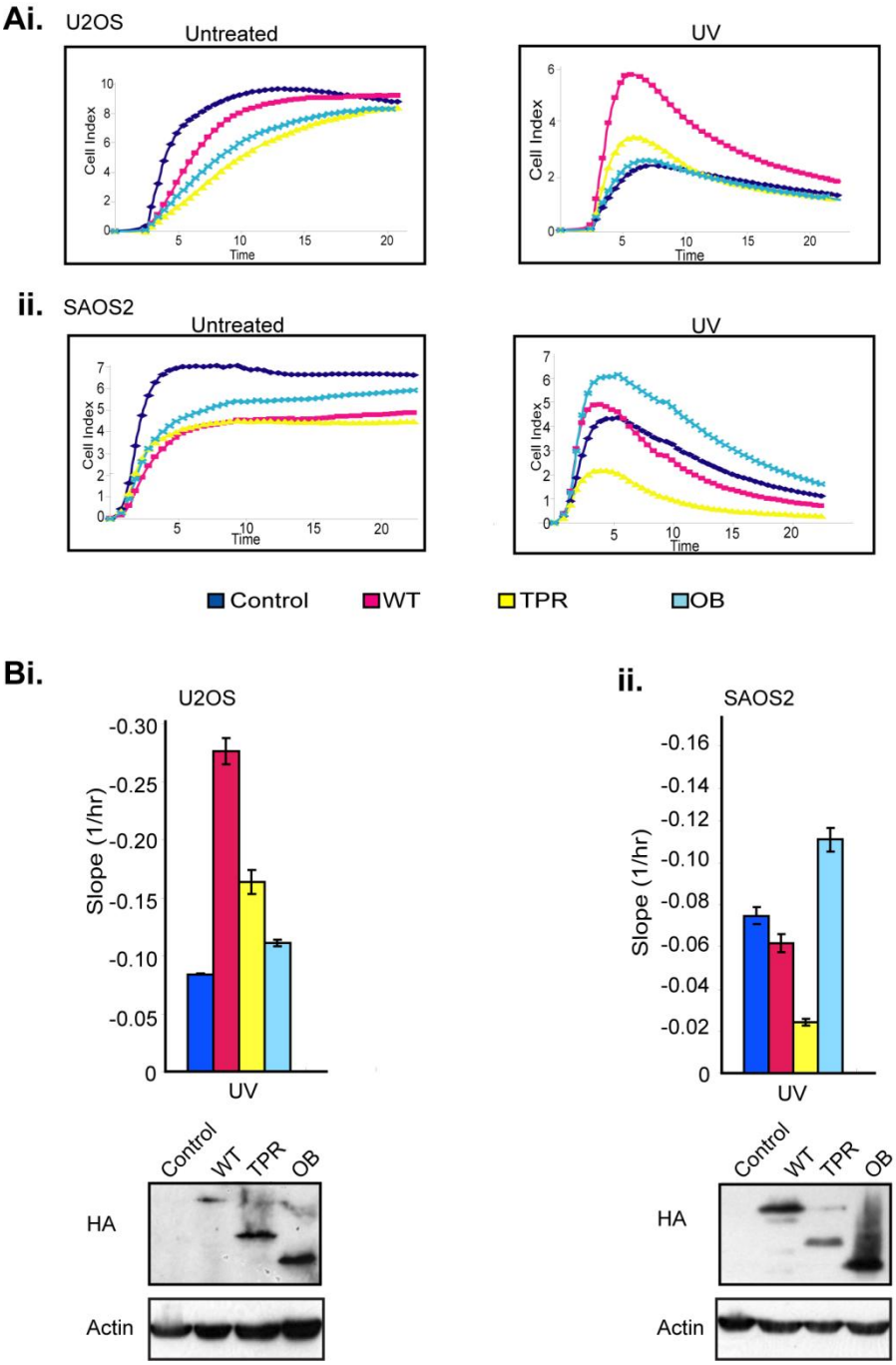



**Figure 3.2 Functional analyses of Strap stable cell lines.**

**A.** Stably transfected empty vector (control), wild type Strap (WT), TPR motif and the OB fold in U2OS (**i**) and SAOS2 (**ii**) were either untreated or treated with UV light (50 J/m$^2$) as indicated.

**B.** Following continuous xCELLigence cell monitoring in **A**, the slope (which represents the rate of change of the cell index from 5 to 20 hr) was calculated in U2OS (**i**) and SAOS2 (**ii**) stably transfected with either vector control, wild type Strap (WT), HA-TPR or HA-OB. The bottom panels represent input protein levels of the stably transfected cell lines. Ectopic Strap was detected using the anti-HAantibody. Actin served as a loading control.

### 3.2 Inducible cell lines

The inducible system is based on the discovery of the tetracycline resistance operon, Transposon (Tn) 10 in *Escherichi*a *Coli*. The tetracycline resistance operon encodes a repressor protein (TetR). The repressor protein binds specifically to Tet Operator (Gossen et al., 1995). This binding represses the transcriptional activity of the adjacent promoter. In the presence of tetracycline, the repressor protein undergoes conformational changes upon binding (Gossen et al., 1995). The conformational changes prevent the repressor protein from binding to the operator, resulting in relieving the negative effect on the adjacent promoter (Gossen et al., 1995). In the inducible U2OS Tet-On® Gene Expression System from Clontech, the cells express a modified Tet regulatory protein that reverses the function of TetR and activates transcription in the presence of doxycycline. Doxycycline is used as an inducer instead of tetracycline due to doxycycline's ability to achieve complete activation at a significantly lower concentration and longer half-life compared to tetracycline (Gossen et al., 1995).

The OB fold has the ability to bind to proteins and interestingly also to oligonucleotides (Theobald et al., 2003). This feature of the OB fold might contribute to Strap's transcriptional role. To pursue this line of enquiry, stable inducible U2OS cells expressing the OB fold were created which served as a convenient tool for subsequent investigations. Stable inducible U2OS cells expressing wild type Strap had been previously created (Jansson et al., 2008). Several attempts were made to create stable inducible U2OS cells expressing the TPR motif which unfortunately, were not successful. The expression and localisation of the stable inducible U2OS cells expressing either the OB fold or wild

type Strap were examined by immunofluorescence and immunoblotting (**Figure 3.3**).

These stable inducible cell lines were used to evaluate the role of wild type Strap and the OB fold. Cells expressing wild type Strap in the presence of UV light showed an increase in cleaved PARP-1 levels, an apoptosis marker. In contrast, U2OS stable inducible cells expressing OB fold exhibited reduced p53 levels and PARP-1 cleavage (**Figure 3.4**). This suggests that the OB fold has a negative impact on p53 levels during DNA damage compared to wild type Strap.

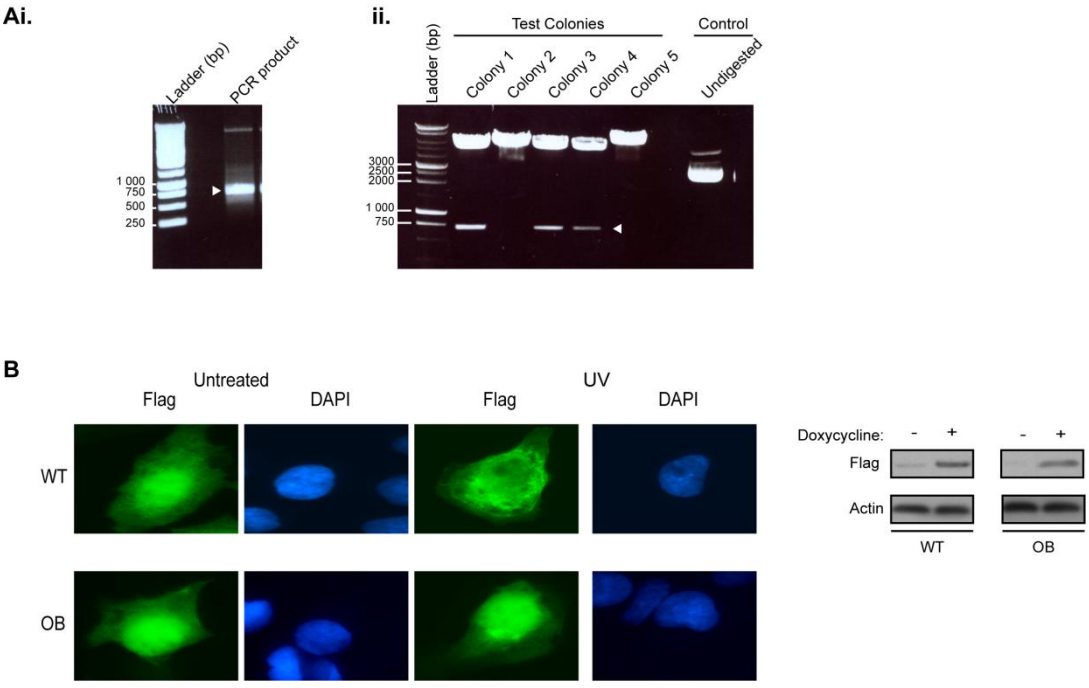



**Figure 3.3 Development of OB fold inducible cell line.**

**Ai.** Amplification of the OB fold fragment by PCR reaction. Arrowhead indicates the OB fold fragment, approximately 687 base pair (bp).

**ii.** Empty pTRE vector or vectors containing the OB fold insert (indicated by arrowhead) were digested with *BamHI* and *Not1* restriction enzymes. Undigested plasmid serves as negative control and the presence of the OB as an insert was detected via agarose gel electrophoresis. Plasmid with OB fold as an insert was verified by sequencing.

**B.** U2OS inducible stable cells expressing wild type Strap (WT) or the OB fold were induced with doxycycline (1 μg/ml) and either untreated or treated with UV light (50 J/m$^2$; 6 hr) as indicated. Samples were immunostained with anti-Flag antibody to detect ectopic Strap. DAPI staining was used to visualise the nuclei. (Magnification X600.) The right panels represent input protein levels of the U2OS inducible stable cells expressing wild type Strap (WT) or the OB fold that were either uninduced (-) or induced (+) with doxycycline (1 μg/ml). Ectopic Strap was detected using the anti-Flag antibody. Actin served as a loading control.

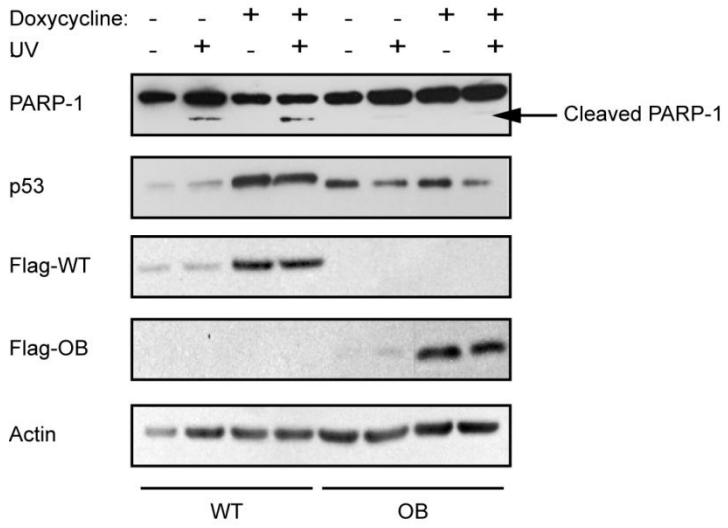



**Figure 3.4 Wild type Strap augments apoptosis in response to damage.**

Wild type Strap (WT) and OB fold inducible cell lines were either uninduced (-) or induced (+) with doxycycline (1 μg/ml) and treated with UV light (50 J/$m^2$, 6 hr) as indicated after which the levels of PARP-1 and p53 were determined by immunoblotting. Ectopic Strap was detected with anti-Flag antibody and actin served as a loading control.

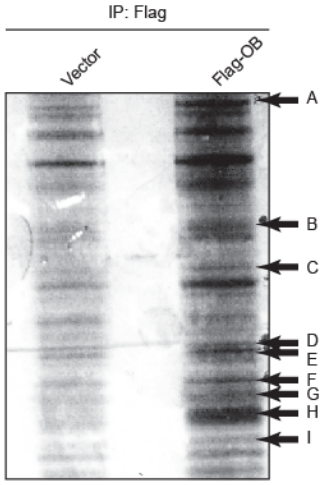
### 3.3 Introduction to proteomic analysis

Protein-protein interaction mapping is of great value in understanding the molecular mechanism of cellular functions as well as disease (Cho et al., 2004). The immunoblot analysis on immunoprecipitated samples is only employed to confirm known or hypothesized interacting proteins whilst mass spectrometry analysis serves as a powerful tool to screen and identify novel interacting proteins. To identify interacting proteins, immunoprecipitation of ectopic protein expressed in cells followed by a mass spectrometry approach was used. The immunoprecipitated samples were silver stained and enzymatically digested before analysed using liquid-chromatography-coupled tandem mass spectrometry (LC/MS-MS). The U2OS stable inducible OB fold cells were employed in the mass spectrometry approach. Further to the Strap crystal structure elucidation as previously discussed (**Chapter 3.1**), it was of interest to identify OB fold interacting proteins. Identifying these proteins may aid in understanding the OB fold's role in Strap's function.

### 3.4 Proteomic analysis of the OB fold

The OB fold is a small structural motif originally named for its oligonucleotide/oligosaccharide binding properties and additionally it was reported that the OB fold facilitates protein-protein interactions as well (Perez-Arellano et al., 2007). The OB fold is derived mainly of β-strands which primarily recognize ssDNA and RNA (Perez-Arellano et al., 2007). The OB fold structure can either exist as a domain within a larger protein or in proteins that are entirely composed of several OB folds (Theobald et al., 2003). OB fold proteins have been identified as critical players in DNA replication, DNA recombination, DNA repair, transcription, translation, cold-shock response and telomere maintenance (Theobald et al., 2003). One of the main functions of the OB fold structure is to bind to nucleic acid (Theobald et al., 2003).

Broad spectrums of proteins were identified from the mass spectrometry analysis using MASCOT software on the OB fold associated protein complexes. This software compares the spectra obtained from the mass spectrometry to a database of theoretical spectra and how well they match. Matched spectra were rated according to ion score; the higher the ion score, the more likely it is not a random event. The interacting proteins identified from the mass spectrometry were scrutinized by MASCOT ion score and the protein's molecular weight (**Figure 3.5**).




| | Description | Score |
|---|---|---|
| A | i. Nucleolin, 76.752 | 583 |
| | ii. Endoplasmin, HSP90, 82.728 | 118 |
| | iii. DNA replication licensing factor, MCM3 | 101 |
| B | i. Eukaryotic translation initiation factor 3 subunit L, 66.912 | 368 |
| | ii. Ras GTPase-activating protein-binding protein 1, 52.217 | 322 |
| | iii. Pyruvate kinase isoenzyme M1/M2, 58.470 | 319 |
| | iv. T-complex protein 1- eta, 59.798 | 319 |
| | Gamma, 61.118 | 197 |
| | Epsilon, 60.089 | 168 |
| | Delta, 58.576 | 145 |
| | v. TGF-beta activated kinase & MAP3K7- binding protein, 54.895 | 106 |
| C | i. Elongation factor 1- alpha-1, 50.435 | 432 |
| | Gamma, 50.429 | 419 |
| | Alpha-2, 50.780 | 271 |
| | ii. 60s ribosomal protein L4, 49.953 | 356 |
| | iii. Dynactin subunit 2, 44.318 | 282 |
| | iv. Alpha enolase, 47.437 | 204 |
| D | i. 40s ribosomal protein 32.961 | 498 |
| | ii. 60s ribosomal protein L6 32.765 | 498 |
| | L10 34.423 | 194 |
| | iii. Eukaryotic translation initiation factor | |
| | 3 sub 1, 36.867 | 216 |
| | 2 sub 1, 36.371 | 55 |
| | Sub J, 29.047 | 54 |
| | iv. MEP50, 37.442 | 154 |
| | v. Poly (rc)- binding protein, 36.955 | 122 |
| | vi. Nucleophosmin, 32.854 | 95 |
| | vii.DNA apurunic lysa- 35.867 | 101 |
| | 35.991 | 100 |

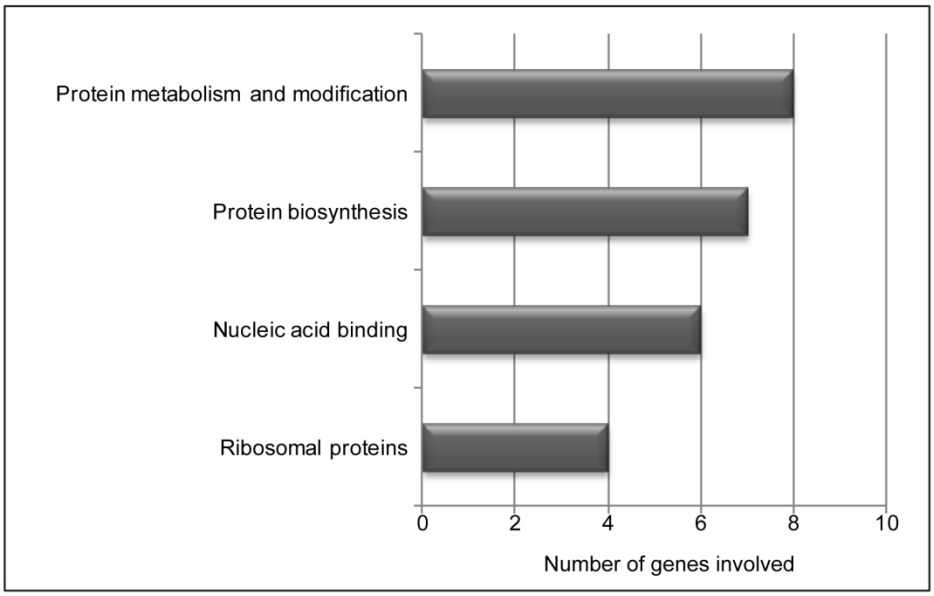
| | Description | Score |
|---|---|---|
| E | i. 60s acid ribosomal protein, 34.42 | 657 |
| | 33.984 | 127 |
| | ii. Eukaryotic translation initiation factor, 29.159 | 384 |
| | 36.371 | 165 |
| | 36.837 | 112 |
| | iii. MEP50, 37.507 | 119 |
| | iv. Nucleophosmin, 32.854 | 95 |
| | v. 40s ribosomal protein 32.961 | 64 |
| | vi. 26s proteasome regulating subunit PRNII, 34.433 | 53 |
| F | i. 60s acid ribosomal protein L7, 30.129 | 436 |
| | ii. 40s ribosomal protein S39 29.796 | 436 |
| | S6 28.834 | 356 |
| | S2 31.590 | 292 |
| | iii.Methylosome subunit pICln, 26.370 | 243 |
| G | i. 40s ribosomal protein S3 26.842 | 545 |
| | S4 29.807 | 520 |
| | S6 28.834 | 485 |
| | ii. 60s acid ribosomal protein L7, 29.264 | 305 |
| | L8, 28.335 | 268 |
| H | i. TTC5/Strap, 49.109 | 648 |
| | ii. 60s acid ribosomal protein L14, 23.535 | 268 |
| | L19, 23.565 | 261 |
| | L13, 24.304 | 204 |
| | L15, 24.425 | 94 |
| | L10, 24.987 | 60 |
| | iii. 40s ribosomal protein S8, 24.475 | 373 |
| I | i. 60s acid ribosomal protein L9, 21.978 | 267 |
| | L10, 25.032 | 256 |
| | L17, 21.611 | 356 |
| | L18, 21.735 | 441 |
| | L29, 17.798 | 150 |
| | ii.40s ribosomal protein S9 22.635 | 229 |

**Figure 3.5 Immunoprecipitation and mass spectrometry of the OB fold.**

U2OS stable inducible cells expressing either the OB fold or vector control (vector) were induced with 1 µg/ml of doxycycline for 16 hr before harvesting and immunoprecipitating with anti-Flag antibody. Immunoprecipitated material was run on SDS-PAGE and silver stained. Bands denoted were excised, in-gel digested with trypsin and analysed by LC-MS/MS. MASCOT score searches of the resulting peptide and its molecular weight are as indicated in the bottom table. Strap is highlighted in yellow.

In an attempt to understand the function of the OB fold, the interacting proteins identified from mass spectrometry were analysed by the bioinformatics analysis tool, DAVID (Database for Annotation, Visualization and Integrated Discovery). DAVID is a web based application consisting of integrated biological information and several analytical modules aimed at systematically extracting enriched biology from a large gene or protein list. To corroborate the findings from DAVID, and further identify pathways that were modulated in cells overexpressing the OB fold, the list of interacting proteins were further analysed using the PANTHER (Protein Analysis Through Evolutionary Relationships) database. PANTHER is a simplified ontology of protein function, which allows browsing of the database by biological function (Thomas et al., 2003). Filtering ($p>1E^{-05}$, Enrichment Score >1) of the interacting proteins identified from the OB fold immunoprecipitation were categorized into four clusters: proteins involved in protein metabolism and modification, protein biosynthesis, nucleic acid binding and ribosomal proteins (**Figure 3.6A**). Interestingly, when the interacting proteins were divided into more specific roles, more than 40% of the proteins identified were involved in DNA and RNA activity (**Figure 3.6B**). This was due to the high number of ribosomal proteins identified from the mass spectrometry analysis. The interacting proteins were also categorised in clusters that are involved in maintaining structural integrity of protein complexes (**Figure 3.6B**). Perhaps this might suggest that the OB fold may also contribute to Strap's function as a scaffolding protein that facilitates the recruitment of other proteins such as JMY and p300 to exert its response.

A




B

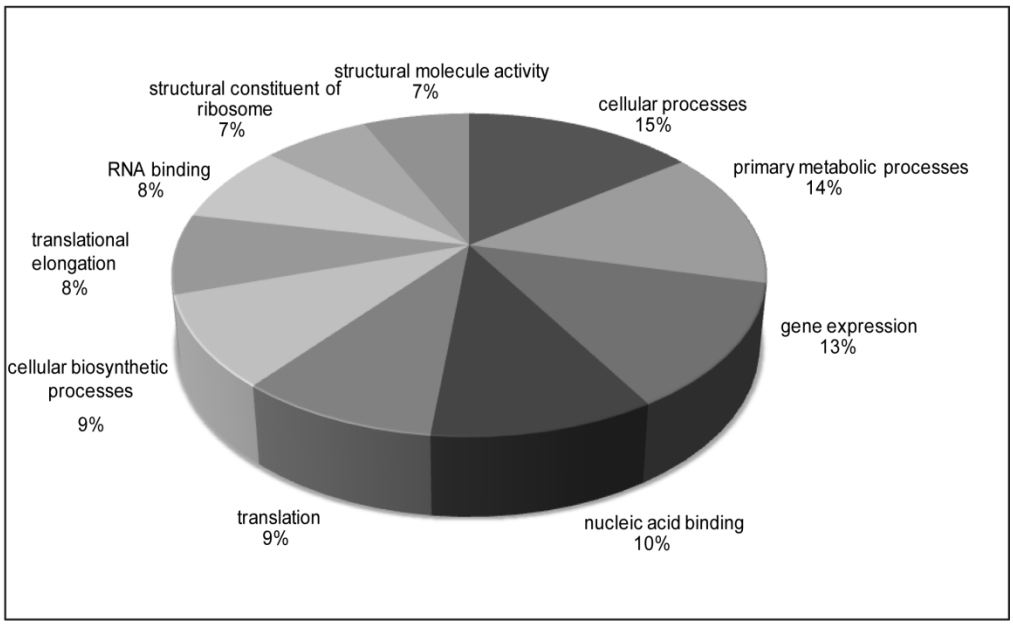



**Figure 3.6 Analysis of OB fold interacting proteins.**

**A.** Functional annotation analysis was performed using DAVID, 2012. The categories used were PANTHER molecular function (MF) and biological process (BP). The categories are shown for OB fold interacting proteins derived from mass spectrometry analysis.

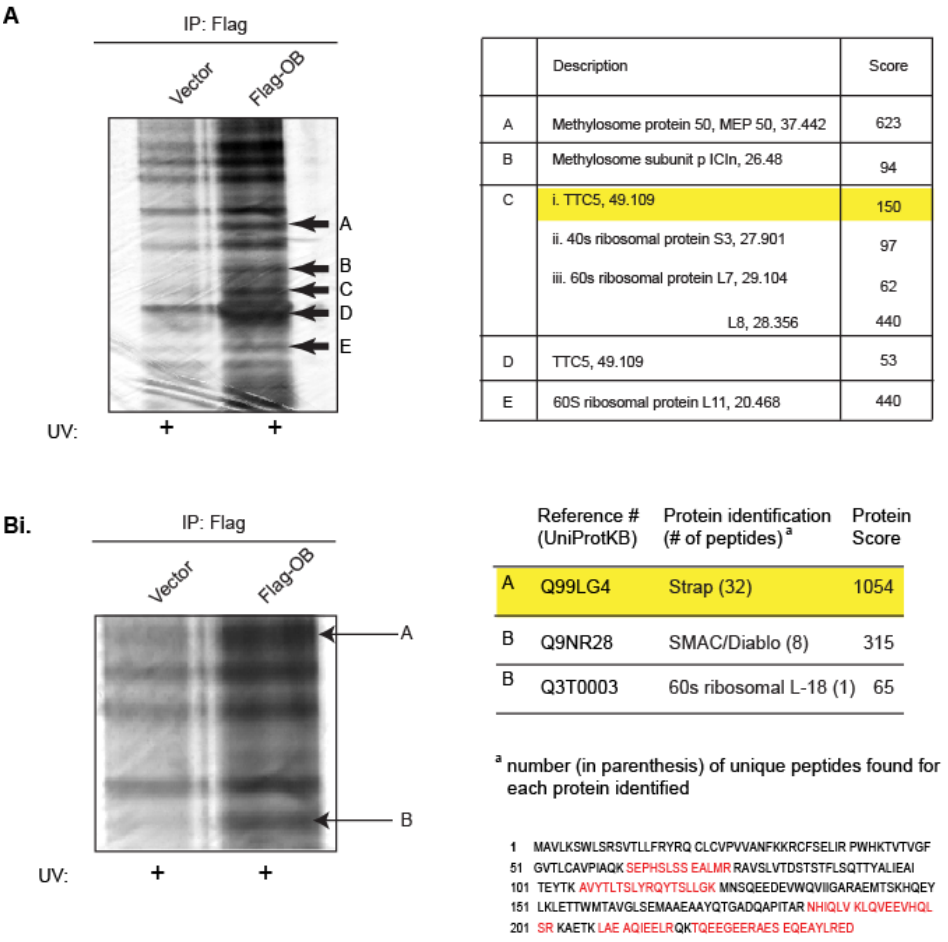
**B.** Pie chart summarizes the specific category according to Gene Ontology.

Taken together, the interacting proteins identified from the mass spectrometry analysis of the OB fold in the absence of damage concur with the function of the OB fold as a nucleic acid binding protein as well as facilitating protein-protein interactions.

### 3.5 Proteomic analysis of the OB fold under damage

In an attempt to compare the interacting proteins identified via mass spectrometry in the absence and presence of damage, U2OS stable inducible cells overexpressing OB fold were subjected to 50 $J/m^2$ of UV light for approximately 6 hr before harvesting and immunoprecipitation. The SDS PAGE gel was silver stained and excised bands were digested and sent for mass spectrometry analysis. Interestingly, compared to undamaged condition, less specific bands were present under damaged conditions (**Figure 3.7A**).

One of the proteins identified from the mass spectrometry analysis under damage conditions was the mitochondrial protein, SMAC/Diablo (**Figure 3.7Bi**). SMAC/Diablo had a MASCOT ion score of 315. To verify this interaction, endogenous immunoprecipitation in U2OS cells showed SMAC/Diablo co-immunoprecipitated with endogenous Strap under damaged and undamaged conditions (**Figure 3.7Bii**). The identification of a mitochondrial protein with high MASCOT ion score and its ability to form a complex with Strap prompted a more detailed investigation of the potential role of Strap at the mitochondria (discussed in depth in **Chapter 4**).




| | Description | Score |
|---|---|---|
| A | Methylosome protein 50, MEP 50, 37.442 | 623 |
| B | Methylosome subunit p ICln, 26.48 | 94 |
| C | i. TTC5, 49.109 | 150 |
| | ii. 40s ribosomal protein S3, 27.901 | 97 |
| | iii. 60s ribosomal protein L7, 29.104 | 62 |
| | L8, 28.356 | 440 |
| D | TTC5, 49.109 | 53 |
| E | 60S ribosomal protein L11, 20.468 | 440 |

| | Reference # (UniProtKB) | Protein identification (# of peptides) [a] | Protein Score |
|---|---|---|---|
| A | Q99LG4 | Strap (32) | 1054 |
| B | Q9NR28 | SMAC/Diablo (8) | 315 |
| B | Q3T0003 | 60s ribosomal L-18 (1) | 65 |

[a] number (in parenthesis) of unique peptides found for each protein identified

1 MAVLKSWLSRSVTLLFRYRQ CLCVPVVANFKKRCFSELIR PWHKTVTVGF
51 GVTLCAVPIAQK SEPHSLSS EALMR RAVSLVTDSTSTFLSQTTYALIEAI
101 TEYTK AVYTLTSLYRQYTSLLGK MNSQEEDEVWQVIIGARAEMTSKHQEY
151 LKLETTWMTAVGLSEMAAEAAYQTGADQAPITAR NHIQLV KLQVEEVHQL
201 SR KAETK LAE AQIEELR QKTQEEGEERAES EQEAYLRED

**Figure 3.7 Immunoprecipitation of OB fold under damage.**

**A & Bi.** U2OS stable inducible cells expressing either OB fold or vector control (vector) were induced with 1 µg/ml of doxycycline for 16 hr and treated with 50 J/m$^2$ of UV light for 6 hr before harvesting and immunoprecipitation with anti-Flag antibody. The bands denoted were excised, digested with trypsin and analysed by LC-MS/MS. MASCOT score searches of the resulting peptide and its molecular weight are as indicated in the table. Strap is highlighted in yellow.

**Bi.** The bold red amino acid residues show the MS/MS peptide coverage of SMAC/Diablo.

**ii.** Endogenous Strap from U2OS cells, treated with UV light (50 J/m$^2$, 6 hr) (+) or untreated (-) was immunoprecipitated and detected with anti-Strap antibody or a non-specific (NS) immunoprecipitation was carried out using rabbit IgG. SMAC was detected with anti-SMAC antibody. Inputs represent 5% of total protein.

### 3.6 Discussion

Mapping protein-protein interactions is an invaluable tool for understanding protein function. Mass spectrometry was used to map protein interactions of the OB fold. The lists of interacting proteins identified from mass spectrometry were categorized according to their biological role using bioinformatics tools. In order to appreciate the data obtained from mass spectrometry, DAVID coupled with PANTHER analysis was used to assemble a summary of the most enriched and pertinent biological functions of the proteins identified.

Mass spectrometry analysis of the OB fold under non damage condition identified many interacting proteins (**Figure 3.5**) but the converse was observed in the presence of damage (**Figure 3.7**). Of note, both ribosomal and methylosome proteins were detected in the presence and absence of damage.

Methylosome protein 50 (MEP50) identified from the mass spectrometry analysis of the OB fold was shown to form a complex with PRMT5 (Friesen et al., 2002). This complex was shown to be involved in small nuclear ribonucleoprotein (snRNP) assembly which is involved in pre-mRNA splicing (Friesen et al., 2002). The roles of MEP50 in snRNP assembly are not well understood. Since Strap was previously shown to aid PRMT5-regulated p53 methylation (Jansson et al., 2008), perhaps Strap may also facilitate the PRMT5-MEP50 interaction. This implies a new role of Strap in regulating pre-mRNA splicing via OB fold, an essential step in many gene expressions.

40% of the proteins identified from the OB fold mass spectrometry analysis were ribosomal and nucleic acid binding proteins. Strap has been shown to bind to ssDNA and dsDNA by biolayer interferometry assay (Adams et al., 2012). Perhaps Strap's nucleic acid-binding ability is provided by the OB fold, given that most OB fold containing proteins are associated with nucleic acids. An example of one such protein is the replication protein A (RPA), a well characterised ssDNA-binding protein that interacts with ssDNA via its OB fold domains (Fanning et al., 2006; Flynn and Zou, 2010).

A ribosome complex is made up of one or more ribosomal RNAs and large and small protein subunits. The complex process in translating mRNA into protein involves ribosomal proteins and occurs in four stages; initiation, elongation, termination and ribosomal recycling. Initiation refers to the assembly of a translation competent ribosome at the AUG start codon on an mRNA. The initiation process requires the separated 40s and 60s subunits which are assembled into an elongation-competent 80s ribosome with initiator methyl-tRNA (Aitken and Lorsch, 2012). The ribosomal proteins identified in the mass spectrometry analysis of the OB fold were the 40s and 60s subunits. The eukaryotic initiation factor (eIF)1a and eIF3 have been implicated in the dissociation of 80s ribosome into 40s and 60s (Kolupaeva et al., 2005). The OB fold mass spectrometry analysis also identified proteins such as the eIF3 which together with the 40s and 60s ribosomes are involved in the ribosome recycling process. It is thus tempting to postulate that the OB fold domain of Strap might be involved in ribosome recycling. Ribosome recycling serves as a link between translation, termination and initiation and ensures the 40s and 60s ribosomes are protected from re-association to prevent another

cycle of mRNA translation (Nurenberg and Tampe, 2013). This implies that Strap might play a role in ensuring the availability of free ribosomal subunits required for a new round of mRNA translation. The concept of the OB fold potentially interacting with the ribosomal proteins is supported by the identification of OB fold domain in bacterial ribosomal and ribosome-associated proteins. Ribosomal proteins S12, S17 and prokaryotic initiation factor work as an integral component within a vast assembly of complexes from various RNA and other relatively small proteins (Theobald et al., 2003).

Besides ribosomal proteins, it was indeed interesting to observe a mitochondrial protein (SMAC/Diablo) in the mass spectrometry analysis of OB fold (**Figure 3.7**). This would suggest that apart from being a transcriptional cofactor, Strap can also be localised to the mitochondria. Ribosomal proteins, metabolic enzymes and chaperones are commonly identified as contaminant protein as they are often present in large amount in cells (Berggard et al., 2007). Moreover, overexpressing a truncated protein in a physiological condition may cause a protein to become incorrectly localised and might not represent its *in vivo* localisation. In this case, the OB fold might be exerting different effects when expressed alone, compared to expression as a part of wild type Strap. In contrast, it is also possible that the interaction of wild type Strap and ribosomal proteins is weak. Nevertheless, it would be of interest to embark on the role of Strap in protein synthesis. Initially, this would mean testing whether Strap binds to RNA or forms an immunocomplex with the ribosomal subunits.

# Chapter 4:

# Results: Strap at the mitochondria

### 4.1 Strap is localised at the mitochondria

Mitochondria are the powerhouses of eukaryotic cells and play important roles in cellular metabolism and regulation. Several reports have shown that pools of transcription factors with well characterised functions in the nucleus are also present at the mitochondria (Szczepanek et al., 2012; Wegrzyn et al., 2009). One of the best studied of these is the transcription factor p53, which has been shown to directly regulate apoptosis at the mitochondria (Chipuk et al., 2004; Leu et al., 2004; Marchenko et al., 2000; Vaseva and Moll, 2009). Given that Strap is a p53 cofactor, the ability of Strap to localise to the mitochondria was investigated.

Initially, mitochondrial fractions from various cell lines were prepared and endogenous Strap was detected (**Figure 4.1A**). The levels of endogenous Strap were compared between total cell lysate, mitochondrial and cytoplasmic fractions (**Figure 4.1B**). Cellular fractionation methods will generally result in mitochondrial fractions with mixed other subcellular organelle. The most common cross-contaminants in mitochondrial fraction come from endoplasmic reticulum, plasma membrane and cytoskeletal elements. A highly enriched mitochondrial fraction allows detailed functional characterisation of Strap at the mitochondria. Highly enriched mitochondrial fractions with minimal cross-contamination of mitochondria and other organelles were determined by comparing different extraction techniques. The levels of Strap were compared in highly enriched mitochondrial fractions obtained using two different isolation kits (**Figure 4.2A**).

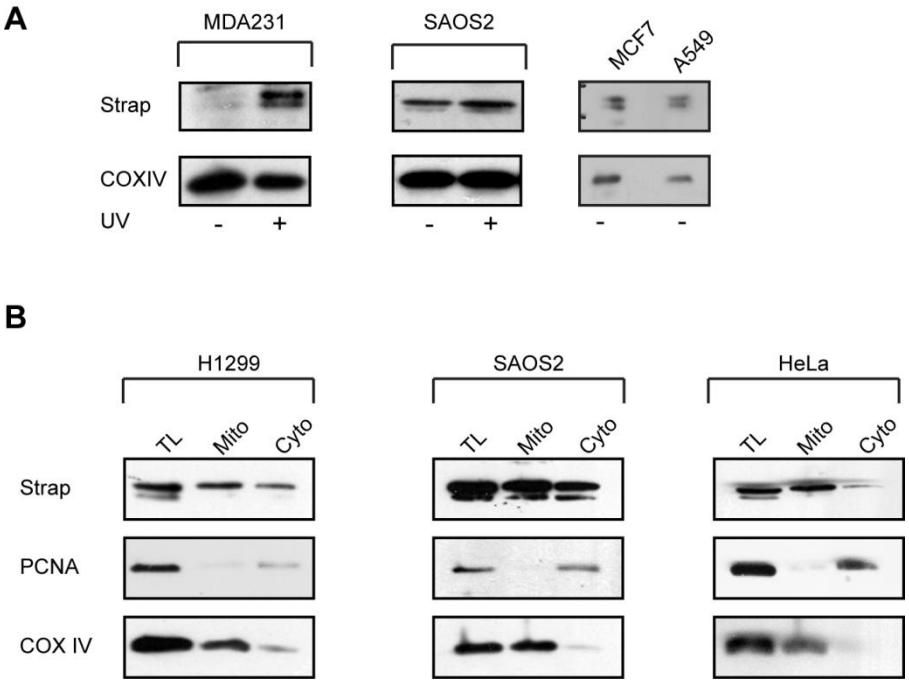



**Figure 4.1 Strap is localised at the mitochondria.**

**A.** Endogenous Strap was detected in mitochondrial fractions in different cell lines. Cytochrome oxidase IV (COXIV) was used as a mitochondrial marker.

**B.** Endogenous Strap was detected in total cell lysate (TL), mitochondrial fraction (Mito) and cytoplasmic fraction (Cyto) in different cell lines. Cytochrome oxidase IV (COXIV) and PCNA were used as mitochondrial and nuclear markers, respectively.

Both methods provided a good level of purified mitochondria with undetectable levels of PARP-1 (nuclear contamination marker) and calnexin (endoplasmic reticular contamination marker) in the mitochondrial fractions. Moreover, Strap was detected in commercially available purified mitochondria from human heart and in a mitochondrial fraction from MCF-7 cells prepared using the conventional sucrose gradient method (**Figure 4.2B**). To further confirm the detection of Strap at mitochondria, ectopic Strap was expressed in increasing concentrations and detected in both the mitochondrial fraction and total cell lysate (**Figure 4.2C**).

Accessibility to proteinase K was used to further asses the localisation of Strap at the mitochondria. Proteinase K, a non-specific serine protease is unable to penetrate the mitochondrial membrane (Reef et al., 2006). Its ability to digest proteins that are exclusively located at the surface of the mitochondria was used to investigate the specific mitochondrial localisation of Strap. TritonX-100 results in solubilisation of the membranes and therefore enables the proteins to be susceptible to proteinase K digestion. Mitochondrially localised Strap was sensitive to proteinase K digestion in the absence and presence of damage, similar to that of BCL-2, an antiapoptotic protein located at the surface of the outer mitochondrial membrane (**Figure 4.3**). This implies that Strap is most likely a mitochondrial surface protein. In contrast, COXIV, a mitochondrial inner membrane space protein, was not affected by the digestion and only disappeared upon treatment with the detergent TritonX-100 (**Figure 4.3**). Collectively, the results from the different biochemical fractionation methods indicate that Strap is localised at the mitochondrial and the Proteinase K digestion suggests that Strap is a mitochondrial surface protein.

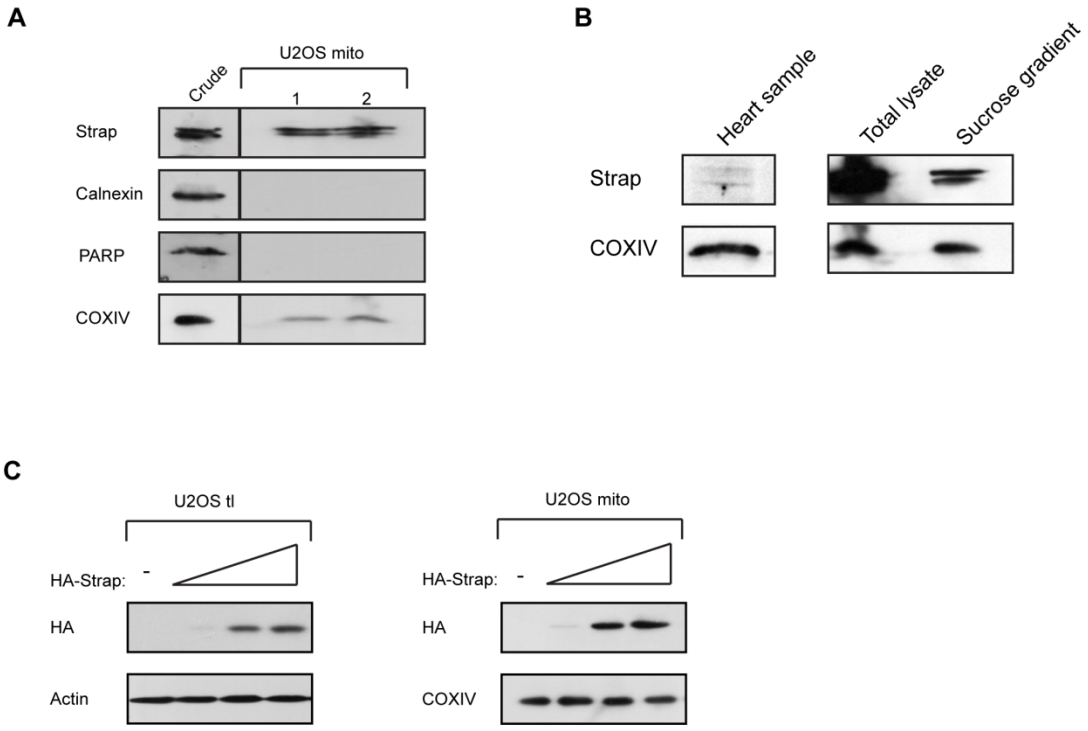



**Figure 4.2 Validation of Strap at mitochondria.**

**A.** Endogenous Strap was detected in the mitochondrial fractions prepared using different commercially available kits (1, 2). Nuclear and endoplasmic reticulum contaminations were monitored using PARP-1 and calnexin antibody respectively.

**B.** Endogenous Strap was detected in mitochondria fractions from heart (commercial) or sucrose gradient preparation. COXIV served as loading control for the mitochondrial fraction.

**C.** Mitochondrial fraction (right panel, mito) and total cell lysate (left panel, tl) were extracted from U2OS cells transfected with increasing concentrations of wild type Strap (HA-Strap). Ectopic Strap was detected using anti-HA antibody. COXIV and actin served as loading controls for the mitochondrial fraction and total cell lysate respectively.

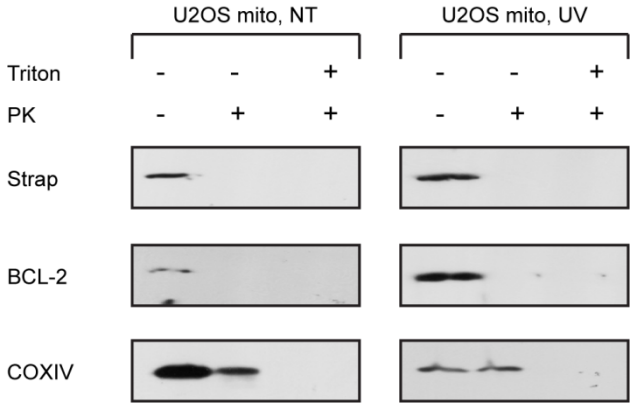



**Figure 4.3 Strap is localised at the outer mitochondrial membrane.**

Mitochondria fractions from U2OS cells were enzymatically digested by proteinase K (PK) in the presence and absence of TritonX-100 (1%) and subsequently analysed by immunoblotting. Mitochondria were isolated from cells that were either untreated (NT) or subjected to UV light (50 J/m$^2$, 3 hr) (UV) as indicated. BCL-2 and COXIV served as markers for the outer and inner mitochondria membrane protein, respectively.

### 4.2 Influence of p53 on mitochondrial Strap

Regulated protein relocalisation is a hallmark of the cellular response to genotoxic drugs that cause DNA damage or DNA replication stress (Tkach et al., 2012). Strap is upregulated upon DNA damage in the presence of p53 (Adams et al., 2008; Coutts and La Thangue, 2006; Demonacos et al., 2004). This prompted a closer examination on the effect of DNA damaging agents on mitochondrial Strap.

To assess Strap accumulation at the mitochondria, detailed time course studies on mitochondrial fractions upon DNA damage were performed. As depicted in **Figure 4.4** (**A & B, left panels**), the presence of Strap at the mitochondria was significantly decreased after 6 hr of damage. This is in contrast to the total cell lysate where Strap levels, as previously reported, were enhanced upon DNA damage (**Figure 4.4A & B, right panels**). This pattern was observed under different types of damage and was specific to Strap as another mitochondrial protein, COXIV, was not affected in the same way.

Collectively, these results indicate that Strap at the mitochondria is damage regulated.

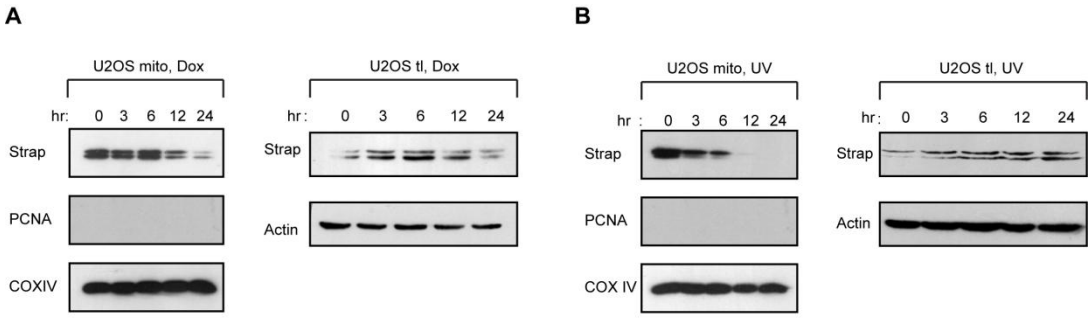



**Figure 4.4 Mitochondrial Strap is damage regulated.**

Levels of Strap were detected in immunoblots of mitochondrial fractions (**left panel**) and total cell lysate, (**right panel**) from U2OS cells before and up to 24 hr after treating with either 10 μM doxorubicin (**A**) or UV light, 50 J/m$^2$ (**B**). The level of PCNA, a nuclear protein, was used to assess the purity of the mitochondrial fraction. COXIV and actin were used as loading controls for mitochondrial fractions and total cell lysates, respectively.

### 4.3 Regulation of nuclear and mitochondrial Strap and p53

The detection of Strap at the mitochondria led to a hypothesis that it may affect mitochondrial p53 given Strap's role as a p53 cofactor (Adams et al., 2012; Demonacos et al., 2004). Initially, isogenic cell line pairs specifically differing in their p53 status were used in time course studies. Time course studies in $HCT116^{+/+}$ cells (which harbour wild type p53), reiterated the results observed earlier in U2OS cells (also wild type p53); a marked decrease in mitochondrial Strap after 6 hr of UV treatment (**Figure 4.5A, left panel**). Of note, in the absence of p53 ($HCT116^{-/-}$), mitochondrial Strap levels remained fairly constant during the DNA damage response (**Figure 4.5A, right panel**). This observation was corroborated in other cell lines harbouring either wild type p53 (U2OS) or devoid of functional p53 (SAOS2) (**Figure 4.5B**). Interestingly, the marked reduction in mitochondrial Strap coincided with decreased mitochondrial p53 (**Figure 4.5A & B, left panels**) suggesting that either p53 or Strap may influence the relocation of each other from the mitochondria during the DNA damage response.

Strap's established role at the nucleus prompted a closer examination of the levels of nuclear and mitochondrial Strap upon DNA damage. As expected, treatment of cells with DNA damaging agents resulted in an accumulation of Strap in total cell lysates (**Figure 4.5D & F**). Interestingly, the absence of p53 resulted in suppressed levels of nuclear Strap (**Figure 4.5C & E**). This was the converse to what was observed in the mitochondrial fraction; that is in the absence of p53, Strap was retained in the mitochondria (**Figure 4.5A & B, right panels**).

These data could be explained by two different possibilities, first is that Strap is a p53 target gene and the changes in the levels of Strap in the nucleus are transcription-dependent. The second is that p53 shuttles Strap from the mitochondria to the nucleus. In order to distinguish between these two possibilities, Strap mRNA levels were examined during the damage response. Quantification of steady state mRNA levels determines whether a protein is regulated at the transcriptional or post-translational level. Under conditions where increased Strap proteins levels were observed (**Figure 4.5D & F**), Strap mRNA levels appeared constant throughout the damage time course independent of p53 status (**Figure 4.6)**. Thus, the p53-regulated changes in Strap levels at the mitochondria and nucleus are not likely due to transcription of *Strap*.

### 4.4 Strap and p53 interact at mitochondria

To assess whether the changes in Strap levels in the absence and presence of p53 reflect a physical interaction, U2OS cells were subjected to UV treatment and p53 was immunoprecipitated. Strap co-immunoprecipitated with p53 under both damage and non damage conditions confirming a physical interaction between p53 and Strap as previously reported (Demonacos et al., 2001) (**Figure 4.7A**). To determine whether this p53-Strap interaction could occur at the mitochondria, L-p53, a full-length p53 construct fused with the BCL-2 targeting signal at the C-terminus (Marchenko et al., 2000) was transfected in a p53-deficient cell line (**Figure 4.8**). SAOS2 cells were transfected with L-p53 and stained with p53 and cytochrome c, a mitochondrial marker, confirming the localisation of L-p53 at the mitochondria (**Figure 4.8A**).

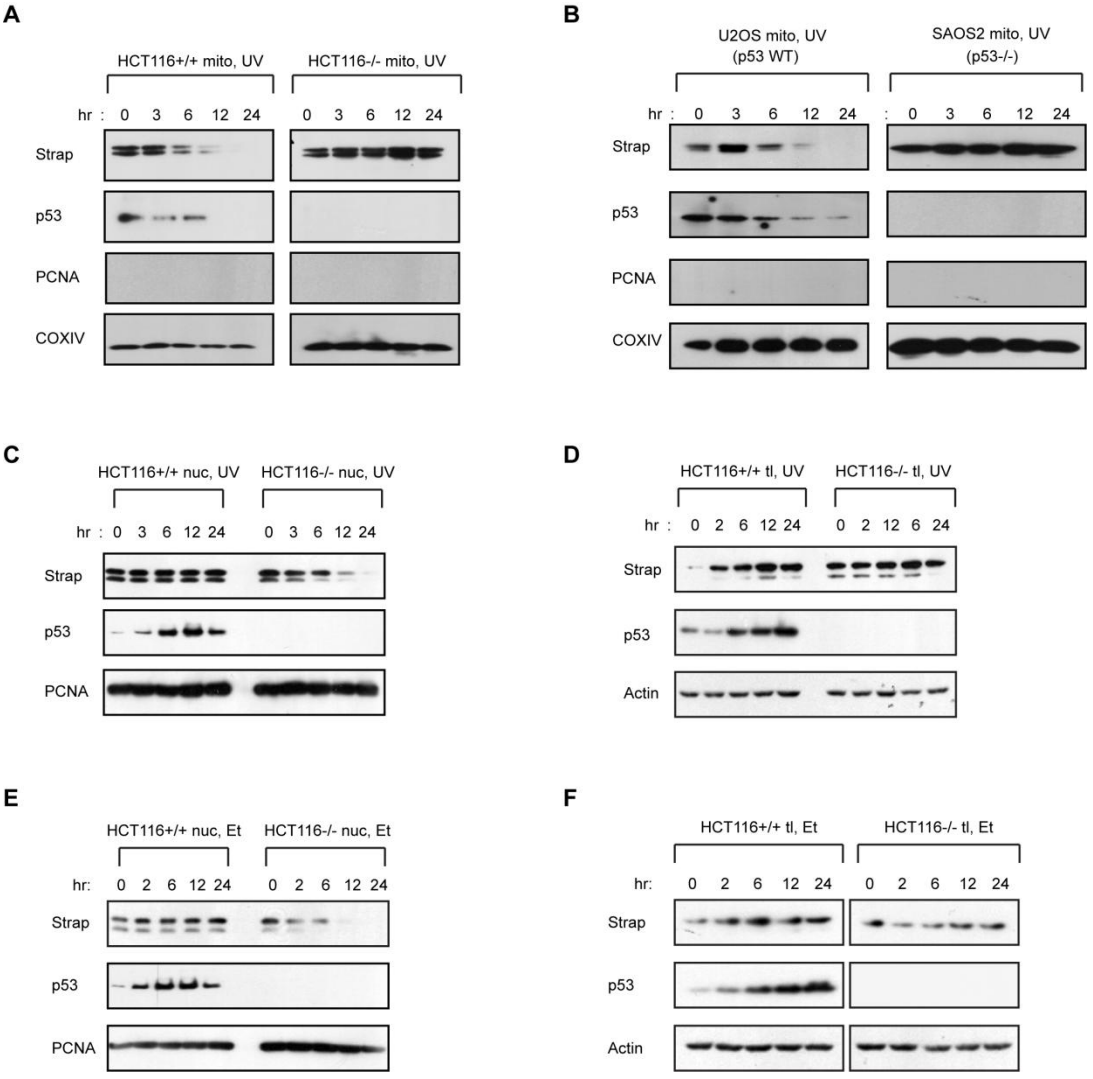



**Figure 4.5 Strap levels are influenced by the presence of p53.**

**A.** Immunoblots of mitochondrial fractions from HCT116$^{+/+}$ and HCT116$^{-/-}$ cells, before and up to 24 hr after treating with UV light (50 J/m$^2$).

**B.** Immunoblots of mitochondrial fractions from U2OS (left panel) and SAOS2 (right panel) cells, before and up to 24 hr after treating with UV light (50 J/m$^2$).

The level of PCNA, a nuclear protein, was used to assess the purity of the mitochondrial fraction. COXIV served as mitochondrial loading control.

Immunoblots of nuclear fractions (**C** & **E**) and total cell lysate (**D & F**) from HCT116$^{-/-}$ and HCT116$^{+/+}$ cells before and up to 24 hr after treated with either UV light (50 J/m$^2$), (**C & D**) or 40 μM of etoposide **(E** & **F**). Actin and PCNA served as loading controls for total cell lysates and nuclear fractions, respectively.

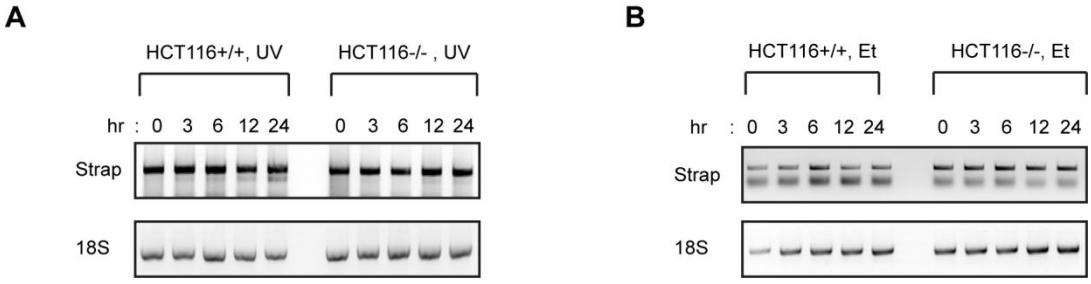



**Figure 4.6 Strap mRNA levels are not affected by damage.**

Semi quantitative RTPCR analysis on total RNA for endogenous Strap expression in $HCT116^{-/-}$ and $HCT116^{+/+}$ cells before and up to 24 hr after treating with either (**A**) UV light, 50 $J/m^2$ or (**B**) 40 μM of etoposide. 18S ribosomal RNA served as a loading control.

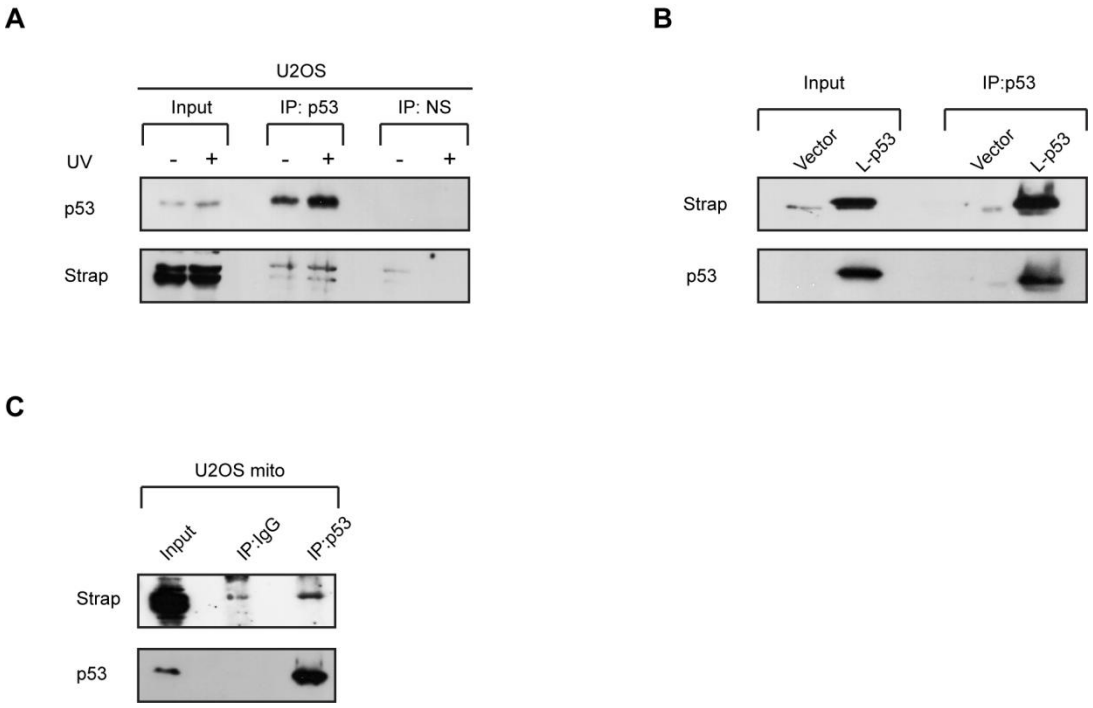



**Figure 4.7 Strap interacts with p53 at the mitochondria.**

**A.** Endogenous p53 from U2OS cells treated with UV light (50 J/m$^2$, 6 hr) (+) or untreated (-) was immunoprecipitated and detected with anti-p53 antibody or a non-specific (NS) immunoprecipitation was carried out using rabbit IgG. Strap was detected with anti-Strap antibody. Inputs represent 5% of total protein loaded.

**B.** p53 was immunoprecipitated from H1299 cells transfected with either L-p53 (mitochondria targeted p53) or vector control. Strap was detected with anti-Strap antibody and p53 was detected with anti-p53 antibody. Inputs represent 5% of total protein loaded.

**C.** Mitochondrial fractions (mito) from U2OS cells were immunoprecipitated and detected with anti-p53 antibody or a non-specific (IgG) immunoprecipitation was carried out using mouse IgG. Strap was detected with anti-Strap antibody. Inputs represent 5% of total mitochondrial extract.

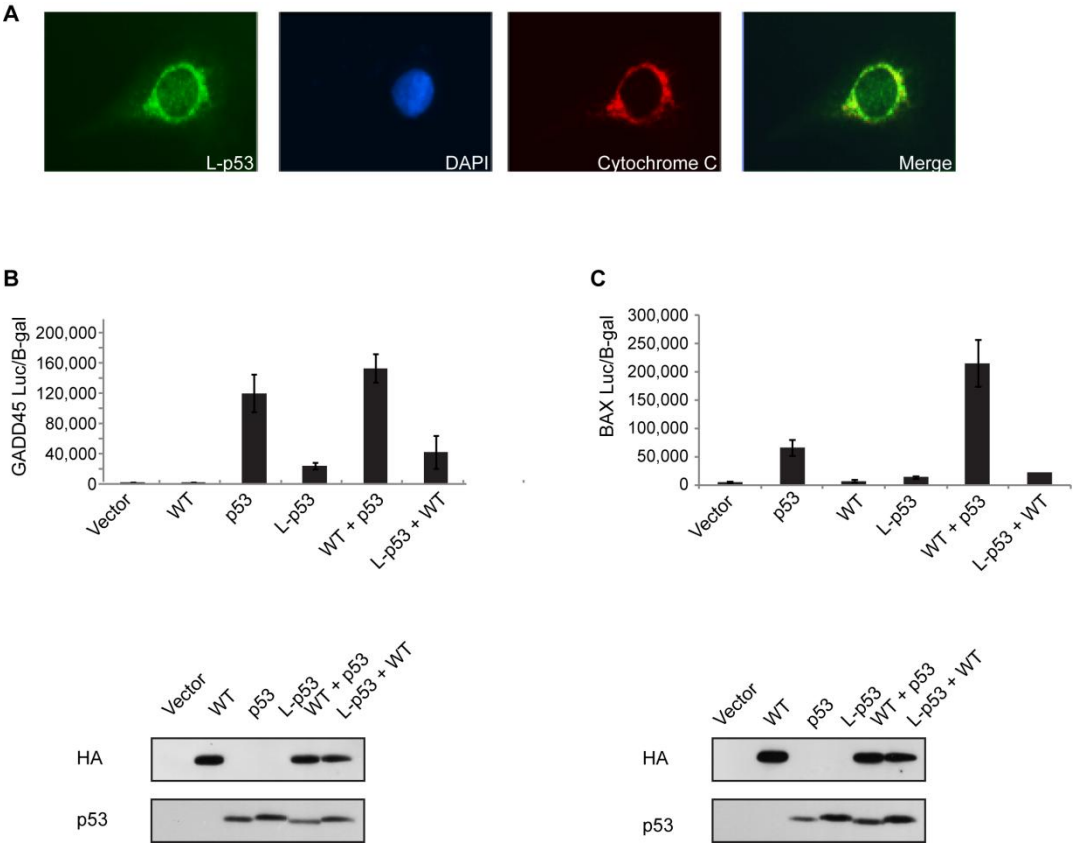



**Figure 4.8 Evaluation of mitochondrially targeted p53.**

**A.** SAOS2 cells were transfected with L-p53 and immunostained with anti-p53 antibody to detect ectopic L-p53. DAPI was used to visualize the nuclei and cytochrome c was used to stain mitochondria. Co-localisation of L-p53 and cytochrome c staining is shown (Merge). (Magnification X600.)

Luciferase reporter assays were performed using U2OS cells transfected with the indicated luciferase reporter construct, (**B**) GADD45 or (**C**) BAX luciferase in the presence of vector, wild type Strap (WT), p53 or L-p53 as indicated. The bottom immunoblots represent input protein levels. Values represent mean ± s.d. n = 3 independent experiments.

L-p53 failed to activate p53 promoters in reporter assays indicating a suppressed transcriptional activity as previously reported (Essmann et al., 2005; Mihara et al., 2003; Palacios and Moll, 2006; Talos et al., 2005) (**Figure 4.8B & C**). Endogenous Strap co-immunoprecipitated with L-p53 in p53 null cells, providing support for an interaction between p53 and Strap at the mitochondria (**Figure 4.7B**). Importantly, immunoprecipitation of endogenous p53 in the mitochondrial fraction from U2OS cells demonstrated a robust interaction between p53 and Strap (**Figure 4.7C**).

### 4.5 Strap reduces mitochondrial p53 levels

To explore the role of Strap and p53 at the mitochondria, Strap was depleted in U2OS cells and the levels of both Strap and p53 were observed. Interestingly, depletion of Strap caused an increase in mitochondrial p53 (**Figure 4.9A**) while the converse result was observed in total cell lysates (**Figure 4.9B**). Moreover, expressing increasing amounts of Strap in $HCT116^{+/+}$ (p53 wild type) cells resulted in a reduction in mitochondrial p53 (**Figure 4.10A**) but an increase in nuclear p53 (**Figure 4.10B**). A similar trend was observed when increasing amounts of ectopic p53 were expressed and levels of endogenous Strap were measured both in nuclear and mitochondrial fractions (**Figure 4.10C & D**).

Collectively, these data suggest that Strap and p53 influence each other's nuclear and mitochondrial localisation and potentially shuttle between the mitochondria and the nucleus upon DNA damage.

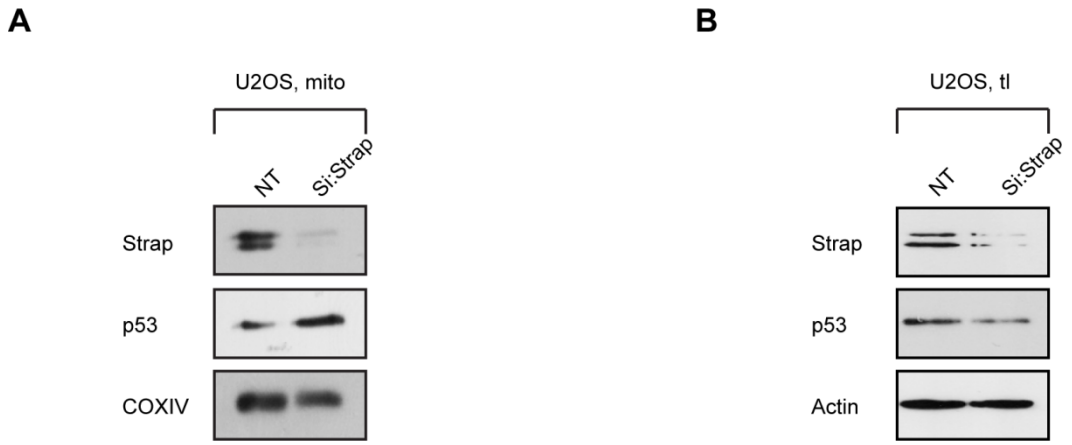



**Figure 4.9 Depletion of Strap enhances mitochondrial p53 levels.**

Mitochondrial fractions (**A**) and total cell lysates (**B**) were prepared from U2OS cells transfected with 90 nM non-targeting (NT) or Strap siRNA for 72 hr. Endogenous Strap and p53 were detected with anti-Strap and anti-p53 antibody respectively. COXIV and actin served as loading controls for mitochondrial fraction and total cell lysate, respectively.

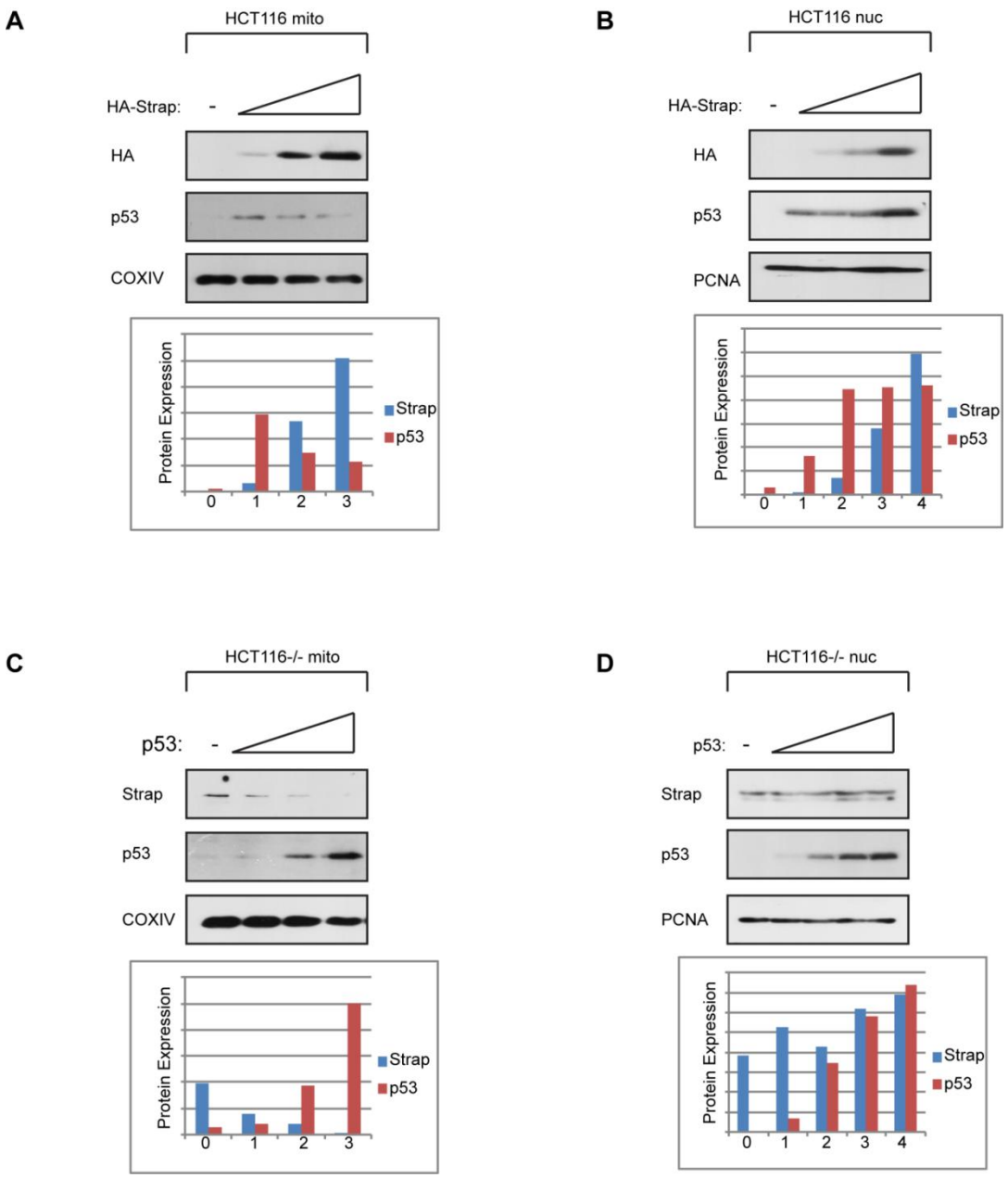



**Figure 4.10 Strap and p53 in the mitochondrial and nuclear fractions.**

Mitochondrial fractions (**A** & **C**) and nuclear fractions (**B** & **D**) were extracted from HCT116$^{+/+}$ and HCT116$^{-/-}$ cells transfected with increasing concentrations of wild type Strap (HA-Strap) in (**A** & **B**) or p53 (**C** & **D**) expression vector as indicated. Ectopic Strap was detected with anti-HA antibody and endogenous Strap was detected with anti-Strap antibody. Both ectopic and endogenous p53 were detected using anti-p53 antibody. COXIV and PCNA served as loading controls for mitochondrial and nuclear fractions, respectively. Quantification is graphically presented.

### 4.6 Strap augments BAK oligomerisation and cytochrome c release

Since Strap was found to be localised at the mitochondria, the functional consequences of this localisation warranted further investigation. The mitochondrial membrane contains pro- and antiapoptotic factors which can induce or prevent a lethal permeabilisation step which is the critical step in commitment to apoptosis in response to DNA damage. Initially, the levels of pro- and antiapoptotic BCL-2 family members, as well as cytochrome c release, in cells depleted of Strap were examined in the presence of damage.

In U2OS cells, depletion of Strap resulted in a decrease in the total level of cytochrome c in the presence of damage (**Figure 4.11A**, **left panel**). Moreover, a decrease in cytochrome c release from the mitochondria into the cytosol was observed upon depleting Strap (**Figure 4.11B**, **left panel**). Interestingly, depleting Strap also affected the BCL-2 family proteins, where a decrease in BAK and enhanced level of BCL-XL were observed in total cell lysate (**Figure 4.11A, right panel**) and mitochondrial fraction (**Figure 4.11B, right panel**) upon UV light treatment. This suggests that the induction of cytochrome c release in the presence of Strap is mediated by regulating the levels of BAK and BCL-XL at the mitochondria. The converse was observed upon depletion of Strap in p53 null cells (SAOS2), suggesting that this effect is p53 dependent (**Figure 4.11C**). The influence of Strap on cytochrome c release was also apparent in HCT116 cells when the level of endogenous Strap was depleted with siRNA, where reduced cytoplasmic cytochrome c was observed in cells with wild type p53 ($HCT116^{+/+}$) and not in p53 null cells ($HCT116^{-/-}$) (**Figure 4.11D**).

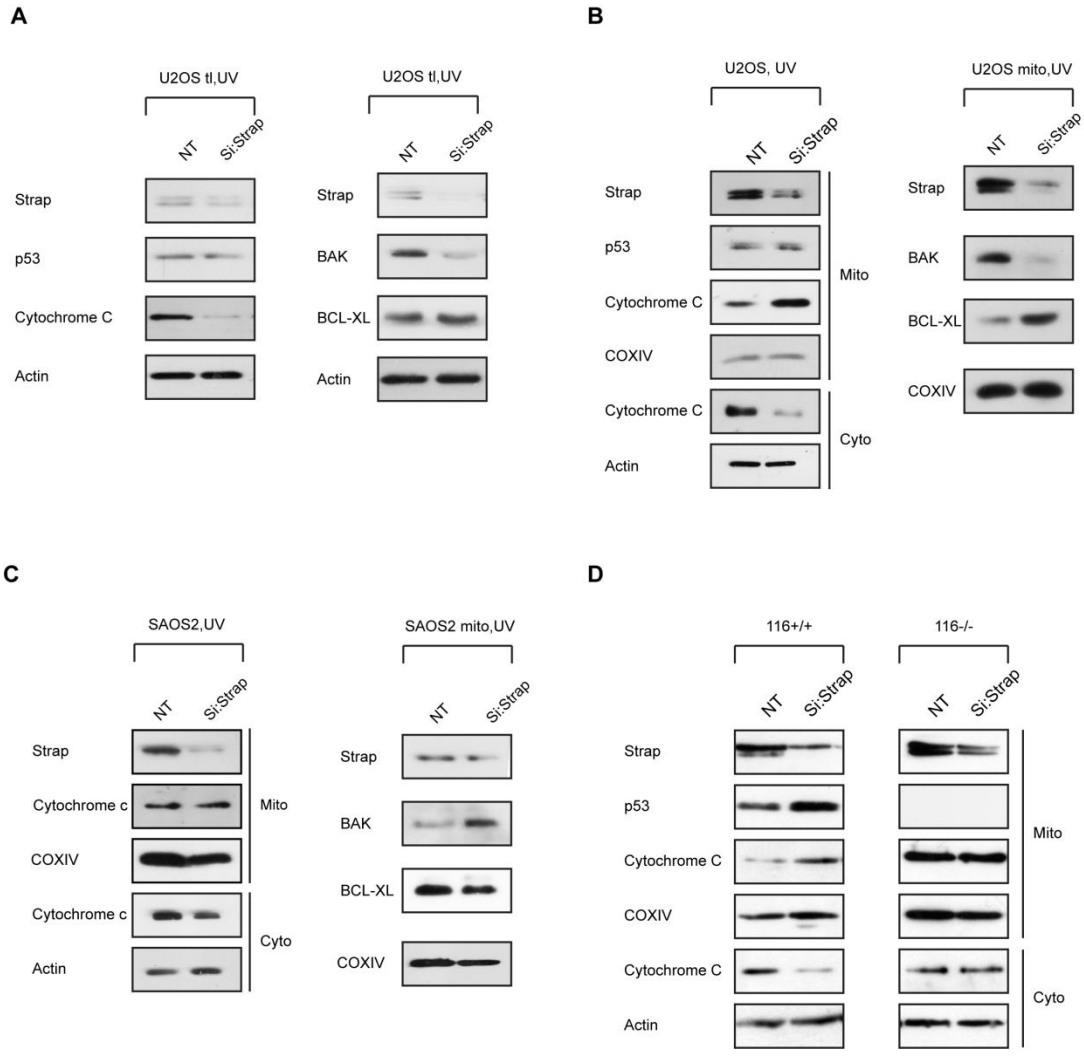



**Figure 4.11 Strap enhances cytochrome c release in the presence of p53.**

(**A**) and (**B**) U2OS cells were transfected with 90 nM non-targeting (NT) or Strap siRNA for 72 hr and were treated with UV light (50 J/m$^2$, 3 hr). Total cell lysate (**A**, **tl**), mitochondrial (mito) and cytoplasmic fractions (cyto) were then immunoblotted with the indicated antibodies. COXIV and actin were used as loading controls for the mitochondrial fraction and total cell lysate, respectively.

**C.** SAOS2 cells were transfected with 90 nM non-targeting (NT) or Strap siRNA for 72 hr and were treated with UV light (50 J/m$^2$, 3 hr). Mitochondrial and cytoplasmic fractions were then immunoblotted with the indicated antibodies. COXIV and actin were used as loading controls for mitochondrial and cytoplasmic fractions, respectively.

**D**. HCT116$^{+/+}$ and HCT116$^{-/-}$ cells were transfected with 90nM non-targeting (NT) or Strap siRNA for 72h and were treated with UV light (50 J/m$^2$, 3h). Mitochondrial (mito) and cytoplasmic fractions (cyto) were then immunoblotted with the indicated antibodies. COXIV and actin were used as loading controls.

The ability of p53 to directly bind and activate BAK (Leu et al., 2004) prompted an investigation on the involvement of Strap in BAK oligomerisation. Upon cross linking treatment, endogenous BAK was mainly detected in the form of dimers and higher order oligomers (**Figure 4.12A**). Reduced formation of BAK oligomers was observed when Strap was depleted in U2OS cells (**Figure 4.12A**). In contrast, no significant effect of BAK oligomerisation was observed in p53 null cells upon depletion of Strap (**Figure 4.12B**).

To establish a cause and effect relationship between p53 and Strap at the mitochondria, Strap was targeted to the mitochondria in the absence and presence of L-p53 in p53 null cells. Stressed-induced mitochondrial localisation of p53 has been shown to be sufficient to induce apoptosis (Mihara et al., 2003; Wolff et al., 2008). Strap targeted to the mitochondria (L-Strap) was generated by fusing the BCL-2 targeting signal at the C-terminus of Strap. The generation of this construct is described in detail in Chapter 5 (**Figure 5.1**). Of note, L-Strap was unable to activate p53 promoter activity (**Figure 4.13**).

In agreement with the literature, targeting p53 to the mitochondria induced cytochrome c release in the absence of DNA damage in p53 null cells (Mihara et al., 2003; Wolff et al., 2008) & (**Figure 4.14**). Interestingly, L-Strap alone was more efficient in its ability to cause cytochrome c release compared to L-p53. The presence of both L-p53 and L-Strap was able to augment the release of cytochrome c compared to expressing either of them alone. These effects were also observed upon treatment with UV light (**Figure 4.14**, **right panel**).

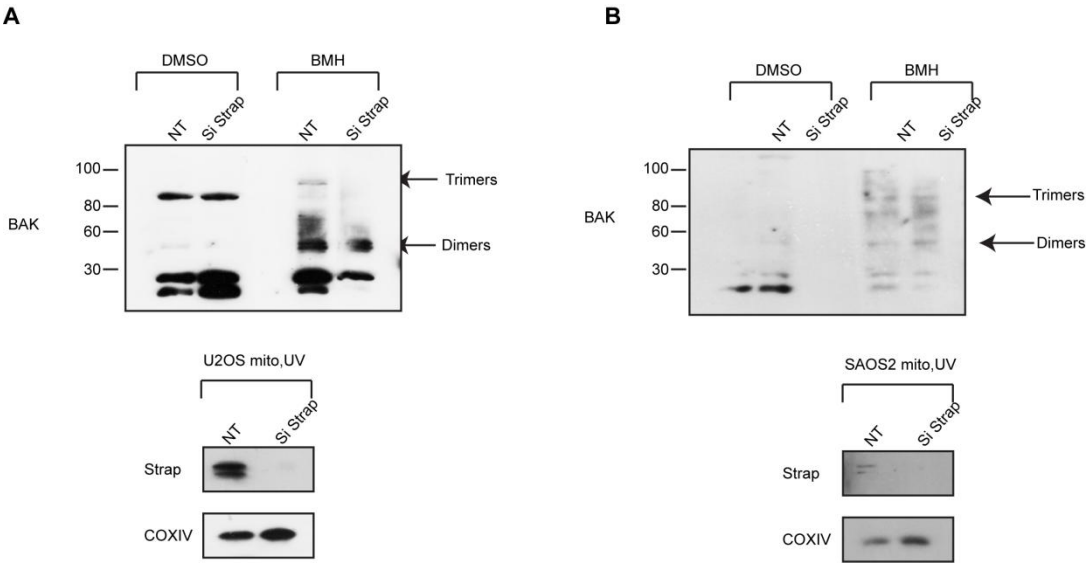



**Figure 4.12 Strap enhances BAK oligomerisation in p53 dependent manner.**

U2OS (**A**) and SAOS2 (**B**) cells were transfected with 90 nM non-targeting (NT) or Strap siRNA for 72 hr and were treated with UV light (50 J/m$^2$, 3 hr) as indicated. Purified mitochondria were crosslinked and immunoblotted with an N-terminal BAK antibody, known to recognize oligomeric BAK (Leu et al., 2004). The levels of Strap proteins are shown in the bottom panels. COXIV was used as loading control for the mitochondrial fraction.

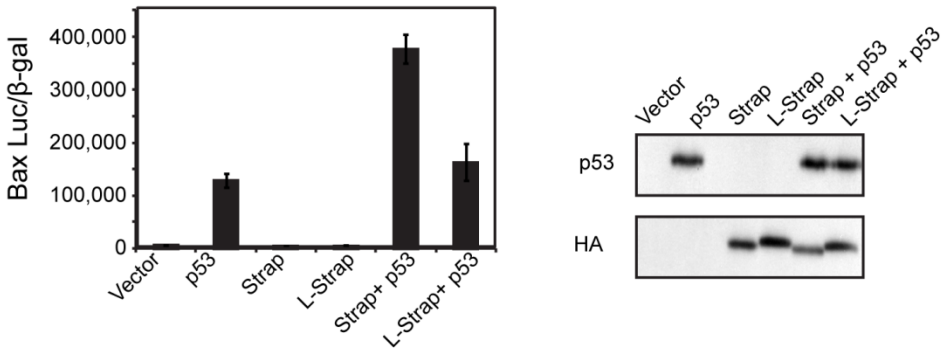



**Figure 4.13 Evaluation of mitochondrially targeted Strap.**

Luciferase reporter assay was performed using U2OS cells transfected with *BAX* luciferase construct in the presence of either vector, p53, wild type Strap (Strap) or L-Strap as indicated. Wild type Strap and L-Strap were detected using anti-HA antibody and p53 was detected using anti-p53 antibody. The immunoblots represent input protein levels. Values represent mean ± s.d. n = 3 independent experiments.

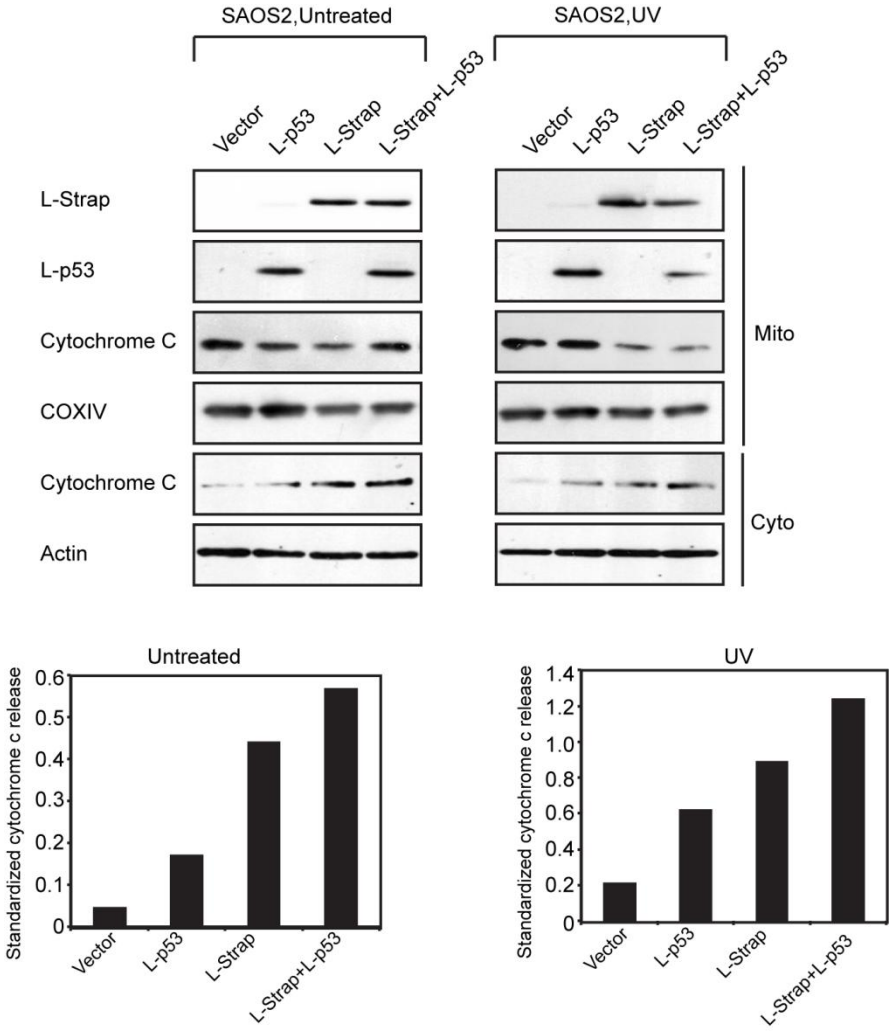



**Figure 4.14 Strap augments cytochrome c release in the presence of L-p53.**

Mitochondrial (Mito) and cytoplasmic (Cyto) fractions from SAOS2 cells transfected with either L-Strap or vector control in the presence or absence of L-p53 were prepared and analysed by immunoblotting with the indicated antibodies. COXIV and actin served as loading controls for mitochondrial and cytoplasmic fractions, respectively. Quantification is shown.

Mitochondrial membrane potential is a sensitive indicator of intrinsic apoptosis as it is often considered as the 'point of no return' in the cascade of events leading to apoptosis (Green and Kroemer, 2004). Cell lines stably expressing Strap were utilised due to the high levels of Strap induction which serves as a useful tool to explore the role of Strap at the mitochondria. U2OS cells expressing stable inducible and SAOS2 cells stably expressing wild type Strap, L-Strap and vector were generated. Initially, cell lines were validated by examining Strap induction in immunofluorescence and immunoblot **(Figure 4.15A & B**).

TMRE was used to measure mitochondrial membrane potential. TMRE is a cationic dye which readily accumulates in active mitochondria due to their relative negative charge (Perry et al., 2011). Approximately 94% of active cells were labelled with TMRE dye which indicated the majority of cells possess functional mitochondria that are able to generate membrane potential (**Figure 4.15C, left panel**). Initially, cells were treated either with specific mitotoxins (CCCP and oligomycin) or UV light. UV light treatment has been shown to cause DNA damage and triggers MOMP which results in mitochondrial membrane depolarization which induces apoptosis. CCCP which is an uncoupling agent (results in membrane depolarization) was used as a negative control whilst oligomycin a specific ATP synthase inhibitor (results in membrane hyperpolarisation) was used as a positive control for TMRE staining. Cells that were treated with UV light showed a shift to the left which is an indication of membrane depolarization (**Figure 4.15C, right panel**).

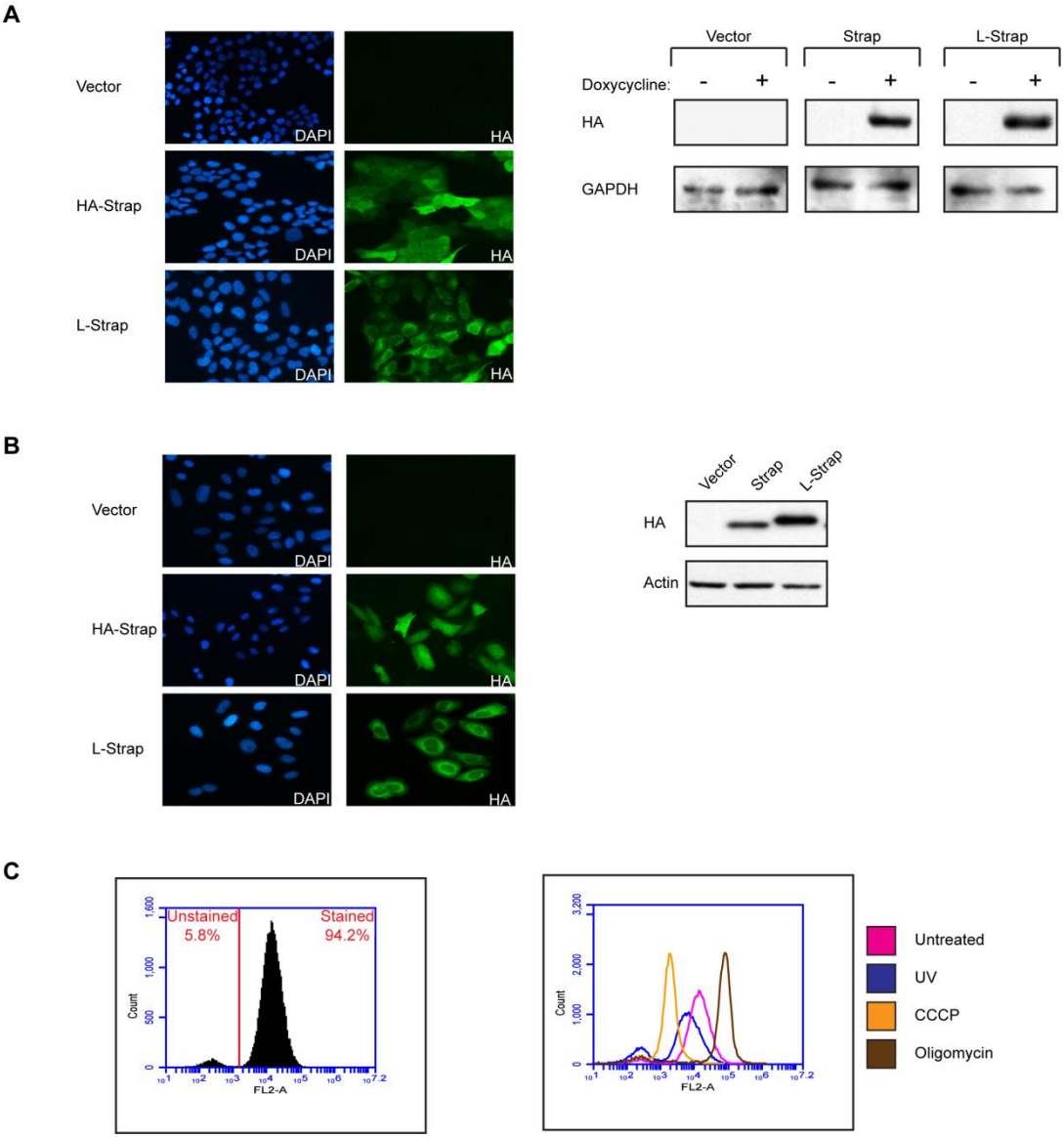



**Figure 4.15 Stably expressing cell lines and control for mitochondrial membrane potential staining.**

**A.** U2OS inducible stable cells were induced with doxycycline (1 µg/ml) and were immunostained with anti-HA antibody to detect ectopic Strap. DAPI staining was used to visualise the nuclei (Magnification X200). Immunoblot represents ectopic protein levels of the inducible stable cell lines either uninduced (-) or induced (+) with doxycycline. GAPDH was used as loading control.

**B.** Stably transfected SAOS2 cells were immunostained with anti-HA antibody to detect ectopic Strap. DAPI staining was used to visualise the nuclei (Magnification X200). Immunoblot represents ectopic protein levels of the stable cell lines. Actin was used as loading control.

**C.** TMRE staining (x axis) was detected in the FL2-A channel. The left profile shows the percentage of cells stained with TMRE. The right profile indicates the FACs profile of cells untreated, treated with CCCP (2.5 µM, 15 min), oligomycin (5 µg/ml, 30 min) and UV light (30 J/m$^2$, 16 hr).

The ability of Strap to induce mitochondrial-dependent apoptosis in the presence of p53 was further investigated by measuring mitochondrial membrane potential in U2OS cells (wild type p53) expressing stable inducible and SAOS2 (devoid of p53) cells stably expressing L-Strap and vector. In unperturbed cells, no significant changes in mitochondrial membrane potential were observed between cells expressing vector and L-Strap in both U2OS and SAOS2 cells (**Figure 4.16C & D**). Interestingly, when the cells were treated with UV light, U2OS cells expressing L-Strap showed a significant increase (10%) in membrane depolarization compared to vector (**Figure 4.16A & C**). No significant difference was observed in SAOS2 cells stably expressing vector and L-Strap (**Figure 4.16B & D**).

Taken together, the data suggest that Strap's effect on BCL-2 family proteins and the ability to enhance cytochrome c release via BAK oligomerisation is p53-dependent. Mitochondrial Strap was also shown to enhance p53-dependent mitochondrial membrane depolarization in the presence of damage. Collectively, Strap mediates p53-dependent apoptosis at the mitochondria.

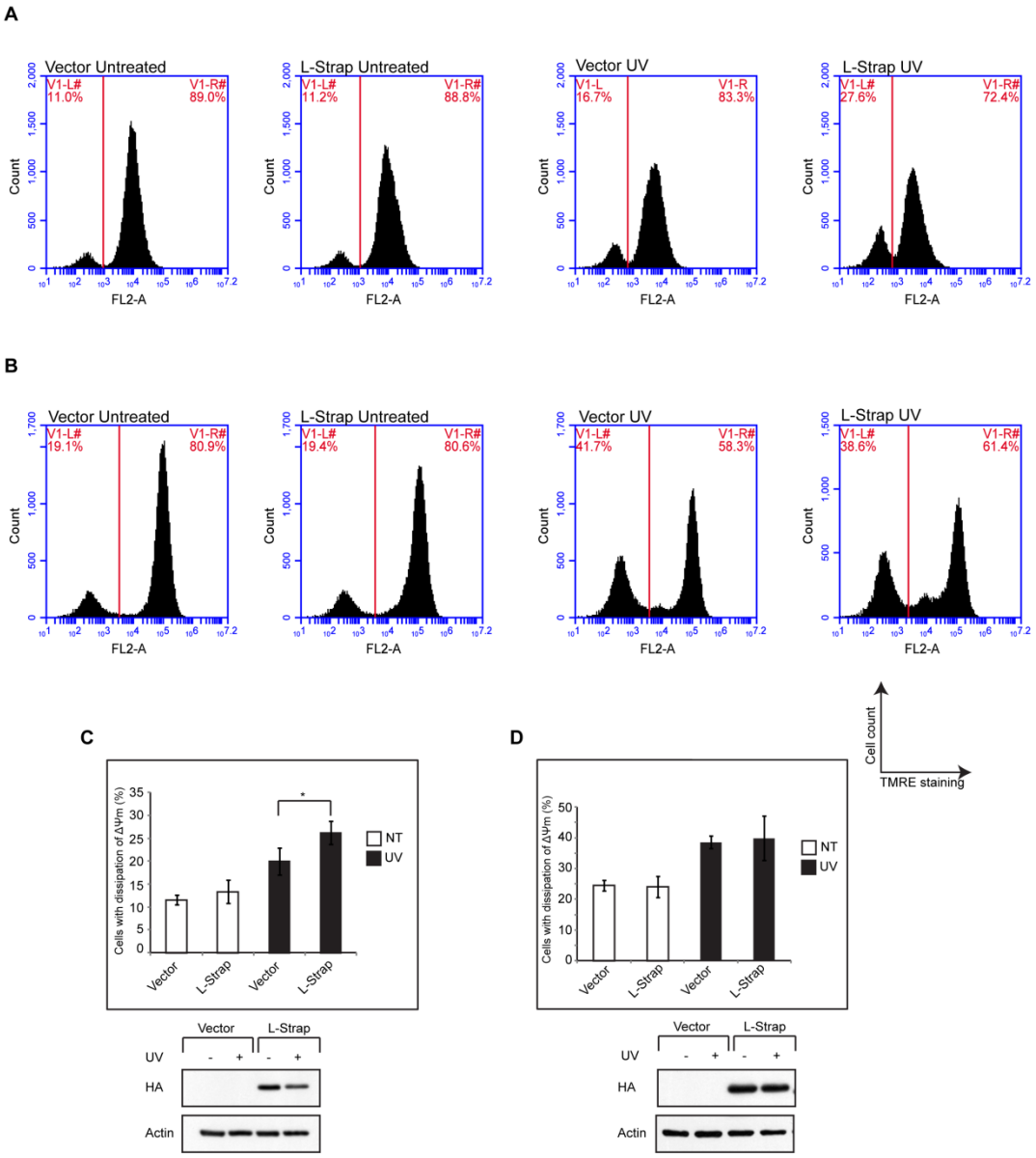



**Figure 4.16 Strap enhances mitochondrial membrane depolarization in the presence of p53.**

FACs profile and analysis of induced (with doxycycline, 1 µg/ml) U2OS stable inducible (**A** & **C**) and SAOS2 (**B** & **D**) cells stably expressing either vector or L-Strap stained with mitochondrial membrane potential specific dye, TMRE. Cells were either untreated (NT) or treated with UV light (30 J/m$^2$, 16 hr) as indicated. The levels of Strap proteins are shown via immunoblotting. Values represent mean ± s.d. * indicates $p<0.05$, Student's t-test, n = 3 independent experiments.

### 4.7 Strap augments apoptosis in the presence of p53

PARP-1 is recognized by cell biologists as a 'death substrate' because PARP-1 was one of the first identified substrates for caspases. PARP-1 cleavage is more appropriately viewed as a marker of apoptosis (Jagtap and Szabo, 2005). The ability of Strap to induce apoptosis was investigated by measuring cleaved PARP-1 levels. Initially, Strap was depleted in U2OS cells and a decrease in the levels of cleaved PARP-1 was observed (**Figure 4.17A**). This observation was extended by measuring the levels of cleaved PARP-1 over time when L-Strap and L-p53 were either expressed alone or co-expressed in p53 null cells (SAOS2). In the absence of L-p53 and L-Strap, cleaved PARP-1 was detected at 6 hr after damage (**Figure 4.17B, left panel**). When L-p53 was expressed alone, a slight increase in cleaved PARP-1 was observed as early as 2 hr after damage (**Figure 4.17B, second panel**). A sharp increase in cleaved PARP-1 was detected at 4 hr after damage when L-Strap was expressed alone (**Figure 4.17B, third panel**). Importantly, co-expression of L-p53 and L-Strap resulted in a dramatic increase in the induction of cleaved PARP-1 even under non damage conditions (**Figure 4.17B, right panel**).

These data collectively suggest that L-Strap and L-p53 have the ability to induce apoptosis and in combination can enhance the apoptotic response even in the absence of damage.

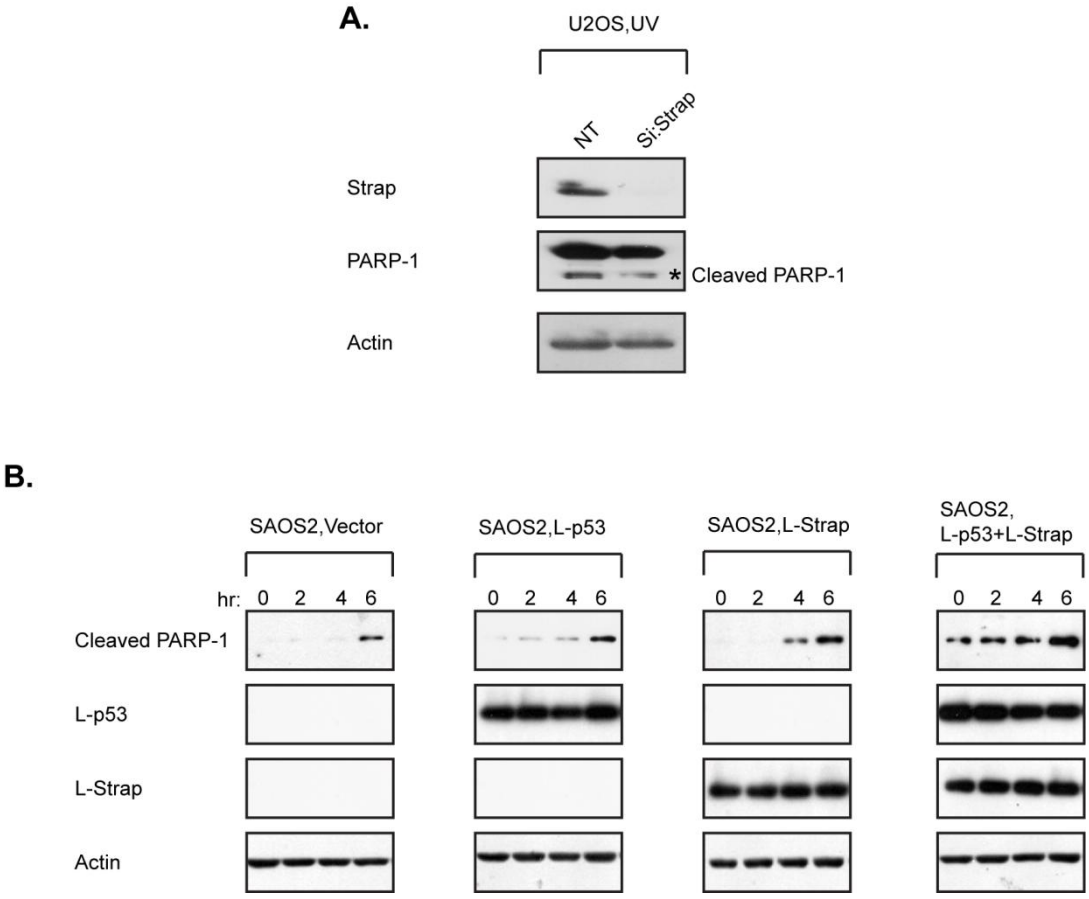



**Figure 4.17 Strap augments cleaved PARP-1 levels in the presence of p53.**

**A.** U2OS cells were transfected with 90 nM non-targeting (NT) or Strap siRNA for 72 hr and were treated with UV light (50 J/m$^2$, 6 hr). Cleaved PARP-1 antibody was used as an apoptotic marker while actin served as loading control. The asterisk indicates the cleaved PARP-1.

**B.** SAOS2 cells were transfected with either L-Strap or vector control in the presence or absence of L-p53. Cells were treated with UV light (50 J/m$^2$) and harvested at indicated time points. L-Strap was detected with anti-HA antibody and L-p53 was detected using anti-p53 antibody. Cleaved PARP-1 was used as an apoptotic marker while actin served as loading control.

To investigate the role of wild type Strap and L-Strap in the cellular stress response, cell viability in stable inducible U2OS cells expressing vector, wild type Strap and L-Strap during DNA damage was measured using the xCELLigence system. This system allows label-free and real-time monitoring of cell viability which is reported as cell index. As depicted in **Figure 4.18A** (**upper left**), in untreated conditions, U2OS cells expressing vector, wild type Strap and L-Strap exhibited similar growth properties. Interestingly, both wild type Strap and L-Strap showed a sharp decrease in cell index compared to vector upon DNA damage (**Figure 4.18A, lower left**). A decrease in cell index implies reduced cell viability. L-Strap showed an approximately 3.5-fold decrease in cell index upon UV treatment compared to vector control (**Figure 4.18A, upper right**). In a parallel study performed in SAOS2 cells, no significant effects were observed between wild type Strap and L-Strap expressing cells (**Figure 4.18B**).

These data suggest that Strap at the mitochondria augments cell death in response to DNA damage in the presence of p53.

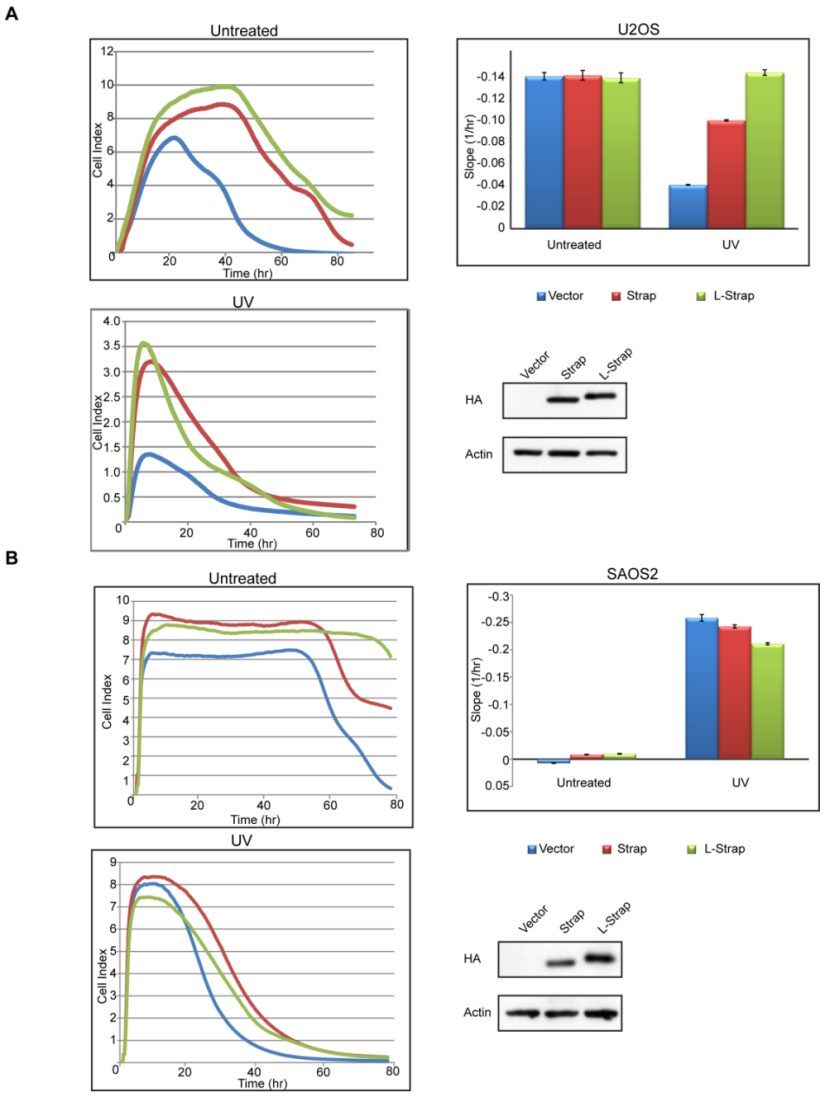



**Figure 4.18 Strap enhances cell death in the presence of p53 upon damage treatment.**

**A.** Stable inducible U2OS cells stably expressing wild type Strap (red), L-Strap (green) or control (dark blue) were induced with 1 µg/ml of doxycycline and were either untreated (**top left panel)** or treated with UV (50 J/m$^2$) (**bottom left panel**) as indicated. 5,000 cells/well were plated into an E-plate 16 and analysed using xCELLigence RTCA DP instrument. Following the continuous xCELLigence cell monitoring, the slope (which represents the rate of change of the cell index from 10 to 60hr after UV treatment) was calculated and presented graphically (**top right**). The levels of Strap proteins are shown via immunoblotting (**bottom right**). Values represent mean ± s.d., n = 3 independent experiments.

**B.** SAOS2 cells stably expressing wild type Strap (red), L-Strap (green) or control (dark blue) were untreated (**top left panel**) or treated with UV (50 J/m$^2$) (**bottom left panel**) as indicated. Following the continuous xCELLigence cell monitoring, the slope (changes in cell index from 5 to 60hr after \uv treatment) was calculated and presented graphically (**top right**). The levels of Strap proteins are shown via immunoblotting (**bottom right**). Values represent mean ± s.d., n = 3 independent experiments.

## 4.8 Summary

Mitochondria play an important role in the initiation of programmed cell death. Although mitochondria contain a genetic and protein synthesis system in the matrix, approximately 99% of mitochondrial proteins are encoded in the nucleus of the cells (Becker et al., 2012; Schmidt et al., 2010). A small but significant amount of Strap is localised at the mitochondria (**Figure 4.1**). This low amount is not surprising as it has been reported that pools of nuclear transcription factors that are localised at the mitochondria are very small compared to the levels in the cytosol or nucleus (Szczepanek et al., 2012). Strap was identified as a mitochondrial surface protein using Proteinase K digestion assay (**Figure 4.3**). Due to the intense cytoplasmic staining of Strap observed via immunofluorescence staining, a detailed investigation on Strap's localisation at the mitochondria using electron microscopy was not possible.

Strap was previously shown to augment the p53 response and importantly Strap levels were regulated under stress (Demonacos et al., 2001). In this study, it was shown that Strap and p53 may facilitate each other's localisation from the mitochondria to the nucleus (**Figure 4.5 & 4.6**). Interestingly, Strap interacts with mitochondrial p53 and this suggests a new transcriptional independent cellular response to stress of Strap in the presence of p53 (**Figure 4.7**).

A wide variety of PTMs were shown to influence p53 nuclear import hence promoting its transcriptional role. Interestingly, in this study, Strap was shown to modulate nuclear p53 levels by regulating the redistribution of p53 from the

mitochondrion to the nucleus. This was shown when an increase in mitochondrial p53 was observed upon Strap depletion (**Figure 4.9**). Furthermore, in an ectopic system when Strap and p53 were overexpressed in p53 wild type and null cells respectively, and the levels of these proteins were measured in the nuclear and mitochondrial fractions; Strap was shown to reduce p53 at the mitochondria and enhance nuclear p53 levels (**Figure 4.10**). Reconciling the overexpression data, the endogenous levels of Strap measured in the mitochondrial and nuclear fractions over time in the presence and absence of p53, further confirms the mitochondria-nuclear shuttling of p53 and Strap in response to cellular stress (**Figure 4.5**).

The hallmark of the transcription independent pathway in p53-mediated apoptosis is the accumulation of p53 at mitochondria that leads to direct activation of BAK and/or BAX (Erster et al., 2004; Leu et al., 2004; Pietsch et al., 2008). Strap was found to suppress the antiapoptotic BCL-2 family proteins and promote BAK oligomerisation in the presence of p53 which result in cytochrome c release (**Figure 4.1 & 4.12**). It is also noted that depletion of Strap leads to reduced level of BAK in total cell lysates (**Figure 4.11A**) and at the mitochondria (**Figure 4.11B**). This would likely explain the reduced BAK oligomerisation observed in the oligomerisation assay (**Figure 4.12**). Since *BAK* is a p53 target gene, the depletion of Strap might reduce p53 transcriptional activity which results in reduced BAK levels and BAK oligomerisation. Depletion of Strap enhances the BCL-XL levels both in the mitochondrial fraction and total cell lysates. This suggests that Strap might influence either the stability of the protein and/or transcription of *BCL-XL*.

The mitochondrial-dependent apoptosis is closely linked with mitochondrial membrane depolarization (Goldstein et al., 2000; Heiskanen et al., 1999). Mitochondrial membrane depolarization can be measured directly by using fluorescent lipophilic dyes such as TMRE, tetramethylrhodamine, methyl ester (TMRM), Rhodamine 123, DiOC6 (3)(3,3-dihexyloxacarbocyanine iodide) and JC-1 (5,5,6,6-tetrachloro-1,1,3,3-tetraethylbenzimidazolyl carbocyanineiodide) (Perry et al., 2011). Using TMRE, Strap was found to enhance mitochondrial membrane depolarization in the presence of p53 upon damage treatment (**Figure 4.16**). Mitochondrial Strap-induced cytochrome c release possibly via BAK oligomerisation and the mitochondrial membrane depolarization observed in the presence of p53 during damage, suggest Strap promotes intrinsic apoptosis in p53-dependent manner.

Interestingly, the co-expression of L-p53 and L-Strap showed an early induction of cleaved PARP-1 levels upon damage treatment over time (**Figure 4.17**). To corroborate these results, L-Strap was also found to decrease cell viability in label-free system (xCELLigence) in the presence of p53 (**Figure 4.18**). Although past work has demonstrated Strap augments transcription of p53 and promotes apoptosis (Demonacos et al., 2004), it is interesting to note that this apoptotic response can also be mediated through mitochondria.

In this study, a new insight into the p53 mitochondrial apoptosis pathway was provided by demonstrating that Strap negatively regulates p53 levels at the mitochondria and at the same time enhances cytochrome c release. It is postulated that mitochondrial accumulation of Strap precedes nuclear stabilization during DNA damage in the presence of p53. Overall, this study identified a new mechanism of Strap-mediated apoptosis during DNA damage that is independent of its transcriptional function.

# Chapter 5

# Results: Proteomic analysis of L-Strap

## 5.1 Generation of mitochondrial targeted Strap

Besides the central role of Strap during DNA damage, the detection of Strap at the mitochondria in this study reflects the complexity of this cofactor in regulating cellular response. Mass spectrometry was used to identify mitochondrial-targeted Strap (L-Strap) interacting proteins may help to provide a better mechanistic understanding of Strap at the mitochondria. Targeting Strap to the mitochondria and analysing the interacting protein provides more insights on the role of Strap at the mitochondria. Fusing a targeting signal as means of transportation of a protein to a specific subcellular compartment within the cell allows a better functional and mechanistic understanding of the protein in that specific compartment. A mitochondrial targeting signal allows a protein to be targeted to either the outer membrane, inner membrane or the mitochondrial matrix. L-Strap was cloned by fusing the BCL-2 mitochondrial targeting signal at the C-terminus of Strap (**Figure 5.1Ai**).

L-Strap was generated in a two-step cloning procedure. Initially, the BCL-2 targeting signal was cloned into the commercially available Flag-tagged vector via oligonucleotide annealing (**Figure 5.1Aii**). Then Strap was amplified via PCR (**Figure 5.1Bi**) and the amplified product was cloned into the Flag-tagged-BCL-2 targeting signal fused vector (**Figure 5.1Bii**). Positive clones were initially determined using restriction digest analysis and the localisation was verified via immunostaining (**Figure 5.1C**). A construct that has both the targeting signal and Strap will generate a 1,420 bp product. All constructs were confirmed by sequencing.

## 5.2 Proteomic analysis of L-Strap

Flag-tagged L-Strap and L-Vector were transiently overexpressed in U2OS cells and harvested 72 hr post transfection. Proteins that were associated with L-Strap were identified by immunoprecipitation using anti-Flag antibody. L-Vector was used to eliminate any false positive proteins that might be associated with the BCL-2 targeting signal. A band at approximately 60 kDa corresponding to Strap was identified in the specific immunoprecipitation lane but not in the vector control lane both in the silver stained gels and immunoblots (**Figure 5.2**). This size was higher than the reported size for Strap due to the presence of the BCL-2 targeting signal fused at the C-terminal end of Strap.

A total of 86 proteins were identified by L-Strap immunoprecipitation and mass spectrometry (**Figure 5.2**). The 86 proteins are categorized according to the PANTHER functional groups: cell structure and motility, intracellular protein traffic, mitosis, chromosome aggregation, tubulin, signal transduction and protein metabolism and modification. Importantly, Strap was identified among these proteins along with the previously reported Strap-interacting proteins; HSP70 (Xu et al., 2008) and PRMT5 (Jansson et al., 2008). The remaining proteins have not previously been reported in the literature to interact with Strap.

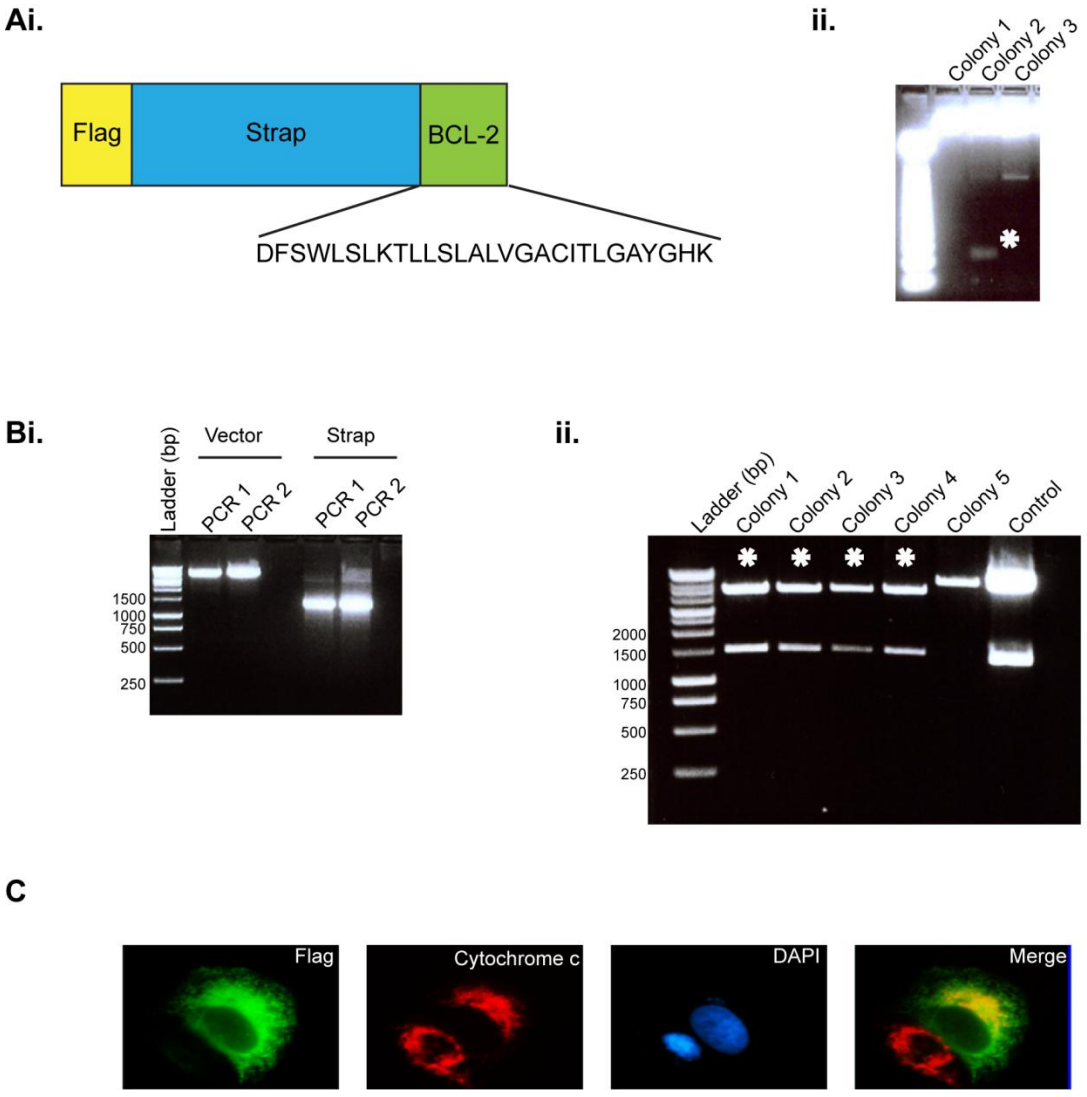



**Figure 5.1 Generation of L-Strap.**

**Ai.** Schematic representation of L-Strap, showing the Flag tag at the N-terminus (yellow), Strap (Red) and the BCL-2 targeting signal at the C-terminus (blue).

**ii.** Screening for clones with annealed BCL-2 targeting signal.

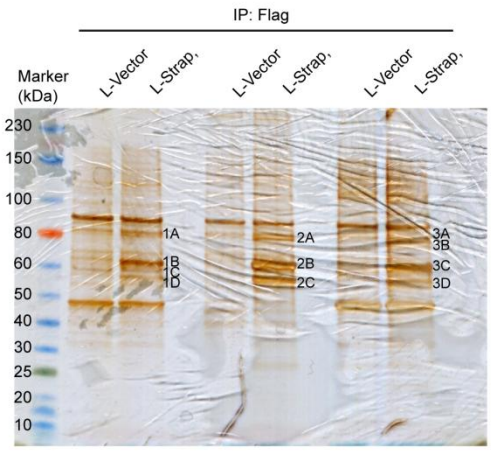
**Bi.** 1,320 bp product (Strap) generated via PCR amplification.

**ii.** Restriction digestion analysis of clones which incorporated the oligonucleotide of interest. Strap without targeting signal from a different backbone vector served as a control.

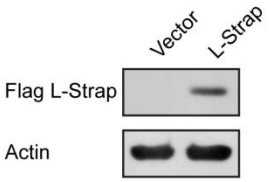
Asterisk denotes positive clones. All constructs were confirmed by sequencing.

**C.** U2OS cells were transfected with L-Strap and immunostained with anti-Flag antibody to detect ectopic L-Strap. DAPI was used to visualize the nuclei and cytochrome c was used to stain mitochondria. Co-localisation of L-Strap and cytochrome c staining is shown (Merge). (Magnification X600.)

**Ai.**




**ii.**



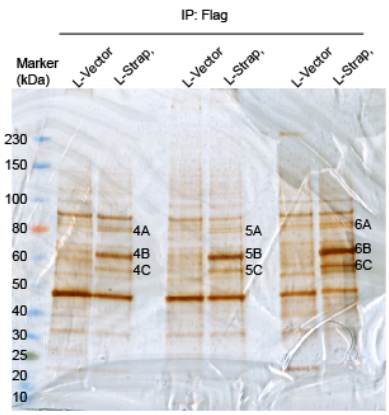

**B.**

| | Description | Score |
|---|---|---|
| 1A | i. Heat shock 70 kDa 1A/1B, 70.294 | 193 |
| | ii. PRMT5, 73.322 | 154 |
| | ii. Beta 1-3 glucosyltransferase, 57.212 | 26 |
| 1B | i. Strap/TTC5, 49.239 | 728 |
| | ii. Serine/Threonine-protein kinase 38, 54.498 | 100 |
| | iii. Heterogenous nuclear ribonucleoprotein K (hnRP K), 51.230 | 378 |
| | iv. Actin cytoplasmic, 42.052 | 508 |
| | v. TGF-beta activated kinase 1 and MAP3K7-binding protein, 54.895 | 97 |
| | vi. Protein phosphatase 1B, 53.180 | 68 |
| 1C | i. Strap/TTC5, 49.239 | 124 |
| | ii. Serine/Threonine-protein kinase 38, 54.498 | 128 |
| 1D | i. Tubulin Beta, 50.095 | 447 |
| | ii. Tubulin Beta-4B, 50.255 | 325 |
| | iii. Tubulin Alpha-1C, 50.788 | 205 |

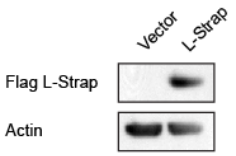
| | Description | Score |
|---|---|---|
| 2A | i. Heat shock 70 kDa 1A/1B, 70.294 | 1628 |
| | ii. PRMT5, 73.322 | 229 |
| | iii. Beta 1-3 glucosyltransferase, 57.212 | 40 |
| | iv. Strap/TTC5, 49.239 | 161 |
| | v. Heterogenous nuclear ribonucleoprotein K (hnRP K), 51.230 | 66 |
| | vi. Transketolase, 68.519 | 64 |
| 2B | i. Strap/TTC5, 49.239 | 1981 |
| | ii. Serine/Threonine-protein kinase 38, 54.498 | 187 |
| | iii. Tubulin Alpha-1C, 50.788 | 95 |
| | iv. Heterogenous nuclear ribonucleoprotein K (hnRP K), 51.230 | 200 |
| 2C | i. Tubulin Beta, 50.095 | 3508 |
| | ii. Tubulin Beta-2A, 50.255 | 2696 |
| | iii. Tubulin Beta-4B, 50.255 | 3207 |
| | iv. Tubulin Beta-8, 50.281 | 1205 |
| | v. Tubulin Beta-3, 50.281 | 2466 |
| | vi. Tubulin Beta-6, 50.281 | 1834 |
| | vii. Tubulin Alpha-4A, 50.634 | 1533 |
| | viii. Strap/TTC5, 49.23 | 266 |

| | Description | Score |
|---|---|---|
| 3A | i. Heat shock 70 kDa 1A/1B, 70.294 | 1315 |
| | ii. PRMT5, 73.322 | 233 |
| | iii. Strap/TTC5, 49.239 | 130 |
| | iv. Tubulin Beta, 50.095 | 170 |
| | v. Tubulin Beta-4B, 50.255 | 155 |
| | vi. Tubulin Alpha-1B, 50.634 | 154 |
| 3B | i. Heat shock 70 kDa 1A/1B, 70.294 | 795 |
| | ii. PRMT5, 73.322 | 341 |
| 3C | i. Strap/TTC5, 49.239 | 836 |
| | ii. Heterogenous nuclear ribonucleoprotein K (hnRP K), 51.230 | 347 |
| | iii. Protein phosphatase 1B, 53.180 | 223 |
| | iv. Serine/Threonine-protein kinase 38, 54.498 | 81 |
| | v. Actin cytoplasmic, 42.052 | 67 |
| 3D | i. Tubulin Alpha-1B, 50.634 | 1529 |
| | ii. Tubulin Alpha-3C, 50.612 | 1153 |
| | iii. Tubulin Beta, 50.095 | 1516 |
| | iv. Tubulin Beta-2B, 50.377 | 1205 |
| | v. Tubulin Beta-4B, 50.255 | 1196 |
| | vi. Tubulin Beta-8, 50.281 | 515 |
| | vii. Tubulin Beta-6, 50.281 | 666 |
| | viii. Strap/TTC5, 49.23 | 300 |
| | ix. ATP synthase subunit Beta, mitochondrial, 56.525 | 77 |

Ci.




ii.




D.

| | Description | Score |
|---|---|---|
| 4A | i. Heat shock 70 kDa 1A/1B, 70.294 | 646 |
| | ii. PRMT5, 73.322 | 134 |
| | ii. Transketolase, 68.519 | 179 |
| 4B | i. Strap/TTC5, 49.239 | 1167 |
| | ii. Serine/Threonine-protein kinase 38, 54.498 | 157 |
| | iii. Serine/Threonine-protein kinase 38-like, 54.196 | 106 |
| | iv. Heterogenous nuclear ribonucleoprotein K (hnRP K), 51.230 | 54 |
| 4C | i. Tubulin Beta, 50.095 | 962 |
| | ii. Tubulin Beta-4B, 50.255 | 668 |
| | iii. Tubulin Beta-6, 50.281 (222) | 222 |
| | iv. Tubulin Alpha-1A, 50.788 (438) | 438 |
| | v. Tubulin Alpha-4A, 50.634 (257) | 257 |
| | vi. Strap/TTC5, 49.23 (104) | 104 |

| | Description | Score |
|---|---|---|
| 6A | i. Heat shock 70 kDa 1A/1B, 70.294 | 468 |
| | ii. PRMT5, 73.322 | 60 |
| 6B | i. Strap/TTC5, 49.239 | 456 |
| | ii. Heterogenous nuclear ribonucleoprotein K (hnRP K), 51.230 | 56 |
| 6C | i. Tubulin Beta, 50.095 | 320 |
| | ii. Tubulin Beta-4B, 50.255 | 160 |
| | iii. Tubulin Alpha-1B, 50.634 | 281 |
| | iv. Tubulin Beta-1A, 50.78 | 249 |
| | v. ATP synthase subunit Beta, mitochondrial, 56.525 | 28 |

| | Description | Score |
|---|---|---|
| 5A | i. Heat shock 70 kDa 1A/1B, 70.294 | 484 |
| | ii. PRMT5, 73.322 | 51 |
| 5B | i. Strap/TTC5, 49.239 | 865 |
| | ii. Heterogenous nuclear ribonucleoprotein K (hnRP K), 51.230 | 70 |
| 5C | i. Tubulin Beta, 50.095 | 523 |
| | ii. Tubulin Beta-4B, 50.255 | 290 |
| | iii. Tubulin Beta-1A, 50.788 | 239 |
| | iv. Tubulin Beta-1B, 50.634 | 287 |
| | v. Tubulin Beta-6, 50.281 | 93 |
| | vi. ATP synthase subunit Beta, mitochondrial 56.625 | 38 |
| | vii. Strap/TTC5, 49.23 | 62 |

**Figure 5.2 Immunoprecipitation of L-Strap.**

**Ai** & **Ci.** Ectopic Strap from U2OS cells transiently expressing either L-Strap or empty vector control (L-Vector) were immunoprecipitated with anti-Flag antibody. Immunoprecipitated material was run on SDS-PAGE and silver stained.

**Aii & Cii.** A fraction of the immunoprecipitates was immunoblotted. L-Strap was detected with anti-Flag antibody. Actin served as loading control.

**B** & **D.** Bands denoted were excised, in-gel digested with trypsin and analysed by LC-MS/MS. MASCOT score searches of the resulting peptides and the molecular weight are as indicated in the bottom tables. Strap is highlighted in yellow.

Proteins involved in protein metabolism and modification that were identified in mass spectrometry were subjected to PANTHER analysis (**Figure 5.3**). This functional group was of interest due to the significant role of the mitochondria in metabolic pathways. Approximately 46% of proteins identified in this group were involved in metabolic processes and the other 54% of proteins identified were involved in protein modifications such co-translational and post-translational modifications (**Figure 5.3B**).

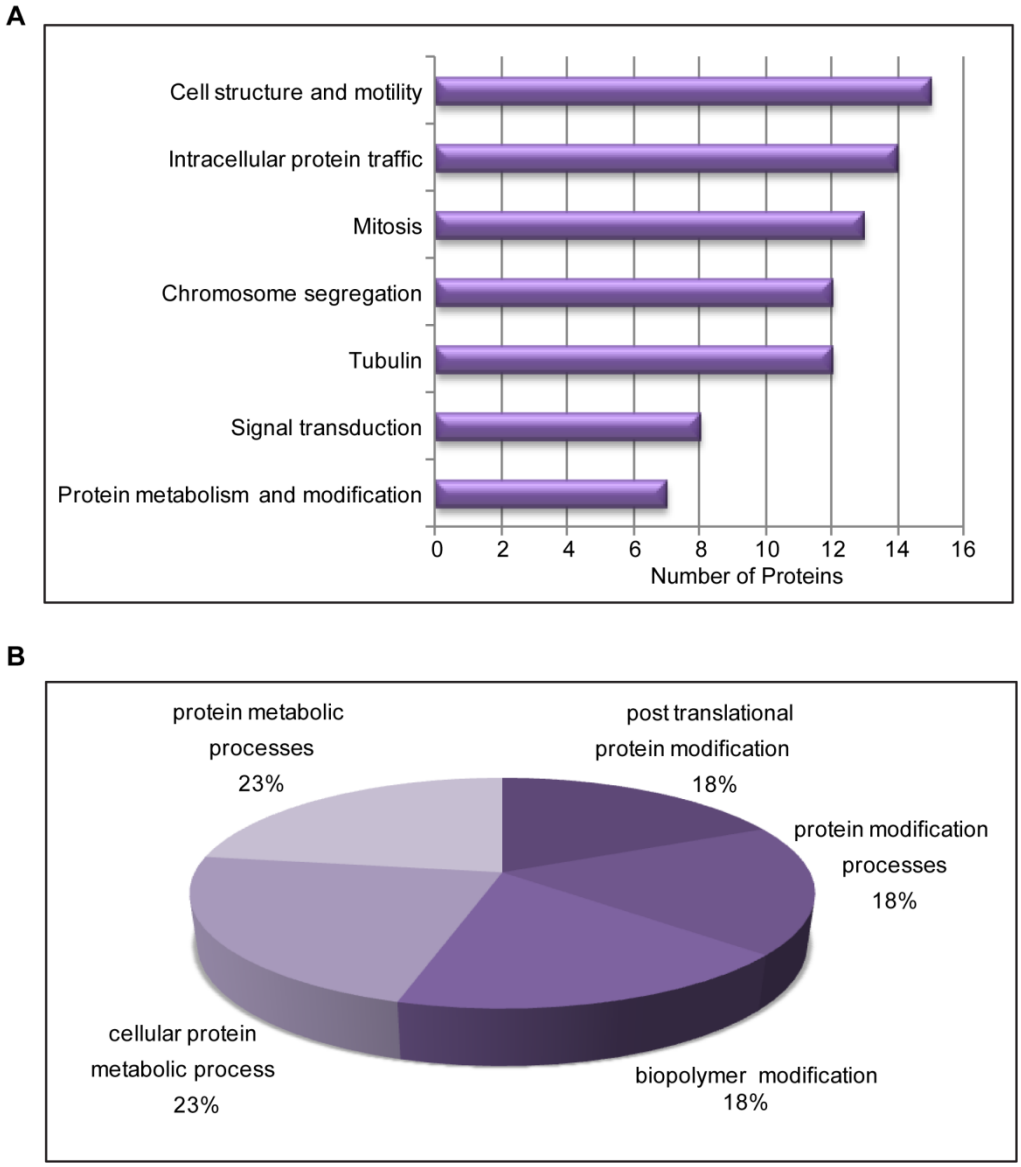



**Figure 5.3 Analysis of L-Strap interacting proteins.**

**A.** Functional annotation analysis was performed using DAVID, 2012. The categories used were PANTHER molecular function (MF) and biological process (BP). The categories are shown for L-Strap interacting proteins derived from mass spectrometry analysis.

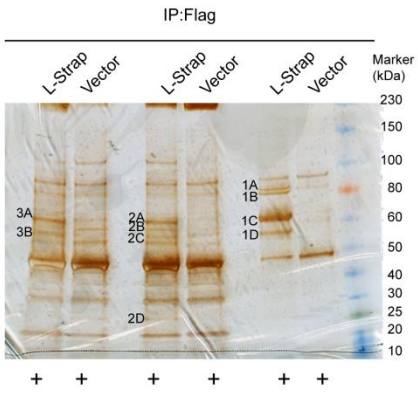
**B.** Pie chart summarizes the specific category according to Gene Ontology.

### 5.3 Proteomic analysis of L-Strap under damage

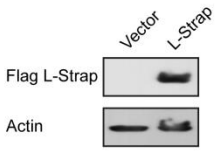
In an effort to determine the role of L-Strap at the mitochondria during damage or how damage modulates Strap at the mitochondria, mass spectrometry was used to identify proteins that interacted with L-Strap upon DNA damage treatment. L-Strap was transiently overexpressed in U2OS cells and treated with 50 $J/m^2$ UV light before immunoprecipitation (**Figure 5.4**). The interacting proteins obtained from the mass spectrometry analysis on L-Strap treated with UV light were grouped according to PANTHER annotation. In the absence of damage, the interacting proteins were categorised to clusters, among others are proteins involved in cell motility, protein trafficking and chromosome segregation. Four additional groups were identified in the list of interacting proteins obtained from the mass spectrometry analysis of UV treated samples compared to the untreated samples. The additional functional groups were proteins involved in the stress response, protein folding, chaperone and protein complex assembly (**Figure 5.5A**).

Interestingly, closer inspection of the protein metabolism and modification group revealed that there was an increase of 26% in the interacting proteins identified in UV light treated samples compared to the untreated (**Figure 5.5B**). More than half of the proteins detected in the absence of damage from this group were involved in protein modifications. In contrast to non damage condition, only 37% of the proteins identified upon damage treatment in this group were involved in protein modifications (**Figure 5.5B**). Collectively, these data suggest a potential regulation in cell metabolism during damage in the presence of L-Strap.

**Ai.**




**ii.**




**B.**

| | Description | Score |
|---|---|---|
| 1A | i. Heat shock 70 kDa 1A/1B, 70.294 | 310 |
| | ii. PRMT5, 73.322 | 150 |
| | iii. Heat shock 70 kDa, 71.440 | 323 |
| | iv. Heat shock cognate 71 kDa, 71.082 | 2132 |
| 1B | i. Heat shock 70 kDa 1A/1B, 70.294 | 2589 |
| | ii. PRMT5, 73.322 | 115 |
| | iii. Heat shock 70 kDa protein 2, 70.263 | 344 |
| | iv. Heat shock cognate 71 kDa, 71.082 | 374 |
| 1C | i. Strap/TTC5, 49.239 | 1633 |
| | ii. Heterogenous nuclear ribonucleoprotein K (hnRP K), 51.230 | 82 |
| | iii. Tubulin Alpha-1B, 50.804 | 92 |
| | iv. Protein phosphatase 1B, 53.180 | 56 |
| 1D | i. Tubulin Alpha-1B, 50.634 | 26099 |
| | ii. Tubulin Alpha-3C/D, 50.612 | 2279 |
| | iii. Tubulin Beta, 50.095 | 2941 |
| | iv. Tubulin Beta-2B, 50.377 | 2114 |
| | v. Tubulin Beta-4B, 50.255 | 2289 |
| | vi. Tubulin Beta-8, 50.281 | 988 |
| | vii. Tubulin Beta-6, 50.281 | 1023 |
| | viii. Tubulin Beta-3, 50.281 | 1683 |
| | ix. Tubulin Beta-2A, 50.255 | 2106 |
| | x. Tubulin Alpha-1C, 50.548 | 2079 |

| | Description | Score |
|---|---|---|
| 2A | i. Strap/TTC5, 49.239 | 714 |
| | ii. Heterogenous nuclear ribonucleoprotein K (hnRP K), 51.230 | 264 |
| | iii. Protein phosphatase 1B, 53.180 | 136 |
| 2B | i. Actin cytoplasmic, 42.052 | 90 |
| | ii. Strap/TTC5, 49.239 | 97 |
| | iii. Tubulin Beta-8, 50.281 | 33 |
| 2C | i. Coronin, 53.899 | 1389 |
| | ii. Tubulin Alpha-1B, 50.634 | 495 |
| | iii. Vimentin, 53.676 | 358 |
| | iv. Trifunctional enzyme subunit beta, 51.547 | 137 |
| | v. Tubulin Beta, 50.096 | 264 |
| 2D | i. Dehydrogenase/reductase SDR family, | 900 |
| | ii. Heat shock protein beta 1, 22.826 | 70 |

| | Description | Score |
|---|---|---|
| 3A | i. Strap/TTC5, 49.239 | 981 |
| | ii. Serine/Threonine-protein kinase 38, 54.498 | 115 |
| | iii. Coronin, 53.899 | 79 |
| | iv. Heterogenous nuclear ribonucleoprotein K (hnRP K), 51.230 | 108 |
| | v. Actin cytoplasmic, 42.052 | 121 |
| 3B | i. Tubulin Beta, 50.095 | 701 |
| | ii. Tubulin 1A, 50.78 | 714 |
| | iii. Tubulin Beta-4B, 50.255 | 591 |
| | iv. Tubulin Alpha-4A, 50.634 | 548 |
| | v. Tubulin Beta-6, 50.281 | 235 |

**Figure 5.4 Immunoprecipitation of L-Strap under damage.**

**Ai.** Ectopic Strap from U2OS cells transiently expressing either L-Strap or empty vector control (L-Vector) treated with 50 J/m$^2$ of UV light for 6 hr were immunoprecipitated with anti-Flag antibody. Immunoprecipitated material was run on SDS-PAGE and silver stained.

**ii.** A fraction of the immunoprecipitates was immunoblotted. Ectopic Strap was detected with anti-Flag antibody. Actin served as loading control.

**B.** Bands denoted were excised, in-gel digested with trypsin and analysed by LC-MS/MS. MASCOT score searches of the resulting peptides and molecular weight are as indicated in the bottom tables. Strap is highlighted in yellow.

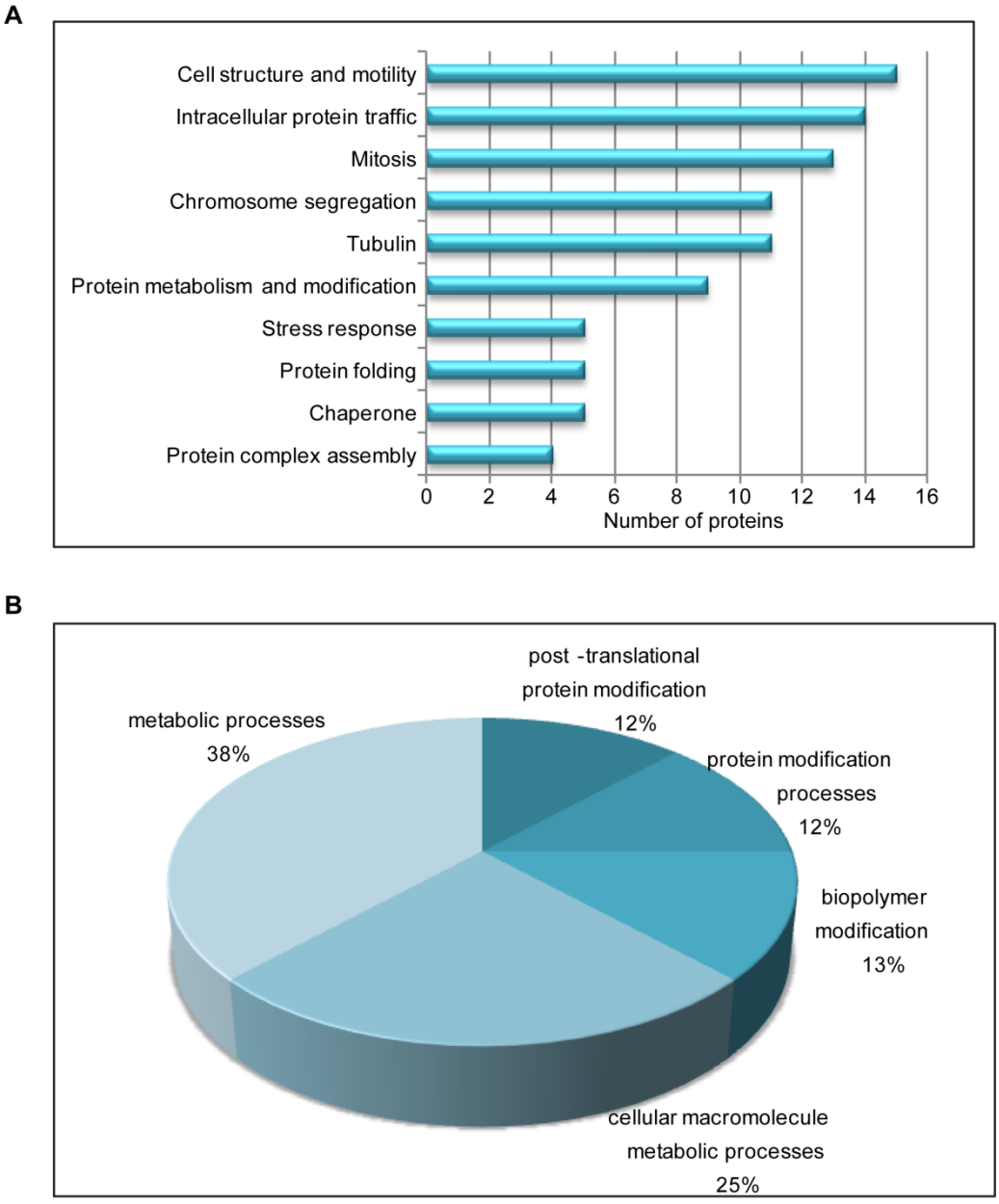



**Figure 5.5 Analysis of L-Strap interacting proteins under damage.**

**A.** Functional annotation analysis was performed using DAVID, 2012. The categories used were PANTHER molecular function (MF) and biological process (BP). The categories are shown for L-Strap interacting proteins derived from mass spectrometry analysis.

**B.** Pie chart summarizing the specific category according to Gene Ontology.

### 5.4 Post-translational modifications

PTMs are involved in most of the cellular response to various stimuli. The term PTM denotes the change in the polypeptide chain as a result of either the addition or removal of distinct chemical moieties to amino acid residues, proteolytic processing of the protein termini or the introduction of a covalent crosslink between domains of the protein (Larsen et al., 2006). One of the PTMs that is often regulated in cells is phosphorylation. It is estimated that one-third of eukaryotic proteins are phosphorylated, as a result of carefully regulated protein kinase and phosphatase activities (Cohen, 2002; Witze et al., 2007).

Five phosphorylation sites (four phosphoserine and one phosphotyrosine) were identified from the L-Strap mass spectrometry analysis in the presence of damage (**Figure 5.6**). One phosphoserine was located in TPR4, two phosphoserine sites were located in TPR6 and one of each phosphoserine and phosphotyrosine sites were located at the OB fold. S221 at TPR5 was previously published as a site targeted by CHK2 phosphorylation (Adams et al., 2008). Interestingly, the adjacent serine (S222) was also detected as a potential phosphorylation site but only during damage. The S138 (phosphoserine site at TPR4) was detected under both damage and non damage conditions. The phosphoserine site located at the OB fold was only detected once during damage and has a poor ion score. Interestingly, a phosphotyrosine site was detected at the OB fold both in the presence and absence of damage. The data obtained from the PTM analysis of L-Strap mass spectrometry postulates that phosphorylation may influence Strap at mitochondria.

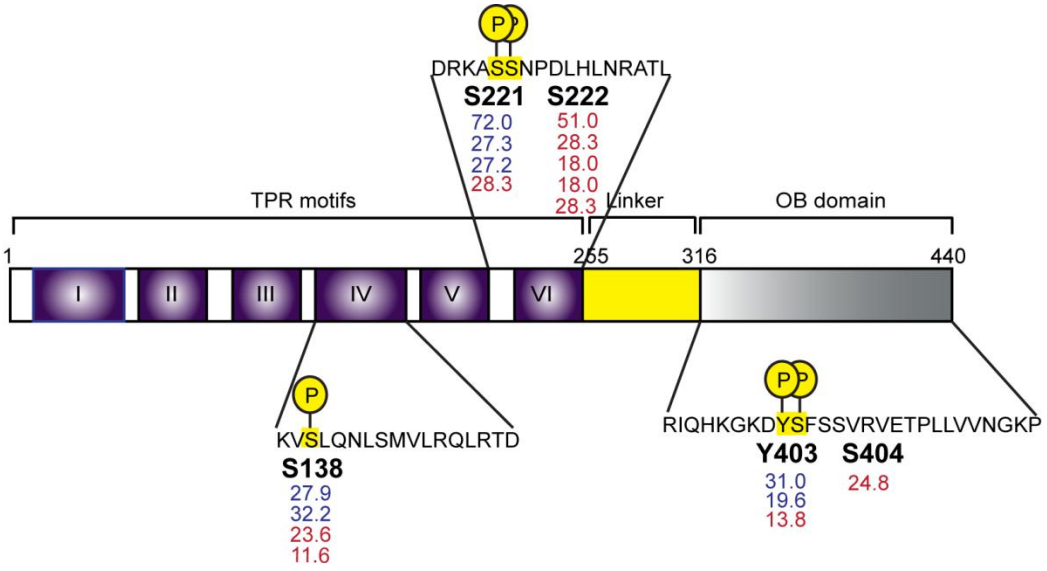



**Figure 5.6 PTMs identified from L-Strap mass spectrometry analysis.**

Strap contains six TPR motifs and an OB fold. The phosphorylation sites identified from L-Strap mass spectrometry analysis are as indicated. Ion score identified under damage conditions are highlighted in red and blue highlights represent ion score identified in the absence of damage.

## 5.5 Discussion

Mass spectrometry analysis of L-Strap identified mixed classes of proteins. In the analysis of L-Strap interacting proteins, the possibility that the protein identified interacted with the BCL-2 targeting signal was eliminated by using vector control which included the targeting signal. L-Strap mass spectrometry analysis identified Strap associated proteins that were previously reported such as PRMT5 and HSP70. The detection of proteins associated with Strap's transcriptional role perhaps might be protein overexpression-induced artifact. This experiment can be repeated using Strap immunoprecipitated from mitochondrial and nuclear fractions in the presence or absence of damage, revealing more detail on the separate roles of Strap.

Several mitochondrial proteins were identified such as transketolase, heterogenous nuclear ribonucleoprotein K (hnRNP K), tubulins and ATP synthase subunit-β. Tubulins that were identified as interacting proteins from the L-Strap mass spectrometry analysis have been shown to be involved in regulation of mitochondrial function (Rostovtseva and Bezrukov, 2012; Rostovtseva et al., 2008). The transketolase enzyme is associated with the non-oxidative branch of the pentose phosphate pathway which plays a crucial role in nucleic acid synthesis (Boros et al., 1997). The proteomic analysis of L-Strap identified ATP synthase subunit-β, an inner mitochondrial membrane protein involved in ATP synthesis during oxidative phosphorylation. The functional consequences of this interaction are discussed in depth in **Chapter 6**. In depth investigation into the mitochondrial Strap interacting proteins, initially by immunoprecipitation would be able to eliminate false positive interactors.

Amongst the interacting proteins identified from the L-Strap mass spectrometry analysis were tubulin-α and –β which were categorised into cell structure and motility group according to PANTHER annotation (**Figure 5.3 & 5.5**). Tubulin was initially thought to be predominantly a cytosolic protein but several studies have demonstrated tubulin in mitochondria (Carre et al., 2002). An interaction between voltage-dependent anion channel (VDAC) and tubulin was observed and this provided a functional link between mitochondrial respiration and the cytoskeleton (Carre et al., 2002). VDAC is located at the OMM and functions as a gatekeeper for the entry and exit of mitochondrial metabolites. Mitochondrial tubulin-VDAC interaction is involved in apoptosis through PTP opening which results in cytochrome c release (Carre et al., 2002). The detection of tubulins in the mass spectrometry analysis suggests that mitochondrial Strap may be involved in facilitating the VDAC –tubulin interaction. This may provide another function of Strap at the mitochondria in regulating mitochondria-induced apoptosis which involves the interaction with tubulin.

Phosphorylation is a widespread PTM (Manning et al., 2002). It is efficient in controlling cellular responses to external and internal signals as it is rapid, reversible and does not require protein synthesis or degradation (Sacco et al., 2012). Eukaryotic phosphorylation typically occurs on serine, threonine and tyrosine residues (Olsen et al., 2006). It was observed that L-Strap was highly phosphorylated at multiple sites under both non damage and damage conditions (**Figure 5.6**). It is postulated that perhaps PTMs influence Strap's localisation to the mitochondria. Moreover, the mass spectrometry analysis of L-Strap in the presence and absence of damage detected proteins involved in intracellular protein trafficking

(**Figure 5.3 & 5.5**). Perhaps the identification of protein phosphatase from the L-Strap mass spectrometry analysis suggests that Strap might also be dephosphorylated at the mitochondria. The phosphorylation and dephosphorylation may modulate the localisation of Strap between mitochondria and nucleus.

In summary, mass spectrometry analysis of Strap generated a large number of possible interacting proteins. It is noted that biochemical validation has to be employed in combination with mass spectrometry analysis to eliminate false positive interactors. The ability of proteomic techniques to identify interacting proteins and PTMs provide a better understanding of the many aspects in the architecture of large multiprotein assemblies which involve Strap.

# Chapter 6

# Results: Strap and cellular metabolism

### 6.1 Strap interacts with ATP synthase subunit-β

To provide a better understanding of Strap at the mitochondria, a mass spectrometry approach was used to identify mitochondrial Strap interacting proteins. L-Strap was overexpressed and immunoprecipitated from U2OS cells and the bound proteins were analyzed by SDS-PAGE and identified by mass spectrometry. Of relevance, the ATP synthase subunit-β was identified from the mass spectrometry analysis (**Figure 6.1A**). ATP synthase subunit-β is an inner mitochondrial membrane that forms the catalytic domain of ATP synthase, the key enzyme involved in the energy production by OXPHOS. Initially, the ATP synthase subunit-β and Strap interaction was confirmed by immunoprecipitation in U2OS cells stably expressing vector, wild type Strap and L-Strap. Both wild type Strap and L-Strap co-immunoprecipitated with ATP synthase subunit-β which further verifies the mass spectrometry analysis (**Figure 6.1B**).

The localisation of the ATP synthase subunit-β at the mitochondria was observed via immunostaining. ATP synthase subunit-β was shown to co-localise with another inner membrane protein, COXIV (**Figure 6.2A**). To further validate the ectopic interaction of ATP synthase subunit-β and Strap, endogenous Strap was shown to co-immunoprecipitate with ATP synthase subunit-β in U2OS (**Figure 6.2B**) and HeLa (**Figure 6.2C**) cells. Importantly, this complex was formed in the mitochondrial fractions (**Figure 6.2D**) which provided further evidence for an interaction between ATP synthase subunit-β and Strap occuring at the mitochondria.

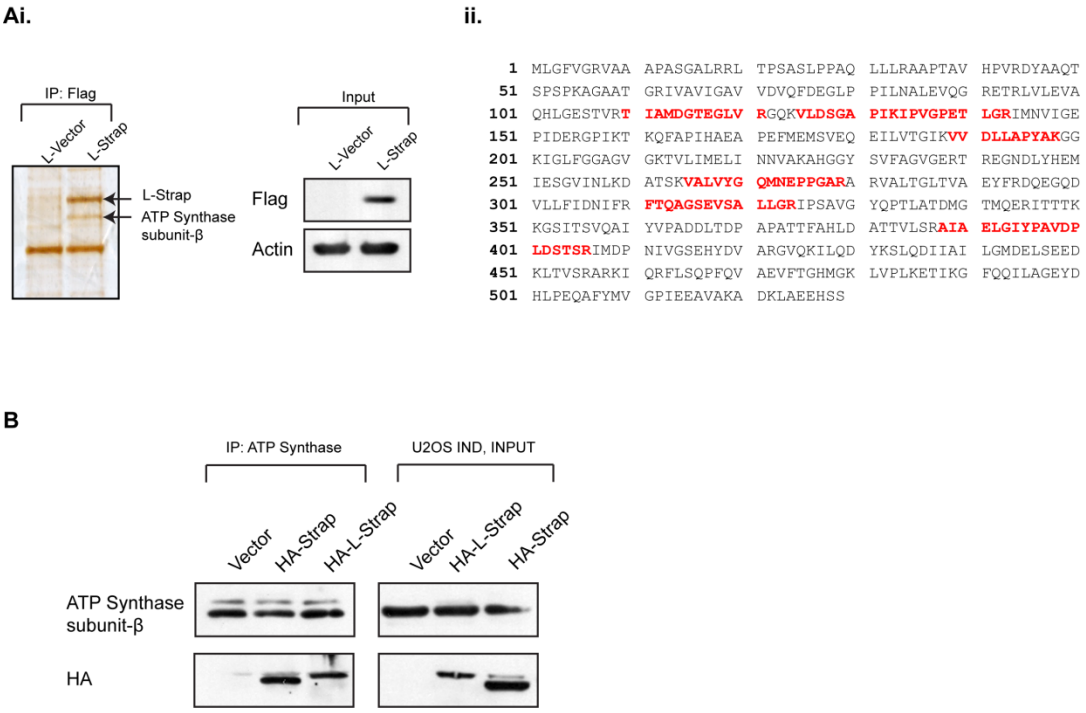



**Figure 6.1 Identification of an interacting partner of L-Strap.**

**Ai**. L-Strap from U2OS cells transfected with either 1 µg of L-vector or L-Strap was immunoprecipitated with anti-Flag antibody. The silver-stained protein band was excised and subjected to tryptic digestion and LC/MS-MS (left panel). The position of Strap and ATP synthase subunit-β are indicated. A fraction of the immunoprecipitates was immunoblotted (right panel). L-Strap was detected with anti-Flag antibody and actin served as loading control.

**ii.** The peptide sequences of ATP synthase subunit-β identified via mass spectrometry indicated in **i** are highlighted. Peptides (indicated in red) were eluted from the tryptic digestion in **i**.

**B.** ATP synthase subunit-β was immunoprecipitated from U2OS cells stably expressing vector, wild type Strap and L-Strap. Endogenous ATP synthase subunit-β was detected with anti-ATP synthase subunit-β antibody and ectopic Strap was detected with anti-HA antibody. Inputs represent 2% of total protein.

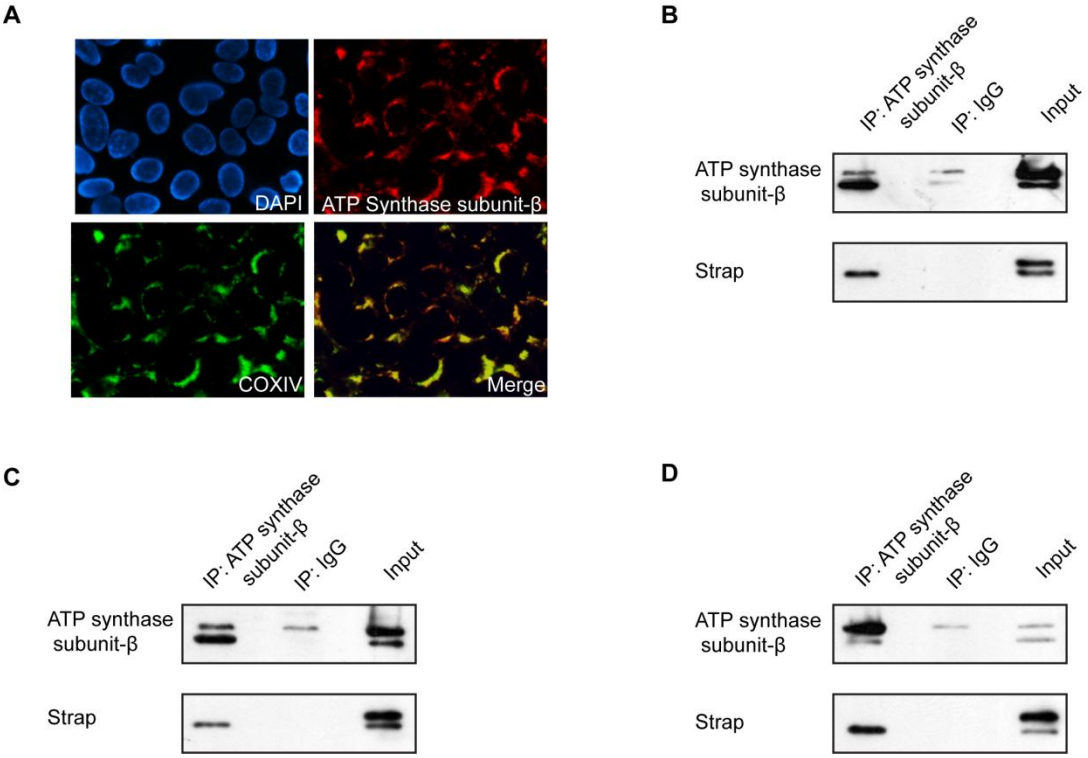



**Figure 6.2 Strap interacts with ATP synthase subunit-β.**

**A.** U2OS cells were immunostained with anti-ATP synthase subunit-β antibody. COXIV serves as an inner mitochondrial membrane marker and DAPI staining was used to visualise the nuclei. Co-localisation of ATP synthase subunit-β and COXIV staining is shown (Merge). (Magnification X200.)

Endogenous ATP synthase subunit-β from U2OS (**B**) and HeLa (**C**) cells was immunoprecipitated and detected with anti-ATP synthase subunit-β antibody or a non-specific (IgG) immunoprecipitation was carried out using mouse IgG. Strap was detected with anti-Strap antibody. Inputs represent 5% of total protein.

**D.** Mitochondrial fractions were immunoprecipitated and detected with anti-ATP synthase subunit-β antibody or a non-specific (IgG) immunoprecipitation was carried out using mouse IgG. Strap was detected with anti-Strap antibody. Inputs represent 2% of total mitochondrial extract.

## 6.2 Regulation of Strap during OXPHOS

ATP synthase is the enzyme complex responsible for ATP synthesis driven by OXPHOS. Cancer cells derive energy from glucose via glycolysis. Glucose restriction promotes cancer cells to rely on OXPHOS instead of glycolysis to produce energy. Glucose deprivation was achieved by substituting glucose in the media with galactose (Marroquin et al., 2007; Rossignol et al., 2004). Galactose is metabolised primarily in the liver which yields one molecule of glucose-1-phosphate per one molecule of galactose. The use of glucose and galactose supplemented media provided a good platform to investigate the influence of Strap on energy production during OXPHOS compared to glycolysis in cultured cell lines.

Initially, levels of Strap in total cell lysates and mitochondrial fractions were examined in glucose and galactose supplemented media. Strap was upregulated both in the total cell lysates (**Figure 6.3Ai & Bi**) and in the mitochondrial fractions (**Figure 6.3Aii & Bii**) when galactose supplemented media (condition that promotes OXPHOS) was used. Interestingly, the converse was observed in the absence of p53 where a decrease in Strap levels was observed in p53 null cells (SAOS2 and HCT116$^{-/-}$) when galactose supplemented media was used (**Figure 6.3A & B**). Of note, an increase in p53 levels were also observed in total cell lysates when cells were grown in galactose supplemented media (**Figure 6.3Ai & Bi**). Interestingly, not much is known about the p53's function in cancer cells grown in galactose supplemented media. To date, overexpression of p53 in yeast grown in galactose supplemented media led to growth inhibition and apoptosis (Palermo et al., 2013).

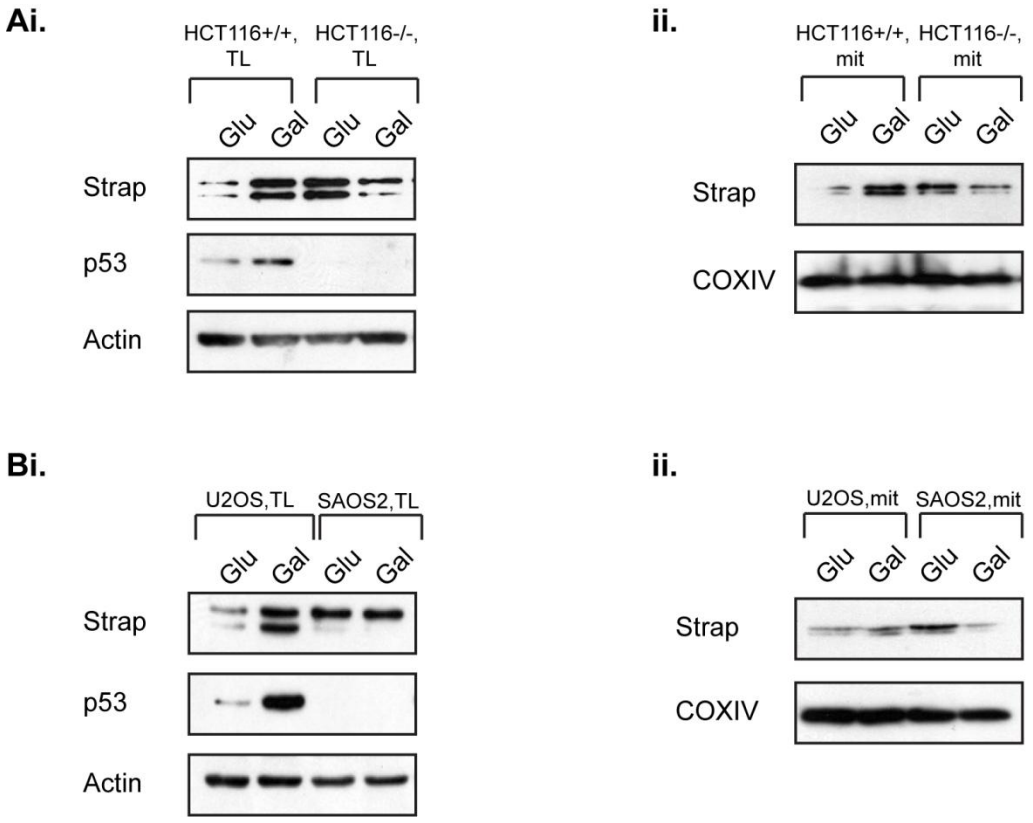



**Figure 6.3 Strap levels in glucose and galactose supplemented media.**

Immunoblots of total cell lysate (TL) and mitochondrial fraction (mit) from $HCT116^{+/+}$ and $HCT116^{-/-}$ (**A**) and U2OS and SAOS2 cells (**B**) grown in either glucose (Glu) or galactose (Gal) supplemented media. COXIV and actin were used to assess mitochondrial and total cell lysate loading, respectively.

Since an increase in Strap levels was detected in galactose supplemented media, the next step was to investigate whether Strap would exhibit differences in binding to ATP synthase subunit-β *in vivo* in glucose versus galactose supplemented media. In an attempt to understand the interaction between Strap and ATP synthase subunit-β, immunoprecipitation-immunoblot analysis was carried out. Endogenous ATP synthase subunit-β was immunoprecipitated from U2OS cells grown in either glucose or galactose supplemented media. An enhanced interaction between endogenous Strap and ATP synthase subunit-β was observed in galactose supplemented media (**Figure 6.4A**). Next, the influence of p53 on the Strap-ATP synthase subunit-β interaction was explored. Endogenous ATP synthase subunit-β was immunoprecipitated from $HCT116^{+/+}$ (wild type p53) and $HCT116^{-/-}$ (devoid of p53) cells. The presence of p53 was shown to upregulate the interaction between Strap and ATP synthase subunit-β (**Figure 6.4B**). The Strap-ATP synthase subunit-β interaction in the presence of p53 was augmented when cells were grown in galactose supplemented media (**Figure 6.4C**). Of note, an increase in Strap when $HCT116^{+/+}$ cells were grown in galactose supplemented media was not observed in the inputs as the lysates were loaded according to volume not total protein concentration.

An enhanced interaction between Strap and p53 was previously shown upon damage treatment (**Figure 4.7A**). Since the presence of damage modulated the Strap-p53 interaction, it was of interest to investigate if this interaction is regulated when cells are grown in either glucose or galactose supplemented media. Intriguingly, an increased association between Strap and p53 was observed when cells were grown in galactose supplemented media during damage (**Figure 6.5A**).

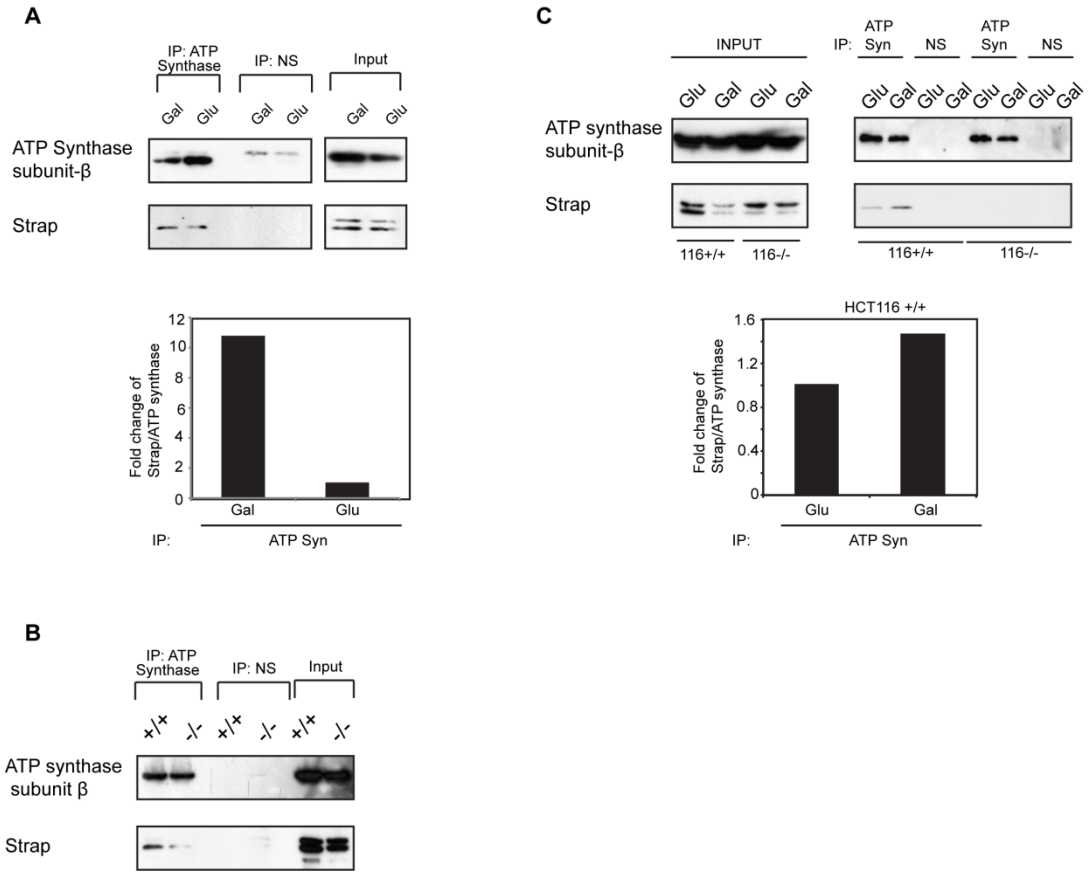



**Figure 6.4 Interaction between Strap and ATP synthase subunit-β.**

**A.** ATP synthase subunit-β was immunoprecipitated from U2OS cells grown either in glucose (Glu) or galactose (Gal) supplemented media. Endogenous ATP synthase subunit-β and Strap were detected with anti-ATP synthase subunit-β and anti-Strap antibody respectively. Inputs represent 2% of total protein. Quantification is shown.

**B.** ATP synthase subunit-β was immunoprecipitated from $HCT116^{+/+}$ (+/+) & $HCT116^{-/-}$ (-/-). Endogenous ATP synthase subunit-β and Strap were detected with anti-ATP synthase subunit-β and anti-Strap antibody respectively. Inputs represent 2% of total protein.

**C.** ATP synthase subunit-β was immunoprecipitated from $HCT116^{+/+}$ & $HCT116^{-/-}$ cells grown either in glucose (Glu) or galactose (Gal) supplemented media. Endogenous ATP synthase subunit-β and Strap were detected with anti-ATP synthase subunit-β and anti-Strap antibody respectively. Inputs represent 2% of total protein. Quantification is shown.

The present data suggest an enhanced Strap and ATP synthase subunit-β interaction in the presence of p53 when cells are grown in galactose supplemented media. Interestingly, the Strap and p53 association was also augmented during damage in galactose supplemented media. This prompted an investigation on whether Strap, p53 and ATP synthase subunit-β formed a ternary complex in galactose supplemented media. Unfortunately, p53 failed to co-immunoprecipitate with ATP synthase subunit-β neither in glucose nor galactose supplemented media in the absence or presence of damage (**Figure 6.5B**). Interestingly, an enhanced association of Strap and ATP synthase subunit-β was observed in galactose supplemented media but this interaction was marginally affected by the presence of damage (**Figure 6.5B**).

Taken together, these data suggest that the Strap-ATP synthase subunit-β and Strap-p53 interactions are enhanced when OXPHOS is predominant in the cells. The Strap-p53 interaction is further upregulated in the presence of damage. This suggests that the Strap and ATP synthase subunit-β interaction is important during OXPHOS and perhaps the interaction between Strap and p53 is damage-regulated.

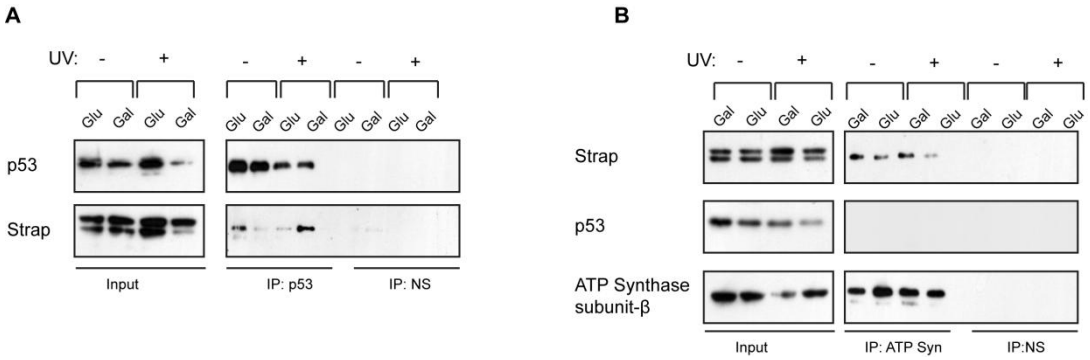



**Figure 6.5 Strap and p53 interaction in glucose or galactose supplemented media.**

p53 (**A**) or ATP synthase subunit-β (**B**) was immunoprecipitated from HCT116$^{+/+}$ cells grown either in glucose (Glu) or galactose (Gal) supplemented media, either left untreated (-) or treated (+) with 50 J/m$^2$ UV light for 6 hr as indicated. ATP synthase subunit-β and Strap were detected with anti-ATP synthase subunit-β and anti-Strap antibody respectively. p53 was detected using p53 antibody. Inputs represent 2% of total protein.

### 6.3 Strap influences ATP/ADP levels during OXPHOS

The α and β catalytic domains of the ATP synthase complex are responsible for ATP synthesis. Thus, regulating ATP synthase activity will affect the cellular energy status which can be assessed by measuring the ratio between ATP and ADP (ATP/ADP). To determine the effects of Strap on cellular energy status, cellular ATP/ADP ratio were measured using high performance liquid chromatography (HPLC). In U2OS cells, depletion of Strap caused an increase in the cellular ATP/ADP ratio (**Figure 6.6A**). Similar results were observed when cells were supplemented with either glucose or galactose media (**Figure 6.6B**). The influence of p53 on the cellular ATP/ADP ratio was of interest since the presence of p53 modulated the Strap-ATP synthase subunit-β interaction. Interestingly, no significant changes in the ATP/ADP ratio were observed in SAOS2 cells (devoid of p53) upon Strap depletion (**Figure 6.6C & D**).

Next, the ATP/ADP ratio was measured in U2OS cells expressing stable inducible vector, wild type Strap and L-Strap in glucose or galactose supplemented media. In glucose supplemented media (**Figure 6.7A**), a marginal decrease in ATP/ADP ratio was observed in wild type Strap and L-Strap expressing cells. The ATP/ADP ratio detected in glucose supplemented media is predominantly produced via glycolysis. When OXPHOS was favoured by using galactose supplemented media, a marked reduction in ATP/ADP ratio was observed in wild type Strap and L-Strap expressing cells (**Figure 6.7B**). Intriguingly, no significant changes in the ATP/ADP ratio were observed in SAOS2 cells stably expressing vector, wild type Strap or L-Strap in glucose (**Figure 6.7C**) or galactose (**Figure 6.7D**) supplemented media.

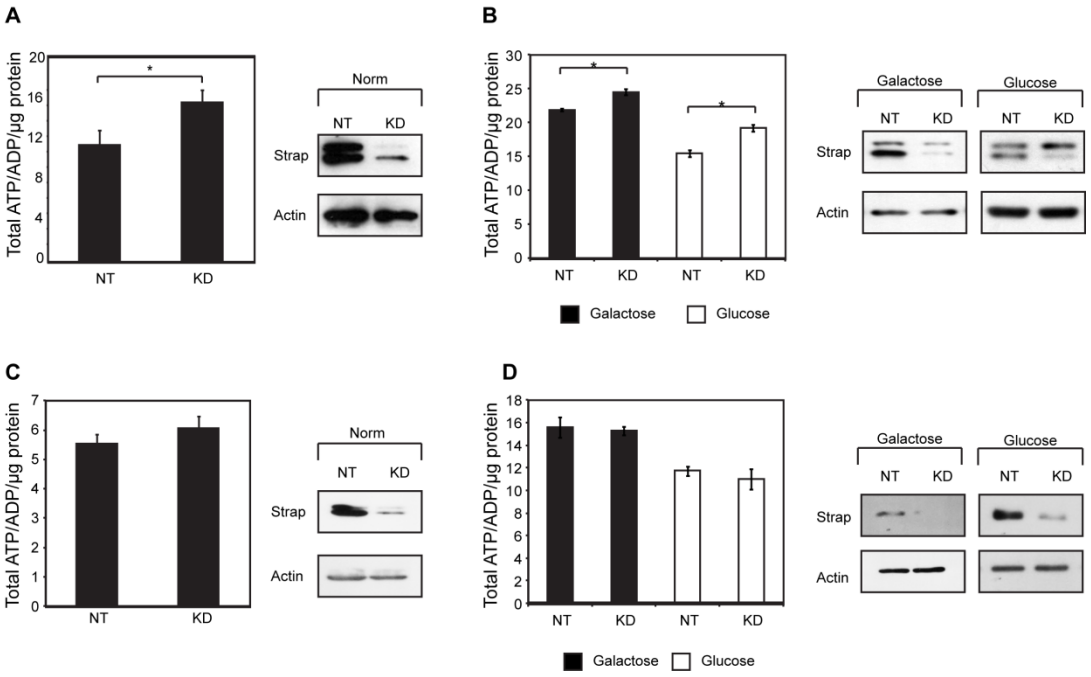



**Figure 6.6 Depletion of Strap increases cellular ATP/ADP ratio.**

U2OS (**A** & **B**) and SAOS2 (**C** & **D**) cells were transfected with 90 nM non-targeting (NT) or Strap siRNA (KD) for 72 hr and cellular ATP/ADP ratio was measured in complete (norm) (**A** & **C**), glucose and galactose (**B** & **D**) supplemented media as indicated. The levels of Strap are shown via immunoblotting. Strap was detected with anti-Strap antibody and actin served as loading control. Values represent mean ± s.d. * indicates $p<0.05$, Student's t-test, n= 3-6 independent experiments. The ATP/ADP ratio was measured by Stratford MR, Department of Oncology, University of Oxford.

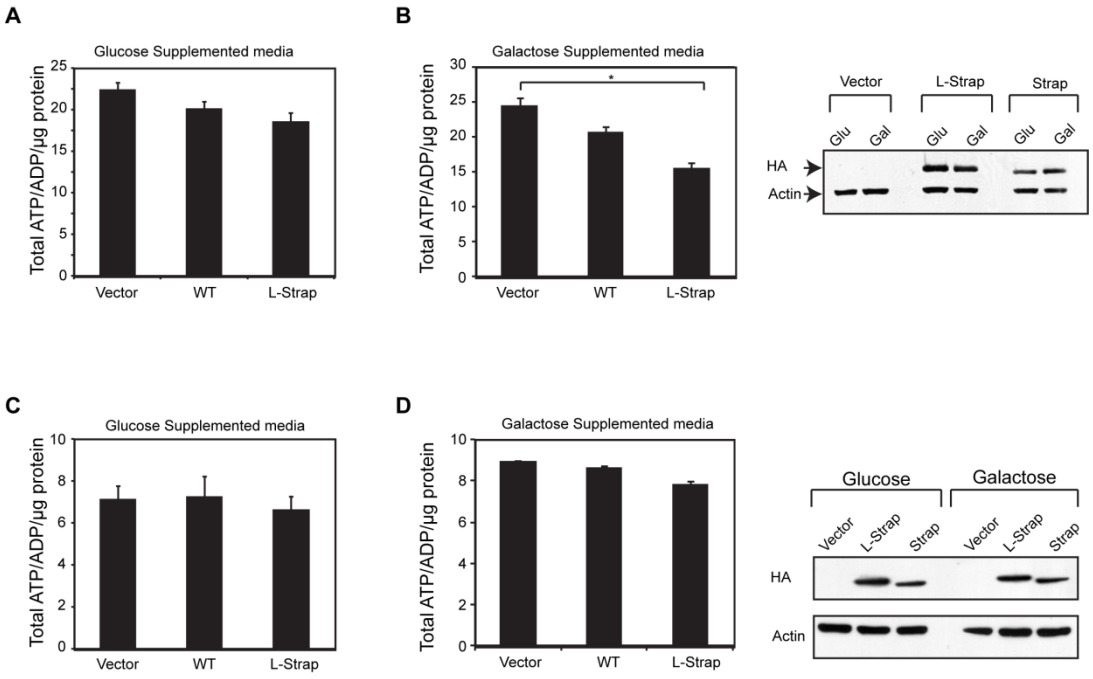



**Figure 6.7 Strap depletes cellular ATP/ADP ratio.**

U2OS inducible stable cells expressing vector, wild type Strap (WT) and L-Strap (**A** & **B**) induced with doxycycline, 1 µg/ml and SAOS2 cells stably expressing vector, wild type Strap (WT) and L-Strap (**C** & **D**) were grown in glucose (**A** & **C**) or galactose supplemented media (**B** & **D**), and then cellular ATP/ADP ratio was measured. The level of Strap proteins are shown via immunoblotting. Ectopic Strap was detected with anti-HA antibody and actin served as loading control. Values represent mean ± s.d. * indicates $p<0.05$, Student's t-test, n = 3 independent experiments. The ATP/ADP ratio was measured by Stratford MR, Department of Oncology, University of Oxford.

Measuring mitochondrial membrane potential has become a commonly used tool for monitoring changes in the mitochondrial membrane that relate to the cells capacity to generate ATP via OXPHOS (Perry et al., 2011). Reduced ATP synthesis associated with impaired ATP synthase activity results in mitochondrial membrane hyperpolarisation. Mitochondrial membrane potential was measured using TMRE staining followed by flow cytometry analysis in stable inducible U2OS cells expressing vector, wild type Strap and L-Strap grown in either glucose or galactose supplemented media. In glucose supplemented media, no changes in the flow cytometry analysis were observed between wild type Strap and vector control (**Figure 6.8A, left panel**). L-Strap expressing cells showed a marginal shift to the right which indicates mitochondrial membrane hyperpolarisation (**Figure 6.8A, left panel**). Stable inducible U2OS cells expressing wild type Strap and L-Strap grown in galactose supplemented media showed progressive mitochondrial membrane hyperpolarisation depicted by shifts to the right, corresponding to higher TMRE staining compared to vector control (**Figure 6.8A, right panel**). This implies the increase levels of Strap at the mitochondria (depicted by L-Strap compared to wild type Strap) during OXPHOS, results in increase in mitochondrial hyperpolarisation.

It was postulated that Strap may affect the cellular ATP/ADP ratio by modulating ATP synthase activity given the interaction between Strap and ATP synthase subunit-β. This hypothesis was tested by measuring the ATP synthase specific activity using an ELISA based assay. Enzyme activity was measured in U2OS cells expressing stable inducible vector, wild type Strap and L-Strap grown in either glucose or galactose supplemented media. U2OS cells treated with oligomycin, a specific ATP synthase inhibitor, was used as a control in this assay.

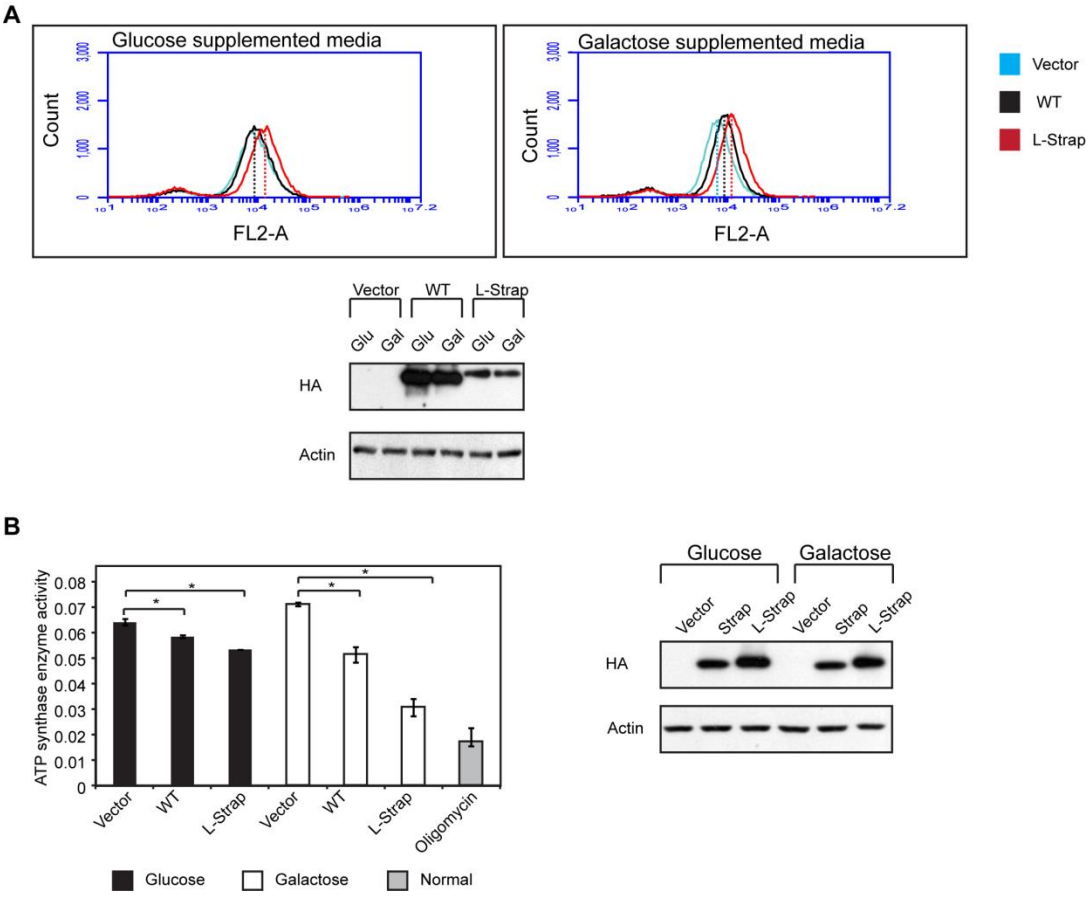



**Figure 6.8 Strap influences the mitochondrial membrane potential and ATP synthase activity.**

**A.** TMRE staining (x axis) of induced (with doxycycline, 1 µg/ml) U2OS cells stably expressing vector, wild type and L-Strap grown in either glucose or galactose supplemented media as indicated. The staining was detected in the FL2-A channel. Immunoblots represent input protein levels. Ectopic Strap was detected with anti-HA antibody and actin served as loading control.

**B.** ATP synthase specific activity was measured in induced (with doxycycline, 1 µg/ml) U2OS inducible stable cells expressing vector, wild type Strap and L-Strap grown in either glucose or galactose supplemented media. Cells treated with oligomycin served as a control. The levels of Strap proteins are shown via immunoblotting. Ectopic Strap was detected with anti-HA antibody and actin served as loading control. Values represent mean ± s.d. * indicates $p<0.05$, Student's t-test, n = 3 independent experiments.

Cells overexpressing wild type Strap and L-Strap resulted in a significant reduction in ATP synthase activity in glucose supplemented media (**Figure 6.8B**). A marked reduction was observed in wild type Strap and L-Strap expressing cells grown in galactose supplemented media (**Figure 6.8B**).

p53 was shown to promote OXPHOS and the absence of p53 results in an increase in glycolysis (Matoba et al., 2006). Interestingly, p53 balancing the use of glycolysis and OXPHOS in energy production does not alter the total ATP levels (Matoba et al., 2006). Strap decreased the ATP/ADP ratio and ATP synthase activity in the presence of p53. Since there are reports which suggest that p53 influences aerobic respiration, the ATP/ADP ratio and the ATP synthase activity were measured in the presence and absence of p53. The HCT116 cell lines which harbour wild type p53 ($^{+/+}$) and the p53 nulls cells ($^{-/-}$) were used. In agreement with previous reports (Maddocks et al., 2013; Matoba et al., 2006), the ATP/ADP ratio was not altered when cells were grown in complete media (**Figure 6.9A**). A small but significant increase in ATP/ADP ratio was observed in cells expressing wild type p53 grown in galactose supplemented media (**Figure 6.9A**). The converse was observed in cells grown in glucose supplemented media where the absence of p53 resulted in an increase in the ATP/ADP ratio (**Figure 6.9A**). Intriguingly, p53 did not alter the ATP synthase activity in either complete, glucose or galactose supplemented media (**Figure 6.9B**).

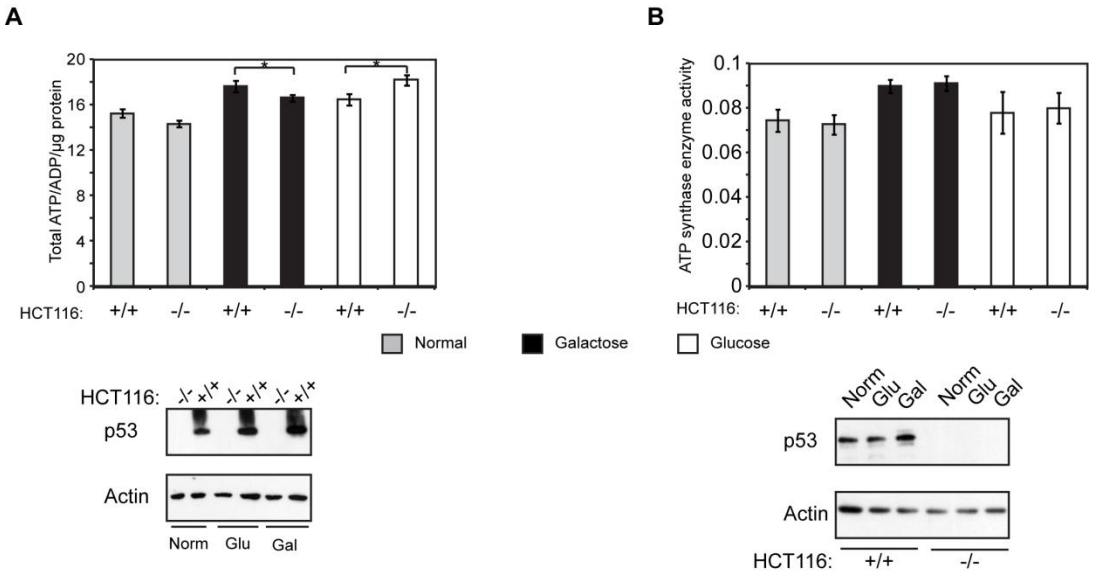



**Figure 6.9 ATP synthase activity and ATP/ADP ratio in the presence and absence of p53.**

**A.** Cellular ATP/ADP ratio was measured in HCT116$^{+/+}$ and HCT116$^{-/-}$ grown in either complete (norm), glucose (glu) or galactose (gal) supplemented media. The levels of p53 are shown via immunoblotting. p53 was detected with anti-p53 antibody and actin served as loading control. Values represent mean ± s.d. * indicates $p<0.05$, Student's t-test, n = 3 independent experiments. The ATP/ADP ratio was measured by Stratford MR, Department of Oncology, University of Oxford.

**B.** ATP synthase specific activity was measured in HCT116$^{+/+}$ and HCT116$^{-/-}$ grown in either complete (norm), glucose (glu) or galactose (gal) supplemented media. The levels of p53 are shown via immunoblotting. p53 was detected with anti-p53 antibody and actin served as loading control.

This study suggests that Strap depletes the cellular ATP/ADP ratio in the presence of p53. L-Strap induces mitochondrial membrane hyperpolarisation, comparable to oligomycin, a specific ATP synthase inhibitor. Collectively these data suggest that mitochondrial Strap reduces the cellular ATP/ADP ratio by deregulating the ATP synthase activity in the presence of p53.

### 6.4 L-Strap augments apoptosis during OXPHOS in the presence of p53

Strap augments p53-induced apoptosis during damage response. The ability of Strap to induce apoptosis was examined in the absence and presence of damage when cells were grown in either glucose or galactose supplemented media.

Initially levels of cleaved PARP-1 were measured in U2OS cells expressing stable inducible vector, wild type Strap and L-Strap grown in either glucose or galactose supplemented media upon DNA damage treatment. Induction of cleaved PARP-1 was observed at 4 hr upon damage in vector control cells grown in either glucose (**Figure 6.10A**) or galactose (**Figure 6.10B**) supplemented media. In cells expressing wild type Strap, cleaved PARP-1 levels were upregulated as early as 1 hr after damage in glucose supplemented media (**Figure 6.10A**) and at 2 hr after damage in galactose supplemented media (**Figure 6.10B**). Interestingly, cells overexpressing L-Strap grown in galactose supplemented media showed an increase in cleaved PARP-1 at an earlier time point compared to vector control (**Figure 6.10B**) but this was not observed in glucose supplemented media (**Figure 6.10A**).

This study was further extended to investigate the influence of p53 on Strap-induced apoptosis in glucose and galactose supplemented media. Levels of cleaved PARP-1 over time were measured when vector, wild type Strap and L-Strap were expressed in $HCT116^{+/+}$ ($p53^{+/+}$) or $HCT116^{-/-}$ ($p53^{-/-}$) cells grown in either glucose or galactose supplemented media. In glucose supplemented media, an increase in cleaved PARP-1 was observed at 2 hr upon damage when wild type Strap was expressed in $HCT116^{+/+}$ cells compared to L-Strap and vector control expressing cells (**Figure 6.10C**). In galactose supplemented media, cleaved PARP-1 was observed at 6 hr in $HCT116^{+/+}$ expressing vector control (**Figure 6.10D**). Wild type Strap and L-Strap showed an induction in cleaved PARP-1 at 4 hr and 2 hr upon damage respectively (**Figure 6.10D**). Cleaved PARP-1 was not detected in p53 null cells ($HCT116^{-/-}$) within the first 6 hr upon damage treatment.

In conclusion, wild type Strap expressing cells were able to induce apoptosis in both glucose and galactose supplemented media whilst L-Strap expressing cells showed an increase in cleaved PARP-1 compared to vector control only when galactose supplemented media was used. The induction of cleaved PARP-1 by wild type Strap and L-Strap expressing cells is p53-dependent.

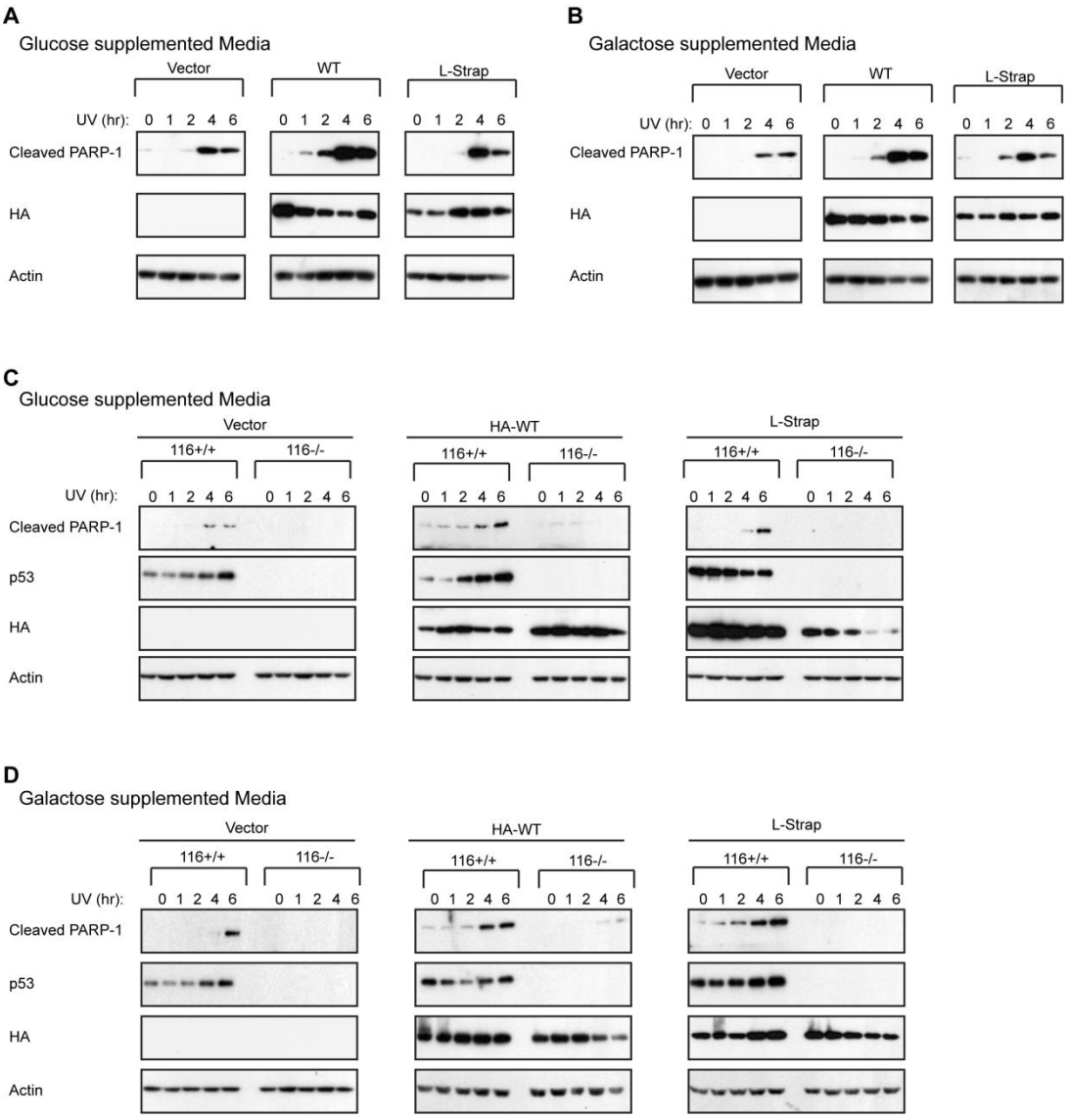



**Figure 6.10 Strap induces apoptosis in a p53-dependent manner.**

U2OS inducible stable cells expressing vector, wild type Strap (WT) and L-Strap induced with doxycycline, 1 µg/ml (**A** & **B**), HCT116$^{+/+}$ and HCT116$^{-/-}$ (**C** & **D**) cells transfected with either 1 µg of vector control, wild type Strap (WT) or L-Strap were grown in glucose (**A** & **C**) or galactose (**B** & **D**) supplemented media as indicated. Cells were treated with UV light (50 J/m$^2$) and harvested at the indicated time points. Ectopic Strap and p53 were detected with anti-HA antibody and anti-p53 antibody respectively. Cleaved PARP-1 was used as an apoptotic marker while actin served as loading control.

To further substantiate the induction of cleaved PARP-1 observed when L-Strap was overexpressed upon DNA damage in galactose supplemented media, the apoptotic cell population (Sub-G1) was measured by FACs analysis. Consistently, an increase in the Sub-G1 population was observed in inducible stable U2OS cells expressing L-Strap grown in galactose supplemented media upon UV treatment compared to vector control (**Figure 6.11A**). This was not observed in SAOS2 cells (p53 null) stably expressing L-Strap either in the presence or absence of damage, grown in either glucose or galactose supplemented media (**Figure 6.11B**).

Oligomycin specifically inhibits ATP synthase activity which results in ATP depletion. If the Strap-regulated ATP synthase activity modulates Strap induced-apoptosis during OXPHOS, complete inhibition of ATP synthase activity will impair Strap-induced apoptosis. To test this hypothesis, ATP synthase activity was modulated in cells overexpressing either vector or L-Strap by treating with different doses of oligomycin.

Initially, a dose escalation study was carried out to obtain a dose of oligomycin that partially or completely inhibited the ATP synthase activity (**Figure 6.12A**). This dose escalation study was further extended by measuring the apoptotic population in U2OS cells expressing stable inducible vector control and L-Strap treated with different doses of oligomycin (**Figure 6.12B & C**). When 20 μM of oligomycin (partial inhibition) was used, an increase in apoptotic cells was observed in cells overexpressing L-Strap compared to vector control (**Figure 6.12B**).

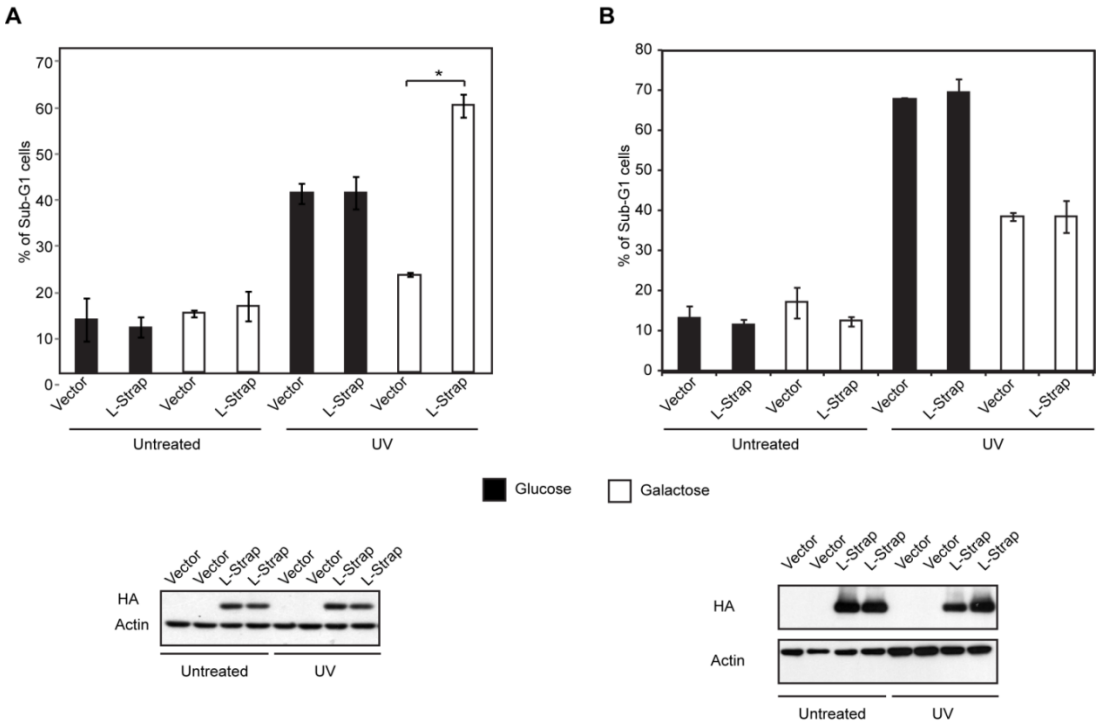



**Figure 6.11 L-Strap induces apoptosis during OXPHOS in a p53-dependent manner in the presence of damage.**

Induced (with doxycycline, 1 µg/ml) U2OS inducible stable cells (**A**) and SAOS2 cells (**B**) stably expressing vector and L-Strap were grown in glucose or galactose supplemented media, and were treated with UV light (30 J/m$^2$, 16 hr) as indicated. Cell viability was assessed by analysing Sub-G1 DNA content. The levels of Strap were shown via immunoblotting. Ectopic Strap was detected with anti-HA antibody and actin served as loading control. Values represent mean ± s.d. * indicates $p<0.05$, Student's t-test, n = 3 independent experiments.

No change in the number of apoptotic cells was observed when a higher dose (40 μM, complete inhibition) was used (**Figure 6.12C**). This suggests mitochondrial Strap mediates apoptosis by regulating ATP synthase activity.

Strap depletes ATP and induces apoptosis. This implies inhibiting Strap-mediated ATP depletion by supplementing exogenous ATP will negate its apoptotic response. Interestingly, restoring the ATP levels with 20 mM of inosine was able to completely revert the apoptotic response of L-Strap upon damage treatment (**Figure 6.12D**).

Taken together, the data in this study suggests Strap induces apoptosis via ATP depletion by regulating ATP synthase activity.

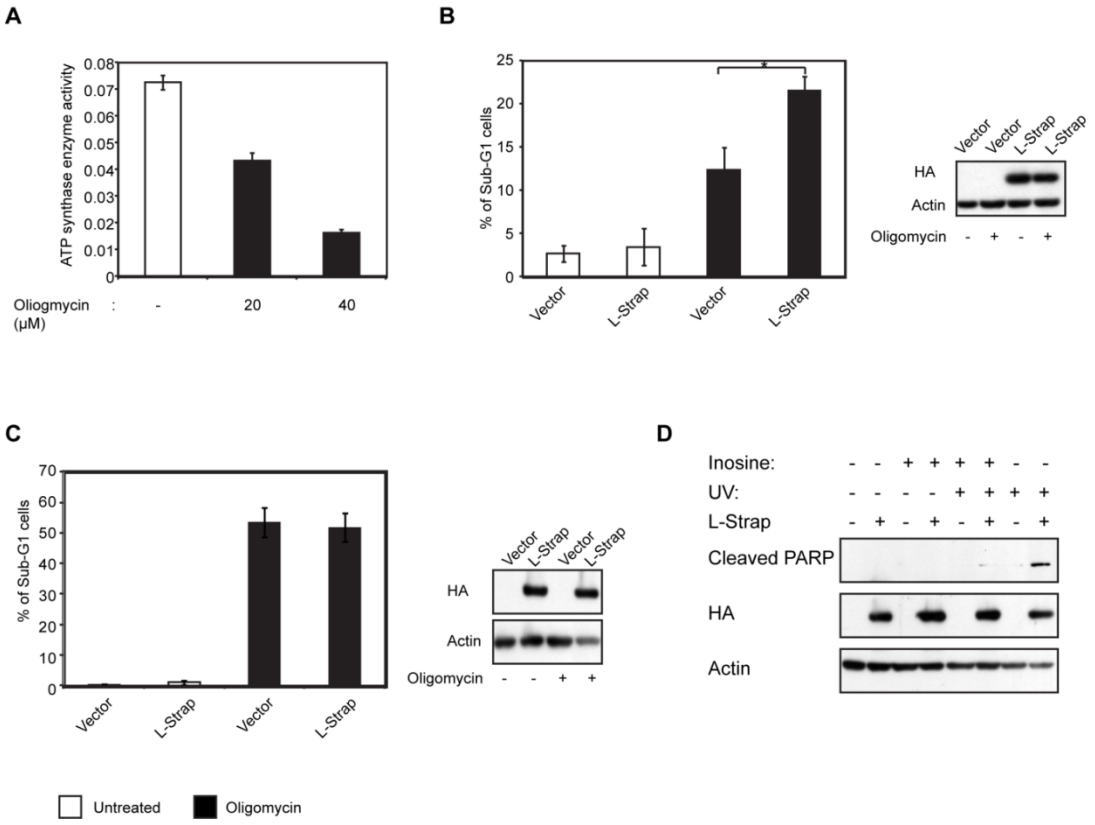



**Figure 6.12 ATP depletion mediates L-Strap induced apoptosis.**

**A.** ATP synthase activity was measured in U2OS cells treated with the indicated doses of oligomycin.

U2OS inducible stable cells expressing vector and L-Strap induced with doxycycline, 1 μg/ml were treated with either 20 μM (**B**) or 40 μM (**C**) of oligomycin. Cell viability was assessed by analysing Sub-G1 DNA content. The levels of Strap were shown via immunoblotting. Ectopic Strap was detected with anti-HA antibody and actin served as loading control. Values represent mean ± s.d. * indicates $p<0.05$, Student's t-test, n = 3 independent experiments.

**D**.U2OS inducible stable cells induced with doxycycline, 1 μg/ml were grown in galactose supplemented media expressing vector or L-Strap and treated with either inosine (20 mM, 6 hr) and/or UV light (50 J/$m^2$, 3 hr) as indicated. Ectopic Strap was detected with anti-HA antibody. Cleaved PARP-1 was used as an apoptosis marker and actin served as loading control.

### 6.5 Regulation of Strap during hypoxia

Cancer cells mainly maintain their energy requirement via glycolysis in the absence and presence of oxygen. Adaptive metabolic responses towards a low oxygen environment are essential to maintain rapid proliferation and are highly relevant for tumour progression. Most mammalian tissue exists at 2-9 % oxygen whilst a hypoxic environment is defined when oxygen is at ≤ 2 % (Bertout et al., 2008). Since Strap was regulated during OXPHOS when the presence of oxygen was essential, it was of interest to explore the regulation of Strap during the converse environment; hypoxia.

Initially, levels of Strap in total cell lysates and mitochondrial fractions were measured during hypoxia. An increase in Strap was observed during hypoxia in total cell lysates (**Figure 6.13A & C**) but the converse was observed in the mitochondrial fractions (**Figure 6.13B & D**). Similar results were observed in total cell lysate when hypoxia-mimetic agent desferrioxamine (DFO) was used (**Figure 6.13E & F**). Upregulation of HIF-1α was used as a marker for hypoxic stress.

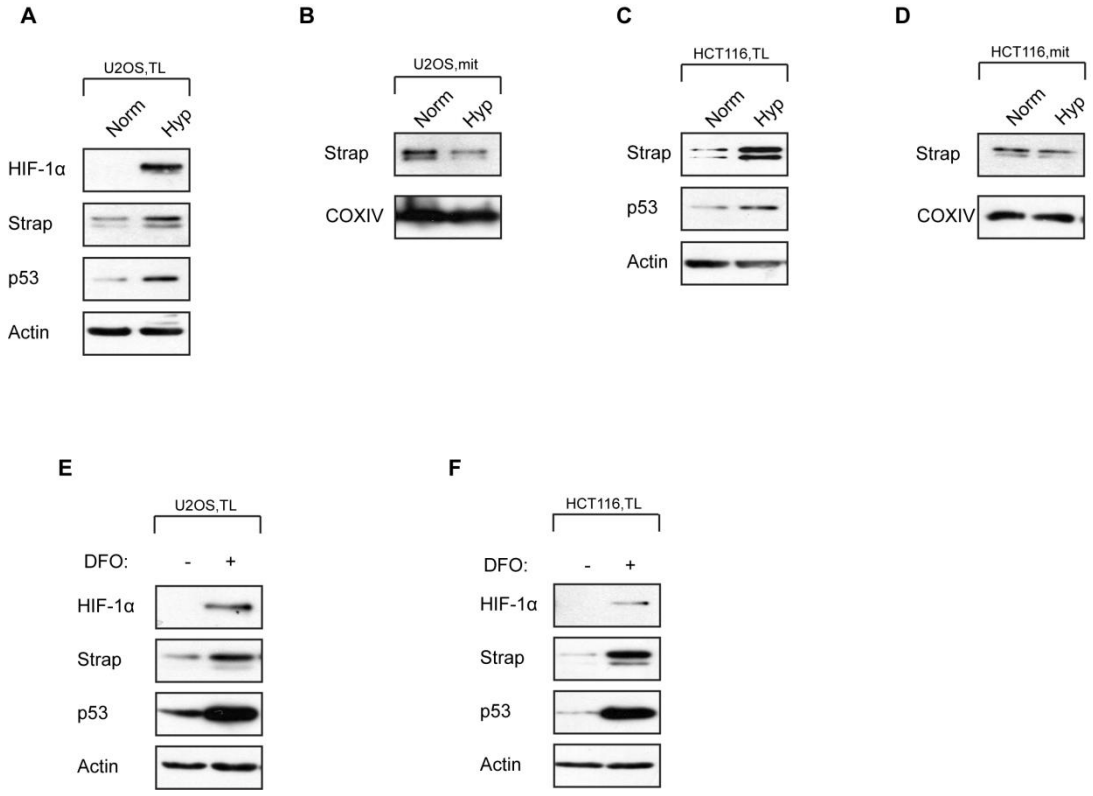



**Figure 6.13 Strap levels during hypoxia.**

U2OS (**A** & **B**) and HCT116$^{+/+}$ (**C** & **D)** cells were incubated under normoxic (Norm) and hypoxic (Hyp, 1 % oxygen) conditions as indicated before harvesting. Total cell lysates (**A** & **C**) and mitochondrial fractions (**B** & **D**) were immunoblotted with the indicated antibodies.

U2OS (**E**) and HCT116$^{+/+}$ (**F**) cells were treated with DFO (100 μM) for 24 hr before harvesting and immunoblotted with antibodies as indicated.

Endogenous Strap and p53 levels were detected using anti-Strap antibody and p53 DO-1 antibody respectively. HIF-1α was detected using HIF-1α antibody. Actin and COXIV served as loading control for total cell lysate and mitochondrial fractions, respectively.

Adaptation to hypoxia in cells is mainly mediated via the regulation of transcription by HIF-1. HIF-1 is a heterodimeric protein that consists of two subunits, HIF-1α and HIF-1β. Both of these subunits form dimers during hypoxia. The dimer binds to the core DNA binding sequence 5'A/G CGTG 3' known as HRE (Semenza, 2010). Close inspection of the promoter region of Strap identified one putative HRE that matches the canonical sequence (**Figure 6.14A**). The transcriptional regulation of Strap during hypoxia was investigated by measuring mRNA levels. Of note, an increase in Strap mRNA levels was observed during hypoxia in U2OS cells (**Figure 6.14B**).

Together, these data indicate Strap level is enhanced during hypoxia and further suggest a transcriptional regulation in response to hypoxia.




**Figure 6.14 Transcriptional regulation of Strap during hypoxia.**

**A.** Sequence of the human Strap 5' promoter region. The grey shading indicates Exon 1. Underlined is the initiating methionine and the yellow highlight is the putative HRE.

**B.** Semi-quantitative RTPCR analysis on total RNA for endogenous Strap expression in U2OS cells during normoxic and hypoxic (16 hr, 1% oxygen) conditions. 18S served as loading control.

## 6.6 Summary

The proteomic analysis of L-Strap identified ATP synthase subunit-β as a potential Strap interacting protein (**Figure 6.1**). The ATP synthase complex is an inner mitochondrial membrane protein and subunit-β is one of the main catalytic domains involved in ATP synthesis during OXPHOS. The interaction between Strap and ATP synthase subunit-β was confirmed via immunoprecipitation using an antibody that specifically detects the ATP synthase subunit-β in cells with overexpressed Strap and endogenous experiments (**Figure 6.2**). Of note, the Strap-ATP synthase subunit-β interaction was enhanced in galactose supplemented media (**Figure 6.4A**).

The increased level of mitochondrial Strap (**Figure 6.3**) and the increased interaction of Strap and ATP synthase subunit-β observed in galactose supplemented media (**Figure 6.4**) suggest that Strap levels are modulated when cells are forced to derive energy by OXPHOS. Interestingly, Strap depletes ATP in a p53-dependent manner (**Figure 6.7**), potentially via ATP synthase subunit-β. The decreased ATP is associated with decreased ATP synthase enzymatic activity and hyperpolarisation of the mitochondrial membrane potential (**Figure 6.8**).

Strap-dependent ATP depletion (**Figure 6.6 & 6.7**) and reduced ATP synthase activity (**Figure 6.8A**) were observed in the absence of damage. Interestingly, Strap-dependent apoptosis during OXPHOS was observed only in the presence of damage (**Figure 6.10 & 6.11**). This suggests that Strap induced ATP depletion (**Figure 6.6 & 6.7**) and mitochondrial hyperpolarisation (**Figure 6.8**) were not

sufficient to induce cell death but perhaps these events sensitise the cells and accelerate the apoptotic response upon cellular stress. These results were reiterated when restoration of Strap-mediated ATP depletion inhibited Strap-induced apoptosis (**Figure 6.12D**).

L-Strap was found to be sensitive to the ATP synthase inhibitor oligomycin (**Figure 6.12B**). L-Strap did not enhance the apoptosis levels when complete inhibition of ATP synthase activity was achieved (**Figure 6.12C**) suggesting the cell death observed in L-Strap overexpressed cells is mediated by regulating ATP synthase activity. Replenishment of ATP by treating the cells with inosine prevented L-Strap-induced apoptosis (**Figure 6.12D**) which further substantiate the hypothesis that L-Strap induces apoptosis via ATP depletion which is mediated by reducing ATP synthase activity. Of note, cellular energy status is not affected by the presence of p53 (Maddocks et al., 2013; Matoba et al., 2006) (**Figure 6.9A**). Impaired cell's ability to produce ATP which results in severe ATP depletion is associated with necrosis. Of note, the data in this study does not preclude cell death via necrosis and perhaps this line of investigation warrants attention.

The current data mainly focused on the role of Strap when OXPHOS is predominant. Nevertheless, an initial study of Strap during hypoxic condition suggests a potential transcriptional regulation of Strap (**Figure 6.13 & 6.14**). It is postulated that perhaps Strap has a dual role in inducing apoptosis depending on its microenvironment. It maybe that Strap's nuclear role is prominent during low

oxygen tension and when cancer cells rely upon OXPHOS for energy, Strap depletes ATP and sensitises the cells to p53-dependent apoptosis.

Together, this study proposes a new mechanism of Strap at the mitochondria which involves deregulating the ATP levels and ATP synthase activity potentially via its interaction with ATP synthase subunit-β to induce p53-dependent apoptosis.

# Chapter 7

# Results: Strap derivatives

### 7.1 Proteomic analysis of the OB fold

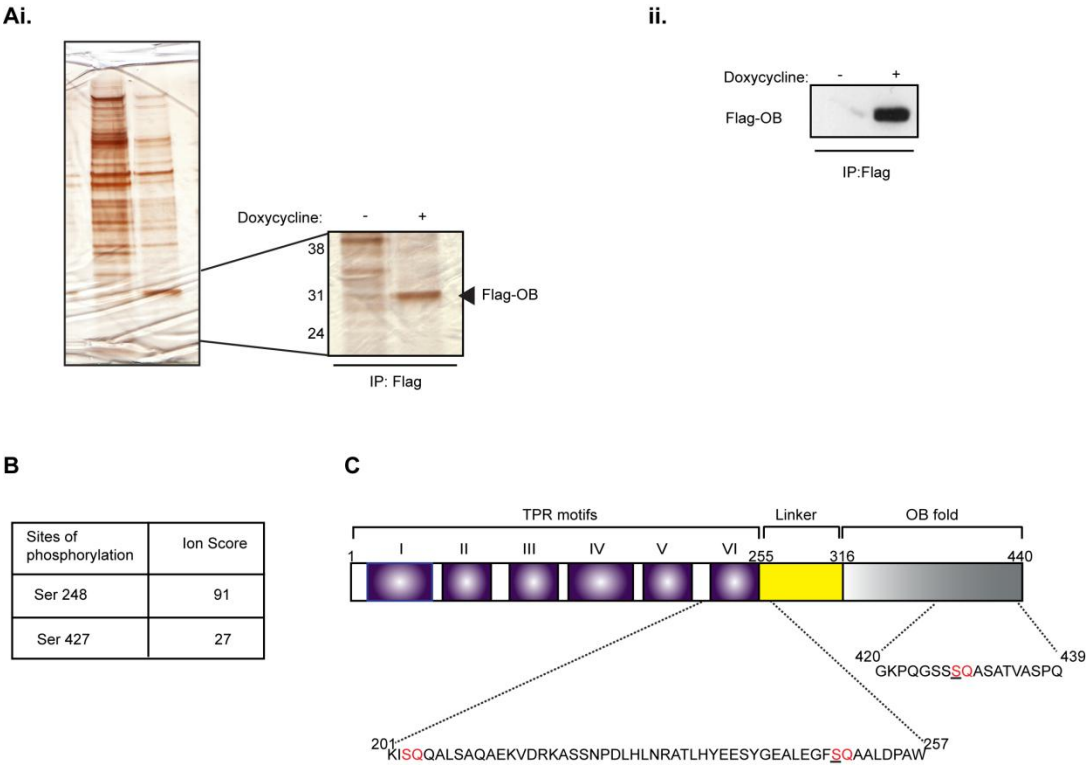
In an effort to detect proteins interacting with the OB fold, proteomic analysis was performed using LC/MS-MS on ectopic OB fold immunoprecipated from inducible U2OS cells stably expressing Flag-tagged OB fold. Besides identifying interacting proteins, PTMs were detected from the immunoprecipitation (**Figure 7.1A**). PTMs are processing events that change the property of a protein by proteolytic cleavage or by addition of a modifying group to one or more amino acids. PTM of a protein influences the physiological activity, localisation, turnover and interaction with other proteins (Mann and Jensen, 2003). Mass spectrometry has long been used as a tool to identify PTMs on an individual protein.

The proteomic analysis of the OB fold construct identified two new plausible sites of phosphorylation; one at S248 located in the sixth TPR motif (with a MASCOT score of 97) and the other S427, located in the OB fold (with a MASCOT score of 27) (**Figure 7.1B**). Both phosphorylation sites identified in the mass spectrometry analysis were at consensus phosphorylation sites for ATM/ATR kinase. The first phosphorylation site at S248 was identified when the peptide fragment covering 236-263 indicated an increase in the mass of the peptide by 98 Da which implied the presence of phosphoric acid ($H_3PO_4$). The increase in mass occurred between peptide covering 248-251 and since there is only one S residue present in this fragment, the phosphorylation was indicated to occur at S248 (**Figure 7.2A**). The low ion score for S427 was due to the detection of four possible phosphorylation sites in the same peptide sequence (426-433) (**Figure 7.2B**), and the MASCOT search engine was unable to confidently distinguish between these sites. Although

all four sites had an equal ion score, S427 was particularly of interest due to its putative ATM/ATR consensus.

ATM and ATR kinases play a key role during the DNA damage response and DNA replication. The ATM/ATR kinase family is highly conserved throughout eukaryotic evolution and preferentially phosphorylate their substrates on S or threonine (T) residues that precede glutamine (Q) residues, "so-called" SQ/TQ motifs (Traven and Heierhorst, 2005). Wild type Strap contains three SQ/TQ motifs (**Figure 7.1C**). Strap was previously shown to be phosphorylated by ATM kinase at S203 (Demonacos et al., 2004). Based on the two new sites identified by mass spectrometry and the known ATM/ATR site, both phosphomutant and phosphomimetic derivatives were generated. The S residue was replaced by an alanine (A) residue to block phosphorylation and constructs mimicking phosphorylation were generated by replacing the S residue with an aspartic acid (D) residue.

In summary, phosphomimetics and phosphomutants were generated based on the two new phosphorylation sites for ATM/ATR kinase identified from the OB fold mass spectrometry and the previously reported S203 site.




| Sites of phosphorylation | Ion Score |
|---|---|
| Ser 248 | 91 |
| Ser 427 | 27 |

**Figure 7.1 Phosphorylation sites identified via mass spectrometry.**

**Ai.** OB fold was immunoprecipitated using anti-Flag antibody from U2OS stable inducible cells expressing OB fold either induced with doxycycline (1 µg/ml, 24 hr) (+) or uninduced (-). The eluates were separated by SDS-PAGE gel and silver stained. The position of the OB fold is indicated.

**ii.** 2% of the immunoprecipitates obtained from (**i**) were used as inputs to confirm the precipitation of the OB fold via immunoblot. The OB fold was detected using the anti-Flag antibody.

**B.** Table summarizing the ion scores for the phosphorylation sites detected via mass spectrometry.

**C.** Red highlight represents three consensus phosphorylation sites (SQ and TQ) ATM/ATR kinase in the Strap peptide sequence. The underlined red amino acid residues are the phosphorylation sites obtained from MASCOT analysis using the UniProt_SwissProt protein database (https://mascot.molbiol.ox.ac.uk).

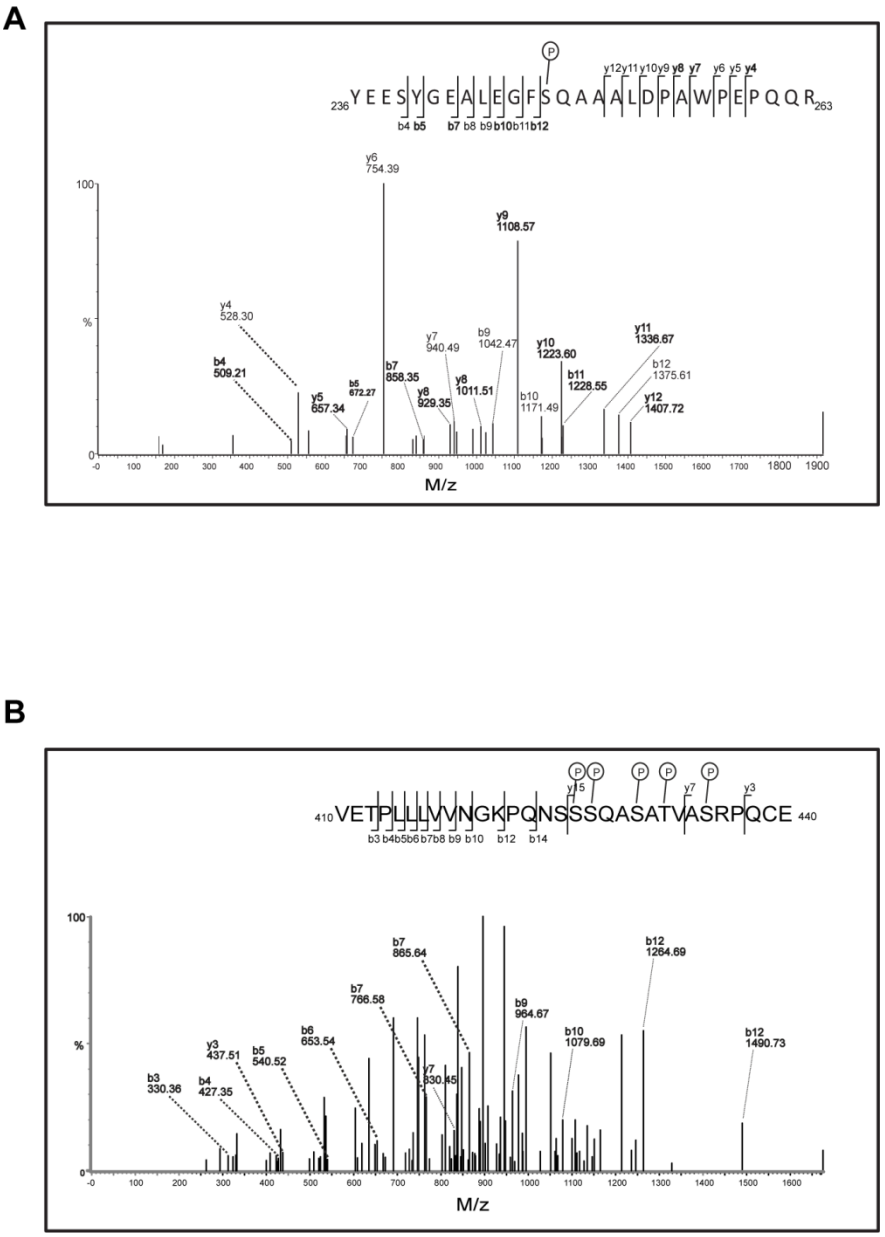



**Figure 7.2 Strap is phosphorylated.**

The sequence of the OB fold (221-440) covering residues 236-263 **(A**) and 410-440 (**B**) are shown and the possible phosphorylation sites are indicated. Fragment ions are indicated as b and y ions. (Spectra were generated by Kessler BM, Nuffield Department of Medicine, University of Oxford.)

### 7.2 Characterization of Strap ATM/ATR consensus sites

Conversion of an S residue to a D or an A residue allows functional assessment of specific phosphorylation events in a cellular context. The D residue mimics phosphorylation due to the presence of the negatively charged carboxyl group. The substitution with the A residue abolishes phosphorylation due to the absence of the charged group. Initially, the SQ/TQ motifs were mutated individually to examine the significance of the phosphorylation site.

As previously reported, reduced nuclear staining was observed in S203A compared to the S203D derivative upon damage treatment (**Figure 7.3**). All the other mutants exhibited an intense staining both in the cytoplasmic and nuclear region similar to that of wild type Strap (**Figure 7.3**). Mutation of all these phosphorylation sites namely S203, S248 and S427 to A (3A) did not alter the localisation of Strap (**Figure 7.4**). The phosphomimetics replacing 203, 248 and 427 from S to D (3D) demonstrated a predominantly cytoplasmic localisation compared to wild type Strap (**Figure 7.4**). Intriguingly, when the cells were treated with UV light, the phosphomimetic mutant exhibited an unusual localisation which was later confirmed to reflect its association with mitochondria (**Figure 7.4**). The association with mitochondria was confirmed by using a cationic dye, mitotracker (MitoTracker®Red CMXRos, MITO), that specifically stains the mitochondria. It binds irreversibly to the polarized mitochondrial membrane enabling it to be used prior to fixing cells (Poot et al., 1996). The localisation of ectopic Strap derivatives is summarized in **Figure 7.5A**.

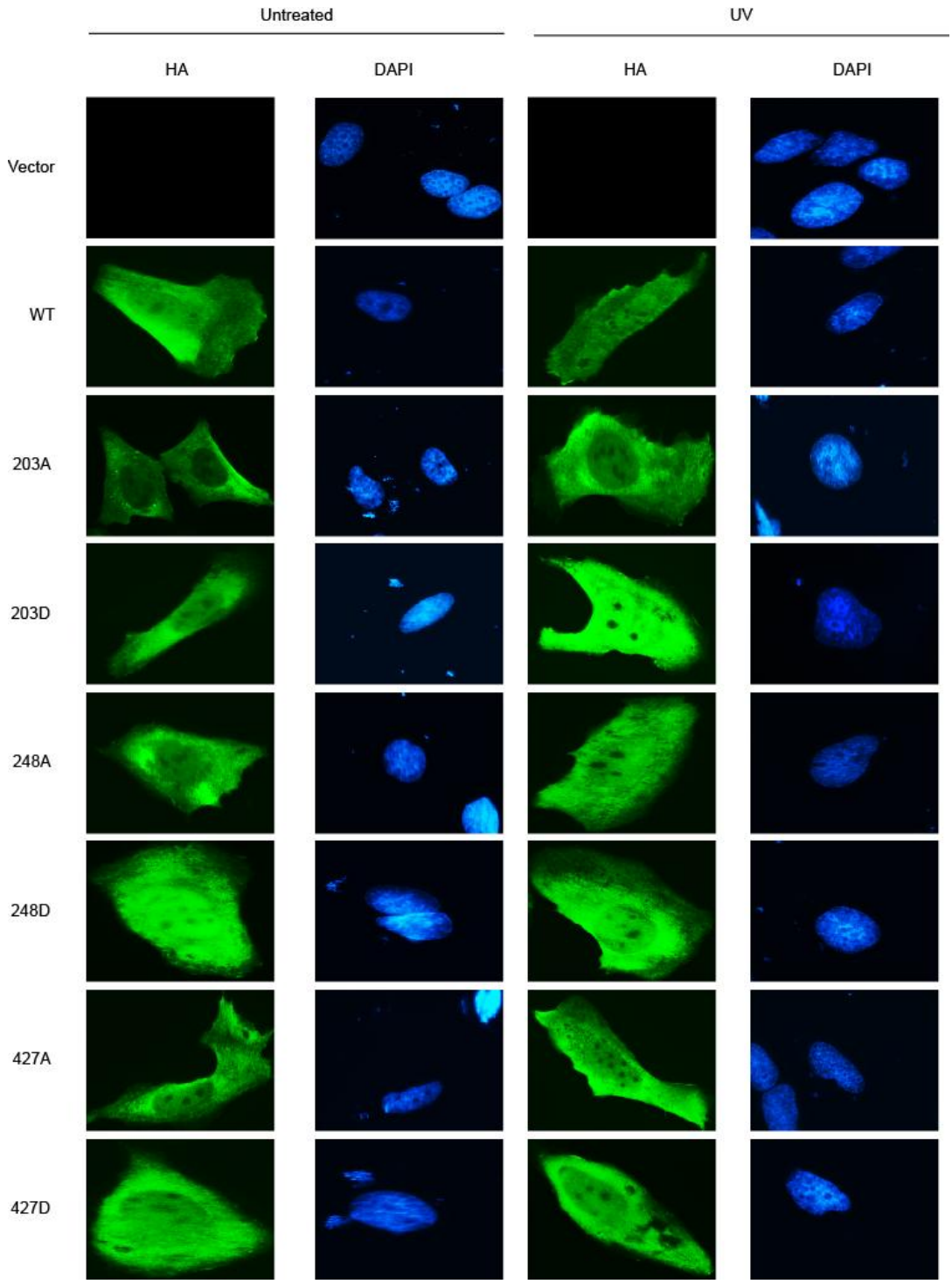



**Figure 7.3 Localisation of Strap derivatives.**

U2OS cells were transfected with wild type Strap (WT), Strap derivatives or empty vector and were either untreated or treated with UV light (50 J/m$^2$, 6 hr) as indicated. Cells were immunostained with anti-HA (HA) antibody to detect ectopic Strap and DAPI was used to visualize the nuclei. (Magnification X600.)

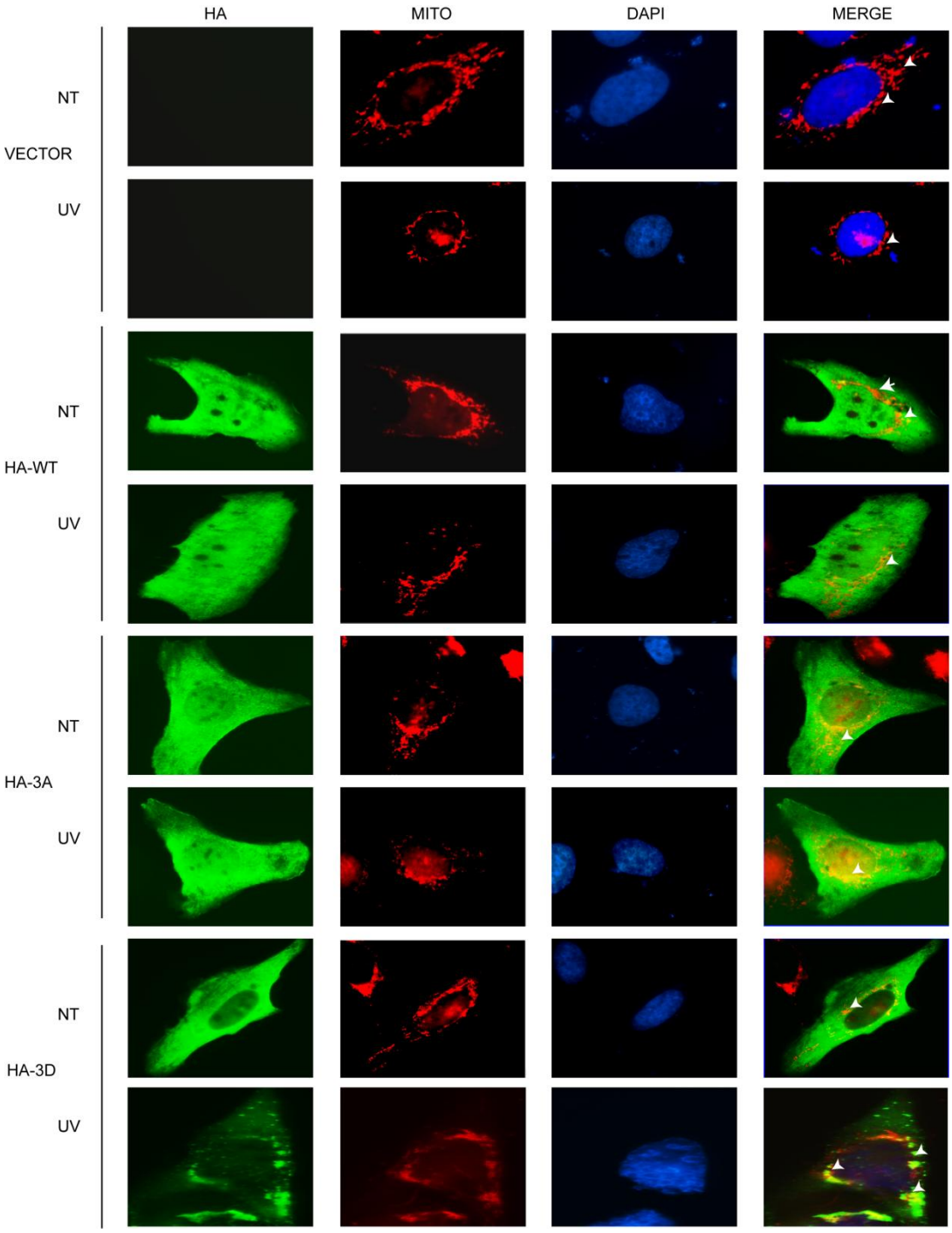



**Figure 7.4 Strap derivative is localised to mitochondria.**

U2OS cells were transfected with wild type Strap (HA-WT), HA-3A, HA-3D or empty vector. Cells were either untreated (NT) or treated with UV light (50 J/m$^2$, 6 hr) as indicated (UV). Cells were immunostained with anti-HA (HA) antibody to detect ectopic Strap. Mitotracker (MITO) was used to stain mitochondria and DAPI was used to visualize the nuclei. Combination of MITO and HA staining is shown (MERGE). Arrowheads indicate colocalisation of Strap and mitotracker (Magnification X600.)

The ability of Strap derivative to localise at the mitochondria was further examined using biochemical fractionation. Mitochondrial fractionation from U2OS cells by differential centrifugation demonstrated that in the absence of damage, ectopic wild type Strap and HA-3D were detected in the mitochondrial fraction (**Figure 7.5Bi**). When the cells were treated with UV light, higher HA-3D levels compared to wild type Strap were observed in the mitochondrial fraction (**Figure 7.5Bii**). An increased level of wild type Strap compared to HA-3D was observed in the cytoplasmic fraction under both damage and non damage conditions (**Figure 7.5Biii & iv**).

Collectively the data observed from the immunostaining and biochemical fractionations suggest that predominant localisation of the HA-3D mutant to the mitochondria in the presence of damage.

**A**

| Derivatives | Localization | |
|---|---|---|
| | Untreated | UV |
| WT | Cytoplasmic & nuclear | Cytoplasmic & nuclear |
| 203A | More cytoplasmic | More cytoplasmic |
| 203D | More cytoplasmic | Cytoplasmic & nuclear |
| 248A | Cytoplasmic & nuclear | Cytoplasmic & nuclear |
| 248D | Cytoplasmic & nuclear | Cytoplasmic & nuclear |
| 427A | Cytoplasmic & nuclear | Cytoplasmic & nuclear |
| 427D | Cytoplasmic & nuclear | Cytoplasmic & nuclear |
| 3A | Cytoplasmic & nuclear | Cytoplasmic & nuclear |
| 3D | More cytoplasmic | Mitochondria |

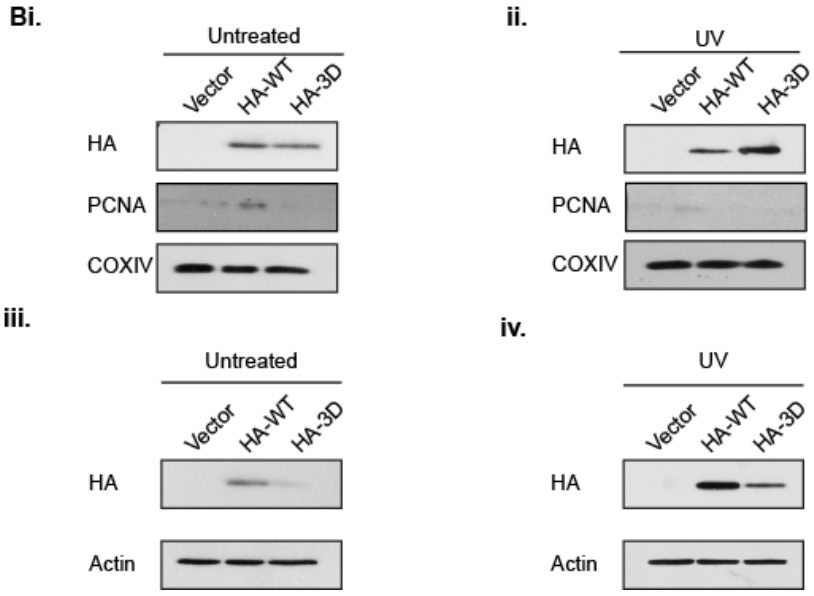



**Figure 7.5 HA-3D is predominantly in the mitochondrial fraction.**

**A.** Table summarising the properties of the Strap derivatives.

**B.** Immunoblots of mitochondrial fractions (**i** & **ii**) and cytoplasmic fractions (**iii** & **iv**) from U2OS cells transfected with either 1 µg of empty vector, wild type Strap (HA-WT) or HA-3D. Cells were either untreated (**i** & **iii**) or treated with UV (**ii** & **iv**) (50 J/m$^2$, 3 hr) as indicated. The level of PCNA, a nuclear protein, was used to assess the purity of the mitochondrial fractions. COXIV and actin were used to assess mitochondrial and cytoplasmic loading, respectively.

### 7.3 Impact of ATM/ATR phosphorylation on Strap at the mitochondria

ATM and ATR collaborate in many ways, but the cellular phenotypes that result from the loss of ATM and ATR are dramatically different. The loss of ATR causes rapid lethality at the earliest embryonic stage (Brown and Baltimore, 2000; de Klein et al., 2000) whilst the homozygous ATM disrupted mice have growth retardation, neurologic dysfunction, infertility, immunologic abnormality, chromosomal instability and extreme sensitivity to IR (Barlow et al., 1996). Since the SQ/TQ motif is a shared consensus between the two kinases, ATM and ATR, further elucidation was required to assess whether Strap is phosphorylated by ATM and/or ATR kinase. The ataxia telangiectasia (AT) cell line which is ATM deficient ($ATM^{-/-}$) and its ATM reconstituted counterpart were used to investigate Strap levels in the absence and presence of DNA damaging agent. To begin with, levels of ATM were verified in these cell lines via immunoblotting (**Figure 7.6A**).

Levels of Strap were determined in these cell lines in the absence or presence of DNA damaging agent. Etoposide was used as it has been shown to activate both ATM and ATR via induction of DSBs (Schonn et al., 2010). In total cell lysates, Strap was upregulated in the presence of ATM upon treatment with etoposide. Reduced levels of Strap were observed in ATM deficient cells upon damage treatment **(Figure 7.6B**). Intriguingly, in the mitochondrial fraction, the converse result was observed; a reduced level of Strap was observed in ATM proficient cells compared to ATM deficient cells and this was further reduced upon damage treatment (**Figure 7.6C**).

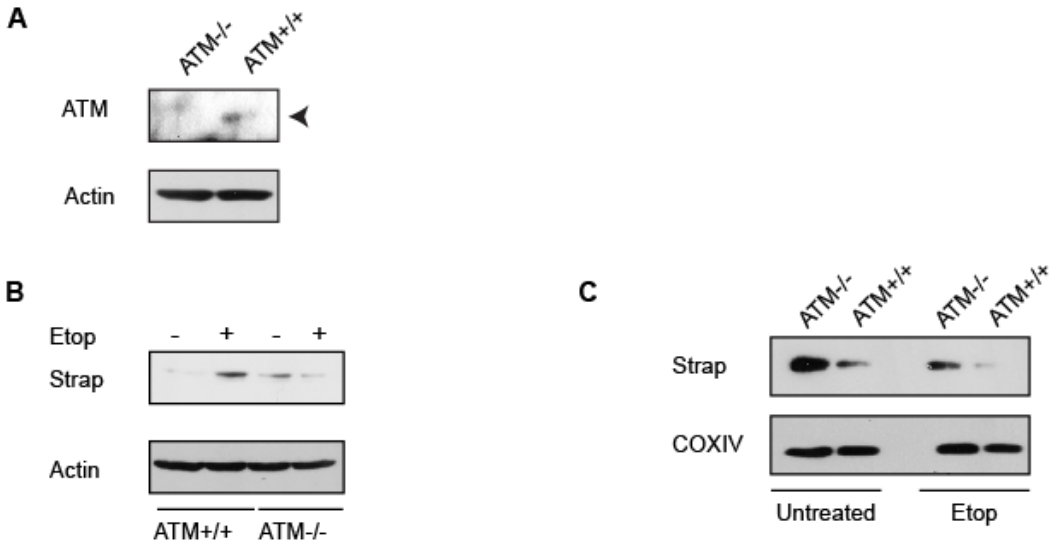



**Figure 7.6 Strap levels in the presence and absence of ATM.**

**A.** $ATM^{-/-}$ and $ATM^{+/+}$ cell lysates were loaded according to total protein content. ATM was detected using ATM antibody and actin serves as a loading control. Arrowhead indicates the ATM band detected.

**B.** $ATM^{-/-}$ and $ATM^{+/+}$ cells were either untreated (-) or treated with 40 μM of etoposide for 6 hr (+) as indicated. Samples were loaded according to total protein content. Endogenous Strap was detected using anti-Strap antibody and actin serves as a loading control.

**C.** Mitochondrial fractions were extracted from $ATM^{-/-}$ and $ATM^{+/+}$ cells were either untreated or treated with etoposide (40 μM, 6 hr) as indicated. Endogenous Strap was detected using anti-Strap antibody and COXIV serves as a loading control.

To investigate the effect of ATM and/or ATR kinases on Strap at the mitochondria, a range of inhibitors were used to inhibit ATM kinase only or both ATM and ATR activity. The ATM kinase inhibitor (2-Morpholin-4-yl-6-thianthren-1-yl-pyran-4-one) specifically inhibits ATM activity by competitive inhibition of ATP. The ATM/ATR kinase inhibitor (CGK 733) inhibits both ATM and ATR phosphorylation. Caffeine was also used as it has been shown to inhibit the catalytic activity of both ATM and ATR (Sarkaria et al., 1999) but is a relatively non-selective agent which causes many effects in cells (Cortez, 2003). Cells were pre-incubated with the appropriate inhibitors prior to treatment with the DNA damaging agents. Etoposide and UV light treatment were used as DNA damaging agents. UV light has been shown to induce SSBs and activate the ATR signalling cascade (Di Siena et al., 2013).

Mitochondrial Strap levels were increased upon treatment with UV light (**Figure 7.7A**). Decreased levels of Strap at the mitochondria were observed when cells were pre-incubated with the ATM/ATR kinase inhibitor and caffeine prior to UV light treatment (**Figure 7.7A**). In cells treated with etoposide (**Figure 7.7B**), a marginal decrease was observed upon pre-incubation with the ATM kinase and ATM/ATR kinase inhibitors. These levels were further reduced upon caffeine treatment (**Figure 7.7B**).

Collectively, these data suggest that both ATM and ATR phosphorylation influence the levels of Strap at the mitochondria upon treatment with DNA damaging agents.

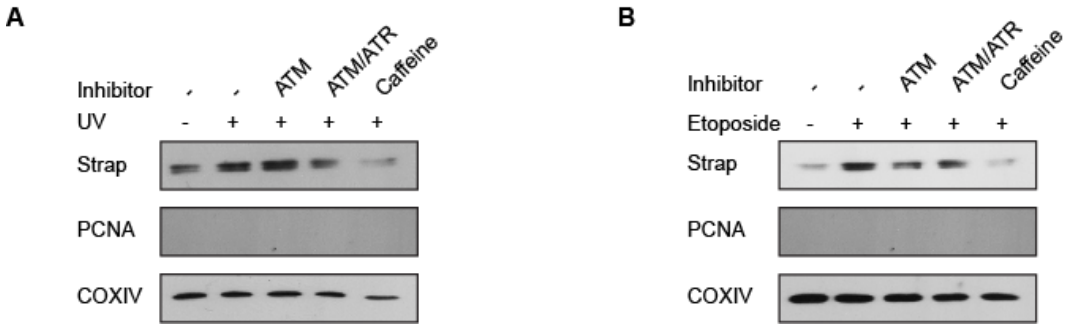



**Figure 7.7 Levels of Strap at mitochondria in the presence of ATM and/or ATR inhibitor.**

Mitochondrial fractions from U2OS cells either untreated (-) or treated (+) with 50 $J/m^2$ of UV light (**A**) or 40 µM of etoposide (**B**) for 4 hr in the presence of either ATM kinase inhibitor (ATM), ATM/ATR kinase inhibitor (ATM/ATR) or caffeine. The level of PCNA, a nuclear protein, was used to assess the purity of the mitochondrial fraction. COXIV served as mitochondrial loading control.

### 7.4 Strap derivatives and p53

Previous work in the laboratory demonstrated that Strap can augment p53 activity (Demonacos et al., 2001). Properties of the Strap derivatives, 3A and 3D, were compared to wild type Strap to address the effects of mutant derivatives on p53 activity. Wild type Strap, the phosphomutant 3A and the 3D mutant were transiently expressed in U2OS cells. Endogenous p53 was immunoprecipitated from cells and the interaction with the Strap derivatives was observed. Both wild type Strap and phosphomutant 3A, co-immunoprecipitated with p53. Intriguingly, the immunoprecipitation and immunoblot analysis showed an enhanced interaction between p53 and the 3D mutant compared to wild type Strap (**Figure 7.8A**).

p53 transcriptionally activates target genes such as *p21/Waf1* and *GADD45* which can lead to cell cycle arrest, or *BAX*, which can lead to cell death (Amundson et al., 1998). As Strap was previously shown to regulate p53 transcriptional activity, the ability of Strap derivatives to activate the p53-responsive promoters, *BAX* (**Figure 7.8B**) and *GADD45* (**Figure 7.8C**) were explored using luciferase assays. Wild type Strap and the 3D mutant were transiently expressed in U2OS cells in the presence or absence of p53. In agreement with published data (Adams et al., 2012), Strap activated both reporter constructs in the presence of p53, confirming its role in enhancing p53 transcriptional activity (**Figure 7.8B & C**). Of interest, the 3D mutant failed to mediate transcriptional activation of both promoters which is in agreement with its cytoplasmic localisation.

Together these data show that 3D mutant has enhanced association with p53 compared to wild type Strap but is unable to activate p53 promoter activity.

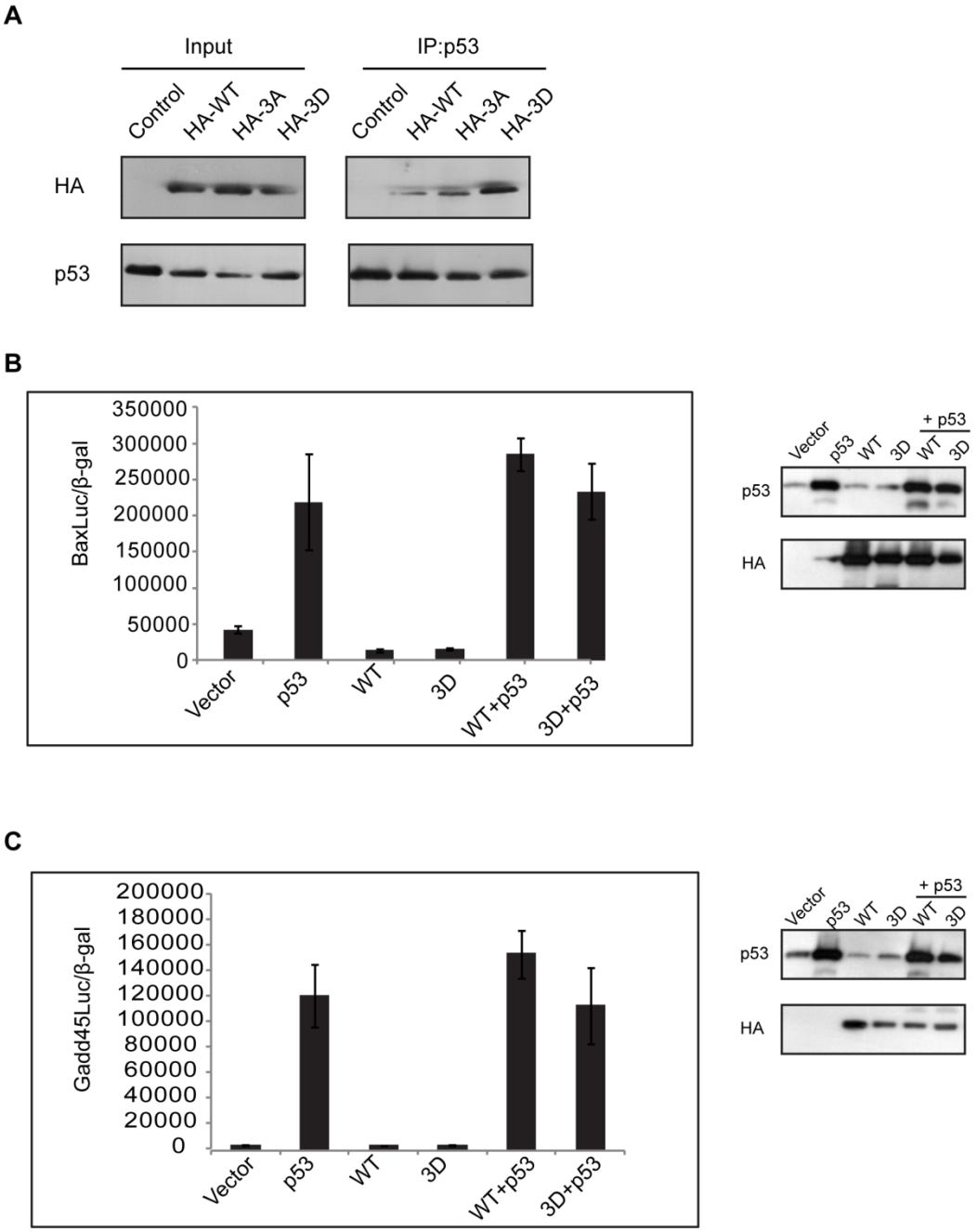



**Figure 7.8 Strap and 3D mutant in the presence of p53.**

**A.** Endogenous p53 was immunoprecipitated from U2OS cells transfected with wild type Strap (HA-WT), HA-3A, HA-3D or vector control using p53 antibody. Ectopic Strap and p53 were detected with anti-HA antibody and p53 antibody, respectively. 2% of the total sample volume was loaded as inputs.

Luciferase reporter assays were performed using U2OS cells transfected with vector, wild type Strap (WT), HA-3D and p53 as indicated. The graph represents luciferase activity derived from *BAX* luciferase (**B**) and *GADD45* (**C**) after normalizing for β-galactosidase activity. Immunoblots represents input protein levels. Ectopic Strap and p53 were detected with anti-HA antibody and p53 antibody, respectively. Values represent mean ± s.d., n= 3 independent experiments.

### 7.5 Strap and 3D mutant augment apoptosis in the presence of p53

The localisation of the 3D mutant at the mitochondria and its ability to interact with p53 prompted a detailed study to investigate the involvement of the 3D mutant in p53-dependent Strap-mediated intrinsic apoptosis as discussed in Chapter 4. One important observation that might complicate the interpretation of the results is the reduced expression of both L-p53 and 3D mutant when they are co-expressed in cells. Initially, Strap derivatives were transiently transfected in U2OS cells and the protein levels were observed in the presence or absence of damage. A marked reduction in protein level of the 3D mutant compared to wild type Strap was observed upon UV light treatment (**Figure 7.9A**). It was noted that co-expressing L-p53 reduces the expression of both wild type Strap and the 3D mutant at the mitochondria (**Figure 7.9B**).

The involvement of Strap derivatives in intrinsic apoptosis was initially measured by the ability to induce cytochrome c release in the absence or presence of L-p53. Cytochrome c release was defined by the release of cytochrome c from the mitochondria into the cytoplasmic fraction. Wild type Strap and the 3D mutant have an impaired ability to induce cytochrome c release in the absence of p53 (**Figure 7.9B**). As previously reported (Marchenko et al., 2000; Mihara et al., 2003), L-p53 expressed in p53 null cells was able to induce cytochrome c release (**Figure 7.9B**). Notably, expression of wild type Strap in the presence of L-p53 resulted in a decreased level of cytochrome c at the mitochondria and this level was further reduced in the presence of the 3D mutant (**Figure 7.9B**).

These observations were further extended to explore the effect of the 3D mutant and wild type Strap on the pro- and antiapoptotic BCL-2 family proteins which are involved in the intrinsic apoptosis pathway. Mitochondria were extracted from p53 null cells transiently expressing either wild type Strap or the 3D mutant in the presence or absence of L-p53. In the absence of L-p53, equal levels of BCL-XL (antiapoptotic protein) were observed (**Figure 7.9C**). Interestingly, reduced levels of BCL-XL were observed when wild type Strap and 3D mutant were co-expressed with L-p53 (**Figure 7.9C**). The converse was observed with respect to BAK (antiapoptotic protein) levels. Enhanced BAK levels were observed when wild type Strap and 3D mutant were expressed in the presence of L-p53 (**Figure 7.9C**).

Two apoptotic markers, cleaved PARP-1 and caspase 3 were used to further asses the apoptotic function of the 3D mutant. Overexpression of wild type Strap in U2OS cells led to increased levels of cleaved PARP-1, cleaved caspase 3 and upregulation of p53 upon damage (**Figure 7.9D**). An increase in the apoptotic markers were observed in cells overexpressing the 3D mutant compared to wild type Strap (**Figure 7.9D**). Cleaved PARP-1 was then measured in HCT116$^{-/-}$ cells, overexpressing either wild type Strap or the 3D mutant in the absence or presence of L-p53. Expression of wild type Strap or the 3D mutant resulted in enhanced PARP-1 cleavage after DNA damage treatment (once the protein expression levels of wild type Strap and the 3D mutant were normalized) (**Figure 7.9E**).

Collectively, these data suggest that the Strap phosphomimetic mutant, 3D has enhanced ability to promote intrinsic apoptosis in the presence of p53 compared to wild type Strap.

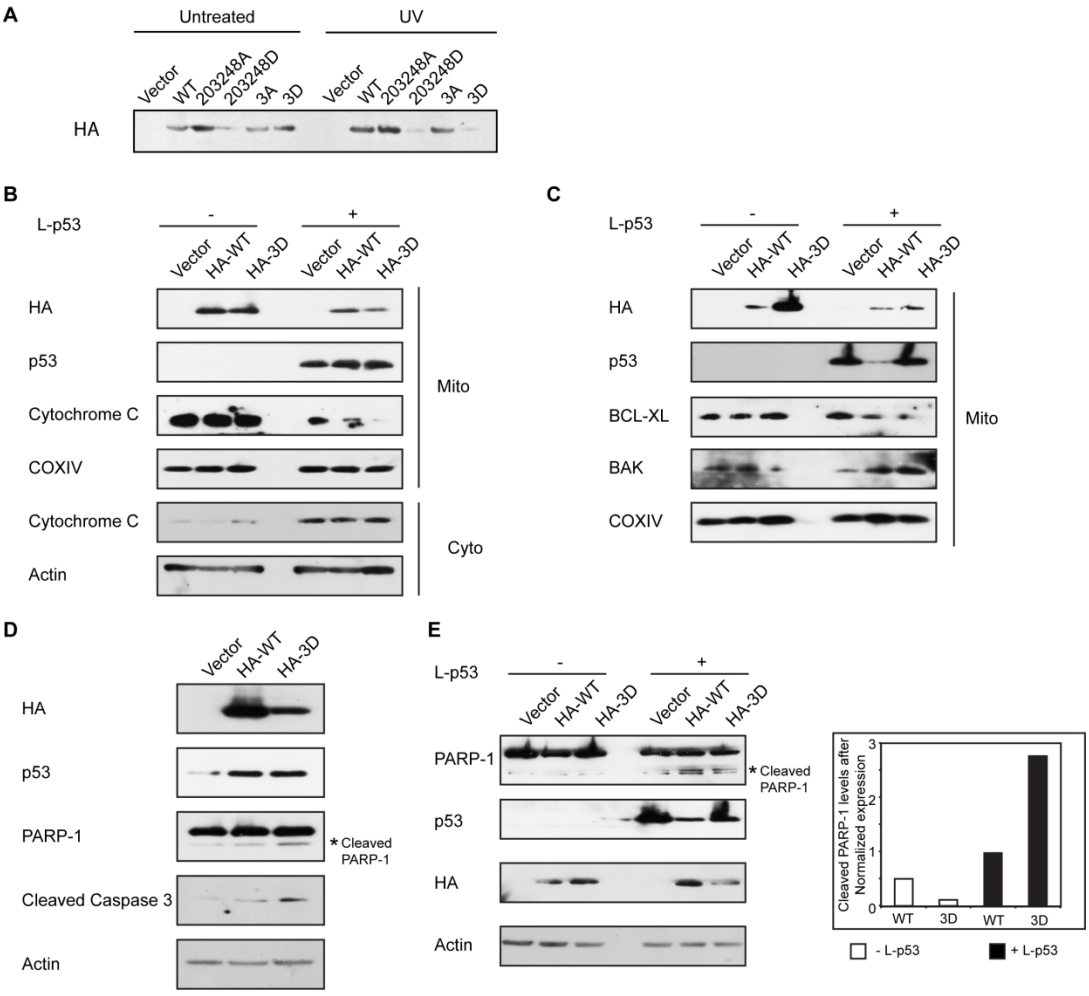



**Figure 7.9 Strap and 3D mutant augment apoptosis in the presence of p53.**

**A.** U2OS cells were transfected with either 1 μg of vector or the indicated Strap derivatives and treated with 50 J/m$^2$ of UV light for 3 hr as indicated. Samples were loaded according to β-galactosidase activity as a measure of transfection efficiency.

**B** & **C.** Mitochondrial (Mito) and cytoplasmic (Cyto) fractions from HCT116$^{-/-}$ cells transfected with wild type Strap (HA-WT), HA-3D or vector control in the presence or absence of L-p53 were prepared and analysed by immunoblotting with the indicated antibodies. COXIV and actin served as loading controls for mitochondrial and cytoplasmic fractions, respectively.

**D.** U2OS cells transfected with either wild type Strap (HA-WT), HA-3D or vector control were treated with UV light (50 J/m$^2$, 6 hr). Immunoblotting was performed with the indicated antibodies. Actin served as a loading control. The asterisk indicates the cleaved PARP-1.

**E.** HCT116$^{-/-}$ cells were transfected with wild type Strap (HA-WT), HA-3D or vector control in the absence or presence of L-p53 and were immunoblotted with the indicated antibodies. Actin served as a loading control. The asterisk indicates the cleaved PARP-1. Quantification of the cleaved PARP-1 levels upon normalizing the expression of wild type Strap and the 3D mutant is shown in the right panel.

## 7.6 Summary

ATM and ATR kinases play critical role in the maintenance of genome integrity upon DNA damage. These kinases phosphorylate proteins which harbour ATM/ATR consensus motifs, S/TQ and it has been reported that more than 900 consensus sites were phosphorylated by ATM/ATR kinase in response to damage (Matsuoka et al., 2007). Analysis of the Strap protein sequence indicates it contains three putative consensus sites for ATM/ATR kinase phosphorylation (**Figure 7.1**). This study has identified two new phosphorylation sites which are at the putative ATM/ATR consensus sites via mass spectrometry analysis of the OB fold (**Figure 7.1 & 7.2**). Our laboratory has previously demonstrated that the S203 site, a putative site for ATM/ATR phosphorylation plays a critical role in Strap nuclear accumulation (Demonacos et al., 2004). The S203 site was not detected via the mass spectrometry analysis as the OB fold construct comprises residues from 220-440 only.

The phosphorylation mimetic mutant of these three sites (3D) was generated and shown to localise at the mitochondria upon DNA damage treatment via immunostaining (**Figure 7.4**) and biochemical fractionation (**Figure 7.5**). The 3D mutant was incapable of activating p53 activity in contrast to wild type Strap (**Figure 7.8B & C**). The 3D mutant was shown to immunoprecipitate with p53 (**Figure 7.8A**) and induce p53-dependent apoptosis (**Figure 7.9B - E**). It was indeed interesting to note that the single site mutants showed similar localisation to the wild type Strap (except for S203A mutant) but the phosphorylation mimetic of all the three sites exhibited an enhanced cytoplasmic localisation in the absence of damage and upon UV treatment, the 3D mutant was shown to localise at the

mitochondria (**Figure 7.3 & 7.4**). This suggests phosphorylation of all the three sites is essential to alter the localisation of Strap.

The AT cell line and its ATM reconstituted counterpart and specific and general inhibitors of the ATM and/or ATR kinase phosphorylation were used to explore the regulation of ATM and/or ATR kinase on Strap's mitochondrial localisation. Strap was upregulated in the ATM proficient cells in total cell lysate upon DNA damage as previously reported (**Figure 7.6B** & (Demonacos et al., 2004)) but the converse was observed in the mitochondrial fractions (**Figure 7.6C**). Etoposide was used as the DNA damaging agent as it induces double-strand breaks that predominantly activate ATM phosphorylation. Inhibition of both ATM and ATR kinases resulted in a decrease level of Strap at the mitochondria upon damage treatment (**Figure 7.7**). Perhaps, ATM phosphorylation leads to nuclear accumulation (Demonacos et al., 2004) whilst ATR and ATM phosphorylation impacts on mitochondrial accumulation of Strap.

Collectively, this study suggests that phosphorylation at all three putative consensus sites of ATM/ATR kinase phosphorylation leads to mitochondrial accumulation of Strap upon DNA damage treatment. Phosphorylated Strap at the mitochondria augments intrinsic apoptosis in the presence of p53. In conclusion, the data from this study offers additional evidence on phosphorylation-regulated mechanism of Strap's apoptotic function.

# Chapter 8

# Discussion

## 8.1 Strap at the mitochondria

Strap was first identified via a yeast two-hybrid assay as a JMY interacting protein (Demonacos et al., 2001). JMY and Strap interact with p300/CBP and this complex is required for the p53 response during DNA damage (Shikama et al., 1999). The studies presented here provide further insight into the function of Strap and importantly ascertain a completely novel subcellular localisation of Strap at the mitochondria (**Figure 4.1** & **Figure 4.2**).

99% of mitochondrial proteins are nuclear-encoded. These nuclear encoded proteins are transported via various ways from the cytosol to the mitochondrial sub compartments. Typically, nuclear encoded mitochondrial precursor proteins possess targeting signal that are recognized by receptors on the mitochondrial surface (Schmidt et al., 2010). Mitochondrial targeting signals do not share distinct consensus sequences but instead display common physicochemical properties and are usually rich in positively charged residues (Abe et al., 2000). Mitochondrial targeting signal allows the protein to be transported to different compartments of mitochondria. For example, targeting signal from ornithine transcarbamylase, cytochrome c oxidase and translocase of outer membrane (TOM) target proteins to the matrix, inner and outer mitochondrial membrane, respectively (Mossalam et al., 2012). Many of the mitochondrial proteins do not contain an N-terminal mitochondrial targeting signal but instead have internal signals. Unfortunately, internal signals are lack of consistent patterns and the nature of these signals remain largely elusive (Neupert and Herrmann, 2007). Besides targeting signal, proteins can be transported to the mitochondria by forming a multichaperone complex with

mitochondrial Hsp70 and Hsp90. These proteins are transferred to the TOM70 core domain prior to chaperone docking (Young et al., 2003).

Sequence analysis of Strap protein showed the absence of a classical mitochondrial targeting signal. This is not surprising as nuclear proteins that have been shown to redistribute to the cytosol and mitochondria such as p53 and Nur77 do not contain mitochondria targeting sequences as well (Lindenboim et al., 2011). The presence of an internal signal can be investigated by identifying the domain in Strap that directs mitochondrial localisation. Perhaps, Strap mitochondrial localisation is chaperone-mediated and this can be explored by examining the interaction between Strap and these chaperones as well as measuring the mitochondrial Strap levels when the two main chaperone proteins, Hsp70 and Hsp90, are depleted.

Evidence from this study showed that the localisation of Strap at the mitochondria is influenced by PTM. Phosphorylation at all three putative ATM/ATR consensus sites upon DNA damage showed an enhanced localisation of Strap at the mitochondria (**Figure 7.4** & **Figure 7.5**). Phosphorylation has been shown to play a role in regulating the mitochondrial localisation of proteins such as MCL-1, a mitochondrial antiapoptotic protein which requires phosphorylation for its localisation and functional role in apoptosis protection at the mitochondria (Thomas et al., 2012). Phosphorylation can be used to modulate the nature and the strength of protein-protein interactions as well as conformational changes which can affect the binding to partner proteins thereby regulating protein binding and coordinating different pathways (Gsponer et al., 2008; Nishi et al., 2011). It was indeed

interesting to observe that Strap phosphorylated at multiple sites, depicted by the 3D mutant, is localised to the mitochondria in the presence of damage (**Figure 7.4**) compared to singly phosphorylated Strap mutant (S203D) which showed nuclear accumulation in response to damage (**Figure 7.3**). To corroborate, several phosphorylation sites were identified from the mass spectrometry analysis of mitochondrially targeted Strap (**Figure 5.6**). It is likely that the localisation of Strap to different subcellular compartments is influenced by conformational changes induced by phosphorylation events or phosphorylation-regulated protein-protein interactions. These findings strongly support that phosphorylation mediates Strap's mitochondrial localisation. Therefore, future studies should aim to elucidate functional consequences of the phosphorylation sites identified in the mass spectrometry analysis.

Of note, Strap was found at the mitochondria even in the absence of damage (**Figure 4.4 & 4.5A & B**). This perhaps suggests other mechanisms besides phosphorylation are responsible for its mitochondrial localisation. The lack of mitochondrial targeting signal in Strap's sequence suggests mitochondrial localisation of Strap might be mediated by chaperone proteins such as mitochondrial Hsp70 and Hsp90. Interestingly, the cytosolic segment of TOM70 contains seven TPR motifs (Wu and Sha, 2006). It is tempting to suggest perhaps there is an interaction between Strap and TOM70 mediated via their TPR motifs given these motifs are involved in augmenting protein-protein interaction.

### 8.2 Shuttling of mitochondrial Strap and p53

Proteins move between the cytoplasm and the nucleus and this shuttling process is important in coordinating and regulating the function of a protein. This study suggests p53 shuttles Strap from the mitochondria to the nucleus.

p53 localisation at the mitochondria precedes its nuclear accumulation during damage (Erster et al., 2004; Zhao et al., 2005). The p53 transcription-independent apoptosis will only be initiated when a certain threshold of p53 is attained in the cytosol or mitochondria (Speidel, 2010). p53's nuclear role is mediated by PTMs which occur in response to damage. The nucleo-cytoplasmic shuttling of p53 which regulates its transcription-dependent and -independent roles depends on the nuclear export signal (NES) and nuclear localisation signal located at the N- and C-termini of p53 (Liang and Clarke, 1999). p53 is able to shuttle between nucleus and cytosol and it accumulates in both compartments when it becomes stabilized upon DNA damage. Regulation of its nuclear export and import and abundance in the cytosol and mitochondria is an obvious mode in modulating the transcription-independent proapoptotic functions of p53 (Speidel, 2010). This study suggests a role for Strap in facilitating the mitochondrial and nuclear localisation of p53. Similar kinetics of Strap and p53 were observed at the mitochondria upon damage treatment (**Figure 4.5A & B**) and the absence of p53 resulted in suppressed levels of nuclear Strap but increased levels of Strap at the mitochondria (**Figure 4.5C & E**). This therefore suggests that Strap and p53 potentially facilitate each other's translocation from the mitochondria to the nucleus. The NES and phosphorylation events modulate Strap's nuclear accumulation (Demonacos et al., 2004). An NES characterised by high leucine content was identified at the N-terminal region of Strap that is conserved

across species (**Figure 8.1**). Perhaps the mitochondria-nuclear shuttling of p53 and Strap is regulated by the NES. Hence, it will be of interest to investigate the levels of nuclear and mitochondrial Strap using a mutant derivative in which the candidate NES is deleted.

Depletion of Strap resulted in an increase in mitochondrial p53 levels (**Figure 4.9A**) but the converse was observed in the total cell lysates (**Figure 4.9B**). Interestingly, the overexpression of Strap enhanced the nuclear p53 levels (**Figure 4.10**). This implies that Strap reduces mitochondrial p53 and facilitates its nuclear localisation. Very few nuclear proteins are known to negatively regulate mitochondrial p53 levels. Nucleophosmin, a nucleolar protein, suppresses mitochondrial p53 levels under normal and stress conditions and competitively inhibits p53-BAX interaction. (Dhar and St Clair, 2009; Kerr et al., 2007; Thompson et al., 2008). Strap on the other hand, negatively regulates mitochondrial p53 levels and at the same time augments the p53 mitochondrial apoptotic response. Together, the data indicate another role of Strap in regulating p53 activity by modulating the mitochondrial and nuclear p53 levels.

It will be of interest to observe the kinetics of mitochondrial p53 upon DNA damage in the absence of Strap which will provide more evidence on the influence of Strap on mitochondrial p53 and nuclear trafficking. The transcriptional influence on Strap and p53 localisation from the mitochondria to the nucleus can be explored with the use of inhibitors that impairs global transcriptional activity such as α-amanitin.

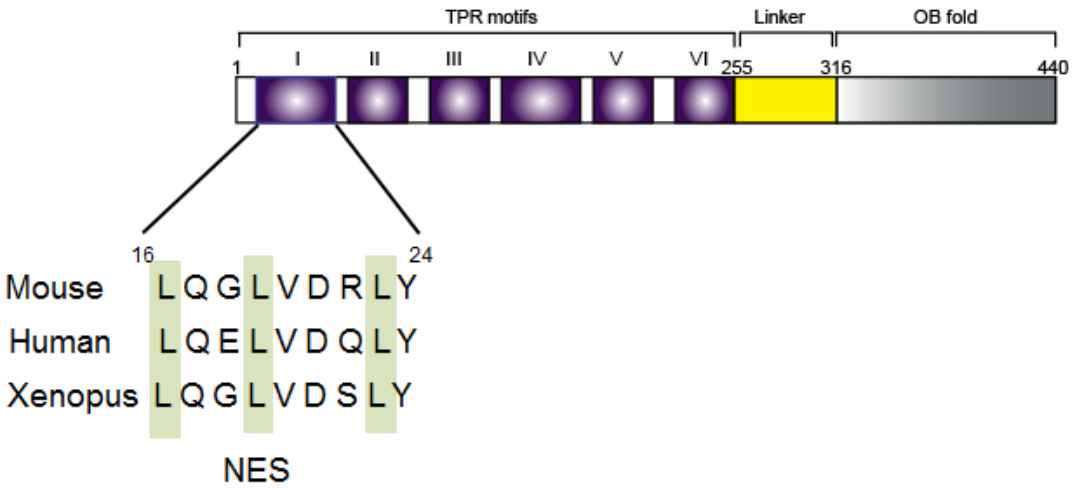



**Figure 8.1 Evolutionarily conserved nuclear export sequences in Strap.**

Strap contains the leucine-rich NES located in the amino N-terminal region (residues 16-24).

An inhibitor that prevents nuclear transport such as leptomycin B would be helpful in eliminating other potential proteins that might facilitate p53 and Strap's localisation from the mitochondria to the nucleus. Example of potential proteins involved in protein shuttling is the heat shock proteins that are known for their nucleo-cytoplasmic activity. Strap was shown to coordinate the p53 activity in response to damage at the mitochondria and nucleus via nucleo-cytoplasmic shuttling. Together, this study implies a new role for the previously characterised transcriptional regulator.

### 8.3 Strap at the mitochondria induces p53-dependent apoptosis

Members of the BCL-2 family tightly regulate the commitment to apoptosis by their ability to govern MOMP which results in the release of apoptogenic factors such as cytochrome c (Taylor et al., 2008). MOMP is a result of oligomerisation of the proapoptotic BCL-2 family members, BAK and BAX that leads to the formation of pore at the OMM and the release of the apoptogenic factors. This study suggests that Strap augments p53-mediated cytochrome c release possibly via regulation of BAK activity.

The hallmark of the transcription-independent pathway in p53-mediated apoptosis is the accumulation of p53 at the mitochondria that leads to direct activation of BAK and/or BAX (Erster et al., 2004; Leu et al., 2004; Pietsch et al., 2008). Strap disrupts the balance between proapoptotic and antiapoptotic proteins of the BCL-2 family and promotes BAK oligomerisation in the presence of p53 to induce cytochrome c release (**Figure 4.11 & 4.12**).

Similarly, the oncogenic transcription factor Myc has been also shown to enhance p53's mitochondrial role via BAK. Myc alters the interaction between phosphorylated p53 and the BAK-BCL-XL complex and enhances the conformational activation of BAK (Nieminen et al., 2013). Perhaps, phosphorylated p53 is important in inducing BAK oligomerisation. It will therefore be interesting to investigate the influence of Strap on the phosphorylation status of p53. Reduced BAK oligomerisation was accompanied by a p53-dependent decrease in BAK protein levels both in mitochondrial fraction and total cell lysate when Strap was depleted (**Figure 4.11**). This implies that the reduced BAK oligomerisation observed is a result of decrease in BAK levels. Since *BAK* is a p53 target gene (Graupner et al., 2011) and Strap has been shown to augment p53 transcriptional activity (Demonacos et al., 2001), perhaps the reduction in BAK levels is due to the reduced p53-dependent *BAK* transcriptional activity in the absence of Strap. Intriguingly, the decrease in BAK levels was also observed in the absence of p53 when Strap was depleted. This reduction of BAK did not affect BAK oligomerisation activity. This might imply that Strap regulates both transcriptional and oligomerisation activity of mitochondrial BAK.

Interestingly, the converse was observed in regards to BCL-XL protein levels; with depletion of Strap enhancing BCL-XL levels both in total cell lysate and mitochondrial fractions (**Figure 4.11**). Strap may inhibit the transcription of *BCL-XL* or alternatively, Strap might influence the stability of BCL-XL. The regulation of Strap on BCL-XL transcription can be explored by measuring the BCL-XL expression in the presence and absence of Strap. Kelch-like ECH-associated protein (KEAP1) was shown to mediate BCL-XL degradation which leads to enhanced

cytochrome c release-induced apoptosis (Niture and Jaiswal, 2011). Perhaps Strap influences the stability of BCL-XL by promoting proteosomal degradation resulting in an increase in the level of active proapoptotic protein, such as BAK which triggers MOMP.

Strap was found to regulate the BAK levels in the presence and absence of p53 (**Figure 4.11**). Depleting Strap resulted in reduced level of p53-dependent BAK oligomerisation (**Figure 4.12**). To explore the possibility that Strap might influence *BAK* expression, the investigation of BAK mRNA levels in the presence and absence of Strap would be essential. Strap influences p53-dependent BAK oligomerisation but no direct interaction between Strap and BAK was provided. A more direct way to assay BAK oligomerisation could be by using purified mitochondria isolated from $HCT116^{+/+}$ (wild type p53 ) and $HCT116^{-/-}$ (devoid of p53) cells to investigate the ability of Strap to induce BAK oligomerisation in the presence and absence of p53. Addition of recombinant full-length Strap to the isolated mitochondria may be able to provide direct evidence of the ability of Strap to effect BAK oligomerisation. Moreover, p53 induces BAK oligomerisation by disrupting BAK/MCL-1 interaction (Leu et al., 2004). It will indeed be interesting to evaluate if Strap alters the p53-mediated BAK/MCL-1 interaction. However, this does not eliminate the possibility that Strap might influence the induction of BAX oligomerisation as p53-induced cytochrome c release can also be mediated by BAX oligomerisation (Chipuk et al., 2004). Perhaps using mitochondrial fractions of MEFs derived from wild type and BAX deficient mice could be used to address if Strap plays a role in BAX-mediated mitochondrial apoptosis. Together the data in this study suggests a model whereby Strap impacts on MOMP. Strap-dependent

regulation of BCL-2 family member proteins such as BAK and BCL-XL, promotes MOMP and the mitochondrial-induced apoptosis.

### 8.4 Strap and cellular metabolism

A mass spectrometry approach was used to explore the role of Strap at the mitochondria. ATP synthase subunit-β was found to interact with Strap in overexpression (**Figure 6.1**) and endogenous (**Figure 6.2**) immunoprecipitation.

The proteinase K digestion assay suggests that Strap resides at the outer mitochondrial membrane (**Figure 4.3**), more detailed investigation would be required to fully elucidate Strap's mitochondrial localisation. Of note, in this study and others (Mancini et al., 2009; Perciavalle et al., 2012) have shown that BCL-2 was sensitive to proteinase K digestion although BCL-2 has been reported to be at the inner mitochondrial membrane (Hockenbery et al., 1990) suggesting the proteinase K digestion assay is not very sensitive (**Figure 4.3**). Due to the intense cytoplasmic staining of Strap in light microscopy, detailed investigation on Strap's localisation at the mitochondria using electron microscopy may not be possible. The Strap- ATP synthase subunit-β interaction indicates that besides the OMM, Strap might be localised at inner mitochondrial membrane as well. Interestingly, recent studies on previously reported surface mitochondrial proteins such as BCL-XL and MCL-1, were shown to localise to the inner membrane. BCL-XL was detected at the outer and matrix of the mitochondria and was shown to regulate the ion leak within ATP synthase complex promoting efficient ATP production via its interaction with ATP synthase subunit-β (Alavian et al., 2011). MCL-1 localised at

the mitochondrial matrix was required for the maintenance of mitochondrial DNA and proper assembly of the ATP synthase complex (Perciavalle et al., 2012). Although ATP synthase subunit-β and Strap were shown to form a complex, this does not provide evidence of direct interaction. Experiments using recombinant proteins to determine the interaction of Strap with the ATP synthase complex would be able to address this issue.

ATP synthase complex was initially thought to be an enzyme located exclusively at the mitochondria, interestingly; this complex has been discovered to reside on cell surface as well (Chi and Pizzo, 2006). The cell surface ATP synthase complex is not efficient in generating extracellular ATP but mainly has roles in intracellular pH regulation in endothelial cells and in mediating high-density lipoprotein (HDL) endocytosis (Chi and Pizzo, 2006). The interaction between Strap and ATP synthase subunit-β was detected in the mitochondrial fraction confirming that this interaction occurs at the mitochondria and not the cell surface (**Figure 6.2D**).

The functional consequences of the Strap-ATP synthase subunit-β interaction were explored during OXPHOS. Since cancer cells rely on aerobic glycolysis, alteration in the microenvironment was essential to switch the energy production machinery from aerobic glycolysis to OXPHOS. As mentioned earlier, cancer cells synthesize ATP by relying on catabolism of substrates mainly glucose and also glutamine. Modulating the glucose level forces cancers cells to switch from glycolysis and the OXPHOS system for energy production.

Cancer cells grown in glucose-free, galactose containing media rely on OXPHOS to synthesize ATP (Alavian et al., 2011; Perciavalle et al., 2012). In this media, galactose will be the only substrate available for oxidation and this process will not yield any ATP. This forces cancer cells to utilize the OXPHOS system for ATP production (Marroquin et al., 2007). Human primary muscle cells showed an increase in oxygen consumption rate and cytochrome oxidase activity when cultured in galactose supplemented media (Aguer et al., 2011). Cells grown in galactose media were reported to adapt morphologically by increasing cristae membrane and by elevating the levels of OXPHOS-related protein such as the respiratory chain complexes (Rossignol et al., 2004). Strap was upregulated in total cell lysates and mitochondrial fractions from cells grown in galactose supplemented media in the presence of p53 (**Figure 6.3**). This indicates that Strap at the mitochondria is likely to be modulated during OXPHOS in a p53-dependent manner.

Interestingly, the galactose-mediated increase in Strap protein levels was accompanied by a decline in ATP synthase activity (**Figure 6.8B**) which resulted in reduced cellular ATP/ADP ratio (**Figure 6.6 & 6.7**). It is postulated the suppression of OXPHOS is potentially via Strap's interaction with ATP synthase subunit-β. Recent studies have identified proteins that interacted with the ATP synthase complex and regulate its activity. Cyclophilin D was shown to interact with the lateral stalk of the ATP synthase complex and the absence of cyclophilin D showed an increase rate in ATP hydrolysis (Giorgio et al., 2009). Htra2 which is an apoptotic factor released upon MOMP was also shown to modulate the ATP synthase activity. HtrA2 was found to interact with the ATP synthase complex under basal conditions and regulate the proton uncoupling during OXPHOS (Plun-

Favreau et al., 2012). Interestingly, unlike cyclophilin D and HtrA2, Strap was shown to suppress the ATP synthase activity and the absence of Strap increased the ATP/ADP ratio. This was indeed surprising as most ATP synthase interacting proteins have been shown to enhance rather than inhibit its activity. More recently, oligomycin sensitivity-conferring protein (OSCP), part of the peripheral stalk of the ATP synthase complex, was identified as a new mitochondrial protein partner of p53 in the mitochondrial matrix (Bergeaud et al., 2013). The authors postulated that the matrix p53 might be involved in the organization and stabilisation of the mature ATP synthase (Bergeaud et al., 2013). Perhaps the Strap-ATP synthase subunit-β interaction in the presence of p53 disrupts the ATP synthase complex organization which reduces its efficiency in producing ATP. Therefore, future studies aim to explore the possibility of a link between mitochondrial Strap and alteration in ATP synthase conformation would be of interest.

ATPase inhibitory factor 1 (IF1), an endogenous protein inhibitor, has been shown to decrease the ATP synthase activity in cancer cells (Sanchez-Cenizo et al., 2010). Overexpression of IF1 in colon cancer inhibited the activity of ATP synthase and promoted the upregulation of glycolysis but did not affect the cellular ATP levels (Formentini et al., 2012; Sanchez-Cenizo et al., 2010). Moreover, the overexpression of IF1 increased cell proliferation and invasiveness with delayed execution of mitochondrial-mediated apoptosis (Formentini et al., 2012). It is interesting to note that both Strap and IF1 negatively regulate the ATP synthase activity. Contrary to IF1, Strap-inhibition of ATP synthase activity altered the cellular energy status and promoted cell death instead of cell survival.

The level of cellular ATP is an important determinant for cell death. In apoptosis, a sufficient supply of ATP is necessary to favour apoptosome formation and to trigger caspase activation (Sanchez-Arago et al., 2012). The severity of reduction in cellular ATP determines the mode of programmed cell death. A three-fold decrease in the intercellular ATP has been shown to initiate cytochrome c release from the inner mitochondrial membrane and triggers apoptosis (Izyumov et al., 2004). Overexpression of mitochondrially targeted Strap resulted in an approximately two-fold decrease in the ATP/ADP ratio in the absence of damage (**Figure 6.7**). It is noted that the decrease alone was not sufficient to elicit an apoptotic response as Strap-induced apoptosis was not observed in the absence of damage (**Figure 6.10 & 6.11**). Instead, the Strap-mediated decrease in the ATP/ADP ratio was shown to sensitise the cells to p53-dependent apoptosis in the presence of damage (**Figure 6.10 & 6.11**).

The overexpression mitochondrially targeted Strap resulted in mitochondrial membrane hyperpolarisation in either glucose or galactose supplemented media (**Figure 6.8A**) Reduced ATP synthesis associated with decrease in ATP synthase activity results in mitochondrial membrane hyperpolarisation. The mitochondrial hyperpolarisation observed in this study strongly suggest it is not associated with MOMP as this hyperpolarisation was observed in the absence of damage (**Figure 6.8A**). MOMP requires the presence of damage which triggers the activation and oligomerisation of the proapoptotic proteins, BAK and/or BAX. The data in this study support the idea that mitochondrial membrane hyperpolarisation occurs at the early stages of apoptosis. This is based on the observation that cytochrome c release

and mitochondrial hyperpolarisation were shown to precede the onset of mitochondrial-induced apoptosis (Banki et al., 1999; Sanchez-Alcazar et al., 2000).

Importantly, the functional consequences of Strap at the mitochondria require the presence of p53. The influence of p53 in Strap-mediated ATP depletion warrants more extensive investigations. Strap depletes cellular ATP/ADP ratio and promotes apoptosis in a p53-dependent manner. Interestingly, no ternary complex between Strap, p53 and the ATP synthase subunit-β was observed (**Figure 6.5B**). p53 neither effects the ATP synthase activity nor the cellular ATP levels in OXPHOS-reliant cancer cells (**Figure 6.9**). The p53 regulation on OXPHOS is mediated via its transcriptional role as discussed earlier (Hu et al., 2010; Matoba et al., 2006). Perhaps, Strap-mediated ATP depletion would activate the AMPK-mediated phosphorylation of p53 at residue S15 similar to that observed during Myc-induced cellular energy alteration (Nieminen et al., 2013). Moreover, the molecular pathway for metabolic stress-induced AMPK activation, p53 stabilization and consequent apoptotic response are not well defined. It will be of interest to evaluate the levels of phosphorylated p53 and AMPK in the absence or presence of Strap to investigate if Strap affects this pathway. This implies that p53 influences both Strap-regulated BAK oligomerisation and ATP depletion.

To further examine the Strap-regulated ATP depletion in mediating the apoptotic response, it will be crucial to exclude the activation of the necrotic pathway. Dual staining with fluorescent Annexin V and PI or measuring the release of high-mobility group box 1 (HMGB1), the classical biochemical hallmark specific for

necrosis (Vaseva et al., 2012), would provide an insight into the mechanism of programmed cell death. Of note, Strap-mediated ATP depletion does not exclude the possibility of a transcriptional influence. To explore this issue, Strap mRNA levels would be measured during glucose and galactose supplemented media. It will also be of interest to measure the mRNA levels of OXPHOS-regulated p53 genes (such as SCO2 and GLS2), in the presence or absence of Strap. These results will help to clarify the involvement of transcription, as well as p53, in Strap-mediated ATP depletion during OXPHOS. This idea could be explored further by using the small molecule inhibitor of p53 transcriptional activity such as pifithrin α or a general transcription inhibitor such as α-amintin.

### 8.5 Regulation of Strap during hypoxia

Wild type Strap induces apoptosis in cells grown in glucose and galactose supplemented media as opposed to L-Strap, whereby an induction of apoptosis was only observed in cells grown in galactose supplemented media upon damage treatment (**Figure 6.10**). Interestingly, reduced mitochondrial Strap was observed in cells grown in glucose compared to galactose supplemented media (**Figure 6.3**). This implies that the presence of glucose alone reduces Strap's activity at the mitochondria. Perhaps Strap might modulate glycolysis instead of OXPHOS in the presence of glucose. HIF1, the major transcription factor during hypoxia mediates the transition from OXPHOS to aerobic glycolysis in cancer cells. Interestingly, both the protein (**Figure 6.13**) and mRNA (**Figure 6.14B**) levels of Strap were upregulated during hypoxia. Further analysis of the Strap promoter sequence identified HRE which suggests Strap might be a HIF1 responsive gene (**Figure**

**6.14A**). It is interesting to hypothesise that Strap induces apoptosis depending on the microenvironment.

Interestingly, p53 has been shown to be an important regulator of cellular metabolism by modulating both glycolysis and OXPHOS. p53 limits glycolytic flux through direct repression of gene expression such as *GLUT1* and *GLUT4* (Thorens and Mueckler, 2010). p53-dependent regulation of OXPHOS is mediated by transcriptional activation OXPHOS-regulated genes such as *SCO2* (Matoba et al., 2006). Similar to p53, Strap might be able to regulate both glycolysis and OXPHOS. Strap-mediated ATP depletion during OXPHOS sensitises cells to apoptosis in response to damage. During hypoxia, when glycolysis is predominant, Strap might inhibit HIF transcriptional activity. If enhanced nuclear localisation of Strap was observed during hypoxia, it is also possible that Strap might augment p53 activity. In order to explore the influence of Strap on HIF transcriptional activity, determining the mRNA levels of HIF target genes such as *GLUT1* and *LDH-A* would be essential. Measuring the expression of p53-regulated genes during OXPHOS and hypoxia may help to address the influence of Strap on p53 activity.

Perhaps, the changes in the microenvironment regulate Strap's localisation either to the nucleus or mitochondria. If *Strap* is a HIF target gene, nuclear Strap induces cell death by supressing HIF transcriptional activity during hypoxia and when cancer cells rely on OXPHOS for energy production, mitochondrial Strap induces apoptosis via p53-dependent ATP depletion during cellular stress response. Initially, future studies measuring the glucose and oxygen consumption rates during hypoxia

and normoxia in the presence and absence of Strap would be essential to explore Strap's role during OXPHOS and glycolysis.

To substantiate that Strap harbours a functional HRE on its promoter, cloning the HRE sequence in a luciferase reporter construct and testing it in a reporter assay will be required. Binding of HIF to the *Strap* promoter can be demonstrated via chromatin immunoprecipitation with specific HIF antibody or by electrophoretic mobility shift assay (EMSA) to investigate if the HIF protein binds *in vitro* to the HRE sequence located on Strap's promoter. Together, this study provides a novel perspective on the metabolic regulatory function of Strap and reveals that Strap has an important role in modulating cellular metabolism which impacts on tumourigenesis.

### 8.6 ATM/ATR phosphorylation of Strap

Strap contains three consensus sites for ATM/ATR kinase phosphorylation (**Figure 7.1**). Two of these sites were shown to be phosphorylated via mass spectrometry analysis (**Figure 7.1 & 7.2**) and a Strap phosphomimetic mutant of all three sites showed mitochondrial localisation upon DNA damage (**Figure 7.4 & 7.5**).

The 3D mutant was shown to interact with p53 (**Figure 7.8A**) and enhance the p53-mediated apoptosis (**Figure 7.9B-E**). Proteins phosphorylation at multiple sites; either simultaneously or cooperatively, has been shown to increase the magnitude of effects and generate a wider array of functions compared to singly phosphorylated proteins (Park et al., 2006). For example, multisite phosphorylation of BCL-2 in the

flexible loop domain positively regulates its antiapoptotic function (Deng et al., 2004). The phosphomimetic mutant of BCL-2 showed a delayed release of cytochrome c from the mitochondria upon stress response (Deng et al., 2004). This study reports that the phosphorylation of Strap at multiple sites enhances the proapoptotic function of Strap. This is supported by the enhance association of the 3D mutant with p53 (**Figure 7.8A**) and an increase in p53-mediated apoptosis compared to wild type Strap (**Figure 7.9B-E**). This suggests multiple phosphorylation events are important in modulating the p53-mediated apoptotic response of mitochondrial Strap.

ATM phosphorylation of Strap was shown to prompt its nuclear accumulation, followed by nuclear Strap stabilization by CHK2 phosphorylation (Adams et al., 2008; Demonacos et al., 2004). Interestingly, enhanced Strap levels in the ATM proficient cells compared to AT cells (ATM deficient) was observed in the total cell lysates but the converse was observed in the mitochondrial fractions (**Figure 7.6**). Perhaps ATM phosphorylation of Strap predominantly promotes nuclear accumulation resulting in less cytoplasmic Strap and the mitochondrial localisation of Strap requires both ATM and ATR phosphorylation (**Figure 7.7**). It will indeed be interesting to explore the effect of CHK2 phosphorylation on mitochondrial Strap which may provide information on the interplay between Strap nuclear stabilization and mitochondrial localisation.

The role of ATM/ATR phosphorylation influencing the Strap's mitochondrial accumulation was further supported when a range of inhibitors were used. A marked decrease in mitochondrial Strap was observed when both ATM and ATR kinases were inhibited compared to inhibiting ATM kinase alone (**Figure 7.7**). This would suggest perhaps ATR and ATM phosphorylation influence mitochondrial localisation of Strap compared to ATM phosphorylation alone. Of note, Strap was observed at the mitochondria even in the absence of damage. The ATM and/or ATR pathway is activated in response to DNA damage which would suggest that the presence of other mechanisms besides ATM and/or ATR phosphorylation influence Strap at the mitochondria.

Reduced 3D mutant levels compared to wild type Strap was observed in the presence of p53 (**Figure 7.9A-C**). This is an interesting observation which might imply that p53 influences the stability of the 3D mutant at the mitochondria. It may be that the reduced expression of the Strap phosphomimetic mutant (3D) is due to its stability or linked to cell toxicity. Perhaps cells overexpressing the Strap phosphomimetic mutant die more rapidly compared to wild type Strap. This hypothesis is supported by the different mitochondria morphology observed in cells overexpressing the 3D mutant compared to the vector control and wild type Strap (**Figure 7.4**). Mitochondria are highly dynamic and are usually dispersed throughout the entire cell (Desagher and Martinou, 2000). However, during the early event of apoptosis, mitochondria undergo perinuclear clustering followed by mitochondria condensation (Desagher and Martinou, 2000). Perhaps a more in depth study is required on the morphological changes observed upon expressing the 3D mutant. The phosphorylation of wild type Strap in cells is perhaps short lived

due to rapid dephosphorylation which would prevent destabilization of phosphorylated Strap. Interestingly, the mass spectrometry analysis of L-Strap detected Protein Phosphatase 1B as a potential mitochondrial Strap interacting protein (**Figure 5.2 &. 5.4**). This substantiates the rationale of a phosphorylation/dephosphorylation event on Strap occurring at the mitochondria. Perhaps the dephosphorylation event is followed by ATM phosphorylation of Strap which stimulates nuclear accumulation and augments p53 transcriptional activity. The use of a small molecule phosphatase inhibitor might shed light on the importance of phosphorylation/dephosphorylation in regulating Strap's localisation.

Measuring the half-life of the 3D mutant and wild type Strap would be essential in determining the stability of these two proteins. To explore the temporal relation between the alterations in mitochondrial dynamics and the 3D mutant upon DNA damage, real-time mitochondria morphology analysis using time-lapse microscopy would be of interest. Time-lapse analysis using mitochondrial-targeted fluorescent proteins and dyes, allows detailed and dynamic visualization of mitochondria. Exploring the 3D mutant crystal structure could also provide essential information regarding the structure and conformational changes of the mutant compared to wild type Strap.

The translocation of proteins between the cytoplasm and nucleus can be triggered by many regulatory mechanisms such as protein association/disassociation and phosphorylation/dephosphorylation. The results from this study suggest that phosphorylation events mediate Strap's subcellular localisation. As mentioned

earlier, phosphorylation of all three ATM/ATR consensus sites promotes mitochondrial translocation. It is likely that a dephosphorylation event takes place in the early phases of damage which prompts nuclear accumulation of Strap. Nuclear accumulation of Strap is followed by stabilization by CHK2 phosphorylation.

### 8.7 Conclusions and future directions

This study has demonstrated that Strap is localised at the mitochondria and forms a complex with p53 at the mitochondria which augments cytochrome c release possibly via BAK oligomerisation in the presence of p53. Intriguingly, Strap was found to negatively regulate the levels of mitochondrial p53 and it enhances nuclear p53 levels; suggesting that Strap and p53 may facilitate each other's localisation from the mitochondria to the nucleus. Mitochondrial Strap was also found to interact with ATP synthase subunit-β and deplete cellular ATP by attenuating ATP synthase activity leading to p53-dependent apoptosis. In addition, ATM/ATR phosphorylation of Strap enhances its mitochondrial localisation during damage. The data from this study postulates that Strap depletes cellular ATP which sensitises the cells to apoptosis in the presence of damage. During the early onset of DNA damage, Strap interacts with mitochondrial p53 and induces cytochrome c release and eventually Strap and p53 are localised to the nucleus where Strap augments p53's transcriptional role. The model is illustrated in **Figure 8.2**.

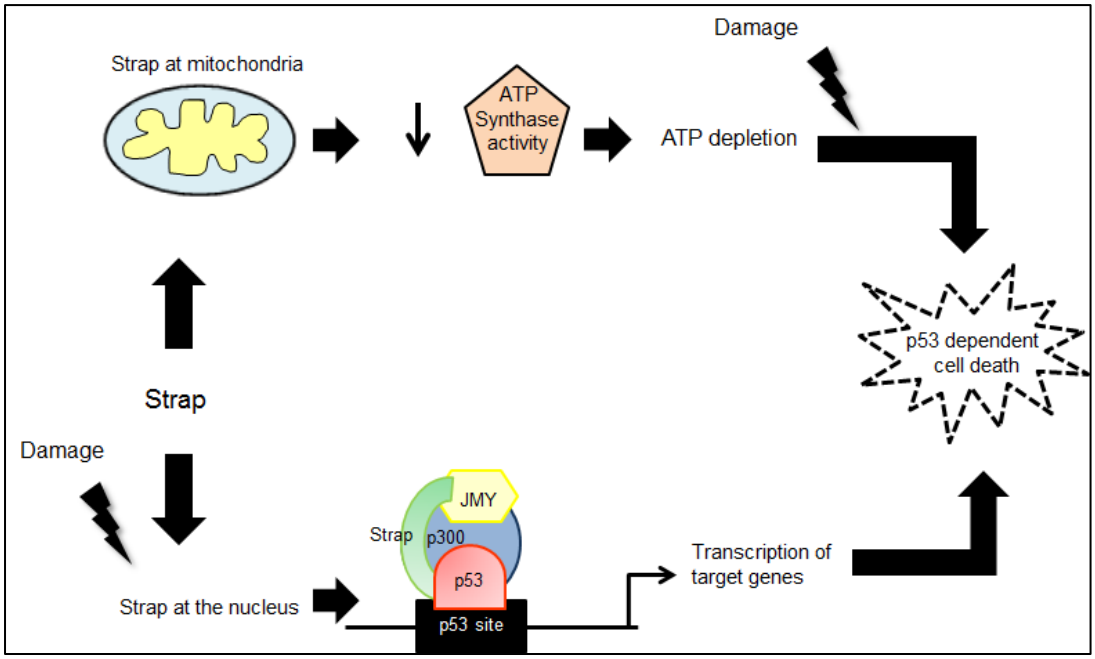



**Figure 8.2 Model.**

Strap at the mitochondria depletes cellular ATP by regulating ATP synthase activity. In the presence of DNA damage, mitochondrial Strap induces p53-dependent cytochrome c release. Mitochondrial function of Strap precedes its nuclear accumulation.

Future studies should capitalize on the results presented here to gain a more detailed picture of the role of mitochondrial Strap. For example, it will be interesting to generate Strap knockout (KO) mice and compare their metabolic status with the wild type Strap mice. A metabolomics approach would be ideal to analyse the alterations in cellular metabolites (Nagrath et al., 2011). The results from this study will aid in further elucidating the role of Strap-mediated apoptosis either via modulating OXPHOS or glycolysis or perhaps both. The data in this study implies that Strap's role during hypoxia is influenced by its transcriptional activity. Gene expression analysis on cells with depleted Strap during hypoxia, normoxia and OXPHOS would provide information on Strap-mediated differential regulation of genes in response to cellular metabolism. This study may also be extended to explore the influence of p53 in Strap transcriptional activity. Further to cell line studies, it will be important to assess Strap levels in tumours with active or dysfunctional mitochondria. Perhaps, if Strap plays a major role at the mitochondria, a decline in Strap levels would be observed in tumours with mitochondrial dysfunction such as phaeochromocytomas (Astuti et al., 2001). Intriguingly, Strap has been shown to promote cell survival instead of apoptosis in AML cells (harbour mutant p53) (Lynch et al., 2013). This may imply that the wild type and mutant p53 might regulate the proapoptotic and prosurvival function of Strap, respectively. Given the growing body of evidence for the role of mutant p53 in tumour progression (Oren and Rotter, 2010), it will be important to explore the implication of mutant p53 on Strap's functional role.

In summary, the detection of a stress responsive p53-cofactor that governs both transcription-independent and –dependent arms of p53's apoptotic program emphasises the cooperative nature of these two functions in fully executing the cellular response to stress stimuli. Strap triggers a first wave of the p53-mediated apoptotic response by inducing mitochondrial membrane permeabilisation via BAK oligomerisation and ATP depletion in the presence of damage. Prolonged signalling along the same axis would further augment p53 transcription in the nucleus, thus amplifying the apoptotic response. Together, this study highlights a previously unrecognised role of Strap in cellular metabolic regulation and thus, making Strap a promising cancer therapeutic target.

This study has yielded provocative results and most importantly these and future studies on Strap likely to be of therapeutic consequence. Developing a small molecule drugs that mimics Strap which is likely to be used in cancers that harbour wild type p53 would be desirable. The presence of functional p53 is essential as Strap enhances p53-dependent apoptosis. The Strap mimetic would be able to re-establish the apoptotic pathway and induces cell death. Alternatively, in tumours that are devoid of functional p53, Strap mimetic can be used as adjuvant treatment to the current p53 based therapy.

# Chapter 9

# References

Abe, Y., Shodai, T., Muto, T., Mihara, K., Torii, H., Nishikawa, S., Endo, T., and Kohda, D. (2000). Structural basis of presequence recognition by the mitochondrial protein import receptor Tom20. Cell *100*, 551-560.

Adams, C.J., Graham, A.L., Jansson, M., Coutts, A.S., Edelmann, M., Smith, L., Kessler, B., and La Thangue, N.B. (2008). ATM and Chk2 kinase target the p53 cofactor Strap. EMBO Rep *9*, 1222-1229.

Adams, C.J., Pike, A.C., Maniam, S., Sharpe, T.D., Coutts, A.S., Knapp, S., La Thangue, N.B., and Bullock, A.N. (2012). The p53 cofactor Strap exhibits an unexpected TPR motif and oligonucleotide-binding (OB)-fold structure. Proc Natl Acad Sci U S A *109*, 3778-3783.

Aguer, C., Gambarotta, D., Mailloux, R.J., Moffat, C., Dent, R., McPherson, R., and Harper, M.E. (2011). Galactose enhances oxidative metabolism and reveals mitochondrial dysfunction in human primary muscle cells. PloS one *6*, e28536.

Aitken, C.E., and Lorsch, J.R. (2012). A mechanistic overview of translation initiation in eukaryotes. Nature structural & molecular biology *19*, 568-576.

Alavian, K.N., Li, H., Collis, L., Bonanni, L., Zeng, L., Sacchetti, S., Lazrove, E., Nabili, P., Flaherty, B., Graham, M., *et al.* (2011). Bcl-xL regulates metabolic efficiency of neurons through interaction with the mitochondrial F1FO ATP synthase. Nat Cell Biol *13*, 1224-1233.

Amundson, S.A., Myers, T.G., and Fornace, A.J., Jr. (1998). Roles for p53 in growth arrest and apoptosis: putting on the brakes after genotoxic stress. Oncogene *17*, 3287-3299.

Astuti, D., Latif, F., Dallol, A., Dahia, P.L., Douglas, F., George, E., Skoldberg, F., Husebye, E.S., Eng, C., and Maher, E.R. (2001). Gene mutations in the succinate

dehydrogenase subunit SDHB cause susceptibility to familial pheochromocytoma and to familial paraganglioma. American journal of human genetics *69*, 49-54.

Atienza, J.M., Zhu, J., Wang, X., Xu, X., and Abassi, Y. (2005). Dynamic monitoring of cell adhesion and spreading on microelectronic sensor arrays. Journal of biomolecular screening *10*, 795-805.

Banki, K., Hutter, E., Gonchoroff, N.J., and Perl, A. (1999). Elevation of mitochondrial transmembrane potential and reactive oxygen intermediate levels are early events and occur independently from activation of caspases in Fas signaling. J Immunol *162*, 1466-1479.

Barlow, C., Hirotsune, S., Paylor, R., Liyanage, M., Eckhaus, M., Collins, F., Shiloh, Y., Crawley, J.N., Ried, T., Tagle, D., *et al.* (1996). Atm-deficient mice: a paradigm of ataxia telangiectasia. Cell *86*, 159-171.

Becker, T., Bottinger, L., and Pfanner, N. (2012). Mitochondrial protein import: from transport pathways to an integrated network. Trends in biochemical sciences *37*, 85-91.

Bensaad, K., Tsuruta, A., Selak, M.A., Vidal, M.N., Nakano, K., Bartrons, R., Gottlieb, E., and Vousden, K.H. (2006). TIGAR, a p53-inducible regulator of glycolysis and apoptosis. Cell *126*, 107-120.

Bergeaud, M., Mathieu, L., Guillaume, A., Moll, U.M., Mignotte, B., Le Floch, N., Vayssiere, J.L., and Rincheval, V. (2013). Mitochondrial p53 mediates a transcription-independent regulation of cell respiration and interacts with the mitochondrial F(1)F(0)-ATP synthase. Cell Cycle *12*, 2781-2793.

Berggard, T., Linse, S., and James, P. (2007). Methods for the detection and analysis of protein-protein interactions. Proteomics *7*, 2833-2842.

Bertout, J.A., Patel, S.A., and Simon, M.C. (2008). The impact of O2 availability on human cancer. Nature reviews Cancer *8*, 967-975.

Boros, L.G., Puigjaner, J., Cascante, M., Lee, W.N., Brandes, J.L., Bassilian, S., Yusuf, F.I., Williams, R.D., Muscarella, P., Melvin, W.S., *et al.* (1997). Oxythiamine and dehydroepiandrosterone inhibit the nonoxidative synthesis of ribose and tumor cell proliferation. Cancer Res *57*, 4242-4248.

Brown, E.J., and Baltimore, D. (2000). ATR disruption leads to chromosomal fragmentation and early embryonic lethality. Genes Dev *14*, 397-402.

Budanov, A.V., Sablina, A.A., Feinstein, E., Koonin, E.V., and Chumakov, P.M. (2004). Regeneration of peroxiredoxins by p53-regulated sestrins, homologs of bacterial AhpD. Science *304*, 596-600.

Budanov, A.V., Shoshani, T., Faerman, A., Zelin, E., Kamer, I., Kalinski, H., Gorodin, S., Fishman, A., Chajut, A., Einat, P., *et al.* (2002). Identification of a novel stress-responsive gene Hi95 involved in regulation of cell viability. Oncogene *21*, 6017-6031.

Cairns, R.A., Harris, I.S., and Mak, T.W. (2011). Regulation of cancer cell metabolism. Nature reviews Cancer *11*, 85-95.

Cano, C.E., Gommeaux, J., Pietri, S., Culcasi, M., Garcia, S., Seux, M., Barelier, S., Vasseur, S., Spoto, R.P., Pebusque, M.J., *et al.* (2009). Tumor protein 53-induced nuclear protein 1 is a major mediator of p53 antioxidant function. Cancer Res *69*, 219-226.

Carre, M., Andre, N., Carles, G., Borghi, H., Brichese, L., Briand, C., and Braguer, D. (2002). Tubulin is an inherent component of mitochondrial membranes that interacts with the voltage-dependent anion channel. J Biol Chem *277*, 33664-33669.

Carvajal, L.A., and Manfredi, J.J. (2013). Another fork in the road--life or death decisions by the tumour suppressor p53. EMBO Rep *14*, 414-421.

Chen, D., Kon, N., Li, M., Zhang, W., Qin, J., and Gu, W. (2005a). ARF-BP1/Mule is a critical mediator of the ARF tumor suppressor. Cell *121*, 1071-1083.

Chen, X.J., and Butow, R.A. (2005). The organization and inheritance of the mitochondrial genome. Nature reviews Genetics *6*, 815-825.

Chen, Z., Trotman, L.C., Shaffer, D., Lin, H.K., Dotan, Z.A., Niki, M., Koutcher, J.A., Scher, H.I., Ludwig, T., Gerald, W., *et al.* (2005b). Crucial role of p53-dependent cellular senescence in suppression of Pten-deficient tumorigenesis. Nature *436*, 725-730.

Cheung, E.C., Ludwig, R.L., and Vousden, K.H. (2012). Mitochondrial localization of TIGAR under hypoxia stimulates HK2 and lowers ROS and cell death. Proc Natl Acad Sci U S A *109*, 20491-20496.

Chi, S.L., and Pizzo, S.V. (2006). Cell surface F1Fo ATP synthase: a new paradigm? Annals of medicine *38*, 429-438.

Chipuk, J.E., Kuwana, T., Bouchier-Hayes, L., Droin, N.M., Newmeyer, D.D., Schuler, M., and Green, D.R. (2004). Direct activation of Bax by p53 mediates mitochondrial membrane permeabilization and apoptosis. Science *303*, 1010-1014.

Cho, S., Park, S.G., Lee, D.H., and Park, B.C. (2004). Protein-protein interaction networks: from interactions to networks. Journal of biochemistry and molecular biology *37*, 45-52.

Ciccia, A., and Elledge, S.J. (2010). The DNA damage response: making it safe to play with knives. Mol Cell *40*, 179-204.

Cohen, P. (2002). The origins of protein phosphorylation. Nat Cell Biol *4*, E127-130.

Cortez, D. (2003). Caffeine inhibits checkpoint responses without inhibiting the ataxia-telangiectasia-mutated (ATM) and ATM- and Rad3-related (ATR) protein kinases. J Biol Chem *278*, 37139-37145.

Coutts, A.S., Boulahbel, H., Graham, A., and La Thangue, N.B. (2007). Mdm2 targets the p53 transcription cofactor JMY for degradation. EMBO Rep *8*, 84-90.

Coutts, A.S., and La Thangue, N. (2006). The p53 response during DNA damage: impact of transcriptional cofactors. Biochem Soc Symp, 181-189.

Coutts, A.S., and La Thangue, N.B. (2005). The p53 response: emerging levels of co-factor complexity. Biochem Biophys Res Commun *331*, 778-785.

Coutts, A.S., Pires, I.M., Weston, L., Buffa, F.M., Milani, M., Li, J.L., Harris, A.L., Hammond, E.M., and La Thangue, N.B. (2011). Hypoxia-driven cell motility reflects the interplay between JMY and HIF-1alpha. Oncogene.

Coutts, A.S., Weston, L., and La Thangue, N.B. (2009). A transcription co-factor integrates cell adhesion and motility with the p53 response. Proc Natl Acad Sci U S A *106*, 19872-19877.

Crighton, D., Wilkinson, S., O'Prey, J., Syed, N., Smith, P., Harrison, P.R., Gasco, M., Garrone, O., Crook, T., and Ryan, K.M. (2006). DRAM, a p53-induced modulator of autophagy, is critical for apoptosis. Cell *126*, 121-134.

Dai, C., and Gu, W. (2010). p53 post-translational modification: deregulated in tumorigenesis. Trends in molecular medicine *16*, 528-536.

Davies, L., Paraskevopoulou, E., Sadeq, M., Symeou, C., Pantelidou, C., Demonacos, C., and Krstic-Demonacos, M. (2011). Regulation of glucocorticoid receptor activity by a stress responsive transcriptional cofactor. Mol Endocrinol *25*, 58-71.

de Klein, A., Muijtjens, M., van Os, R., Verhoeven, Y., Smit, B., Carr, A.M., Lehmann, A.R., and Hoeijmakers, J.H. (2000). Targeted disruption of the cell-cycle checkpoint gene ATR leads to early embryonic lethality in mice. Current biology : CB *10*, 479-482.

Demonacos, C., Krstic-Demonacos, M., and La Thangue, N.B. (2001). A TPR motif cofactor contributes to p300 activity in the p53 response. Mol Cell *8*, 71-84.

Demonacos, C., Krstic-Demonacos, M., Smith, L., Xu, D., O'Connor, D.P., Jansson, M., and La Thangue, N.B. (2004). A new effector pathway links ATM kinase with the DNA damage response. Nat Cell Biol *6*, 968-976.

Deng, X., Gao, F., Flagg, T., and May, W.S., Jr. (2004). Mono- and multisite phosphorylation enhances Bcl2's antiapoptotic function and inhibition of cell cycle entry functions. Proc Natl Acad Sci U S A *101*, 153-158.

Desagher, S., and Martinou, J.C. (2000). Mitochondria as the central control point of apoptosis. Trends Cell Biol *10*, 369-377.

Dewson, G., Kratina, T., Sim, H.W., Puthalakath, H., Adams, J.M., Colman, P.M., and Kluck, R.M. (2008). To trigger apoptosis, Bak exposes its BH3 domain and homodimerizes via BH3:groove interactions. Mol Cell *30*, 369-380.

Dhar, S.K., and St Clair, D.K. (2009). Nucleophosmin blocks mitochondrial localization of p53 and apoptosis. J Biol Chem *284*, 16409-16418.

Di Siena, S., Campolo, F., Rossi, P., Jannini, E.A., Dolci, S., and Pellegrini, M. (2013). UV and genotoxic stress induce ATR relocalization in mouse spermatocytes. The International journal of developmental biology *57*, 281-287.

Du, C., Fang, M., Li, Y., Li, L., and Wang, X. (2000). Smac, a mitochondrial protein that promotes cytochrome c-dependent caspase activation by eliminating IAP inhibition. Cell *102*, 33-42.

Dumont, P., Leu, J.I., Della Pietra, A.C., 3rd, George, D.L., and Murphy, M. (2003). The codon 72 polymorphic variants of p53 have markedly different apoptotic potential. Nature genetics *33*, 357-365.

Eguchi, Y., Shimizu, S., and Tsujimoto, Y. (1997). Intracellular ATP levels determine cell death fate by apoptosis or necrosis. Cancer Res *57*, 1835-1840.

Elstrom, R.L., Bauer, D.E., Buzzai, M., Karnauskas, R., Harris, M.H., Plas, D.R., Zhuang, H., Cinalli, R.M., Alavi, A., Rudin, C.M., *et al.* (2004). Akt stimulates aerobic glycolysis in cancer cells. Cancer Res *64*, 3892-3899.

Eng, C., Kiuru, M., Fernandez, M.J., and Aaltonen, L.A. (2003). A role for mitochondrial enzymes in inherited neoplasia and beyond. Nature reviews Cancer *3*, 193-202.

Erster, S., Mihara, M., Kim, R.H., Petrenko, O., and Moll, U.M. (2004). In vivo mitochondrial p53 translocation triggers a rapid first wave of cell death in response to DNA damage that can precede p53 target gene activation. Mol Cell Biol *24*, 6728-6741.

Essmann, F., Pohlmann, S., Gillissen, B., Daniel, P.T., Schulze-Osthoff, K., and Janicke, R.U. (2005). Irradiation-induced translocation of p53 to mitochondria in the absence of apoptosis. J Biol Chem *280*, 37169-37177.

Fanning, E., Klimovich, V., and Nager, A.R. (2006). A dynamic model for replication protein A (RPA) function in DNA processing pathways. Nucleic Acids Res *34*, 4126-4137.

Ferlay, J., Shin, H.R., Bray, F., Forman, D., Mathers, C., and Parkin, D.M. (2010). Estimates of worldwide burden of cancer in 2008: GLOBOCAN 2008. Int J Cancer *127*, 2893-2917.

Flynn, R.L., and Zou, L. (2010). Oligonucleotide/oligosaccharide-binding fold proteins: a growing family of genome guardians. Critical reviews in biochemistry and molecular biology *45*, 266-275.

Fokas, E., Prevo, R., Hammond, E.M., Brunner, T.B., McKenna, W.G., and Muschel, R.J. (2013). Targeting ATR in DNA damage response and cancer therapeutics. Cancer treatment reviews.

Formentini, L., Sanchez-Arago, M., Sanchez-Cenizo, L., and Cuezva, J.M. (2012). The mitochondrial ATPase inhibitory factor 1 triggers a ROS-mediated retrograde prosurvival and proliferative response. Mol Cell *45*, 731-742.

Friesen, W.J., Wyce, A., Paushkin, S., Abel, L., Rappsilber, J., Mann, M., and Dreyfuss, G. (2002). A novel WD repeat protein component of the methylosome binds Sm proteins. J Biol Chem *277*, 8243-8247.

Giaccia, A.J., and Kastan, M.B. (1998). The complexity of p53 modulation: emerging patterns from divergent signals. Genes Dev *12*, 2973-2983.

Giam, M., Huang, D.C., and Bouillet, P. (2008). BH3-only proteins and their roles in programmed cell death. Oncogene *27 Suppl 1*, S128-136.

Giorgio, V., Bisetto, E., Soriano, M.E., Dabbeni-Sala, F., Basso, E., Petronilli, V., Forte, M.A., Bernardi, P., and Lippe, G. (2009). Cyclophilin D modulates mitochondrial F0F1-ATP synthase by interacting with the lateral stalk of the complex. J Biol Chem *284*, 33982-33988.

Goldstein, J.C., Waterhouse, N.J., Juin, P., Evan, G.I., and Green, D.R. (2000). The coordinate release of cytochrome c during apoptosis is rapid, complete and kinetically invariant. Nat Cell Biol *2*, 156-162.

Gossen, M., Freundlieb, S., Bender, G., Muller, G., Hillen, W., and Bujard, H. (1995). Transcriptional activation by tetracyclines in mammalian cells. Science *268*, 1766-1769.

Graupner, V., Alexander, E., Overkamp, T., Rothfuss, O., De Laurenzi, V., Gillissen, B.F., Daniel, P.T., Schulze-Osthoff, K., and Essmann, F. (2011). Differential regulation of the proapoptotic multidomain protein Bak by p53 and p73 at the promoter level. Cell Death Differ *18*, 1130-1139.

Green, D.R., and Kroemer, G. (2004). The pathophysiology of mitochondrial cell death. Science *305*, 626-629.

Gsponer, J., Futschik, M.E., Teichmann, S.A., and Babu, M.M. (2008). Tight regulation of unstructured proteins: from transcript synthesis to protein degradation. Science *322*, 1365-1368.

Hainaut, P., and Wiman, K.G. (2009). 30 years and a long way into p53 research. Lancet Oncol *10*, 913-919.

Hanahan, D., and Weinberg, R.A. (2000). The hallmarks of cancer. Cell *100*, 57-70.

Hanahan, D., and Weinberg, R.A. (2011). Hallmarks of cancer: the next generation. Cell *144*, 646-674.

Harper, J.W., and Elledge, S.J. (2007). The DNA damage response: ten years after. Mol Cell *28*, 739-745.

Haupt, Y., Rowan, S., Shaulian, E., Vousden, K.H., and Oren, M. (1995). Induction of apoptosis in HeLa cells by trans-activation-deficient p53. Genes Dev *9*, 2170-2183.

Hegde, R., Srinivasula, S.M., Zhang, Z., Wassell, R., Mukattash, R., Cilenti, L., DuBois, G., Lazebnik, Y., Zervos, A.S., Fernandes-Alnemri, T., *et al.* (2002). Identification of Omi/HtrA2 as a mitochondrial apoptotic serine protease that

disrupts inhibitor of apoptosis protein-caspase interaction. J Biol Chem *277*, 432-438.

Heiskanen, K.M., Bhat, M.B., Wang, H.W., Ma, J., and Nieminen, A.L. (1999). Mitochondrial depolarization accompanies cytochrome c release during apoptosis in PC6 cells. J Biol Chem *274*, 5654-5658.

Hockenbery, D., Nunez, G., Milliman, C., Schreiber, R.D., and Korsmeyer, S.J. (1990). Bcl-2 is an inner mitochondrial membrane protein that blocks programmed cell death. Nature *348*, 334-336.

Holmquist-Mengelbier, L., Fredlund, E., Lofstedt, T., Noguera, R., Navarro, S., Nilsson, H., Pietras, A., Vallon-Christersson, J., Borg, A., Gradin, K., *et al.* (2006). Recruitment of HIF-1alpha and HIF-2alpha to common target genes is differentially regulated in neuroblastoma: HIF-2alpha promotes an aggressive phenotype. Cancer cell *10*, 413-423.

Holt, I.J., He, J., Mao, C.C., Boyd-Kirkup, J.D., Martinsson, P., Sembongi, H., Reyes, A., and Spelbrink, J.N. (2007). Mammalian mitochondrial nucleoids: organizing an independently minded genome. Mitochondrion *7*, 311-321.

Hu, W., Zhang, C., Wu, R., Sun, Y., Levine, A., and Feng, Z. (2010). Glutaminase 2, a novel p53 target gene regulating energy metabolism and antioxidant function. Proc Natl Acad Sci U S A *107*, 7455-7460.

Izyumov, D.S., Avetisyan, A.V., Pletjushkina, O.Y., Sakharov, D.V., Wirtz, K.W., Chernyak, B.V., and Skulachev, V.P. (2004). "Wages of fear": transient threefold decrease in intracellular ATP level imposes apoptosis. Biochim Biophys Acta *1658*, 141-147.

Jackson, R.J., Hellen, C.U., and Pestova, T.V. (2010). The mechanism of eukaryotic translation initiation and principles of its regulation. Nat Rev Mol Cell Biol *11*, 113-127.

Jagtap, P., and Szabo, C. (2005). Poly(ADP-ribose) polymerase and the therapeutic effects of its inhibitors. Nature reviews Drug discovery *4*, 421-440.

Jansson, M., Durant, S.T., Cho, E.C., Sheahan, S., Edelmann, M., Kessler, B., and La Thangue, N.B. (2008). Arginine methylation regulates the p53 response. Nat Cell Biol *10*, 1431-1439.

Javadov, S., and Karmazyn, M. (2007). Mitochondrial permeability transition pore opening as an endpoint to initiate cell death and as a putative target for cardioprotection. Cellular physiology and biochemistry : international journal of experimental cellular physiology, biochemistry, and pharmacology *20*, 1-22.

Jones, R.G., and Thompson, C.B. (2009). Tumor suppressors and cell metabolism: a recipe for cancer growth. Genes Dev *23*, 537-548.

Kastan, M.B., Zhan, Q., el-Deiry, W.S., Carrier, F., Jacks, T., Walsh, W.V., Plunkett, B.S., Vogelstein, B., and Fornace, A.J., Jr. (1992). A mammalian cell cycle checkpoint pathway utilizing p53 and GADD45 is defective in ataxia-telangiectasia. Cell *71*, 587-597.

Kazak, L., Reyes, A., and Holt, I.J. (2012). Minimizing the damage: repair pathways keep mitochondrial DNA intact. Nat Rev Mol Cell Biol *13*, 659-671.

Kerr, L.E., Birse-Archbold, J.L., Short, D.M., McGregor, A.L., Heron, I., Macdonald, D.C., Thompson, J., Carlson, G.J., Kelly, J.S., McCulloch, J., *et al.* (2007). Nucleophosmin is a novel Bax chaperone that regulates apoptotic cell death. Oncogene *26*, 2554-2562.

Kilbride, S.M., and Prehn, J.H. (2012). Central roles of apoptotic proteins in mitochondrial function. Oncogene.

Kim, J.W., Tchernyshyov, I., Semenza, G.L., and Dang, C.V. (2006). HIF-1-mediated expression of pyruvate dehydrogenase kinase: a metabolic switch required for cellular adaptation to hypoxia. Cell metabolism *3*, 177-185.

Kohn, A.D., Summers, S.A., Birnbaum, M.J., and Roth, R.A. (1996). Expression of a constitutively active Akt Ser/Thr kinase in 3T3-L1 adipocytes stimulates glucose uptake and glucose transporter 4 translocation. J Biol Chem *271*, 31372-31378.

Kolupaeva, V.G., Unbehaun, A., Lomakin, I.B., Hellen, C.U., and Pestova, T.V. (2005). Binding of eukaryotic initiation factor 3 to ribosomal 40S subunits and its role in ribosomal dissociation and anti-association. RNA *11*, 470-486.

Koopman, W.J., Distelmaier, F., Smeitink, J.A., and Willems, P.H. (2013). OXPHOS mutations and neurodegeneration. EMBO J *32*, 9-29.

Kruse, J.P., and Gu, W. (2008). SnapShot: p53 posttranslational modifications. Cell *133*, 930-930 e931.

Laemmli, U.K. (1970). Cleavage of structural proteins during the assembly of the head of bacteriophage T4. Nature *227*, 680-685.

Lane, D.P., and Crawford, L.V. (1979). T antigen is bound to a host protein in SV40-transformed cells. Nature *278*, 261-263.

Larsen, M.R., Trelle, M.B., Thingholm, T.E., and Jensen, O.N. (2006). Analysis of posttranslational modifications of proteins by tandem mass spectrometry. BioTechniques *40*, 790-798.

Leist, M., Single, B., Castoldi, A.F., Kuhnle, S., and Nicotera, P. (1997). Intracellular adenosine triphosphate (ATP) concentration: a switch in the decision

between apoptosis and necrosis. The Journal of experimental medicine *185*, 1481-1486.

Lemasters, J.J., Qian, T., Bradham, C.A., Brenner, D.A., Cascio, W.E., Trost, L.C., Nishimura, Y., Nieminen, A.L., and Herman, B. (1999). Mitochondrial dysfunction in the pathogenesis of necrotic and apoptotic cell death. Journal of bioenergetics and biomembranes *31*, 305-319.

Leng, R.P., Lin, Y., Ma, W., Wu, H., Lemmers, B., Chung, S., Parant, J.M., Lozano, G., Hakem, R., and Benchimol, S. (2003). Pirh2, a p53-induced ubiquitin-protein ligase, promotes p53 degradation. Cell *112*, 779-791.

Leu, J.I., Dumont, P., Hafey, M., Murphy, M.E., and George, D.L. (2004). Mitochondrial p53 activates Bak and causes disruption of a Bak-Mcl1 complex. Nat Cell Biol *6*, 443-450.

Levine, A.J., and Puzio-Kuter, A.M. (2010). The control of the metabolic switch in cancers by oncogenes and tumor suppressor genes. Science *330*, 1340-1344.

Li, H., Zhu, H., Xu, C.J., and Yuan, J. (1998). Cleavage of BID by caspase 8 mediates the mitochondrial damage in the Fas pathway of apoptosis. Cell *94*, 491-501.

Li, M., Chen, D., Shiloh, A., Luo, J., Nikolaev, A.Y., Qin, J., and Gu, W. (2002). Deubiquitination of p53 by HAUSP is an important pathway for p53 stabilization. Nature *416*, 648-653.

Li, T., Kon, N., Jiang, L., Tan, M., Ludwig, T., Zhao, Y., Baer, R., and Gu, W. (2012). Tumor suppression in the absence of p53-mediated cell-cycle arrest, apoptosis, and senescence. Cell *149*, 1269-1283.

Liang, S.H., and Clarke, M.F. (1999). A bipartite nuclear localization signal is required for p53 nuclear import regulated by a carboxyl-terminal domain. J Biol Chem *274*, 32699-32703.

Linares, L.K., Hengstermann, A., Ciechanover, A., Muller, S., and Scheffner, M. (2003). HdmX stimulates Hdm2-mediated ubiquitination and degradation of p53. Proc Natl Acad Sci U S A *100*, 12009-12014.

Lindenboim, L., Borner, C., and Stein, R. (2011). Nuclear proteins acting on mitochondria. Biochim Biophys Acta *1813*, 584-596.

Liu, B., Chen, Y., and St Clair, D.K. (2008). ROS and p53: a versatile partnership. Free radical biology & medicine *44*, 1529-1535.

Liu, X., Kim, C.N., Yang, J., Jemmerson, R., and Wang, X. (1996). Induction of apoptotic program in cell-free extracts: requirement for dATP and cytochrome c. Cell *86*, 147-157.

Logan, N., Graham, A., Zhao, X., Fisher, R., Maiti, B., Leone, G., and La Thangue, N.B. (2005). E2F-8: an E2F family member with a similar organization of DNA-binding domains to E2F-7. Oncogene *24*, 5000-5004.

Lynch, J.T., Somerville, T.D., Spencer, G.J., Huang, X., and Somervaille, T.C. (2013). TTC5 is required to prevent apoptosis of acute myeloid leukemia stem cells. Cell death & disease *4*, e573.

MacKenzie, S.H., and Clark, A.C. (2012). Death by caspase dimerization. Advances in experimental medicine and biology *747*, 55-73.

Maddocks, O.D., Berkers, C.R., Mason, S.M., Zheng, L., Blyth, K., Gottlieb, E., and Vousden, K.H. (2013). Serine starvation induces stress and p53-dependent metabolic remodelling in cancer cells. Nature *493*, 542-546.

Maltzman, W., and Czyzyk, L. (1984). UV irradiation stimulates levels of p53 cellular tumor antigen in nontransformed mouse cells. Mol Cell Biol *4*, 1689-1694.

Mancini, F., Di Conza, G., Pellegrino, M., Rinaldo, C., Prodosmo, A., Giglio, S., D'Agnano, I., Florenzano, F., Felicioni, L., Buttitta, F., *et al.* (2009). MDM4 (MDMX) localizes at the mitochondria and facilitates the p53-mediated intrinsic-apoptotic pathway. EMBO J *28*, 1926-1939.

Mann, M., and Jensen, O.N. (2003). Proteomic analysis of post-translational modifications. Nature biotechnology *21*, 255-261.

Manning, G., Whyte, D.B., Martinez, R., Hunter, T., and Sudarsanam, S. (2002). The protein kinase complement of the human genome. Science *298*, 1912-1934.

Marchenko, N.D., Wolff, S., Erster, S., Becker, K., and Moll, U.M. (2007). Monoubiquitylation promotes mitochondrial p53 translocation. EMBO J *26*, 923-934.

Marchenko, N.D., Zaika, A., and Moll, U.M. (2000). Death signal-induced localization of p53 protein to mitochondria. A potential role in apoptotic signaling. J Biol Chem *275*, 16202-16212.

Marroquin, L.D., Hynes, J., Dykens, J.A., Jamieson, J.D., and Will, Y. (2007). Circumventing the Crabtree effect: replacing media glucose with galactose increases susceptibility of HepG2 cells to mitochondrial toxicants. Toxicological sciences : an official journal of the Society of Toxicology *97*, 539-547.

Matoba, S., Kang, J.G., Patino, W.D., Wragg, A., Boehm, M., Gavrilova, O., Hurley, P.J., Bunz, F., and Hwang, P.M. (2006). p53 regulates mitochondrial respiration. Science *312*, 1650-1653.

Matsuoka, S., Ballif, B.A., Smogorzewska, A., McDonald, E.R., 3rd, Hurov, K.E., Luo, J., Bakalarski, C.E., Zhao, Z., Solimini, N., Lerenthal, Y., *et al.* (2007). ATM

and ATR substrate analysis reveals extensive protein networks responsive to DNA damage. Science *316*, 1160-1166.

Meng, X.W., Lee, S.H., Dai, H., Loegering, D., Yu, C., Flatten, K., Schneider, P., Dai, N.T., Kumar, S.K., Smith, B.D., *et al.* (2007). Mcl-1 as a buffer for proapoptotic Bcl-2 family members during TRAIL-induced apoptosis: a mechanistic basis for sorafenib (Bay 43-9006)-induced TRAIL sensitization. J Biol Chem *282*, 29831-29846.

Mihara, M., Erster, S., Zaika, A., Petrenko, O., Chittenden, T., Pancoska, P., and Moll, U.M. (2003). p53 has a direct apoptogenic role at the mitochondria. Mol Cell *11*, 577-590.

Miyashita, T., and Reed, J.C. (1995). Tumor suppressor p53 is a direct transcriptional activator of the human bax gene. Cell *80*, 293-299.

Modjtahedi, N., Giordanetto, F., Madeo, F., and Kroemer, G. (2006). Apoptosis-inducing factor: vital and lethal. Trends Cell Biol *16*, 264-272.

Moss, J., Tinline-Purvis, H., Walker, C.A., Folkes, L.K., Stratford, M.R., Hayles, J., Hoe, K.L., Kim, D.U., Park, H.O., Kearsey, S.E., *et al.* (2010). Break-induced ATR and Ddb1-Cul4(Cdt)(2) ubiquitin ligase-dependent nucleotide synthesis promotes homologous recombination repair in fission yeast. Genes Dev *24*, 2705-2716.

Mossalam, M., Matissek, K.J., Okal, A., Constance, J.E., and Lim, C.S. (2012). Direct induction of apoptosis using an optimal mitochondrially targeted p53. Molecular pharmaceutics *9*, 1449-1458.

Nagrath, D., Caneba, C., Karedath, T., and Bellance, N. (2011). Metabolomics for mitochondrial and cancer studies. Biochim Biophys Acta *1807*, 650-663.

Nakano, K., and Vousden, K.H. (2001). PUMA, a novel proapoptotic gene, is induced by p53. Mol Cell *7*, 683-694.

Neupert, W., and Herrmann, J.M. (2007). Translocation of proteins into mitochondria. Annual review of biochemistry *76*, 723-749.

Nieminen, A.I., Eskelinen, V.M., Haikala, H.M., Tervonen, T.A., Yan, Y., Partanen, J.I., and Klefstrom, J. (2013). Myc-induced AMPK-phospho p53 pathway activates Bak to sensitize mitochondrial apoptosis. Proc Natl Acad Sci U S A *110*, E1839-1848.

Nishi, H., Hashimoto, K., and Panchenko, A.R. (2011). Phosphorylation in protein-protein binding: effect on stability and function. Structure *19*, 1807-1815.

Niture, S.K., and Jaiswal, A.K. (2011). Inhibitor of Nrf2 (INrf2 or Keap1) protein degrades Bcl-xL via phosphoglycerate mutase 5 and controls cellular apoptosis. J Biol Chem *286*, 44542-44556.

Nunnari, J., and Suomalainen, A. (2012). Mitochondria: in sickness and in health. Cell *148*, 1145-1159.

Nurenberg, E., and Tampe, R. (2013). Tying up loose ends: ribosome recycling in eukaryotes and archaea. Trends in biochemical sciences *38*, 64-74.

Oda, E., Ohki, R., Murasawa, H., Nemoto, J., Shibue, T., Yamashita, T., Tokino, T., Taniguchi, T., and Tanaka, N. (2000). Noxa, a BH3-only member of the Bcl-2 family and candidate mediator of p53-induced apoptosis. Science *288*, 1053-1058.

Olsen, J.V., Blagoev, B., Gnad, F., Macek, B., Kumar, C., Mortensen, P., and Mann, M. (2006). Global, in vivo, and site-specific phosphorylation dynamics in signaling networks. Cell *127*, 635-648.

Olsson, M., and Zhivotovsky, B. (2011). Caspases and cancer. Cell Death Differ.

Oren, M., and Rotter, V. (2010). Mutant p53 gain-of-function in cancer. Cold Spring Harb Perspect Biol *2*, a001107.

Osaki, M., Oshimura, M., and Ito, H. (2004). PI3K-Akt pathway: its functions and alterations in human cancer. Apoptosis : an international journal on programmed cell death *9*, 667-676.

Palacios, G., and Moll, U.M. (2006). Mitochondrially targeted wild-type p53 suppresses growth of mutant p53 lymphomas in vivo. Oncogene *25*, 6133-6139.

Palermo, V., Mangiapelo, E., Piloto, C., Pieri, L., Muscolini, M., Tuosto, L., and Mazzoni, C. (2013). p53 death signal is mainly mediated by Nuc1(EndoG) in the yeast S. cerevisiae. FEMS yeast research.

Papa, S., Martino, P.L., Capitanio, G., Gaballo, A., De Rasmo, D., Signorile, A., and Petruzzella, V. (2012). The oxidative phosphorylation system in mammalian mitochondria. Advances in experimental medicine and biology *942*, 3-37.

Papandreou, I., Cairns, R.A., Fontana, L., Lim, A.L., and Denko, N.C. (2006). HIF-1 mediates adaptation to hypoxia by actively downregulating mitochondrial oxygen consumption. Cell metabolism *3*, 187-197.

Park, K.S., Mohapatra, D.P., Misonou, H., and Trimmer, J.S. (2006). Graded regulation of the Kv2.1 potassium channel by variable phosphorylation. Science *313*, 976-979.

Perciavalle, R.M., Stewart, D.P., Koss, B., Lynch, J., Milasta, S., Bathina, M., Temirov, J., Cleland, M.M., Pelletier, S., Schuetz, J.D., *et al.* (2012). Anti-apoptotic MCL-1 localizes to the mitochondrial matrix and couples mitochondrial fusion to respiration. Nat Cell Biol *14*, 575-583.

Perez-Arellano, I., Gallego, J., and Cervera, J. (2007). The PUA domain - a structural and functional overview. The FEBS journal *274*, 4972-4984.

Perry, S.W., Norman, J.P., Barbieri, J., Brown, E.B., and Gelbard, H.A. (2011). Mitochondrial membrane potential probes and the proton gradient: a practical usage guide. BioTechniques *50*, 98-115.

Pietsch, E.C., Leu, J.I., Frank, A., Dumont, P., George, D.L., and Murphy, M.E. (2007). The tetramerization domain of p53 is required for efficient BAK oligomerization. Cancer biology & therapy *6*, 1576-1583.

Pietsch, E.C., Perchiniak, E., Canutescu, A.A., Wang, G., Dunbrack, R.L., and Murphy, M.E. (2008). Oligomerization of BAK by p53 utilizes conserved residues of the p53 DNA binding domain. J Biol Chem *283*, 21294-21304.

Plun-Favreau, H., Burchell, V.S., Holmstrom, K.M., Yao, Z., Deas, E., Cain, K., Fedele, V., Moisoi, N., Campanella, M., Miguel Martins, L., *et al.* (2012). HtrA2 deficiency causes mitochondrial uncoupling through the F(1)F(0)-ATP synthase and consequent ATP depletion. Cell death & disease *3*, e335.

Poirier, M.C. (2004). Chemical-induced DNA damage and human cancer risk. Nature reviews Cancer *4*, 630-637.

Poot, M., Zhang, Y.Z., Kramer, J.A., Wells, K.S., Jones, L.J., Hanzel, D.K., Lugade, A.G., Singer, V.L., and Haugland, R.P. (1996). Analysis of mitochondrial morphology and function with novel fixable fluorescent stains. The journal of histochemistry and cytochemistry : official journal of the Histochemistry Society *44*, 1363-1372.

Reef, S., Zalckvar, E., Shifman, O., Bialik, S., Sabanay, H., Oren, M., and Kimchi, A. (2006). A short mitochondrial form of p19ARF induces autophagy and caspase-independent cell death. Mol Cell *22*, 463-475.

Renault, T.T., and Manon, S. (2011). Bax: Addressed to kill. Biochimie *93*, 1379-1391.

Riedl, S.J., and Salvesen, G.S. (2007). The apoptosome: signalling platform of cell death. Nat Rev Mol Cell Biol *8*, 405-413.

Rossignol, R., Gilkerson, R., Aggeler, R., Yamagata, K., Remington, S.J., and Capaldi, R.A. (2004). Energy substrate modulates mitochondrial structure and oxidative capacity in cancer cells. Cancer Res *64*, 985-993.

Rostovtseva, T.K., and Bezrukov, S.M. (2012). VDAC inhibition by tubulin and its physiological implications. Biochim Biophys Acta *1818*, 1526-1535.

Rostovtseva, T.K., Sheldon, K.L., Hassanzadeh, E., Monge, C., Saks, V., Bezrukov, S.M., and Sackett, D.L. (2008). Tubulin binding blocks mitochondrial voltage-dependent anion channel and regulates respiration. Proc Natl Acad Sci U S A *105*, 18746-18751.

Sablina, A.A., Budanov, A.V., Ilyinskaya, G.V., Agapova, L.S., Kravchenko, J.E., and Chumakov, P.M. (2005). The antioxidant function of the p53 tumor suppressor. Nat Med *11*, 1306-1313.

Sacco, F., Perfetto, L., Castagnoli, L., and Cesareni, G. (2012). The human phosphatase interactome: An intricate family portrait. FEBS letters *586*, 2732-2739.

Sanchez-Alcazar, J.A., Ault, J.G., Khodjakov, A., and Schneider, E. (2000). Increased mitochondrial cytochrome c levels and mitochondrial hyperpolarization precede camptothecin-induced apoptosis in Jurkat cells. Cell Death Differ *7*, 1090-1100.

Sanchez-Arago, M., Formentini, L., and Cuezva, J.M. (2012). Mitochondria-Mediated Energy Adaption in Cancer: The H(+)-ATP Synthase-Geared Switch of Metabolism in Human Tumors. Antioxidants & redox signaling.

Sanchez-Cenizo, L., Formentini, L., Aldea, M., Ortega, A.D., Garcia-Huerta, P., Sanchez-Arago, M., and Cuezva, J.M. (2010). Up-regulation of the ATPase

inhibitory factor 1 (IF1) of the mitochondrial H+-ATP synthase in human tumors mediates the metabolic shift of cancer cells to a Warburg phenotype. J Biol Chem *285*, 25308-25313.

Sansome, C., Zaika, A., Marchenko, N.D., and Moll, U.M. (2001). Hypoxia death stimulus induces translocation of p53 protein to mitochondria. Detection by immunofluorescence on whole cells. FEBS letters *488*, 110-115.

Sarkaria, J.N., Busby, E.C., Tibbetts, R.S., Roos, P., Taya, Y., Karnitz, L.M., and Abraham, R.T. (1999). Inhibition of ATM and ATR kinase activities by the radiosensitizing agent, caffeine. Cancer Res *59*, 4375-4382.

Schmidt, O., Pfanner, N., and Meisinger, C. (2010). Mitochondrial protein import: from proteomics to functional mechanisms. Nat Rev Mol Cell Biol *11*, 655-667.

Schonn, I., Hennesen, J., and Dartsch, D.C. (2010). Cellular responses to etoposide: cell death despite cell cycle arrest and repair of DNA damage. Apoptosis : an international journal on programmed cell death *15*, 162-172.

Schulze, A., and Harris, A.L. (2012). How cancer metabolism is tuned for proliferation and vulnerable to disruption. Nature *491*, 364-373.

Schwartzenberg-Bar-Yoseph, F., Armoni, M., and Karnieli, E. (2004). The tumor suppressor p53 down-regulates glucose transporters GLUT1 and GLUT4 gene expression. Cancer Res *64*, 2627-2633.

Semenza, G.L. (2010). Defining the role of hypoxia-inducible factor 1 in cancer biology and therapeutics. Oncogene *29*, 625-634.

Shen, L., Sun, X., Fu, Z., Yang, G., Li, J., and Yao, L. (2012). The fundamental role of the p53 pathway in tumor metabolism and its implication in tumor therapy. Clin Cancer Res *18*, 1561-1567.

Shikama, N., Lee, C.W., France, S., Delavaine, L., Lyon, J., Krstic-Demonacos, M., and La Thangue, N.B. (1999). A novel cofactor for p300 that regulates the p53 response. Mol Cell *4*, 365-376.

Shiloh, Y., and Ziv, Y. (2013). The ATM protein kinase: regulating the cellular response to genotoxic stress, and more. Nat Rev Mol Cell Biol *14*, 197-210.

Shiozaki, E.N., and Shi, Y. (2004). Caspases, IAPs and Smac/DIABLO: mechanisms from structural biology. Trends in biochemical sciences *29*, 486-494.

Speidel, D. (2010). Transcription-independent p53 apoptosis: an alternative route to death. Trends Cell Biol *20*, 14-24.

Stoddart, M.J. (2011). Cell viability assays: introduction. Methods Mol Biol *740*, 1-6.

Stratton, M.R. (2011). Exploring the genomes of cancer cells: progress and promise. Science *331*, 1553-1558.

Suzuki, S., Tanaka, T., Poyurovsky, M.V., Nagano, H., Mayama, T., Ohkubo, S., Lokshin, M., Hosokawa, H., Nakayama, T., Suzuki, Y., *et al.* (2010). Phosphate-activated glutaminase (GLS2), a p53-inducible regulator of glutamine metabolism and reactive oxygen species. Proc Natl Acad Sci U S A *107*, 7461-7466.

Suzuki, Y., Imai, Y., Nakayama, H., Takahashi, K., Takio, K., and Takahashi, R. (2001). A serine protease, HtrA2, is released from the mitochondria and interacts with XIAP, inducing cell death. Mol Cell *8*, 613-621.

Szczepanek, K., Lesnefsky, E.J., and Larner, A.C. (2012). Multi-tasking: nuclear transcription factors with novel roles in the mitochondria. Trends Cell Biol *22*, 429-437.

Takahashi, R., Deveraux, Q., Tamm, I., Welsh, K., Assa-Munt, N., Salvesen, G.S., and Reed, J.C. (1998). A single BIR domain of XIAP sufficient for inhibiting caspases. J Biol Chem *273*, 7787-7790.

Talos, F., Petrenko, O., Mena, P., and Moll, U.M. (2005). Mitochondrially targeted p53 has tumor suppressor activities in vivo. Cancer Res *65*, 9971-9981.

Tasdemir, E., Maiuri, M.C., Galluzzi, L., Vitale, I., Djavaheri-Mergny, M., D'Amelio, M., Criollo, A., Morselli, E., Zhu, C., Harper, F., *et al.* (2008). Regulation of autophagy by cytoplasmic p53. Nat Cell Biol *10*, 676-687.

Taylor, R.C., Cullen, S.P., and Martin, S.J. (2008). Apoptosis: controlled demolition at the cellular level. Nat Rev Mol Cell Biol *9*, 231-241.

Theobald, D.L., Mitton-Fry, R.M., and Wuttke, D.S. (2003). Nucleic acid recognition by OB-fold proteins. Annu Rev Biophys Biomol Struct *32*, 115-133.

Thomas, L.W., Lam, C., Clark, R.E., White, M.R., Spiller, D.G., Moots, R.J., and Edwards, S.W. (2012). Serine 162, an essential residue for the mitochondrial localization, stability and anti-apoptotic function of Mcl-1. PloS one *7*, e45088.

Thomas, P.D., Kejariwal, A., Campbell, M.J., Mi, H., Diemer, K., Guo, N., Ladunga, I., Ulitsky-Lazareva, B., Muruganujan, A., Rabkin, S., *et al.* (2003). PANTHER: a browsable database of gene products organized by biological function, using curated protein family and subfamily classification. Nucleic Acids Res *31*, 334-341.

Thompson, J., Finlayson, K., Salvo-Chirnside, E., MacDonald, D., McCulloch, J., Kerr, L., and Sharkey, J. (2008). Characterisation of the Bax-nucleophosmin interaction: the importance of the Bax C-terminus. Apoptosis : an international journal on programmed cell death *13*, 394-403.

Thorens, B., and Mueckler, M. (2010). Glucose transporters in the 21st Century. American journal of physiology Endocrinology and metabolism *298*, E141-145.

Tkach, J.M., Yimit, A., Lee, A.Y., Riffle, M., Costanzo, M., Jaschob, D., Hendry, J.A., Ou, J., Moffat, J., Boone, C., *et al.* (2012). Dissecting DNA damage response pathways by analysing protein localization and abundance changes during DNA replication stress. Nat Cell Biol *14*, 966-976.

Towbin, H., Staehelin, T., and Gordon, J. (1979). Electrophoretic transfer of proteins from polyacrylamide gels to nitrocellulose sheets: procedure and some applications. Proc Natl Acad Sci U S A *76*, 4350-4354.

Traven, A., and Heierhorst, J. (2005). SQ/TQ cluster domains: concentrated ATM/ATR kinase phosphorylation site regions in DNA-damage-response proteins. Bioessays *27*, 397-407.

Vafai, S.B., and Mootha, V.K. (2012). Mitochondrial disorders as windows into an ancient organelle. Nature *491*, 374-383.

Vaseva, A.V., Marchenko, N.D., Ji, K., Tsirka, S.E., Holzmann, S., and Moll, U.M. (2012). p53 opens the mitochondrial permeability transition pore to trigger necrosis. Cell *149*, 1536-1548.

Vaseva, A.V., and Moll, U.M. (2009). The mitochondrial p53 pathway. Biochim Biophys Acta *1787*, 414-420.

Velasco-Miguel, S., Buckbinder, L., Jean, P., Gelbert, L., Talbott, R., Laidlaw, J., Seizinger, B., and Kley, N. (1999). PA26, a novel target of the p53 tumor suppressor and member of the GADD family of DNA damage and growth arrest inducible genes. Oncogene *18*, 127-137.

Verhagen, A.M., Ekert, P.G., Pakusch, M., Silke, J., Connolly, L.M., Reid, G.E., Moritz, R.L., Simpson, R.J., and Vaux, D.L. (2000). Identification of DIABLO, a

mammalian protein that promotes apoptosis by binding to and antagonizing IAP proteins. Cell *102*, 43-53.

Vogelstein, B., Papadopoulos, N., Velculescu, V.E., Zhou, S., Diaz, L.A., Jr., and Kinzler, K.W. (2013). Cancer genome landscapes. Science *339*, 1546-1558.

Vousden, K.H., and Prives, C. (2009). Blinded by the Light: The Growing Complexity of p53. Cell *137*, 413-431.

Walensky, L.D., and Gavathiotis, E. (2011). BAX unleashed: the biochemical transformation of an inactive cytosolic monomer into a toxic mitochondrial pore. Trends in biochemical sciences *36*, 642-652.

Wallace, D.C. (1999). Mitochondrial diseases in man and mouse. Science *283*, 1482-1488.

Wallace, D.C. (2012). Mitochondria and cancer. Nature reviews Cancer *12*, 685-698.

Warburg, O. (1956). On the origin of cancer cells. Science *123*, 309-314.

Wegrzyn, J., Potla, R., Chwae, Y.J., Sepuri, N.B., Zhang, Q., Koeck, T., Derecka, M., Szczepanek, K., Szelag, M., Gornicka, A., *et al.* (2009). Function of mitochondrial Stat3 in cellular respiration. Science *323*, 793-797.

Wei, M.C., Zong, W.X., Cheng, E.H., Lindsten, T., Panoutsakopoulou, V., Ross, A.J., Roth, K.A., MacGregor, G.R., Thompson, C.B., and Korsmeyer, S.J. (2001). Proapoptotic BAX and BAK: a requisite gateway to mitochondrial dysfunction and death. Science *292*, 727-730.

Westphal, D., Dewson, G., Czabotar, P.E., and Kluck, R.M. (2011). Molecular biology of Bax and Bak activation and action. Biochim Biophys Acta *1813*, 521-531.

Wheeler, H.E., Maitland, M.L., Dolan, M.E., Cox, N.J., and Ratain, M.J. (2013). Cancer pharmacogenomics: strategies and challenges. Nature reviews Genetics *14*, 23-34.

Witze, E.S., Old, W.M., Resing, K.A., and Ahn, N.G. (2007). Mapping protein post-translational modifications with mass spectrometry. Nature methods *4*, 798-806.

Wolff, S., Erster, S., Palacios, G., and Moll, U.M. (2008). p53's mitochondrial translocation and MOMP action is independent of Puma and Bax and severely disrupts mitochondrial membrane integrity. Cell research *18*, 733-744.

Wolter, K.G., Hsu, Y.T., Smith, C.L., Nechushtan, A., Xi, X.G., and Youle, R.J. (1997). Movement of Bax from the cytosol to mitochondria during apoptosis. The Journal of cell biology *139*, 1281-1292.

Wu, Y., and Sha, B. (2006). Crystal structure of yeast mitochondrial outer membrane translocon member Tom70p. Nature structural & molecular biology *13*, 589-593.

Xu, D., Zalmas, L.P., and La Thangue, N.B. (2008). A transcription cofactor required for the heat-shock response. EMBO Rep *9*, 662-669.

Xue, W., Zender, L., Miething, C., Dickins, R.A., Hernando, E., Krizhanovsky, V., Cordon-Cardo, C., and Lowe, S.W. (2007). Senescence and tumour clearance is triggered by p53 restoration in murine liver carcinomas. Nature *445*, 656-660.

Youle, R.J., and Strasser, A. (2008). The BCL-2 protein family: opposing activities that mediate cell death. Nat Rev Mol Cell Biol *9*, 47-59.

Young, J.C., Hoogenraad, N.J., and Hartl, F.U. (2003). Molecular chaperones Hsp90 and Hsp70 deliver preproteins to the mitochondrial import receptor Tom70. Cell *112*, 41-50.

Zhao, Y., Chaiswing, L., Velez, J.M., Batinic-Haberle, I., Colburn, N.H., Oberley, T.D., and St Clair, D.K. (2005). p53 translocation to mitochondria precedes its nuclear translocation and targets mitochondrial oxidative defense protein-manganese superoxide dismutase. Cancer Res *65*, 3745-3750.

Zuchero, J.B., Coutts, A.S., Quinlan, M.E., Thangue, N.B., and Mullins, R.D. (2009). p53-cofactor JMY is a multifunctional actin nucleation factor. Nat Cell Biol *11*, 451-459.